THE UNIVERSITY OF
SYDNEY

BIOCHAR CARBON STABILITY IN SOME CONTRASTING SOILS FROM AUSTRALIA

A thesis submitted in fulfilment of the requirements for the degree of Doctor of Philosophy in
Faculty of Agriculture and Environment at
The University of Sydney

Yunying Fang
August 2013

献给我心爱的儿子–吴芮

TO MY BELOVED SON – WU RUI

CERTIFICATE OF ORIGINALITY

I hereby declare that this submission is my own work and that, to the best of my knowledge and belief, it contains no material previously published or written by another person nor material which to a substantial extent has been accepted for the award of any other degree or diploma of the university or other institute of higher learning, except where due acknowledgment has been made in the text.

Signature: 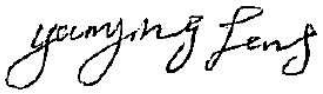

Author Name: Yunying Fang

Date: 30.8.2013

STATEMENT OF AUTHORSHIP

Chapters 3, 4 and 5 are written as separate manuscripts for publication. Consequently there is some repeated information in the method sections of each chapter, which is appropriately referenced to direct the readers for additional information in other relevant chapters.

I am the primary author of each of the three manuscripts. The contributions of the co-authors of each manuscript are given below.

Fang Y, Singh B, Singh BP and Krull E. 2014. Biochar carbon stability in four contrasting soils. European Journal of Soil Science, 65, 60–71.

Fang Y was responsible for conducting all experimental and data analysis and for preparation of the manuscript.

Singh B planned the experiment, supervised the laboratory work and was involved in interpretation of the results and reviewed the manuscript.

Singh BP planned the experiment, provided technical advice and was involved in interpretation of the results and reviewed the manuscript.

Krull E was involved in planning of the experiment and reviewing the manuscript.

Balwant Singh Bhupinder Pal Singh Evelyn Krull

Fang Y, Singh BP and Singh B. Temperature sensitivity of biochar and native carbon mineralisation in biochar-amended soils. Revised version has been resubmitted to Agriculture, Ecosystems and Environment in August 2013.

Fang Y was responsible for conducting all experimental and data analysis and for preparation of the manuscript.

Singh BP planned the experiment, provided technical advice and was involved in interpretation of the results and reviewed the manuscript.

Singh B planned the experiment, supervised the laboratory work and was involved in interpretation of the results and reviewed the manuscript.

Bhupinder Pal Singh Balwant Singh

Fang Y, Singh B and Singh BP. Biochar carbon stability and priming effects in four contrasting biochar-amended soils: long-term incubations at different temperatures. It has been submitted to Soil Biology and Biochemistry in August 2013.

Fang Y was responsible for conducting all experimental and data analysis and for preparation of the manuscript.

Singh B planned the experiment, supervised the laboratory work and was involved in interpretation of the results and reviewed the manuscript.

Singh BP planned the experiment, provided technical advice and was involved in interpretation of the results and reviewed the manuscript.

Balwant Singh

Bhupinder Pal Singh

ABSTRACT

Climate change is one of the biggest challenges facing the world. The largest contributor to climate change is the greenhouse gas CO_2, which is released through anthropogenic activities such as burning of fossil fuel and agricultural waste. To find solutions to mitigate climate change, research has been proposed to reduce greenhouse gas emissions or off-setting emissions through carbon (C) sequestration in soil – the largest C pool of terrestrial ecosystems. In this context, long-term C storage through biochar application to agricultural soils has been becoming a priority area of research in the last two decades.

For wide-spread biochar application to soil, it is important to understand its turnover rate and stability in different soil type and different temperatures. Moreover, the addition of biochar may influence the mineralisation or turnover of organic C in soil, therefore influencing C sequestration potential of biochar in soil. In this thesis, my research has: (i) quantified the effect of pyrolysis temperature, soil type and incubation temperature on biochar-C mineralisation over a relatively long period (2 years) and estimated biochar mean residence time (MRT); (ii) measured the influence of biochar on native soil organic carbon (SOC) mineralisation in different soils and temperatures; (iii) evaluated the temperature sensitivity of biochar-C and native SOC in biochar-amended soils; (iv) undertook a semi-quantitative analysis of C functional groups in fresh and aged biochars using light density fraction of native and biochar amended; and (v) assessed the interactive priming effect of biochar and labile organic matter (LOM) in a clayey soil over 2.1-year period.

Two wood biochars, produced by slow pyrolysis at 450 and 550 °C from a $\delta^{13}C$-depleted (-36.4‰) *Eucalyptus saligna*, were incubated with four soils (Inceptisol, Entisol, Oxisol and Vertisol) at different temperatures (20, 40 and 60 °C) over a 2-year period. The mineralisation of biochar-C or SOC was monitored through the analyses of evolved CO_2 and associated ^{13}C during the incubation period. Using a two-pool isotopic mixing model, biochar-derived and soil-derived CO_2 were determined. Concurrently, any decreases or increases in native SOC mineralisation caused by the presence of biochar, so-called “priming effects”, were quantified.

The proportion of added biochar-C mineralised over the two years was significantly ($p < 0.001$) greater in the 450 °C biochar (0.80−10.58%) amended samples than in the 550 °C biochar (0.43−3.28%) samples across the soil and temperature treatments. The biochar-C mineralisation increased with increasing incubation temperature. The proportion of the 450 °C biochar-C mineralised was significantly ($p < 0.05$) smaller in the Oxisol and Inceptisol than in the Entisol and Vertisol across all temperatures. The effect of soil characteristics, particularly clay mineralogy on biochar-C mineralisation can be clearly observed when the biochar-C mineralisation was expressed as per unit basis of initial native SOC. The smallest proportion of biochar-C was mineralised in the Oxisol and the greatest in the Inceptisol. In comparison, the mineralisation of 550 °C biochar-C was less affected by soil properties. Near-edge X-ray absorption fine structure (NEXAFS) spectroscopy results show that the C functional groups (i.e. aromatic C) of the light fraction (< 1.8 g cm^{-3}) of soil amended with biochars (fresh and aged for 1 and 2 years) did not show any change after 12 months at various incubation temperature.

The MRT of biochar-C, estimated from the 2-year mineralisation data, decreased with increasing incubation temperature. The MRT of the two woody biochars ranged between 25 and 1061 years in the four soils across the three temperatures. Although the MRT values decreased with increasing temperature, at elevated temperatures (40 and 60 °C) the MRT values of the 550 °C biochar in the soils was still in the range of a century to several centuries. Therefore, wood biochar produced at 550 °C can be useful for long-term C storage.

Biochar was found to enhance the stabilisation of native SOC over time, especially in clayey soils. However, a small loss of the native SOC was observed in a sandy soil at different temperatures over the 2-year incubation period. Biochar in a Vertisol produced positive or negative priming effects on LOM-C (labile organic matter-C) mineralisation depending on the LOM application rates. On the other hand, input of LOM (e.g. plant litter) at higher rates can decrease biochar-C stability; biochar may still persist in the soil in the range of a few centuries.

Biochar-C temperature sensitivity (Q_{10}) decreased at the high temperature range (40 to 60 °C) compared to the low temperature range (20 to 40 °C). Temperature sensitivity of biochar did not vary with pyrolysis temperature, and was

either smaller or similar to the native SOC across the four soils. Furthermore, the presence of biochar was found to decrease the temperature sensitivity of native SOC mineralisation and consequently this may enhance the C sequestration of biochar under climate warming.

Taken together, data from the current study indicate that biochar may store C in soil in the range of a few centuries or about a century at elevated temperatures, particularly when produced by slow pyrolysis at 550 °C. This research provides a direct support on the capability of biochar for long-term C storage in soil by quantification of biochar-C mineralisation in a range of soils and at different temperatures. The stability of biochar produced at low temperature can be influenced by soil type, with the greatest stability occurring in the Oxisol at elevated temperatures (40 and 60 °C). In contrast, biochar produced at the higher pyrolysis temperature contain greater proportion of aromatic C and consequently less affected by soil type. Concurrently, biochar may stabilise native SOC in clayey soils, which is found to be greater for the 550 °C biochar than the 450 °C biochar therefore to increase long-term C sequestration by biochar. On the other hand, biochar may increase native SOC mineralisation in a sandy soil. There was some indirect evidence for increased biochar-C stability through its interaction with variable charge minerals, particularly Fe and Al oxides. However, more research examining the mechansims of biochars interaction with soil minerals and native SOC, and the effect of soil envrionmental conditions, such as pH and redox conditions on biochar-C stability are needed.

ACKNOWLEDGEMENTS

I would like to acknowledge the University of Sydney for awarding me an International Scholarship (USydIS) for my postgraduate studies. With great sincerity, I would like to thank the people who have guided me through all aspects of this process. I am highly grateful to my supervisor, Associate Professor Balwant Singh, for his continuous support and encouragement during my PhD study. He has been deeply involved and dedicated in my research endeavours at all the time. He provided help beyond his responsibility as a supervisor. I would like to sincerely thank my associate supervisor, Dr Bhupinder Pal Singh from NSW Department of Primary Industries (NSW DPI) who was always available to provide technical advice, valuable ideas, edits and input.

I also would like to thank Claudia Keitel of the University of Sydney (USYD) for the $\delta^{13}C$ analysis; Neil Wilson of USYD for microbial community analysis; Bruce Cowie and Lars Thomsen from the Australian Synchrotron for the NEXAFS analysis, Bill Gong from the University of New South Wales for the XPS analysis; Matthew Foley from the Australian Centre for Microscopy & Microanalysis (ACMM) at the University of Sydney for the SEM analysis. I am thankful to Craig Barton (NSW DPI) and Burhan Amiji (University of Western Sydney) for supplying the labelled woody biomass; Adriana Downie (Pacific Pyrolysis) for producing the labelled wood biochars; David Giles, Kamaljeet Kaur and Simranjeet Singh Randhawa of NSW DPI for assistance in the laboratory work; Damian Collins of NSW DPI for assistance with the statistical analysis. I would like to thank Alexandra Keith, Nabeel Niazi and Daojarus Ketrot of USYD for their help in setting up the incubation experiments; Ming Zhang from IBM Beijing for data processing in Chapter 5. I also thank technical support from Loraine Watson, Michael Turner, Iona Gyorgy, Ivan Desailly from the Faculty of Agriculture and Environment. Many thanks to the administration staff, Ms Fiona Lawrence. I am thankful to Malcolm Possell for providing transport help when I travelled to Cobbitty for isotope analysis. I thank Dr Evelyn Krull for providing comments in Chapter 3. Alexandra Keith and Lai Poon provided some useful comments in Chapter 7.

Thank you to my fellow graduate students, Lucy Liu, Fei Wang, Wei Sun, Maryam Montazerolghaem, Waqar Ahmad, Kai Yang, Khwunta Khawmee, Mohmmam Witt, Daojarus Ketrot, Irshad Bibi, Chun Liang, Robert Pallasser, Kanika Singh, Nirmala Liyanage and all the great people I've met along the way that have encouraged me to pursue my PhD with great enthusiasm. I would also like to thank my flatmates Weipo Ding and Zhujun Li for creating a pleasant living environment.

Finally, I want to especially thank my family for their unwavering support throughout my endeavours.

PUBLICATIONS

Refereed scientific journals (Published/submitted):

1. Fang Y, Singh B, Singh BP and Krull E. 2014. Biochar carbon stability in four contrasting soils. Accepted by European Journal of Soil Science, 65, 60–71.

2. Fang Y, Singh BP and Singh B. Temperature sensitivity of biochar and native carbon mineralisation in biochar-amended soils. Agriculture, Ecosystems and Environment. This paper has been revised and resubmitted to Agriculture, Ecosystems & Environment in August 2013.

3. Fang Y, Singh B and Singh BP. Biochar carbon stability and priming effects in four contrasting biochar-amended soils: long-term incubations at different temperatures. Submitted to Soil Biology and Biochemistry in August 2013.

4. Nagodavithane C, Singh B, Fang Y. The effect of ageing on surface charge characteristics and adsorption behaviour of cadmium and arsenate in two contrasting soils amended with biochar. Accepted for publication in Soil Research.

Refereed scientific journals (in preparation)

1. Fang Y, Singh B, Wilson N, Keith A and Singh BP. A long-term study of interactive priming of biochar and soil carbon mineralisation in a Vertisol.

2. Singh B, Fang Y, Johnston CT. FTIR spectroscopy based index to evaluate changes in the carbon form of biochars with ageing in different soils.

Conference papers (Abstract/oral presentation):

1. Fang Y, Singh B, Singh BP. "Biochar stability in Australian Soils" Invited talk presented at the Biochar Symposium organised by Climate and Water Research Unit of the NSW Govt. - Industry and Investment at Wollongbar on 10 th Feb 2011.

2. Fang Y, Singh B, Singh BP. "Application of depleted-^{13}C labeling approach for quantifying biochar carbon stability in contrasting soils" oral paper presented at the 11th Australasian Environmental Isotope Conference and the 4th Australasian Hydrogeology Research Conference in Cairns from 12-14 July 2011.

3. Fang Y, Singh B, Singh BP. “Stability of biochar in contrasting soils of Australia” oral paper presented at the 2nd Asia Pacific Biochar Conference held in Kyoto, Japan from 14-18 September 2011.

4. Fang Y, Singh B, Singh BP. “Biochar carbon stability in contrasting soils as influenced by pyrolysis and incubation temperatures” oral paper presented at the ASA-CSSA-SSSA International Annual Meetings held in San Antonio, TX, USA from 16-19 October 2011.

5. Singh BP, Singh B, Fang Y. Biochar carbon stability and stabilisation in Australian soils. In: Climate and Soils Symposium, West Pennant Hills, Sydney, 21-22 September 2011.

6. Fang Y, Singh B, Singh BP, Krull E. “Biochar carbon stability and priming effect in contrasting soils of Australia” oral paper presented at European Geosciences Union General Assembly held in Vienna, Austria, 22-27 April 2012.

7. Fang Y, Singh B, Singh BP, Krull E. “Biochar stability in agricultural soils of Australia” key note presentation at the workshop “Biochar in Agriculture-An Update for Farmers” held at the Wollongbar Primary Industries Institute, Wollongbar, NSW on 6th June, 2012.

8. Fang Y, Singh B, Singh BP, Krull E. “Biochar carbon stability and priming effect in contrasting soils of Australia” oral paper presented at the 4th International Congress of the European Confederation of Soil Science Societies held in Bari (Italy) from, 2-6 July 2012.

9. Fang Y. “Can biochar mitigate climate change through soil carbon sequestration?” oral presented at 3 Minutes Thesis Challenge on 17 July 2012.

10. Fang Y, Singh B, Singh BP, Krull E. “Biochar carbon mineralization in relation to clay content and clay composition of soils” oral presented at 4th International Biochar Congress in Beijing from 16-20 th September, 2012.

11. Fang Y, Singh B, Singh BP, Krull E. “An isotopic study to determine the stability of biochar carbon in Australian agricultural soils” has been accepted for an oral presentation at Joint Australian and New Zealand Soil Science conference to be held at the Wrest Point Convention Centre, Hobart, 2-7 December 2012.

CONTENTS

Contents

LIST OF TABLES

Supporting Information

Chapter 5: Temperature sensitivity of biochar and native carbon mineralisation in biochar-amended soil

Supporting Information

Chapter 6: Application of NEXAFS spectroscopy and XPS for the characterisation of carbon functional groups of aged biochars in soils

Chapter 7: A long-term study of interactive priming of biochar and labile carbon mineralisation in a Vertisol

LIST OF FIGURES

Chapter 2: Literature review

Chapter 3: Biochar carbon stability in four contrasting soils

Chapter 5: Temperature sensitivity of biochar and native carbon mineralisation in biochar-amended soil

Supporting Information

Chapter 6: Application of NEXAFS spectroscopy and XPS for the characterisation of carbon functional groups of aged biochars in soils

Supporting Information

Chapter 7: A long-term study of interactive priming of biochar and labile carbon mineralisation in a Vertisol

Chapter 1: General introduction

1.1. Introduction

Biochar is a solid material obtained from the thermochemical conversion of biomass in an oxygen-limited environment (International Biochar Initiative, 2012). It has been used as a potential soil amendent (Lehmann and Joseph, 2009) with aims to improve soil nutrient retention, water holding capacity, soil pH and cation exchange capacity, and possibly increasing crop yield (Glaser et al., 2002; Lehmann and Rondon, 2006; Liang et al., 2006; Van Zwieten et al., 2010). More importantly, biochar can increase stable forms of carbon (C) in soil, by diverting waste biomass C from a rapid to a slow C-cycling pool. Therefore, biochar has been evaluated globally as a means to sequestrate C to mitigate climate change (Lehmann et al., 2006).

The feasibility of biochar as a technology to mitigate climate change rests on its stability relative to parent feedstock, which generally decomposes faster than the pyrolysed or charred biomass (Santos et al. 2012). Biochar stability varies depending on biomass feedstock and pyrolysis or charring temperature, which can influence aromatic C condensation and the compositions of different C forms (i.e. aromatics, aliphatics, water-soluble organics) within biochar (Keiluweit et al., 2010; Lin et al., 2012a; McBeath and Smernik, 2009). The degree of condensation of aromatic C and the compositions of C components can influence biochar degradation via biotic and abiotic processes (Baldock and Smernik, 2002; Cheng et al., 2006; Hilscher and Knicker, 2011; Zimmermann et al., 2012). Biochar in soil may be stabilised through interaction with soil clay minerals and occlusion within soil aggregates (Brodowski et al., 2005; Brodowski et al., 2006; Glaser et al., 2000). However, the role of organo-mineral interactions and other soil properties (e.g. native organic carbon content and quality, clay content and clay mineralogy) in the stabilisation of biochar has not been well studied. Considering the increased public interest in the use of biochar as a soil amendment for C sequestration and other benefits, it is vital to understand biochar-C stability and its stabilisation mechanisms in contrasting soils.

Compared to biochar-C stability, even less work has been done to investigate the influence of biochar on native soil organic carbon (SOC) mineralisation, i.e.

priming effect, in different soils. It has been suggested, for example, that biochar can increase (positive priming effect) the loss of native organic C (Wardle et al., 2008), thus possibly diminishing its C sequestration potential. On the other hand, Zimmerman et al. (2011) reported both positive and negative priming of biochar on native SOC mineralisation in a range of biochar-amended soils. To distinguish between biochar-C and SOC mineralisation and to quantify the priming effect of biochar on the mineralisation of native SOC, it is necessary to differentiate the CO_2 emission sources from biochar-amended soil. Recently, biochars with isotopically distinct C (^{14}C or ^{13}C) have been employed to isolate biochar-C and added organic C or native SOC mineralisation (Hamer et al., 2004; Jones et al., 2011; Keith et al., 2011; Kuzyakov et al., 2009; Liang et al., 2010; Luo et al., 2011). In these studies, the priming effects of biochar have also been reported to range from positive, negative, or no effect on native or added organic C in soil. On the other hand, the addition of labile organic matter (LOM) in soil can positively increase the mineralisation of biochar-C (Hamer et al., 2004; Keith et al., 2011; Kuzyakov et al., 2009; Luo et al., 2011), or there may be no significant effect on aged biochar (Liang et al., 2010). Over a longer term period, the effects (i.e. organo-mineral interaction, biochar adsorption and microbial activity or structure) contributing to interactive priming may change, and consequently, the direction and magnitude of interactive priming may also change with time. The dynamics and mechanisms of interactive priming of biochar on native SOC mineralisation in soils are poorly understood and require further investigation.

Biochar-C and SOC mineralisation can be accelerated by increasing temperature (Nguyen et al., 2010; Zimmermann et al., 2012). Interest in the temperature sensitivity of SOC decomposition is high due to its importance in global C cycle and potential feedbacks to climate change (Davidson and Janssens, 2006). However, there has been a lack of studies providing insights about the temperature sensitivity of biochar-C decomposition in soils of contrasting characteristics. The studies of SOC temperature sensitivity show that the relatively stable C in soil can be more, equally, or less sensitive to temperature, than the relatively labile C, and these divergent observations may result from the confounding influence of soil properties and environmental conditions (Conant et al., 2008; Davidson and Janssens, 2006; Fang et al., 2005; Liski et al., 1999). Biochar in soil could potentially interact with

SOC and soil minerals to alter SOC mineralisation (Mikutta et al., 2006; Torn et al., 1997) and consequently influence SOC temperature sensitivity to decomposition. However, so far there is no study that has demonstrated if the presence of biochar alters the temperature sensitivity of native SOC mineralisation in contrasting soils.

Research on historical charcoal or black carbon demonstrates that biochar molecular structure changes with time after biochar application to soil (Cheng and Lehmann, 2009; Cheng et al., 2006; Hilscher et al., 2009; Lehmann et al., 2005; Nguyen et al., 2009). The knowledge of chemical structure of biochar can be useful in understanding the interaction mechanisms of biochar with minerals and organic matter in soils. The functional groups on biochar surface can interact with native organic matter and soil minerals which are relevant to biochar stability (Brodowski et al., 2005; Hilscher and Knicker, 2011; Nguyen et al., 2009). Spectroscopy techniques have been used for characterising C functional groups of biochar and SOC. Near-edge X-ray absorption fine spectroscopy (NEXAFS) can reveal the oxidation degree from the small changes of C functional groups in biochar, for example, the nanoscale spatial analysis of the BC particle indicated a significant oxidation of BC surfaces with a reduction of aromatic C and an increase of carboxylic C (Lehmann et al., 2005). X-ray photoelectron spectroscopy (XPS), a surface sensitive technique, can provide complementary information on the development of surface functional groups and the changes in element composition with biochar ageing (Cheng and Lehmann, 2009; Cheng et al., 2006; Lin et al., 2012b; Nguyen et al., 2009). Moreover, the negatively charged functional groups can contribute to soil alkalinity through association with H^+, such as $–COO^-$ (–COOH) and $–O^-$(–OH) (Yuan et al., 2011). However, limited research has been done to investigate the C functional groups of biochar during its ageing process in different soils at different temperatures.

1.2. Aim

The specific aims of the research presented in this thesis are:

1. To quantify biochar-C stability in different soils at different temperatures over a long-term period.
2. To assess the priming effect of biochar on native SOC mineralisation in different soils at different temperatures over a long-term period.

3. To determine the temperature sensitivity of biochar and native SOC mineralisation in biochar-amended soils.
4. To characterise C functional groups of aged biochar in different soils at different temperatures using spectroscopic techniques.
5. To assess the long-term interactive priming effects of biochar and added labile organic matter and the microbial community structure changes in a clayey soil.

The thesis is organised into 8 chapters, including 5 research chapters. The introductory chapter (Chapter 1) is followed by a review of literature (Chapter 2) relevant to the research topic. The results from the research work are presented in Chapters 3−7 and each research chapter targets specific aims and hypotheses. Chapter 3 presents estimates of biochar-C stability in four contrasting soils (Inceptisol, Entisol, Oxisol and Vertisol) at 20 and 40 °C, evaluated over a one-year incubation period and the results presented here in this chapter has been accepted in European Journal of Soil Science. Chapter 4 presents estimates of biochar-C stability in the four contrasting soils, including the priming effects of biochar on native SOC mineralisation at 20, 40 and 60 °C, evaluated over a longer term (two-year incubation period). Chapter 5 presents temperature sensitivity of biochar and native SOC mineralisation in the four biochar-amended soils. Chapter 6 presents the chemical structure changes of aged biochar-C in different soils at different temperatures using near edge X-ray absorption fine structure (NEXAFS) and X-ray photoelectron spectroscopy (XPS) technique. Chapter 7 presents the interactive priming effect of biochar and labile organic matter and the microbial community structure changes over a 2.1-year incubation period. The final chapter of this thesis (Chapter 8) summarises the results presented in the research chapters, and suggests direction for future research in the field of biochar stability and priming effects.

1.3. References

Baldock, J.A., Smernik, R.J., 2002. Chemical composition and bioavailability of thermally, altered Pinus resinosa (Red Pine) wood. Organic Geochemistry 33, 1093-1109.

Brodowski, S., Amelung, W., Haumaier, L., Abetz, C., Zech, W., 2005. Morphological and chemical properties of black carbon in physical soil fractions as revealed by scanning electron microscopy and energy-dispersive X-ray spectroscopy. Geoderma 128, 116-129.

Brodowski, S., John, B., Flessa, H., Amelung, W., 2006. Aggregate-occluded black carbon in soil. European Journal of Soil Science 57, 539-546.

Cheng, C.H., Lehmann, J., 2009. Ageing of black carbon along a temperature gradient. Chemosphere 75, 1021-1027.

Cheng, C.H., Lehmann, J., Thies, J.E., Burton, S.D., Engelhard, M.H., 2006. Oxidation of black carbon by biotic and abiotic processes. Organic Geochemistry 37, 1477-1488.

Conant, R.T., Drijber, R.A., Haddix, M.L., Parton, W.J., Paul, E.A., Plante, A.F., Six, J., Steinweg, J.M., 2008. Sensitivity of organic matter decomposition to warming varies with its quality. Global Change Biology 14, 868-877.

Davidson, E.A., Janssens, I.A., 2006. Temperature sensitivity of soil carbon decomposition and feedbacks to climate change. Nature 440, 165-173.

Fang, C.M., Smith, P., Moncrieff, J.B., Smith, J.U., 2005. Similar response of labile and resistant soil organic matter pools to changes in temperature. Nature 436, 881-881.

Glaser, B., Balashov, E., Haumaier, L., Guggenberger, G., Zech, W., 2000. Black carbon in density fractions of anthropogenic soils of the Brazilian Amazon region. Organic Geochemistry 31, 669-678.

Glaser, B., Lehmann, J., Zech, W., 2002. Ameliorating physical and chemical properties of highly weathered soils in the tropics with charcoal - a review. Biology and Fertility of Soils 35, 219-230.

Hamer, U., Marschner, B., Brodowski, S., Amelung, W., 2004. Interactive priming of black carbon and glucose mineralisation. Organic Geochemistry 35, 823-830.

Hilscher, A., Heister, K., Siewert, C., Knicker, H., 2009. Mineralisation and structural changes during the initial phase of microbial degradation of pyrogenic plant residues in soil. Organic Geochemistry 40, 332-342.

Hilscher, A., Knicker, H., 2011. Degradation of grass-derived pyrogenic organic material, transport of the residues within a soil column and distribution in soil organic matter fractions during a 28 month microcosm experiment. Organic Geochemistry 42, 42-54.

Jones, D.L., Murphy, D.V., Khalid, M., Ahmad, W., Edwards-Jones, G., DeLuca, T.H., 2011. Short-term biochar-induced increase in soil CO_2 release is both biotically and abiotically mediated. Soil Biology & Biochemistry 43, 1723-1731.

Keiluweit, M., Nico, P.S., Johnson, M.G., Kleber, M., 2010. Dynamic molecular structure of plant biomass-derived black carbon (biochar). Environmental Science & Technology 44, 1247-1253.

Keith, A., Singh, B., Singh, B.P., 2011. Interactive priming of biochar and labile organic matter mineralisation in a smectite-rich soil. Environmental Science & Technology 45, 9611-9618.

Kuzyakov, Y., Subbotina, I., Chen, H.Q., Bogomolova, I., Xu, X.L., 2009. Black carbon decomposition and incorporation into soil microbial biomass estimated by ^{14}C labeling. Soil Biology & Biochemistry 41, 210-219.

Lehmann, J., Gaunt, J., Rondon, M., 2006. Bio-char sequestration in terrestrial ecosystems–a review. Mitigation and Adaptation Strategies for Global Change 11, 403-427.

Lehmann, J., Joseph, S., 2009. Biochar for environmental management: Science and technology. Earthscan, London.

Lehmann, J., Liang, B.Q., Solomon, D., Lerotic, M., Luizao, F., Kinyangi, J., Schafer, T., Wirick, S., Jacobsen, C., 2005. Near-edge X-ray absorption fine structure (NEXAFS) spectroscopy for mapping nano-scale distribution of organic carbon forms in soil: Application to black carbon particles. Global Biogeochemical Cycles 19, GB1013. doi 10.1029/2004gb002435.

Lehmann, J., Rondon, M., 2006. Bio-char soil management on highly weathered soils in the humid tropics. Biological Approaches to Sustainable Soil Systems 113, 517-530.

Liang, B., Lehmann, J., Solomon, D., Kinyangi, J., Grossman, J., O'Neill, B., Skjemstad, J.O., Thies, J., Luizao, F.J., Petersen, J., Neves, E.G., 2006. Black carbon increases cation exchange capacity in soils. Soil Science Society of America Journal 70, 1719-1730.

Liang, B.Q., Lehmann, J., Sohi, S.P., Thies, J.E., O'Neill, B., Trujillo, L., Gaunt, J., Solomon, D., Grossman, J., Neves, E.G., Luizão, F.J., 2010. Black carbon affects the cycling of non-black carbon in soil. Organic Geochemistry 41, 206-213.

Lin, Y., Munroe, P., Joseph, S., Henderson, R., Ziolkowski, A., 2012a. Water extractable organic carbon in untreated and chemical treated biochars. Chemosphere 87, 151-157.

Lin, Y., Munroe, P., Joseph, S., Kimber, S., Van Zwieten, L., 2012b. Nanoscale organo-mineral reactions of biochars in ferrosol: an investigation using microscopy. Plant and Soil, 369-380.

Liski, J., Ilvesniemi, H., Makela, A., Westman, C.J., 1999. CO_2 emissions from soil in response to climatic warming are overestimated - The decomposition of old soil organic matter is tolerant of temperature. Ambio 28, 171-174.

Luo, Y., Durenkamp, M., De Nobili, M., Lin, Q., Brookes, P.C., 2011. Short term soil priming effects and the mineralisation of biochar following its incorporation to soils of different pH. Soil Biology & Biochemistry 43, 2304-2314.

McBeath, A.V., Smernik, R.J., 2009. Variation in the degree of aromatic condensation of chars. Organic Geochemistry 40, 1161-1168.

Mikutta, R., Kleber, M., Torn, M.S., Jahn, R., 2006. Stabilization of soil organic matter: Association with minerals or chemical recalcitrance? Biogeochemistry 77, 25-56.

Nguyen, B.T., Lehmann, J., Hockaday, W.C., Joseph, S., Masiello, C.A., 2010. Temperature sensitivity of black carbon decomposition and oxidation. Environmental Science & Technology 44, 3324-3331.

Nguyen, B.T., Lehmann, J., Kinyangi, J., Smernik, R., Riha, S.J., Engelhard, M.H., 2009. Long-term black carbon dynamics in cultivated soil. Biogeochemistry 92, 163-176.

Torn, M.S., Trumbore, S.E., Chadwick, O.A., Vitousek, P.M., Hendricks, D.M., 1997. Mineral control of soil organic carbon storage and turnover. Nature 389, 170-173.

Van Zwieten, L., Kimber, S., Morris, S., Chan, K.Y., Downie, A., Rust, J., Joseph, S., Cowie, A., 2010. Effects of biochar from slow pyrolysis of papermill waste on agronomic performance and soil fertility. Plant and Soil 327, 235-246.

Wardle, D.A., Nilsson, M.C., Zackrisson, O., 2008. Fire-derived charcoal causes loss of forest humus. Science 320, 629-629.

Yuan, J.H., Xu, R.K., Zhang, H., 2011. The forms of alkalis in the biochar produced from crop residues at different temperatures. Bioresource Technology 102, 3488-3497.

Zimmerman, A.R., Gao, B., Ahn, M.Y., 2011. Positive and negative carbon mineralization priming effects among a variety of biochar-amended soils. Soil Biology & Biochemistry 43, 1169-1179.

Zimmermann, M., Bird, M.I., Wurster, C., Saiz, G., Goodrick, L., Barta, J., Capek, P., Santruckova, H., Smernik, R., 2012. Rapid degradation of pyrogenic carbon. Global Change Biology 18, 3306–3316.

Chapter 2: Literature review

2.1. Introduction

Black carbon (BC) contributes to the Earth's slow-cycling carbon pools (Baldock and Smernik, 2002; Lehmann et al., 2006). Estimates suggest that 0.05 to 0.2 Tg (10^9 t) of BC is annually produced and stored in soil (Kuhlbusch, 1998). It can constitute 35% of soil organic carbon (SOC) in German arable soils (Brodowski et al., 2007), 9% in the grassland soils along a climosequence in North America (Glaser and Amelung, 2003), and 30% in Australian soils (Skjemstad et al., 1996). Amazonian Dark Earths (so called "*Terra preta*") are anthropogenic soils that were created by the addition of charcoal, bone and manure to infertile soil between 500 and 2500 years ago. Black carbon constitutes significant amounts of C stocks even several thousand years after they were abandoned (Glaser et al., 2001). Moreover, BC has been reported to be the oldest fraction of C in soils, with mean residence times (MRTs) of several thousand years (Gavin et al., 2003; Lehmann et al., 2009). Consequently, BC seems to be both a large and inert soil organic C pool.

Biochar is considered functionally identical to BC and is obtained from the thermochemical conversion of biomass in an oxygen-limited environment (IBI, 2012). Lehmann (2007) suggested that the application of biochar to soil can lead to the sequestration of about 20% of the net photosynthesis C withdrawal from the atmosphere to soil. Therefore, biochar may offer an opportunity to store biomass C in soil in relatively stable forms and potentially offset the CO_2 emission by humans. Furthermore, when biochar is added to soil, there are secondary benefits of improved nutrient contents, nutrient retention capacity and crop yields (Mukherjee and Zimmerman, 2013; Van Zwieten et al., 2010). Also, biochar can improve soil quality by increasing cation exchange capacities (Glaser et al., 2002), water retention and aeration of soils (Case et al., 2012), microbial functions (Steinbeiss et al., 2009), and reducing aluminium availability (Chan and Xu, 2009).

Considering biochar as a potential soil amendment for long-term C storage, it is important to understand its turnover rate and stability (estimated by mean residence time, MRT) in different soils and environments. This chapter will present the current

knowledge of biochar molecular structure, its production conditions and their relationship with biochar-C stability. In order to understand biochar-C stability, I have summarised a table to compare biochar-C mineralisation that has been measured under laboratory conditions and its MRT as estimated by various means or modelling approaches. This chapter will also present the current knowledge of factors that influence biochar-C stability in soil, including soil minerals and soil temperature. Biochar and soil organic carbon (SOC) mineralisation may also be changed by the addition of biochar to soil, including in the presence of labile organic matter with implications for its C sequestration potential. In this chapter, I will also present the interactive effect of biochar and soil organic carbon (SOC) mineralization, including with added labile organic matter, and the possible mechanisms.

2.2. Biochar molecular structure and production conditions

2.2.1. Definition

Black carbon (BC) is produced by incomplete combustion of fossil fuels and vegetation (Goldberg, 1985). Black carbon can be best described with the combustion continuum model (**Figure 2.1**) (Masiello, 2004). The BC continuum contains different charred residues, ranging from slightly charred biomass, char, charcoal, and highly condensed refractory soot (Glaser et al., 2001; Masiello, 2004). Black carbon has a high C content, is chemically heterogeneous, and dominated by aromatic structures (Masiello, 2004). Biomass forms aromatic ring structures, and then a progressive condensation of smaller aromatic units into larger conjugated sheets (**Figure 2.2**) (Schmidt and Noack, 2000). Recently, biochar has been called BC (Hamer et al., 2004; Nguyen and Lehmann, 2009), or pyrogenic carbon (Hilscher and Knicker, 2011a), produced by humans for soil improvement and C sequestration purposes (Lehmann, 2007; Spokas et al., 2012). Biochar is a solid elemental carbonaceous material obtained from the thermochemical conversion of biomass in an oxygen-limited environment (IBI, 2012). But BC may also specifically refer to charcoal produced through artificial or natural burning process in terrestrial ecosystems.

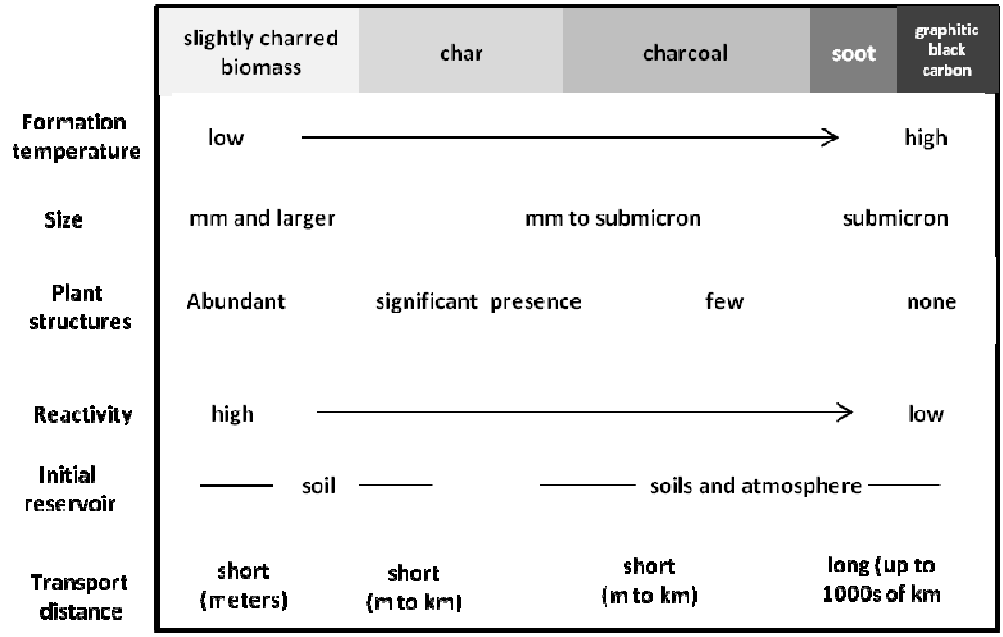

Figure 2.1. The black carbon combustion continuum (adapted from Masiello, (2004)).

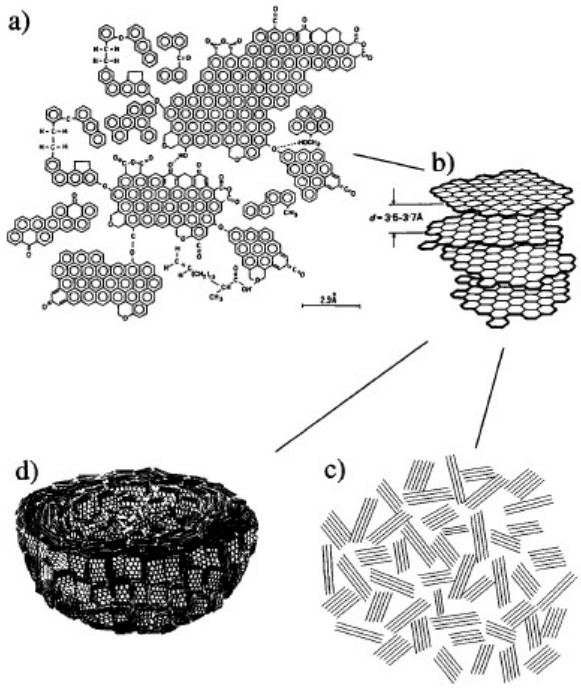

Figure 2.2. Black carbon basic structural units and two principal structures. (a) Basic structure of BC, forms (b) units of three to four layers. (c) Randomly oriented basic structural units. (d) Onion-type particle with several condensation seeds (Schmidt and Noack, 2000).

2.2.2. Biochar molecular structures and H/C ratio change with temperature

Keiluweit et al. (2010) developed a model of the molecular structure of biochar with charring temperature (**Figure 2.3**). At intial charring stage, the native structure of plant material remains preserved. With increasing charring temperature, the initial stage is followed by the formation of volatile dissociation products and phenols (transition char), and aliphatic and aromatic (amorphous char) (**Figure 2.3**). The degree of aromaticity of biochar increases with increasing charring temperature (Czimczik et al., 2002; Ghani et al., 2013; McBeath and Smernik, 2009). For example, Nguyen et al. (2010) evidenced 5−15% more C in aromatic rings when charring temperature increased from 350 to 600 °C, protonated aromatic C increased by 43−57%, and aromatic bridgehead C by 39%. Similarly, based on the solid state ^{13}C DP NMR analysis, McBeath et al. (2011) found that the proportion of aromatic C of biochar increases abruptly from 14% at 200 °C to 88% at 350 °C, and aromaticity of biochar produced at charring temperatures higher than 400°C was found to be > 90%. At high charring temperatures, the degree of aromatic condensation is relatively high and long-range order turbostratic crystallites are formed (**Figure 2.3**). The volatile matter (i.e. non-aromatic and aliphatic) in biochar decreases with increasing temperature.

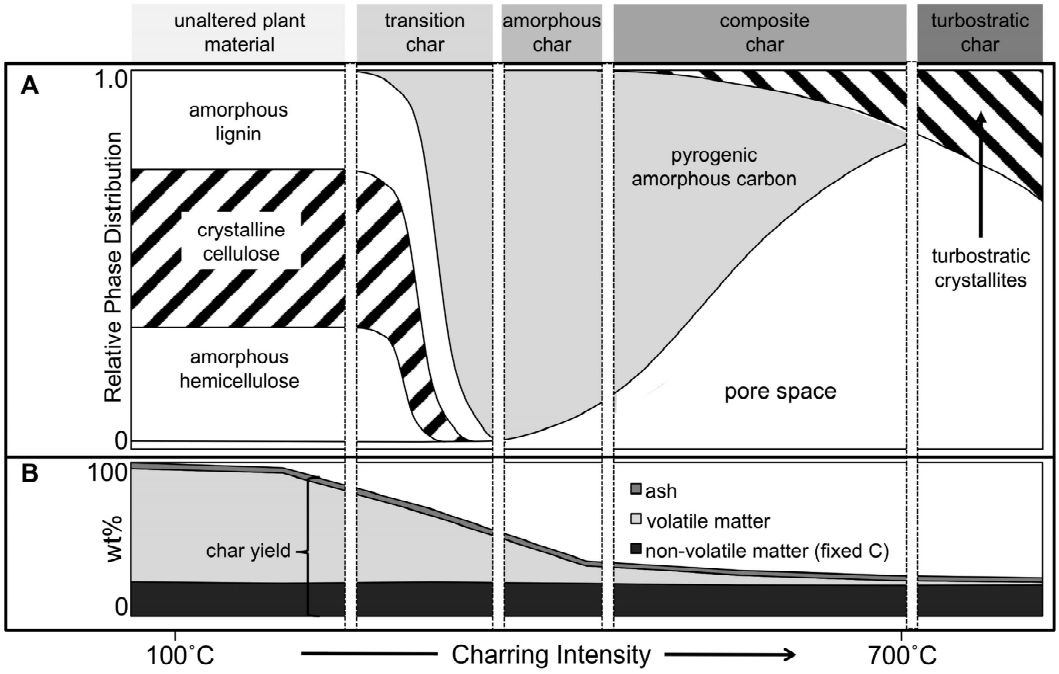

Figure 2.3. Dynamic molecular structure of plant biomass-derived black carbon (biochar) across a charring temperature gradient (Keiluweit et al., 2010).

The degree of condensation of aromatic rings in biochars varies depending on biomass feedstock (Keiluweit et al., 2010; Smernik et al., 2006). The molar H/C and O/C ratios of biochar are negatively correlated with aromaticity and degree of aromatic condensation (Pereira et al., 2011; Schimmelpfennig and Glaser, 2012). Since aromaticity increases with temperature (McBeath et al. 2011), so H/C and O/C ratios will decrease with increasing temperature (Crombie et al., 2013; Keiluweit et al., 2010) and may indicate condensed aromatic structures (Preston and Schmidt, 2006). According to the International Biochar Initiative (2012), a H/C_{org} ratio below 0.7 can be distinguished as biochar that has been thermochemically altered from the unaltered biomass (**Figure 2.4**). This biochar has a greater proportion of fused aromatic ring structures when the H/C_{org} ratio is below 0.7. The ratio of H/C has been proposed to identify whether biochar has been thermochemically altered to recalcitrant C forms and hence could be used for long-term C sequestration purposes. However, it is under debate whether the limit of less than 0.7 proposed by IBI is appropriate for evaluating biochar-C sequestration potential. For example, Schimmelpfennig and Glaser (2012) recommended that biochar is suitable for C sequestration when the H/C and O/C ratios are less than 0.6 and 0.4, respectively.

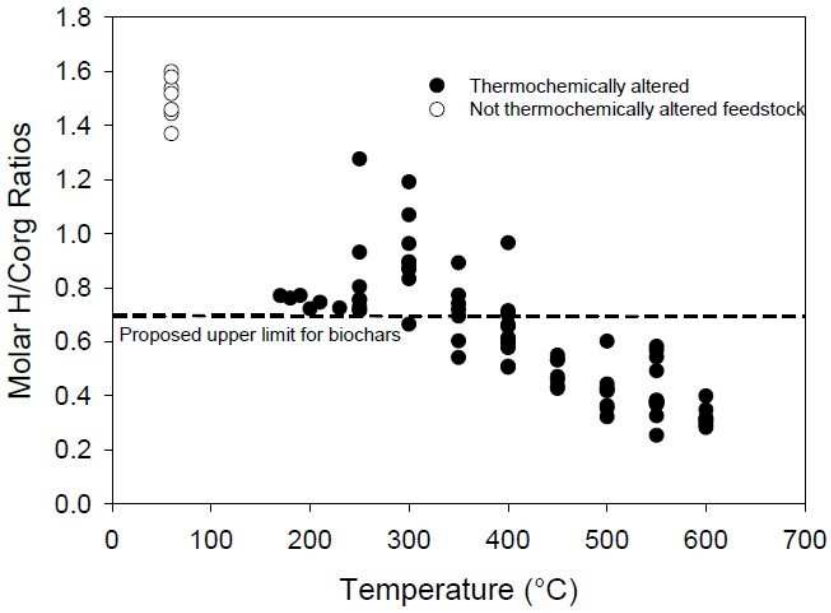

Figure 2.4. Relationship between molar H/Corg ratio and temperature of themochemically altered organic matter in comparison to untreated biomass (IBI, 2012).

Aromatic structure from different biomass sources (parent materials) can be different. Knicker et al. (2008) found that a significant amount of nitrogen (N) in grass leads to char consisting of N-heteroaromatic C with an average cluster size of the aromatic units smaller than six rings. Additionally, smaller rings would have considerable N, O and S substitutions, thus making them more easily amenable to biological and chemical oxidation than larger clusters with limited N, O and S substitutions (Knicker et al., 2008). However, when pyrolysis temperature is high, i.e. 550−600 °C, biochar derived from different materials (wood, corn and manure) would have more fused aromatic structures (Singh et al., 2012; Sun et al., 2012), thus narrowing down biochar-C stability differences between biochars produced from different feedstocks (Singh et al. 2012).

2.2.3. Molecular structure change with ageing

The molecular structure of biochar may change after incubation (Hilscher and Knicker, 2011a; Nguyen et al., 2009). The spatial analysis of a BC particle by near-edge X-ray absorption fine structure (NEXAFS) spectroscopic analysis indicated a significant surface oxidation of BC with a reduction of aromatic C and an increase of carboxylic C (Lehmann et al., 2005). Hilscher and Knicker (2011a) also found that the proportion of O-containing functional groups (such as carboxyl and carbonyl)

increased with the ageing of char in soil, leading to an increase in O/C ratio (Cheng et al., 2008a). High temperature can accelerate the oxidation process, i.e. the O/C ratios were evidenced to increase with increasing temperature (Nguyen et al., 2010). Other BC characteristics may also change with ageing. For example, compared to fresh biochar, aged BC has higher surface acidity and negative surface charge, but lower pH, surface basicity, and adsorption capacity of organic matter such as hydroquinone (Cheng and Lehmann, 2009; Cheng et al., 2008a).

2.3. Biochar-C stability

In general, biochar is not easily amenable to chemical and biological decomposition, and may be more stable than other organic matter forms in soil. The term 'stability' here refers to biochar's resistance to loss via degradation or mineralisation, with higher stability translating to a longer mean residence time (MRT). Biochar-C degradation or mineralisation can be monitored by measuring biochar-derived CO_2 emissions and then estimating biochar MRT from fitting models to the CO_2 emission kinetics data (Kuzyakov et al., 2009; Singh et al., 2012; Zimmerman, 2010). Due to relatively high chemical recalcitrance of biochar-C, it takes a reasonable duration of time to detect biochar-C mineralisation. Moreover, by utilising C isotopes, biochar-C mineralisation can be distinguished from mineralisation of SOC. Biochar-C stability may also be predicted by measuring O/C or H/C molar ratios (Schimmelpfennig and Glaser, 2012; Spokas, 2010), as discussed in the previous section. Additionally, Cross and Sohi (2013) proposed that biochar-C stability could be determined from accelerated biochar ageing induced by chemical oxidation.

2.3.1. Incubation studies of biochar-C mineralisation

In recent years, there have been a large number of incubation studies investigating biochar-C stability, and the results from these studies are summarised in **Table 2.1**. In these studies, biochars were incubated alone or mixed with sand/soil medium in closed chambers with a CO_2 trap, maintaining soil moisture to 50~70% water holding capacity, keeping temperatures between 20 and 32 °C, and then the total CO_2 emissions were measured over a certain time period. The results show that biochar-C mineralisation in soils varies widely in different studies, ranging from 0.5−8.9% (in a Vertisol over 5 years) (Singh et al., 2012), 4.5% (in a sandy-loamy soil over 3.2

years) (Kuzyakov et al., 2009), 0.4−3% (in a sand over 1-year) (Zimmerman, 2010), to 6−21% (in a sand over 1-year) (Nguyen and Lehmann, 2009).

Some studies of biochar or BC stability were conducted in a sandy medium or in a soil without quantifying the source of C mineralised. However, the stability of biochar in sand and soil may be different since biochar can be degraded by both biotic and abiotic processes. Other recent studies have been used ^{13}C / ^{14}C labelled biochars to distinguish between the mineralisation of biochar-C and native SOC (**Table 2.1**). Moreover, since the biochar added to the soil is isotopically distinct from native SOC, any decreases or increases in native SOC mineralisation due to biochar can be quantified, and priming effect can be determined (Keith et al., 2011; Zimmerman et al., 2011). The priming effects of biochar on SOC mineralisation will be discussed separately.

2.3.2. The influence of production condition and feedstock type on biochar-C stability

The mineralisation of biochar-C varies depending on its production condition and feedstock type (**Table 2.1**) due to their influence on the C forms in biochar e.g. low molecular weight organics, and aliphatic and aromatic structures (Keiluweit et al., 2010; Lin et al., 2012; McBeath et al., 2011).

Generally, biochar-C stability increases with increasing charring or pyrolysis temperature (Bruun et al., 2008; Zimmerman et al., 2011). For example, Nguyen et al. (2010) found greater C mineralised in the 350 °C than the 600 °C biochar after 1-year. Keith et al. (2011) also reported that the C mineralisation of eucalyptus biochar produced at 450 °C was 1.5−1.9 times greater than that of the biochar produced at 550 °C when the two biochars were incubated in a Vertisol in the absence and presence of sugarcane residue. As the production temperature for biochar increases, the aromaticity and the degree of aromatic condensation increase (Ghani et al., 2013; McBeath and Smernik, 2009; Schmidt and Noack, 2000), and the fraction of aliphatic C decreases (McBeath and Smernik, 2009).

Singh et al. (2012) reported that biochar-C was mineralised faster in the manure-based biochars than the plant-based biochars. Nguyen et al. (2010) found the oak-derived biochar was more stable than corn-derived biochar. Furthermore, biochars produced from woody biomass are more stable than those produced from

grasses (Hilscher et al., 2009; Zimmerman, 2010). A molecular study by NMR clearly showed that wood-derived biochar has more aromatic C component than other biomass-derived biochars, such as leaves and poultry litter (McBeath and Smernik, 2009; Singh et al., 2012). However, the difference in molecular structure may decrease when they were produced at a high temperature, e.g. similar fused aromatic ring cluster size were found in wood and corn-derived biochars produced at 600 °C (Sun et al., 2012).

Clearly, biochar production temperature and feedstock source are the two major determinants of biochar properties (Singh et al., 2010), including its C stability (Singh et al., 2012; Zimmerman, 2010). Nevertheless, biochar-C stability may also be influenced by soil type and incubation temperature. Biochar was found to be incorporated in organo-mineral fractions in a mineral soil after a short period of one-month (Hilscher and Knicker, 2011b), this could protect biochar from microbial degradation. The fast association of biochar with mineral soil suggests that the influence of soil properties, particularly clay mineral content and composition, need to be considered on biochar stability. The influence of soil-biochar interaction on biochar-C stability will be discussed in the next section. Biochar-C mineralisation by biotic and abiotic processes may increase with increasing temperature (Cheng et al., 2006; Knicker et al., 2013; Zimmerman, 2010). Other factors, such as the heating rate, residence time at highest heating temperature (HHT) and feedstock particle size can also alter the chemical composition and physical stucture of a biochar (McBeath and Smernik, 2009; Sun et al., 2012; Zimmerman, 2010), consequently influence its stability in the soil.

2.3.3. Biochar-C stability as influenced by biotic and abiotic processes

Biochar or BC can be slowly oxidised or mineralised by biotic and abiotic processes (Cheng et al., 2006; Zimmerman, 2010; Zimmermann et al., 2012). Zimmerman (2010) reported that biochar-C mineralisation in a microbial inoculated sand medium was 1.1−2.0 fold greater than that of the abiotic incubations. Some studies have reported that BC decomposition was enhanced by co-metabolic reactions where added labile C served as a C and energy source for microorganisms, therefore increasing microbial activity and enhancing the decomposition rate of biochar or BC

in soils (e.g. Hamer et al. 2004; Kuzyakov et al. 2009; Keith et al. 2011). Furthermore, aromatic C in biochar was found to be degraded by 9−12% during a 7-month incubation study and the authors hypothesised that this was related to the growth of microbial community which can utilise the aromatic core of pyrogenic organic matter as a C and energy source (Knicker et al., 2013). Similarly, 'aromatic transformation' enzymes (phenoloxidases and peroxidises) were found to be active at degrading aromatic rings in biochar (Zimmermann et al., 2012).

Biochar-C mineralisation may increase at well aerated conditions due to the increased soil microbial activities. Nguyen and Lehmann (2009) found a significantly higher biochar-C loss under altering saturated and unsaturated conditions than under saturated conditions, and the difference in C loss between different soil moisture conditions is possibly related to availability of oxygen (Nguyen and Lehmann, 2009). Knoblauch et al. (2011) reported that 5.9 and 8.5% of the biochar derived from rice husk was mineralised under anaerobic and aerobic conditions, when the biochar was incubated with Typha-marsh soil. In Mollisols, Glaser and Amelung (2003) found that at a given temperature regime, the wetter sites accumulated more charcoal than the drier sites.

The studies of biochar properties showed that biochar oxidation occurs over a wide range of temperatures (e.g. -22 °C to 70 °C) (Cheng and Lehmann, 2009; Zimmermann et al., 2012). Abiotic oxidation of biochar was reported to increase with increasing temperature from -22 °C to 70 °C (Cheng and Lehmann, 2009). The reported oxidation of biochar surface due to abiotic and biotic process may vary in different studies. For example, Cheng et al. (2006) found the biochar surface oxidation was mainly contributed to abiotic process at 30 °C instead of biotic process. By comparison, Zimmermann et al. (2012) reported that only 29−35% of biochar-C mineraliation was caused by abiotic process at 30 °C, and the rest was attributed to biotic mineralisation process. The temperature variations can affect microbial activities (Zimmermann et al. 2012), therefore biochar-C mineralisation. Additionally, the contributions of biotic mineralisation relative to abiotic mineralisation decreases with increasing incubation temperature from 30 to 60 °C for young biochar (Zimmermann et al., 2012). The effect of temperature on biochar-C stability will be further discussed in Section 2.6.

Table 2.1. A summary of biochar or BC mineralisation and mean residence time (MRT) data reported in recent published studies.

Biochar or BC type	Experiment	Medium	Biochar or BC mineralised	Model	MRT	Reference
Woody and grass derived biochar produced at 250, 400, 525 or 650 °C	1-year laboratory incubation, 32 °C	Pure sand	0.4−3%	Power model	1.4×10^{2}−1.4×10^{7} years	Zimmerman (2010)
Two biochar pyrolysed at 350 or 700 °C	180 days laboratory incubation, 25 °C	Aquic Paleudalf	0.1−0.8%	−	−	Luo et al. (2011)
Corn and oak derived biochar produced at 350 or 600 °C	1-year laboratory incubation, 30 °C	Pure sand	6−21%	−	−	Nguyen and Lehmann (2009)
Aged black carbon with SOC	177 days laboratory incubation, 30 °C	A range of soils	−	Single-pool exponential model	115 years	Cheng et al. (2008b)
Natural BC with SOC	532 days laboratory incubation, 30 °C	Anthrosol (developed on Oxisols, Ultisols, or Spodosols)	2.8−3.3%	Two-pool exponential model	44−52 years (BC rich soil)	Liang et al. (2008)
Carbonised rice husks	2.9-year laboratory incubation, 28 °C	Typic fluvaquents and Aquic udifluvents	4.4−8.5%	Single-pool exponential model	34.1−66.2 years	Knoblauch et al. (2011)
Maize and straw derived biochars (350°C), and woody biochar (800 °C)	60 days laboratory incubation, 20 °C	Haplic Phaeozem	0.3−1.2%	Two-pool exponential model	39−76 years	Hamer et al. (2004)
Charred plant residue (250 °C)	280 days laboratory incubation, 25 °C	Volcanic ash soil	Not detected	−	−	Shindo (1991)
Charred plant residue produced at 350 °C under oxic conditions	28-month laboratory incubation, 30 °C	Cambisol	35−38% loss	Two-pool exponential model	3−5 years	Hilscher and Knicker (2011b)

Biochar or BC type	Experiment	Medium	Biochar or BC mineralised	Model	MRT	Reference
^{14}C labelled grass biochar (400 °C)	3.2-year laboratory incubation, 20 °C	Haplic Luvisol	3.8−4.5%	Single-pool exponential model	200 years	Kuzyakov et al. (2009)
^{13}C labelled biochars (made from plant, manure, papermill sludge) pyrolysed at 400 or 550 °C	A long-term 5-year laboratory incubation, 20 °C	Vertisol	0.5−8.9%	Two-pool exponential model	90−1600 years	Singh et al. (2012)
^{13}C labelled woody biochar produced at 450 or 550 °C	120 days laboratory incubation, 20 °C	Vertisol	0.14−1.1%	Two-pool exponential model	62−428 years	Keith et al. (2011)
^{13}C labelled woody biochar (450 °C)	6-month laboratory incubation, 25 °C	Haploxeralfs	0.37−0.41%	Two-pool exponential model	389−605 years	(Santos et al., 2012)
^{13}C labelled wheat and eucalypt shoot biochars produced at 450 °C	74 days laboratory incubation, 25/12 °C	Arenosol (FAO WRB)	0.24−0.30%	Two-pool exponential model, with an asymptote	−	Farrell et al. (2013)
^{13}C labelled woody biochar using the traditional mound kiln technique	2-year field study	Oxisol	~2.2%	Two-pool exponential model	600 years	Major et al. (2010a)
BC collected after natural fire (1 and 11 years)	6-month laboratory incubation, variable temperatures (20–50 °C)	Over glass beads	1.5% per year	Single-pool exponential model, Arrhenius function	67 years	Zimmermann et al. (2012)
Woody and grass derived biochar produced at 250 or 650 °C	1-year laboratory incubation, 32 °C	Pure sand	0.2−2.4%	Two-pool exponential model	78−74921 years	Zimmerman and Gao (2013)

2.4. Biochar mean residence time

Biochar is relatively recalcitrant form of C compared to other organic C forms that exist in the soils. **Table 2.1** shows the estimated mean residence time (MRT) of biochars in recent studies. The MRT of biochar or BC ranged from decadal to century timescales (Bird et al., 1999; Hilscher and Knicker, 2011b; Liang et al., 2008; Singh et al., 2012; Zimmermann et al., 2012). The variable MRTs may be because of the variations in biochar type, incubation medium and different models employed to estimate MRT in different studies.

Various models used to estimate biochar MRT are given below.

(i) Single-pool exponential model (Cheng et al., 2008b; Singh et al., 2011):

$$C_{Bt} = C \times \left(1 - e^{-kt}\right) \quad (2.1)$$

where C_{Bt} is the cumulative biochar-C mineralised at time (t); C represents the amount of "potential" mineralisable biochar-C; k is the mineralisation rate constant for potential C mineralisation.

(ii) Two-pool exponential model (Hamer et al., 2004):

$$C_{Bt} = C_L \times \left(1 - e^{-k_L t}\right) + (100 - C_L) \times (1 - e^{-k_R t}) \quad (2.2)$$

where C_{Bt} is the cumulative of added biochar-C mineralised at time (t); C_L and $(100-C_L)$ are the proportions of labile (easily-mineralisable) and recalcitrant (slowly-mineralisable) pools in biochar-C, respectively; k_L and k_R are the mineralisation rate constants for the labile and recalcitrant C pools, respectively. MRT of labile and recalcitrant C pools are the inverse of rate constants.

(iii) Power model (Zimmerman 2010; Zimmerman and Gao, 2013):

$$\frac{dC}{dt} = -C_0 e^b t^m \quad (2.3)$$

$$C_{lost} = C_0 - C_t = \left(\frac{C_0 e^b}{m+1}\right) t^{m+1} \quad (2.4)$$

$$C_{t_{1/2}} = \left(\frac{m+1}{2e^b}\right)^{\left(\frac{1}{m+1}\right)} \quad (2.5)$$

$$MRT = \frac{C_{t_{1/2}}}{Ln\,(2)} \quad (2.6)$$

Where C_0 is initial biochar-C amount; Ct is biochar-C amount at time (t); m and b are the slope and intercept, respectively; $C_{t_{1/2}}$ is the half-life of biochar.

Exponential decay models have been widely used to model the dynamics of soil C mineralisation. The one-pool exponential model (Equation 2.1) assumes C as a homogeneous or a single pool. The two-pool exponential model (Equation 2.2) assumes that C in a substrate is made up of two group of organic constituents; one is relatively labile and degrades at a rapid rate, and the other is relatively recalcitrant, degrades slowly. Singh et al. (2011) used the one-pool exponential model to estimate the MRT of BC using data from several published studies, and reported MRT ranging from 4−109 years in soils and 2−181 years in sands. The two-pool exponential model has been used to fit biochar-C mineralisation data to estimate MRT of biochars in several recent studies (Keith et al., 2011; Santos et al., 2012; Singh et al., 2012). Kätterer et al. (1998) used both one-pool and two-pool exponential models to fit the soil C mineralisation data from a wide range of incubation experiments with varying soil types under different climates and found the two-pool exponential model to be more suitable than the one-pool exponential model in describing and fitting the C mineralisation dynamics. Although similar proportions of the added biochar-C were mineralised in one year, much higher MRTs were reported in Zimmerman's (2010) study (ranged between 1.4×10^2 and 1.4×10^7 years, estimated from Equation 2.3, 2.4 2.5 and 2.6) compared to other studies (Kuzyakov et al., 2009; Major et al., 2010b; Singh et al., 2012). This large difference in the estimates of MRT between Zimmerman's (2010) study and other studies can be attributed to the use of power model (Equations 2.3, 2.4 and 2.5) versus the exponential model. The power model assumes infinite C pools in a substrate (i.e. biochar) with increasing slow degradation rates along a degradation continuum (Zimmerman 2010). Future research needs to identify which model can predict MRT more precisely.

Furthermore, duration of incubation, i.e. short-term (weeks to months) to long-term (years) may also result in differences in the estimated MRT of biochar (Keith et al., 2011; Singh et al., 2012). Short-term studies capture mainly the mineralisation of more labile biochar-C fraction, and hence underestimate biochar

MRT. Therefore, longer-term incubations (i.e. two years or more) are needed to obtain realistic estimates of biochar-C stability (Singh et al. 2012).

2.5. Biochar–soil interaction in relation to biochar-C stability

There have been a number of recent publications investigating the stabilisation mechanisms of biochar in soils (Czimczik and Masiello, 2007; Knicker, 2011; Lehmann et al., 2009). Biochar is considered to be stabilised by the following mechanisms: (i) chemical or molecular recalcitrance of C in the biochar structure, (ii) interactions with soil minerals, or (iii) occlusion within soil aggregates. Biochar chemical recalcitrance is related to its high aromaticity and degree of aromatic condensation (see sections 2.2 and 2.3; Hilscher et al., 2009; Keiluweit et al., 2010; Singh et al., 2012). Also, BC was found to be associated with plaques of Fe and Al oxides on mineral surfaces (Glaser et al., 2000; Lin et al., 2012). The highest BC and soil organic C is generally found in heavy density fraction and clay-associated organic fraction (Brodowski et al., 2007; Brodowski et al., 2006). The stabilisation of BC could be due to the reaction of its surface oxygen functional groups, i.e. carboxyl and aromatic functional groups, with soil minerals (Lehmann et al., 2005; Lin et al., 2012). However, there are very few studies about the role of biochar-mineral interactions, particularly clay content and composition, and other properties of soil (such as native C content) in influencing biochar-C stability.

There are other mechanisms of interactions of organic matter or biochar with different minerals. In a smectite-rich soil, alkyl C can be intercalated into smectites in a flat extended conformation in an acid environment, which enables van der Waals interactions to be established between clay and polymer (Baldock et al., 1997; Theng et al., 1986). Mollisols and "*Terra preta*", both have high BC concentration (Glaser and Amelung, 2003; Glaser et al., 2001), which could also be attributed to bonding of anionic organic functional groups with the negatively charged clay surfaces and aided by cation bridges in the presence of calcium (Czimczik and Masiello, 2007; Muneer and Oades, 1989; Theng et al., 1986).

Thus, organo-mineral interactions play an important role in physically and chemically protecting BC or biochar from mineralisation. Furthermore, the multitude of organo-mineral interactions may lead to the formation of water-stable aggregates (Tisdall and Oades, 1982), which not only physically protect soil organic matter and

biochar, but also reduces their accessibility to microorganisms and their enzymes (Six et al., 2004). Various experiments were conducted as a part of this thesis enhancing our understanding of the role of these soil properties in altering biochar-C mineralisation and stability in soils (see Chapters 3, 4 and 7).

2.6. Incubation temperature effect on biochar-C stability

Incubation temperature may also affect biochar-C mineralisation. For example, Nguyen (2010) reported biochar-C loss increased from 1.5−10% at 4 °C to 14−20% at 60 °C after one-year incubation across corn and oak derived biochar produced at 350°C or 600°C. Similarly, Cheng et al. (2008b) observed that the decomposition of charcoal was greater at high than low mean annual temperature (MAT). Cheng et al. (2008a) found a significant positive relationship between MAT and oxidation (O/C ratio) of charcoal collected from historical furnace sites. In tropical environments the longevity of BC in soils has been reported in the range of decadal timescales (Bird et al., 1999; Zimmermann et al., 2012). By contrast, due to the colder temperature in European chernozems soils, BC longevity was reported in several millennia (1160–5040 years) of radiocarbon age (Schmidt et al., 2002).

The temperature sensitivity of soil C mineralisation, referred to Q_{10}, is defined as the rate of increase in soil CO_2 emission with a 10 °C increase in temperature (Kirschbaum, 1995). It is an important parameter to evaluate the feedback intensity between CO_2 emission and global warming (Luo et al., 2001; Zhou et al., 2009). Since biochar has been advocated as a soil amendment for long-term C squestration across different agro-climatic regions, it is important to understand the temperature sensitivity of biochar decomposition in response to increasing temperature or climate warming. However, there are very few studies on the sensitivity of biochar-C decomposition to temperature change in soil environments. Nguyen et al. (2010) esimated the Q_{10} of corn and oak derived biochars when they were incubated in pure sand; the Q_{10} values ranged between 1.6 and 5.8 at 4−10 °C, and between 1 and 1.8 at 10−60 °C, with higher values for relatively recalcitrant biochars and vice-versa. Similarly, Zimmermann et al. (2012) reported a decrease of biochar Q_{10} values from 1.73 at 20°C to 1.53 at 60°C.

According to the kinetics of enzymatic theory, activation energies are related to the ambient temperature and to the molecular structure of organic C (Davidson and

Janssens, 2006). Biochar contains low-quality organic C fractions, which may have inherently low reactivity and require high activation energy for decomposition, and hence possess greater temperature sensitivity than other C fractions in soil (Davidson and Janssens, 2006). Consistent with the theory, a lot of studies on SOC temperature sensitivity have shown a higher temperature sensitivity for old or stable C than labile C (Bol et al., 2003; Conant et al., 2008a; Conant et al., 2008b; Craine et al., 2010; Fierer et al., 2005; Knorr et al., 2005; Leifeld and Fuhrer, 2005; Vanhala et al., 2007). But the opposite findings also exist, e.g., no difference in the temperature sensitivity between different SOC fractions or pools (Fang et al., 2005; Giardina and Ryan, 2000), or lower temperature sensitivity for old SOC (Liski et al., 1999). Davidson and Janssens (2006) summarised the possible reasons of conflicting temperature sensitivity results for different soil organic C pools. They suggested the factors that influence the temperature sensitivity of soil organic C include the chemical structure of C fractions, incubation temparature, clay mineralogy and soil aggregation. For example, organo-mineral interaction and physical occlusion of C in the interior of soil aggregate can protect C mineralisation in soil, therefore, decreasing the temperature sensitivity of soil C. Although there are a lot of studies on the temperature sensitivity of native SOC, the studies evaluating the temperature sensitivity of biochar-C in soil, including their influence on the temperature sensitivity of native SOC are limited. The studies are required across soils of contrasting mineralogies and other soil properties to determine the realistic biochar-C sequestration potential in soil.

The theory of soil C decomposition kinetics with temperature has been widely researched. However, there is no agreement about the functional equations to describe the relationship between C mineralisation and temperature. Currently, there are three main approaches to obtain SOC temperature sensitivity (i) soil respiration rate (Luo et al., 2001), (ii) the time required for the loss in a given proportion of C (Conant et al., 2008b) and (iii) total mass loss (Fang et al., 2005; Giardina and Ryan, 2000; Liski et al., 1999). The most common expressions of temperature sensitivity are by comparing instantaneous CO_2 efflux rates (Davidson et al., 2006), as given below:

van't Hoff: $\text{Resp} = \alpha e^{\beta T}$, where $Q_{10} = e^{\beta \times 10}$ (2.6)

Modified van't Hoff: $Q_{10} = (\frac{Resp_{T_2}}{Resp_{T_1}})^{\frac{10}{T_2 - T_1}}$ (2.7)

Arrhenius: $Resp = \alpha e^{E_0/RT}$ (2.8)

Where Resp is respiration, α, β, E_0 are fitted paratmeters, T, T_1 and T_2 are measured temperatures (°C or °F for the Arrhenius function), R is the universal gas constant (8.314 $J\,K^{-1}\,mol^{-1}$), and Q_{10} is the factor by which respiration is multiplied when tempeature increases by 10 °C.

Some researchers have incorprated a temperature scaling function in an exponential decompostion model which can be optimized and converted into Q_{10} (Kätterer et al., 1998; Reichstein et al., 2000), as given below:

$$C_{min}(t, T) = C_1 \times \left(1 - e^{-r(T)\,k_1 t}\right) + C_2 \times (1 - e^{-r(T) k_2 t}) \quad (2.9)$$

$$Q_{10} = r(T)^{\frac{10}{T - T_{ref}}} \quad (2.10)$$

Where C_{min} (t, T) is the cumulative proportion of added C mineralised as a function of temperature (T) and time (t); r(T) is a temperature scaling function, relating mineralisation rate at a temperature T to the rate at a reference temperature T_{ref}. This approach assumes that both rate constants (k_1, k_2) are equally affected by temperature (Kätterer et al., 1998; Reichstein et al., 2000).

2.7. Interactive priming effect of biochar and labile organic carbon mineralisation

Biochar application to a soil can influence the mineralisation of native or added SOC and interactively, native or added labile organic matter in a soil can also influence the mineralisation of biochar (Hamer et al. 2004; Keith et al. 2011). The increased or decreased mineralisation rates of organic C, relative to respective controls, have been defined as positive or negative priming, respectively. It is, however, difficult to isolate the effect of native SOC on biochar from the other factors, such as soil pH, clay content or clay composition, which can also influence the biochar-C mineralisation.

2.7.1. Priming effect on native or added organic carbon (by biochar)

Biochar addition to soil may increase the loss of native organic C ("positive priming effect"), and thereby decrease its C sequestration potential (**Table 2.2**). Hamer et al. (2004) found the addition of biochar accelerated glucose mineralisation, up to 17%, after 26 days. Luo et al. (2011) reported the addition of biochar increased native SOC loss by 66−514% in 87 days. Wardle et al. (2008) reported that charcoal buried in the humus layer of boreal forests in northern Sweden promoted the loss of humus-C in soil. The increased mineralisation of native organic C by biochar or BC may reduce or negate the C sequestration benefit of biochar in the soil. On the other hand, the negative priming effect of biochar on SOC mineralisation in clayey mineral soils has also been reported. For example, Keith et al. (2011) found that biochar application decreased the mineralisation of added labile organic C in a smectite-rich soil over a 4-month incubation period. Similarly, Liang et al. (2010) also found the negative priming effect of BC on the added LOM. On the other hand, Santos et al (2012) reported that BC addition to Haploxeralfs (14−19% clay) did not affect the native soil C mineralisation. These contrasting observations on the direction of biochar priming effect on native or added SOC may be related to biochar lability. Zimmerman et al. (2011) found the positive priming in soils with the addition of more labile biochar, and negative priming in soils with the addition of relatively recalcitrant biochar. Similarly, the larger positive priming effect was reported in biochar with relatively higher labile C than biochar with more recalcitrant C (Hamer et al., 2004; Luo et al., 2011).

Priming effects of biochar on native soil organic C have been shown in field and laboratory experiments; however, the mechanisms involved in the process are still not well understood. The positive, negative or no priming effects in published studies suggest that several different mechanisms may occur in soil. Firstly, the positive priming of native SOM could be triggered by enhanced microbial activity and the accompanying increase in enzyme production by labile-C components in biochar (Hamer et al., 2004; Kuzyakov et al., 2009; Luo et al., 2011). The short-term primed CO_2 may also orginate from the dissolution of inorganic C in biochar (Jones et al., 2011). Secondly, the stabilisation of organic C in mineral soil may be caused by organo-biochar-mineral interaction (Liang et al. 2010; Keith et al. 2011). Thirdly, biochars possess large specific surface area and could stablise or decrease C

mineralisation through the sorption of organic substrates on biochar (Kasozi et al., 2010; Kwon and Pignatello, 2005).

Most of the published studies have been conducted over a short-term period. The positive priming effect triggered by labile C in biochar may decrease with the depletion of labile C. Consequently, the positive priming effect of biochar on soil organic C may not be large in magnitude over a longer term. Therefore, the cumulative negative or positive priming may not influence the C squestration potential of biochar application to soil. Woolf and Lehmann (2012b) argued the priming effect of biochar on SOC mineraliation is negligible over a longer period, and only equated to a maximum 3−4% loss of SOC over 100 years in humic Acrisol, Mollisol and Oxisol (clay: 29−38%).

2.7.2. Priming effect on biochar (by added labile organic C)

Biochar-C mineralisation can be enhanced with increasing input of labile organic matter in soil or sand (**Table 2.3**). Kuzyakov et al. (2009) found up to a six times increase in biochar-C mineralisation rate over two weeks after the addition of glucose. Similarly, Keith et al. (2011) reported the mineralisation of woody biochar-C was increased significantly with the increasing application rates of labile organic matter (sugarcane residues) at early stages of incubation in a smectitic-rich soil. However, over time, biochar-C mineralisation was decreased or stabilised in the presence of added organic matter in Vertisol (Keith et al. 2011). Also, Hamer et al. (2004) found that glucose C addition increased mineralisation of biochar-C at 36 to 189% in a sand mixture in a 2-month of incubation period. Moreover, Luo et al. (2011) reported a 33−137% increase in biochar-C mineralisation with the addition of ryegrass in a 3-month incubation study. Contrary to these observations, Liang et al. (2010) reported that the addition of labile organic matter (LOM) did not increase the mineralisation of aged BC in an Anthrosol of Central Amazon, but the added residues were incorporated and stabilised within an organo-mineral fraction in the kaolinitic soils. These results suggest that LOM input may only enhance the mineralisation of labile biochar-C components and once biochar is aged (i.e. depleted in labile components), the stabilisation of added C may be enhanced in biochar-amended mineral soils. Longer-term incubations are required to discern the role of biochar in the stabilisation of added LOM upon interactions with soil clay minerals.

Table 2.2. Priming effect (PE) of biochar on native or added organic carbon in soil.

Biochar type	Soil type	Experimental period and conditions	Magnitude and direction of priming	References
Maize, rye and wood (350 °C)	Pure sand with glucose treated	Up to 26−60 d at 20 °C	+37% to +64%	Hamer et al. (2004)
Grass (400 °C)	Haplic Luvisol	3.2-year at 20 °C	-31% to +6%	Kuzyakov et al. (2009)
Straw (350 or 700 °C)	Aquic Paleudalf	87 d at 25 °C	+66% to +514%	Luo et al. (2011)
Natural charcoal	Anthrosol (developed on Oxisols, Ultisols, or Spodosols)	532 d at 30 °C	-15 to +21%	Liang et al. (2010)
Wood (450 or 550 °C)	Vertisol with sugarcane addition at 0, 1, 2 and 4% rates	120 d at 20 °C	-150% to +20%	Keith et al. (2011)
Fired-derived charcoal	Boreal forest buried with humus	10-year buried in field	Increased about 80% of humus loss	Wardle et al. (2008)
Maize (500 °C)	Acrisol, Mollisiol, Oxisol	50% of above-ground maize residues converted to biochar and return to soil	+3 to +4% in 100 years time (Modeled)	Woolf and Lehmann (2012a)
Wood (450 °C)	Eutric Cambisol	3-year field study	No effect	Jones et al. (2012)
Sugarcane (350, 450 and 550 °C)	Agriculture soil	28 d at 30 °C	No effect to slightly negative priming	Cross and Sohi (2011)
Wood (450 °C)	Fypic Dystrochrept	5 d at 20 °C	No effect	Jones et al. (2011)
Woody and grass (250, 400, 525 and 650 °C)	Alfisol, Entisol and Mollisol	1-year at 32 °C	-52% to 89%	Zimmerman et al. (2011)
Pecan-shell (700 °C)	Typic Kandiudult	67 d at 17−27°C	+0.18 to +11.99%	Novak et al. (2010)
Woody (450 °C)	Haploxeralfs	180 d at 25 °C	No effect	Santos et al. (2012)
Wheat and wood (450 °C)	Arenosol (FAO WRB)	74 d at 25/12 °C	+20% to +30%	Farrell et al. (2013)

Table 2.3. Priming effect (PE) of added organic carbon in soil or sand on biochar-C mineralisation.

Biochar type	**Soil type**	**Experimental period and conditions**	**Magnitude and direction of priming**	**References**
Maize, rye and wood (350 °C)	Pure sand with glucose treated	Up to 26−60 d at 20 °C	+36% to +189%	Hamer et al. (2004)
Grass (400 °C)	Haplic Luvisol with glucose addition	3.2-year at 20 °C	+20% to +160%	Kuzyakov et al. (2009)
Straw (350 and 700 °C)	Aquic Paleudalf	87 d at 25 °C	+33% to +137%	Luo et al. (2011)
Natural BC	Anthrosol (developed on Oxisols, Ultisols, or Spodosols)	532 d at 30 °C	No effect	Liang et al. (2010)
Wood (450 and 550 °C)	Vertisol with sugarcane addition at 1, 2 and 4% rates	120 d at 20 °C	-20% to +40%	Keith et al. (2011)

2.8. Spectroscopic analyses in relation to biochar oxidation and stability

Spectroscopy techniques, including Fourier transform infrared (FTIR), X-ray photoelectron spectroscopy (XPS), near-edge X-ray absorption fine structure spectroscopy (NEXAFS), can provide direct information of biochar surface or bulk C chemistry including changes in carbon functional groups or structure during the oxidation process (Cheng and Lehmann, 2009; Cheng et al., 2006; Hilscher et al., 2009; Lehmann et al., 2005; Lin et al., 2012; McBeath and Smernik, 2009; Nguyen et al., 2009). The surface functional groups can interact with soil minerals (Gu et al., 1994; Kaiser and Guggenberger, 2003; Lin et al., 2012) and spectroscopic techniques can be useful in evaluating biochar-mineral interactions. For example, Fourier transform infrared (FTIR) spectroscopy has been used to examine the type of surface functional groups on biochar surfaces (Cheng et al., 2008a; Cheng et al., 2006) and to clarify mechanism of biochar functionality in soil. These functional groups can interact with native organic matter and soil minerals which are relevant to biochar stability (Brodowski et al., 2005; Hilscher and Knicker, 2011b; Nguyen et al., 2009). Moreover, the negatively charged functional groups can buffer the acid addition and contribute to alkalinity through association with H^+, such as $–COO^-$ (–COOH) and $–O^-$(–OH) (Yuan et al., 2011). Similar to FTIR, XPS can also provide complementary information on the development of surface functional groups with biochar ageing, especially carboxylic and phenolic groups (Cheng and Lehmann, 2009; Cheng et al., 2006). Near-edge X-ray absorption fine structure spectroscopy has been developed to explore the electronic and structural properties of organic matter such as biochar or BC (Heymann et al., 2011; Keiluweit et al., 2010). Similar to XPS, NEXAFS spectra can reveal the oxidation degree from the small changes of C functional groups in biochar, for example, the spatial analysis of the BC particle indicated a significant oxidation of BC surfaces with a reduction of aromatic C and an increase of carboxylic C (Lehmann et al., 2005). Near-edge X-ray absorption fine structure spectroscopy can semi-quantitatively determine the C forms of BC and non-BC (Liang et al., 2006; Liang et al., 2008), therefore understanding the mechanisms of different stability of BC-rich soil and adjacent soils. Moreover, advances in biochar-mineral interactions could further benefit from the progress made in nondestructive microscopic and microscale X-ray spectroscopy techniques such as scanning electron

microscopy (SEM) and energy dispersive x-ray (EDX) analysis (Brodowski et al., 2005; Lin et al., 2012).

The increasing proportions of aromatic C with charring can be directly examined by ^{13}C nuclear magnetic resonance (NMR) (Knicker et al., 2013; McBeath et al., 2011; Preston and Schmidt, 2006). The ^{13}C NMR technique can also quantify the condensed or "graphitic" biochar, so called the degree of aromatic condensation (Smernik et al., 2006). Furthermore, changes in bulk C functional groups can also be examined by NMR, e.g. an increase of carboxyl/carbonyl C ratio and a decrease of O-alkyl/alkyl-C ratio with time (Hilscher et al., 2009).

Spectroscopic techniques mainly qualitatively determine surface or bulk C functional groups rather than quantifying them; these techniques are complicated and expensive, but can complement biochar stability studies in relation to understanding mechanisms.

2.9. Summary

Biochar-C stability estimates range from decadal to millennia timescales and it seems to be influenced by intrinsic physical-chemical recalcitrance and environmental conditions (i.e. soil minerals and temperature). However, most of the studies have been conducted in a sandy medium or in limited soil types. Furthermore, it has been shown that biochar-C stability estimates may change with incubation time, and longer incubation times (years) can provide more realistic MRTs than shorter incubation studies (months). There is clearly a gap in our understanding of the biochar-C stability and the stabilisation effects of biochars produced at different pyrolysis temperatures on native SOC in a range of soils and under different incubation temperatures. The addition of biochar in soil may increase the loss of SOC; therefore negate the C sequestration potential of biochar in soil. Current studies show that the positive priming occurs in the shorter term; however, over a longer-time period the direction of priming may change to negative priming. Overall, the research on biochar-C stability and stabilisation in soils possessing variable properties, such as clay content, clay composition, native C content, over a long-term period is urgently needed to underpin the long-term biochar-C sequestration potential under contrasting environmental (temperature) conditions.

2.10. References

Baldock, J.A., Oades, J.M., Nelson, P.N., Skene, T.M., Golchin, A., Clarke, P., 1997. Assessing the extent of decomposition of natural organic materials using solid-state 13C NMR spectroscopy. Australian Journal of Soil Research 35, 1061-1083.

Baldock, J.A., Smernik, R.J., 2002. Chemical composition and bioavailability of thermally, altered Pinus resinosa (Red Pine) wood. Organic Geochemistry 33, 1093-1109.

Bird, M.I., Moyo, C., Veenendaal, E.M., Lloyd, J., Frost, P., 1999. Stability of elemental carbon in a savanna soil. Global Biogeochemical Cycles 13, 923-932.

Bol, R., Bolger, T., Cully, R., Little, D., 2003. Recalcitrant soil organic materials mineralize more efficiently at higher temperatures. Journal of Plant Nutrition and Soil Science-Zeitschrift Fur Pflanzenernahrung Und Bodenkunde 166, 300-307.

Brodowski, S., Amelung, W., Haumaier, L., Abetz, C., Zech, W., 2005. Morphological and chemical properties of black carbon in physical soil fractions as revealed by scanning electron microscopy and energy-dispersive X-ray spectroscopy. Geoderma 128, 116-129.

Brodowski, S., Amelung, W., Haumaier, L., Zech, W., 2007. Black carbon contribution to stable humus in German arable soils. Geoderma 139, 220-228.

Brodowski, S., John, B., Flessa, H., Amelung, W., 2006. Aggregate-occluded black carbon in soil. European Journal of Soil Science 57, 539-546.

Bruun, S., Jensen, E.S., Jensen, L.S., 2008. Microbial mineralization and assimilation of black carbon: Dependency on degree of thermal alteration. Organic Geochemistry 39, 839-845.

Case, S.D.C., McNamara, N.P., Reay, D.S., Whitaker, J., 2012. The effect of biochar addition on N2O and CO2 emissions from a sandy loam soil - The role of soil aeration. Soil Biology & Biochemistry 51, 125-134.

Chan, K., Xu, Z., 2009. Biochar–nutrient properties and their enhancement, In: Lehmann, J., Joseph, S. (Eds.), Biochar for Environmental Management: Science and Technology. Earthscan London, pp. 67-84.

Cheng, C.H., Lehmann, J., 2009. Ageing of black carbon along a temperature gradient. Chemosphere 75, 1021-1027.

Cheng, C.H., Lehmann, J., Engelhard, M.H., 2008a. Natural oxidation of black carbon in soils: Changes in molecular form and surface charge along a climosequence. Geochimica Et Cosmochimica Acta 72, 1598-1610.

Cheng, C.H., Lehmann, J., Thies, J.E., Burton, S.D., 2008b. Stability of black carbon in soils across a climatic gradient. Journal of Geophysical Research-Biogeosciences 113, doi 10.1029/2007jg000642.

Cheng, C.H., Lehmann, J., Thies, J.E., Burton, S.D., Engelhard, M.H., 2006. Oxidation of black carbon by biotic and abiotic processes. Organic Geochemistry 37, 1477-1488.

Conant, R.T., Drijber, R.A., Haddix, M.L., Parton, W.J., Paul, E.A., Plante, A.F., Six, J., Steinweg, J.M., 2008a. Sensitivity of organic matter decomposition to warming varies with its quality. Global Change Biology 14, 868-877.

Conant, R.T., Steinweg, J.M., Haddix, M.L., Paul, E.A., Plante, A.F., Six, J., 2008b. Experimental warming shows that decomposition temperature sensitivity increases with soil organic matter recalcitrance. Ecology 89, 2384-2391.

Craine, J.M., Fierer, N., McLauchlan, K.K., 2010. Widespread coupling between the rate and temperature sensitivity of organic matter decay. Nature Geoscience 3, 854-857.

Crombie, K., Masek, O., Sohi, S.P., Brownsort, P., Cross, A., 2013. The effect of pyrolysis conditions on biochar stability as determined by three methods. Global Change Biology Bioenergy 5, 122-131.

Cross, A., Sohi, S.P., 2011. The priming potential of biochar products in relation to labile carbon contents and soil organic matter status. Soil Biology & Biochemistry 43, 2127-2134.

Cross, A., Sohi, S.P., 2013. A method for screening the relative long-term stability of biochar. Global Change Biology Bioenergy 5, 215-220.

Czimczik, C.I., Masiello, C.A., 2007. Controls on black carbon storage in soils. Global Biogeochemical Cycles 21, GB3005.

Czimczik, C.I., Preston, C.M., Schmidt, M.W.I., Werner, R.A., Schulze, E.D., 2002. Effects of charring on mass, organic carbon, and stable carbon isotope composition of wood. Organic Geochemistry 33, 1207-1223.

Davidson, E.A., Janssens, I.A., 2006. Temperature sensitivity of soil carbon decomposition and feedbacks to climate change. Nature 440, 165-173.

Davidson, E.A., Janssens, I.A., Luo, Y.Q., 2006. On the variability of respiration in terrestrial ecosystems: moving beyond Q10. Global Change Biology 12, 154-164.

Fang, C.M., Smith, P., Moncrieff, J.B., Smith, J.U., 2005. Similar response of labile and resistant soil organic matter pools to changes in temperature. Nature 436, 881-881.

Farrell, M., Kuhn, T.K., Macdonald, L.M., Maddern, T.M., Murphy, D.V., Hall, P.A., Singh, B.P., Baumann, K., Krull, E.S., Baldock, J.A., 2013. Microbial utilisation of biochar-derived carbon. Science of the Total Environment, in press.

Fierer, N., Craine, J.M., McLauchlan, K., Schimel, J.P., 2005. Litter quality and the temperature sensitivity of decomposition. Ecology 86, 320-326.

Gavin, D.G., Brubaker, L.B., Lertzman, K.P., 2003. Holocene fire history of a coastal temperate rain forest based on soil charcoal radiocarbon dates. Ecology 84, 186-201.

Ghani, W.A.W.A.K., Mohd, A., da Silva, G., Bachmann, R.T., Taufiq-Yap, Y.H., Rashid, U., Al-Muhtaseb, A.H., 2013. Biochar production from waste rubber-wood-sawdust and its potential use in C sequestration: Chemical and physical characterization. Industrial Crops and Products 44, 18-24.

Giardina, C.P., Ryan, M.G., 2000. Evidence that decomposition rates of organic carbon in mineral soil do not vary with temperature. Nature 404, 858-861.

Glaser, B., Amelung, W., 2003. Pyrogenic carbon in native grassland soils along a climosequence in North America. Global Biogeochemical Cycles 17, 1064. doi 10.1029/2002gb002019.

Glaser, B., Balashov, E., Haumaier, L., Guggenberger, G., Zech, W., 2000. Black carbon in density fractions of anthropogenic soils of the Brazilian Amazon region. Organic Geochemistry 31, 669-678.

Glaser, B., Haumaier, L., Guggenberger, G., Zech, W., 2001. The 'Terra Preta' phenomenon: a model for sustainable agriculture in the humid tropics. Naturwissenschaften 88, 37-41.

Glaser, B., Lehmann, J., Zech, W., 2002. Ameliorating physical and chemical properties of highly weathered soils in the tropics with charcoal - a review. Biology and Fertility of Soils 35, 219-230.

Goldberg, E.D., 1985. Black carbon in the environment: properties and distribution. J. Wiley, New York, 198 pp.

Gu, B.H., Schmitt, J., Chen, Z.H., Liang, L.Y., Mccarthy, J.F., 1994. Adsorption and desorption of natural organic-matter on iron-oxide–mechanisms and models. Environmental Science & Technology 28, 38-46.

Hamer, U., Marschner, B., Brodowski, S., Amelung, W., 2004. Interactive priming of black carbon and glucose mineralisation. Organic Geochemistry 35, 823-830.

Heymann, K., Lehmann, J., Solomon, D., Schmidt, M.W.I., Regier, T., 2011. C 1s K-edge near edge X-ray absorption fine structure (NEXAFS) spectroscopy for characterizing functional group chemistry of black carbon. Organic Geochemistry 42, 1055-1064.

Hilscher, A., Heister, K., Siewert, C., Knicker, H., 2009. Mineralisation and structural changes during the initial phase of microbial degradation of pyrogenic plant residues in soil. Organic Geochemistry 40, 332-342.

Hilscher, A., Knicker, H., 2011a. Carbon and nitrogen degradation on molecular scale of grass-derived pyrogenic organic material during 28 months of incubation in soil. Soil Biology & Biochemistry 43, 261-270.

Hilscher, A., Knicker, H., 2011b. Degradation of grass-derived pyrogenic organic material, transport of the residues within a soil column and distribution in soil organic matter fractions during a 28 month microcosm experiment. Organic Geochemistry 42, 42-54.

IBI, 2012. Standardized product definition and product testing guidelines for biochar that is used in soil. http://www.biochar-international.org/sites/default/files/Guidelines_for_Biochar_That_Is_Used_in_Soil_Final.pdf, (cited 5 March, 2013).

Jones, D.L., Murphy, D.V., Khalid, M., Ahmad, W., Edwards-Jones, G., DeLuca, T.H., 2011. Short-term biochar-induced increase in soil CO2 release is both biotically and abiotically mediated. Soil Biology & Biochemistry 43, 1723-1731.

Jones, D.L., Rousk, J., Edwards-Jones, G., DeLuca, T.H., Murphy, D.V., 2012. Biochar-mediated changes in soil quality and plant growth in a three year field trial. Soil Biology & Biochemistry 45, 113-124.

Kaiser, K., Guggenberger, G., 2003. Mineral surfaces and soil organic matter. European Journal of Soil Science 54, 219-236.

Kasozi, G.N., Zimmerman, A.R., Nkedi-Kizza, P., Gao, B., 2010. Catechol and humic acid sorption onto a range of laboratory-produced black carbons (biochars). Environmental Science & Technology 44, 6189-6195.

Kätterer, T., Reichstein, M., Andrén, O., Lomander, A., 1998. Temperature dependence of organic matter decomposition: a critical review using literature data analyzed with different models. Biology and Fertility of Soils 27, 258-262.

Keiluweit, M., Nico, P.S., Johnson, M.G., Kleber, M., 2010. Dynamic molecular structure of plant biomass-derived black carbon (biochar). Environmental Science & Technology 44, 1247-1253.

Keith, A., Singh, B., Singh, B.P., 2011. Interactive priming of biochar and labile organic matter mineralization in a smectite-rich soil. Environmental Science & Technology 45, 9611-9618.

Kirschbaum, M.U.F., 1995. The temperature dependence of soil organic matter decomposition, and the effect of global warming on soil organic C storage. Soil Biology & Biochemistry 27, 753-760.

Knicker, H., 2011. Pyrogenic organic matter in soil: Its origin and occurrence, its chemistry and survival in soil environments. Quaternary International 243, 251-263.

Knicker, H., Gonzalez-Vila, F.J., Gonzalez-Vazquez, R., 2013. Biodegradability of organic matter in fire-affected mineral soils of Southern Spain. Soil Biology & Biochemistry 56, 31-39.

Knicker, H., Hilscher, A., Gonzalez-Vila, F.J., Almendros, G., 2008. A new conceptual model for the structural properties of char produced during vegetation fires. Organic Geochemistry 39, 935-939.

Knoblauch, C., Maarifat, A.A., Pfeiffer, E.M., Haefele, S.M., 2011. Degradability of black carbon and its impact on trace gas fluxes and carbon turnover in paddy soils. Soil Biology & Biochemistry 43, 1768-1778.

Knorr, W., Prentice, I.C., House, J.I., Holland, E.A., 2005. Long-term sensitivity of soil carbon turnover to warming. Nature 433, 298-301.

Kuhlbusch, T.A.J., 1998. Black carbon and the carbon cycle. Science 280, 1903-1904.

Kuzyakov, Y., Friedel, J.K., Stahr, K., 2000. Review of mechanisms and quantification of priming effects. Soil Biology & Biochemistry 32, 1485-1498.

Kuzyakov, Y., Subbotina, I., Chen, H.Q., Bogomolova, I., Xu, X.L., 2009. Black carbon decomposition and incorporation into soil microbial biomass estimated by 14C labeling. Soil Biology & Biochemistry 41, 210-219.

Kwon, S., Pignatello, J.J., 2005. Effect of natural organic substances on the surface and adsorptive properties of environmental black carbon (char): Pseudo pore blockage by model lipid components and its implications for N2-probed surface properties of natural sorbents. Environmental Science & Technology 39, 7932-7939.

Lehmann, J., 2007. A handful of carbon. Nature 447, 143-144.

Lehmann, J., Czimczik, C., Laird, D., Sohi, S., 2009. Stability of biochar in soil, In: Lehmann, J., Joseph, S. (Eds.), Biochar for Environmental Management: Science and Technology. Earthscan London, pp. 183-205.

Lehmann, J., Gaunt, J., Rondon, M., 2006. Bio-char sequestration in terrestrial ecosystems–a review. Mitigation and Adaptation Strategies for Global Change 11, 403-427.

Lehmann, J., Joseph, S., 2009. Biochar for environmental management: Science and technology. Earthscan, London.

Lehmann, J., Liang, B.Q., Solomon, D., Lerotic, M., Luizao, F., Kinyangi, J., Schafer, T., Wirick, S., Jacobsen, C., 2005. Near-edge X-ray absorption fine structure (NEXAFS) spectroscopy for mapping nano-scale distribution of organic carbon forms in soil: Application to black carbon particles. Global Biogeochemical Cycles 19, GB1013.

Leifeld, J., Fuhrer, J., 2005. The temperature response of CO_2 production from bulk soils and soil fractions is related to soil organic matter quality. Biogeochemistry 75, 433-453.

Liang, B., Lehmann, J., Solomon, D., Kinyangi, J., Grossman, J., O'Neill, B., Skjemstad, J.O., Thies, J., Luizao, F.J., Petersen, J., Neves, E.G., 2006. Black carbon increases cation exchange capacity in soils. Soil Science Society of America Journal 70, 1719-1730.

Liang, B., Lehmann, J., Solomon, D., Sohi, S., Thies, J.E., Skjemstad, J.O., Luizao, F.J., Engelhard, M.H., Neves, E.G., Wirick, S., 2008. Stability of biomass-derived black carbon in soils. Geochimica Et Cosmochimica Acta 72, 6069-6078.

Liang, B.Q., Lehmann, J., Sohi, S.P., Thies, J.E., O'Neill, B., Trujillo, L., Gaunt, J., Solomon, D., Grossman, J., Neves, E.G., Luizão, F.J., 2010. Black carbon affects the cycling of non-black carbon in soil. Organic Geochemistry 41, 206-213.

Lin, Y., Munroe, P., Joseph, S., Kimber, S., Van Zwieten, L., 2012. Nanoscale organo-mineral reactions of biochars in ferrosol: an investigation using microscopy. Plant and Soil, 369-380.

Liski, J., Ilvesniemi, H., Makela, A., Westman, C.J., 1999. CO2 emissions from soil in response to climatic warming are overestimated - The decomposition of old soil organic matter is tolerant of temperature. Ambio 28, 171-174.

Luo, Y., Durenkamp, M., De Nobili, M., Lin, Q., Brookes, P.C., 2011. Short term soil priming effects and the mineralisation of biochar following its incorporation to soils of different pH. Soil Biology & Biochemistry 43, 2304-2314.

Luo, Y.Q., Wan, S.Q., Hui, D.F., Wallace, L.L., 2001. Acclimatization of soil respiration to warming in a tall grass prairie. Nature 413, 622-625.

Major, J., Lehmann, J., Rondon, M., Goodale, C., 2010a. Fate of soil-applied black carbon: downward migration, leaching and soil respiration. Global Change Biology 16, 1366-1379.

Major, J., Rondon, M., Molina, D., Riha, S.J., Lehmann, J., 2010b. Maize yield and nutrition during 4 years after biochar application to a Colombian savanna oxisol. Plant and Soil 333, 117-128.

Masiello, C.A., 2004. New directions in black carbon organic geochemistry. Marine Chemistry 92, 201-213.

McBeath, A.V., Smernik, R.J., 2009. Variation in the degree of aromatic condensation of chars. Organic Geochemistry 40, 1161-1168.

McBeath, A.V., Smernik, R.J., Schneider, M.P.W., Schmidt, M.W.I., Plant, E.L., 2011. Determination of the aromaticity and the degree of aromatic condensation of a thermosequence of wood charcoal using NMR. Organic Geochemistry 42, 1194-1202.

Mukherjee, A., Zimmerman, A.R., 2013. Organic carbon and nutrient release from a range of laboratory-produced biochars and biochar-soil mixtures. Geoderma 193, 122-130.

Muneer, M., Oades, J.M., 1989. The role of Ca-organic interactions in soil aggregate stability .1. Laboratory studies with glucose-14C, CaCO3 and CaSO4.2H2O. Australian Journal of Soil Research 27, 389-399.

Nguyen, B.T., Lehmann, J., 2009. Black carbon decomposition under varying water regimes. Organic Geochemistry 40, 846-853.

Nguyen, B.T., Lehmann, J., Hockaday, W.C., Joseph, S., Masiello, C.A., 2010. Temperature sensitivity of black carbon decomposition and oxidation. Environmental Science & Technology 44, 3324-3331.

Nguyen, B.T., Lehmann, J., Kinyangi, J., Smernik, R., Riha, S.J., Engelhard, M.H., 2009. Long-term black carbon dynamics in cultivated soil. Biogeochemistry 92, 163-176.

Novak, J.M., Busscher, W.J., Watts, D.W., Laird, D.A., Ahmedna, M.A., Niandou, M.A.S., 2010. Short-term CO2 mineralization after additions of biochar and switchgrass to a Typic Kandiudult. Geoderma 154, 281-288.

Pereira, R.C., Kaal, J., Arbestain, M.C., Lorenzo, R.P., Aitkenhead, W., Hedley, M., Macias, F., Hindmarsh, J., Macia-Agullo, J.A., 2011. Contribution to characterisation of biochar to estimate the labile fraction of carbon. Organic Geochemistry 42, 1331-1342.

Preston, C.M., Schmidt, M.W.I., 2006. Black (pyrogenic) carbon: A synthesis of current knowledge and uncertainties with special consideration of boreal regions. Biogeosciences 3, 397-420.

Reichstein, M., Bednorz, F., Broll, G., Kätterer, T., 2000. Temperature dependence of carbon mineralisation: conclusions from a long-term incubation of subalpine soil samples. Soil Biology & Biochemistry 32, 947-958.

Santos, F., Torn, M.S., Bird, J.A., 2012. Biological degradation of pyrogenic organic matter in temperate forest soils. Soil Biology & Biochemistry 51, 115-124.

Schimmelpfennig, S., Glaser, B., 2012. One step forward toward characterization: Some important material properties to distinguish biochars. Journal of Environmental Quality 41, 1001-1013.

Schmidt, M.W.I., Noack, A.G., 2000. Black carbon in soils and sediments: Analysis, distribution, implications, and current challenges. Global Biogeochemical Cycles 14, 777-793.

Schmidt, M.W.I., Skjemstad, J.O., Jäger, C., 2002. Carbon isotope geochemistry and nanomorphology of soil black carbon: Black chernozemic soils in central

Europe originate from ancient biomass burning. Global Biogeochemical Cycles 16, 1123.

Shindo, H., 1991. Elementary composition, humus composition, and decomposition in soil of charred grassland plants. Soil Science and Plant Nutrition 37, 651-657.

Singh, B., Singh, B.P., Cowie, A.L., 2010. Characterisation and evaluation of biochars for their application as a soil amendment. Australian Journal of Soil Research 48, 516-525.

Singh, B.P., Cowie, A.L., Smernik, R.J., 2012. Biochar carbon stability in a clayey soil as a function of feedstock and pyrolysis temperature. Environmental Science & Technology 46, 11770-11778.

Singh, N., Abiven, S., Torn, M.S., Schmidt, M.W.I., 2011. Fire-derived organic carbon turnover in soils on a centennial scale. Biogeosciences Discuss 8, 12179-12195.

Six, J., Bossuyt, H., Degryze, S., Denef, K., 2004. A history of research on the link between (micro)aggregates, soil biota, and soil organic matter dynamics. Soil & Tillage Research 79, 7-31.

Skjemstad, J.O., Clarke, P., Taylor, J.A., Oades, J.M., McClure, S.G., 1996. The chemistry and nature of protected carbon in soil. Australian Journal of Soil Research 34, 251-271.

Smernik, R.J., Kookana, R.S., Skjemstad, J.O., 2006. NMR characterization of 13C-benzene sorbed to natural and prepared charcoals. Environmental Science & Technology 40, 1764-1769.

Spokas, K.A., 2010. Review of the stability of biochar in soils: predictability of O:C molar ratios. Carbon Management 1, 289-303.

Spokas, K.A., Cantrell, K.B., Novak, J.M., Archer, D.W., Ippolito, J.A., Collins, H.P., Boateng, A.A., Lima, I.M., Lamb, M.C., McAloon, A.J., Lentz, R.D., Nichols, K.A., 2012. Biochar: A synthesis of its agronomic impact beyond carbon sequestration. Journal of Environmental Quality 41, 973-989.

Steinbeiss, S., Gleixner, G., Antonietti, M., 2009. Effect of biochar amendment on soil carbon balance and soil microbial activity. Soil Biology & Biochemistry 41, 1301-1310.

Sun, H., Hockaday, W.C., Masiello, C.A., Zygourakis, K., 2012. Multiple controls on the chemical and physical structure of biochars. Industrial & Engineering Chemistry Research 51, 3587-3597.

Theng, B.K.G., Churchman, G.J., Newman, R.H., 1986. The occurrence of interlayer clay-organic complexes in 2 New-Zealand soils. Soil Science 142, 262-266.

Tisdall, J.M., Oades, J.M., 1982. Organic-matter and water-stable aggregates in soils. Journal of Soil Science 33, 141-163.

Van Zwieten, L., Kimber, S., Morris, S., Chan, K.Y., Downie, A., Rust, J., Joseph, S., Cowie, A., 2010. Effects of biochar from slow pyrolysis of papermill waste on agronomic performance and soil fertility. Plant and Soil 327, 235-246.

Vanhala, P., Karhu, K., Tuomi, M., Sonninen, E., Jungner, H., Fritze, H., Liski, J., 2007. Old soil carbon is more temperature sensitive than the young in an agricultural field. Soil Biology & Biochemistry 39, 2967-2970.

Wardle, D.A., Nilsson, M.C., Zackrisson, O., 2008. Fire-derived charcoal causes loss of forest humus. Science 320, 629-629.

Woolf, D., Lehmann, J., 2012a. Modelling the long-term response to positive and negative priming of soil organic carbon by black carbon. Biogeochemistry 111, 83-95.

Woolf, D., Lehmann, J., 2012b. Modelling the long-term response to positive and negative priming of soil organic carbon by black carbon. Biogeochemistry, 111, 83-95.

Yuan, J.H., Xu, R.K., Zhang, H., 2011. The forms of alkalis in the biochar produced from crop residues at different temperatures. Bioresource Technology 102, 3488-3497.

Zhou, T., Shi, P.J., Hui, D.F., Luo, Y.Q., 2009. Global pattern of temperature sensitivity of soil heterotrophic respiration (Q10) and its implications for carbon-climate feedback. Journal of Geophysical Research-Biogeosciences 114, G02016.

Zimmerman, A.R., 2010. Abiotic and microbial oxidation of laboratory-produced black carbon (biochar). Environmental Science & Technology 44, 1295-1301.

Zimmerman, A.R., Gao, B., 2013. The stability of biochar in the environment, In: Ladygina, N., Rineau, F. (Eds.), Biochar and Soil Biota. CRC Press, pp. 1-40.

Zimmerman, A.R., Gao, B., Ahn, M.Y., 2011. Positive and negative carbon mineralization priming effects among a variety of biochar-amended soils. Soil Biology & Biochemistry 43, 1169-1179.

Zimmermann, M., Bird, M.I., Wurster, C., Saiz, G., Goodrick, L., Barta, J., Capek, P., Santruckova, H., Smernik, R., 2012. Rapid degradation of pyrogenic carbon. Global Change Biology 18, 3306–3316.

Chapter 3: Biochar carbon stability in four contrasting soils[1]

Abstract

There is a limited understanding of the effects of soil properties on biochar carbon (C) stability. This knowledge is essential to fully evaluate the capacity of biochar for long-term soil C sequestration. In this study, two biochars, produced by slow pyrolysis at 450 or 550 °C from a $\delta^{13}C$-depleted (-36.4‰) *Eucalyptus saligna* Sm. woody material, were incubated in four soils (Inceptisol, Entisol, Oxisol, Vertisol) of contrasting chemical and mineralogical properties. The total biochar-C mineralised over 12 months was 0.30−1.14% and 0.97−2.71% from the soil-biochar mixtures incubated at 20 and 40 °C, respectively. The total biochar-C mineralised (mg CO_2-C per unit of native soil organic C, SOC basis) from soils incubated with the 450 °C biochar was approximately twice the corresponding amount mineralised from the 550 °C biochar systems. The influence of soil properties on biochar-C mineralisation was greater for the 450 °C biochar than the 550 °C biochar. The smallest proportion of C mineralised from the 450 °C biochar occurred in the Inceptisol incubated at 20 °C and in the Oxisol at 40 °C. However, when expressed on a per unit of native SOC basis, the C mineralisation of the 450 and 550 °C biochars was least in the Oxisol and greatest in the Inceptisol at both incubation temperatures. Mean residence times (MRT) of the biochars estimated using the two-pool exponential model varied between 44 and 610 years. The estimated MRT of the biochars may vary under field conditions depending upon the environmental conditions and addition of labile carbon from plants. Our results indicate that biochar-C was stabilised by variable charge minerals in the Oxisol and that the stabilisation occurred rapidly at high temperatures.

[1] This chapter has been published in European Journal of Soil Science under the title "Biochar carbon stability in four contrasting soils" in August 2013. Authors are Yunying Fang, Balwant Singh, Bhupinder Pal Singh and Evelyn Krull.

3.1. Introduction

Biochar is a solid material obtained from the thermochemical conversion of biomass in an oxygen-limited environment (IBI, 2012). In recent years, biochar has been promoted as a technology that can provide multiple environmental benefits upon application to soil, including long-term sequestration of carbon (C) in soil (Woolf et al., 2010). Because of their predominantly aromatic nature (McBeath & Smernik, 2009), biochars are considered as a recalcitrant form of C with long mean residence times (MRT) in the range of centuries to millennia (Kuzyakov et al., 2009; Zimmerman, 2010; Keith et al., 2011; Singh et al., 2012). However, observations of reduced stability in the range of a few decades for natural and laboratory produced char or biochar have also been made, especially under high (≥ 30° C) incubation temperatures (Bird et al., 1999; Murage et al., 2007; Hilscher et al., 2009; Hilscher & Knicker, 2011; Zimmermann et al., 2012). Thus, the stability of biochar-C requires further understanding so that the potential of biochar technology as a long-term C sequestration method can be assessed (Lehmann et al., 2006).

Some of the uncertainties in the estimates of biochar-C stability have been related to production conditions and feedstock type (Nguyen et al., 2010; Zimmerman, 2010; Keith et al., 2011; Singh et al., 2012). For example, biochars produced at lower temperatures (400−450 °C) have been reported to mineralise faster than the higher temperatures (550−650 °C) counterparts. Large production temperatures generally increase the aromaticity and degree of aromatic condensation in the biochar (McBeath & Smernik, 2009; McBeath et al., 2011; Pereira et al., 2011; Kaal et al., 2012) and consequently its intrinsic chemical recalcitrance against biological and chemical decomposition (Zimmerman, 2010; Singh et al., 2012).

The stability of biochar in soils may not be solely attributable to its chemical characteristics but also to its reduced accessibility when involved in organo-mineral associations. Biochar can be stabilised through chemical interactions with soil minerals and subsequent physical occlusion in organo-mineral fractions, thereby limiting its spatial accessibility to soil microorganisms and their enzymes (Lehmann et al., 2011). For instance, Brodowski et al. (2006) found aged char-C in micro-aggregates and aggregate-occluded fractions and hypothesized that reactive surfaces on aged char can contribute actively to aggregate formation and consequently

stabilisation of char in a mineral soil. Furthermore, char-C was embedded within plaques of iron (Fe) and aluminium (Al) oxides on mineral surfaces (Glaser et al., 2000). Lin et al. (2012) found a relatively large concentration of Al at the interface between biochar and mineral phases following short-term ageing of biochar in a Ferrosol. Eckmeier et al. (2010) found that organo-metallic or organo-mineral complexes and intrinsic recalcitrance of char were responsible for large SOC stocks in sesquioxides-rich Cryptopodzols. Although biochar-C is intrinsically chemically recalcitrant, the above studies have demonstrated the importance of organo-mineral complexes to enhance biochar-C stability in the soil. Considering the growing interest in biochar for long-term C sequestration in soil, a greater understanding of the biochar-C stability in soils with varying clay and organic matter contents and compositions is required.

In addition to biochar-soil interactions, soil environmental conditions, such as temperature, may have considerable effects on the stability of biochar-C in soil. Nguyen et al. (2010) observed increasing loss of biochar-C from biochar-sand mixtures (from 1.5 to 20% of the applied biochar-C over a one-year incubation experiment) with increasing incubation temperature from 4 to 60 °C. Cheng et al. (2006) found an increase in the abiotic oxidation of biochar with increasing temperature over a four-month incubation period. High incubation temperatures can increase biochar-C mineralisation (Zimmermann et al., 2012), but whether biochar-soil mineral interactions play a role in counteracting the effect of temperature on biochar-C mineralisation is not known.

Biochar-C mineralisation may be enhanced with increasing organic matter content in soil. For example, the mineralisation of wood biochar-C was increased with the increasing application rates of sugarcane residues at early stages of incubation (positive priming) followed by the stabilisation of biochar-C mineralisation (negative priming) in a smectite-rich soil (Keith et al., 2011). The stabilisation of biochar was attributed to the possible interactions of biochar with minerals and native/added organic matter in the soil. Similarly, Hamer et al. (2004) found that addition of glucose-C increased the mineralisation of biochar-C in a sand mixture. Contrary to these observations, Liang et al. (2010) reported that the addition of sugarcane residues did not increase the mineralisation of aged black C in

Anthrosols of Central Amazon, rather that the added residues were incorporated and stabilised within an organo-mineral fraction in kaolinite dominated soils.

Most previous studies on biochar-C stability were carried out in pure sand or in soils with a limited range of clay minerals, clay content and native organic C content. We still have a poor understanding of the influence of soil properties on biochar-C mineralisation and hence its stability (MRT) in a variety of soils. Here, we used two wood biochars with distinctly different $\delta^{13}C$ signature (-36.4‰) from the soils (-14.1–28.2‰) (**Table 3.1**), which allowed us to quantify the mineralisation of biochar-C and soil C fractions using an isotopic mixing model. The biochars were incubated in four soils of contrasting properties including clay mineral composition, clay content and organic C content under controlled conditions of temperature (20 or 40 °C) and moisture (70% of maximum water holding capacity). Our hypotheses were that (i) biochar-C stability will vary across soils of contrasting properties, and (ii) biochar produced at high temperature (550 °C) will have greater stability than that from low temperature (450 °C) in these soils.

3.2. Material and methods

3.2.1. Biochars and soils

Two wood biochars were produced at 450 and 550 °C using slow pyrolysis (5−10 °C per minute heating rate, 40 minutes residence time) by Pacific Pyrolysis (Somersby, Australia) from ^{13}C-depleted woody biomass of *Eucalyptus saligna* Sm. trees that had been grown for two years under an elevated CO_2 environment (Barton et al., 2010). The biochars were ground and sieved through a 2-mm sieve for the incubation experiments.

Surface soil samples (0−15 cm) were collected from agricultural fields in Australia located at: Wongan Hills in Western Australia (Inceptisol; 35°89´S, 116°38´E); Port Kenny in South Australia (Entisol; 33°14´S, 134°72´E); Wollongbar in New South Wales (Oxisol; 28°50´S, 153°25´E); and Hermitage Research Station, Warwick in Queensland (Vertisol; 28°13´S, 152°6´E) (Soil survey staff, 2010). Soil samples were air-dried, and roots and other visible plant remains were removed. Soil samples were ground and sieved to obtain the < 2 mm size fraction for the incubation experiment.

The measured properties of biochars and soils (n = 4) are shown in **Table 3.1** and Appendix 2. The pH of biochars and soils was measured in 1:5 solid / solution ratio in deionised water using a pre-calibrated pH electrode. Electrical conductivity (EC) was also measured in 1:5 solid / solution extracts using an electrical conductivity meter. Soil particle size was analysed by the hydrometer method. Cation exchange capacity (CEC) and exchangeable cations were determined by the silver thiourea $(AgTU)^{+}$ method. Biochar and soil samples were ground to obtain a <53 μm fraction to measure total C and nitrogen (N) by dry combustion using a vario MAX CNS elemental analyser (Germany). The Entisol was treated with 1 M HCl (at 60 °C) to dissolve carbonate C (Midwood & Boutton, 1998). The acid-treated Entisol was washed repeatedly with deionised water until neutral pH was obtained, dried at 40 °C, and the total organic C content was analysed as described above. The $\delta^{13}C$ signatures of the ground (<53 μm) soil and biochar samples were determined by a Delta V Thermo Finnigan IRMS.

Clay minerals were analysed by X-ray diffraction (XRD) following standard pretreatments (Brown & Brindley, 1980) (details given in the Supporting Information and Appendix 3). Specific surface area and pore volume analyses of biochars were made with a Micromeritics ASAP 2020 surface area and porosity analyser (details given in the Supporting Information 3.7).

Table 3.1. Important properties of soils and biochars used in the incubation experiment.

Property	**Inceptisol**	**Entisol**	**Oxisol**	**Vertisol**	**450 °C biochar**	**550 °C biochar**
WRB order (FAO, 2006)	Arenosols	Calcisol	Ferralsol	Vertisol	–	–
pH (1:5 H_2O)	5.70 (±0.01)	8.77 (±0.01)	5.65 (±0.01)	7.89 (±0.01)	8.64 (±0.05)	9.96 (±0.01)
EC (1:5) / mS m^{-1}	8.2 (±2.3)	24.5 (±2.3)	15.0 (±0.5)	13.0 (±2.6)	89.4 (±21.7)	112.7 (±52.4)
Sand / %	97.5 (±0.1)	66.3 (±0.1)	24.3 (±2.0)	27.3 (±0.7)	–	–
Silt / %	1.2 (±0.1)	12.2 (±0.2)	31.6 (±1.4)	28.5 (±0.8)	–	–
Clay / %	1.3 (±0.1)	21.5 (±0.4)	44.1 (±0.6)	44.2 (±0.1)	–	–
CEC / $mmol_c$ kg^{-1}	24.4 (±2.5)	99.1 (±3.3)	119.9 (±2.9)	265.4 (±3.1)	11.4 (±3.9)	54.0 (±4.4)
Organic carbon / %	0.95 (±0.02)	2.53 (±0.09)	4.39 (±0.02)	2.25 (±0.04)	67.40 (±0.20)	73.19 (±0.14)
Inorganic carbon / %	–	6.01 (±0.06)	–	–	–	–
$\delta^{13}C$ / ‰	-28.17 (±0.02)	-14.08 (±0.01)	-21.35 (±0.01)	-17.32 (±0.01)	-36.34 (±0.01)	-36.53 (±0.02)
Total N / %	0.07 (±0.01)	0.16 (±0.01)	0.43 (±0.02)	0.16 (±0.01)	0.52 (±0.02)	0.62 (±0.01)
SSA / m^2 g^{-1}	–	–	–	–	191.0	228.3
Pore volume / cm^3 g^{-1}	–	–	–	–	57.2	67.5
Clay minerals	Kaol*****, Qtz*, Ill*	Ill****, Kaol***, Qtz*	Goe***, Gib***, Kaol***, Hem**, Ant**, HIV*	Sm*****, Kaol**	–	–

EC: electrical conductivity; CEC: cation-exchange capacity measured by the silver thiorurea method; SSA: specific surface area measured by a CO_2 adsorption method (see Supporting Information).

Kaol=kaolinite; Sm= smectite; Ill= illite; Qtz= quartz; Goe= goethite; Gib= gibbsite; Hem= hematite; Ant= anatase; HIV= hydroxy interlayered vermiculite; numbers represent the ratio of each clay, *****, ****, ***, **, * represents 60% over, 40−60%, 20−40%, 5−20% and less than 5%, respectively.

The numbers in parentheses are the standard error of the mean (n=4).

3.2.2. Incubation experiment

The two biochars were uniformly mixed with each soil type (300 g oven-dry) at 2% (w/w); a non-amended control soil was also included. Biochar-soil mixtures were placed into 300 ml containers (maintaining a bulk density of 1.2 g cm^{-3}) and incubated separately in 1.2 l plastic jars sealed with Vaseline or silicon grease at 20 and 40 °C for up to 12 months. These temperatures occur commonly in temperate and tropical regions (Zimmermann et al., 2012). Each treatment was replicated four times. A CO_2-trap (40 ml of 2.5 M NaOH in 70 ml jar) and a jar of deionized water (40 ml water in 70 ml jar) were placed in each incubation chamber to absorb the CO_2 produced and maintain a constant humidity, respectively. To account for headspace CO_2, four control incubation chambers were set up in the same fashion but containing a closed, empty container instead of the biochar-soil container. A nutrient solution (see Appendix 1) that contained (kg^{-1} soil) aprroximately 183 mg N, 28 mg P, 220 mg K, 13 mg S and required amounts of trace elements was uniformly mixed with each of the soils or soil-biochar mixtures to support microbial growth during the incubation period (Chapman, 1997). A microbial inoculum was prepared by mixing soil samples collected from fields under different vegetations (native eucalyptus forests, pine plantation, maize cropping and grazed pastures), thus introducing a diverse range of microbial communities to the soils or soil biochar-mixtures (Keith et al., 2011). The microbial inoculum was prepared as a soil extract (50 g soil : 100 ml water, seived to < 100 µm). The soil extract was mixed with the nutrient solution in a ratio of 1:125 and applied to the soil-biochar mixtures. The control soils and biochar-soil mixtures were maintained at 70% of maximum water holding capacity. The CO_2 traps were changed at days 3, 9, 18, 38, 94, 183, 276, 365 for the 20 °C incubation experiment, and days 2, 4, 8, 16, 30, 51, 80, 130, 183, 246, 313, 365 for the 40 °C incubation experiment for total CO_2-C and $\delta^{13}C$ analyses. The sampling intervals were varied for the two incubation temperatures because of the expected differences in the CO_2 emission rates at the two temperatures.

3.2.3. Total and biochar carbon mineralisation

The amount of CO_2 respired from biochar amended and control soils was determined by titrating a 1 ml aliquot of the CO_2 trap solution against 0.1 M HCl, using phenolphthalein as the indicator. To determine $\delta^{13}C$ signature of the CO_2 evolved

from soil and soil-biochar mixtures, a 10 ml aliquot of the CO_2 trap solution was mixed with 10 ml of 1.25 M $SrCl_2$ to precipitate the trapped CO_2 as $SrCO_3$. The precipitates were analysed for $\delta^{13}C$ using the procedure described by Keith et al. (2011).

The proportion of biochar-derived CO_2-C ($C_{Biochar}$ (%)) in the total CO_2-C produced was determined using the following two-pool ^{13}C isotopic mixing model:

$$C_{Biochar}\,(\%) = \frac{(\delta_T{}^{13}CO_2 - \delta_C{}^{13}CO_2)}{(\delta_B{}^{13}CO_2 - \delta_C{}^{13}CO_2)} \times 100\,, \qquad (3.1)$$

where $\delta_T{}^{13}CO_2$ is the $\delta^{13}C$ value of the total CO_2-C evolved from biochar-soil mixtures, $\delta_C{}^{13}CO_2$ is the $\delta^{13}C$ value for the CO_2-C evolved from the same soil without biochar amendment and $\delta_B{}^{13}C$ is the $\delta^{13}C$ isotopic composition of the fresh biochar. Using the proportion of CO_2-C derived from biochar, the proportion and amount of native soil C mineralised was determined. The results on the dynamics and magnitude of priming effect of biochars on soil organic C mineralisation will be published separately.

The daily rates of C mineralisation from native soil and biochar were calculated from the amounts of CO_2-C released over a given sampling period and the number of days in the sampling period (Kuzyakov et al., 2009; Luo et al., 2011; Singh et al., 2012).

The cumulative proportion of added biochar-C mineralised over 12 months across all treatments was fitted to a two-pool exponential model to estimate the MRT of biochars (Keith *et al.*, 2011):

$$C_{Bt}(\%) = C_L \times \left(1 - e^{-k_L t}\right) + (100 - C_L) \times (1 - e^{-k_R t}), \qquad (3.2)$$

where C_{Bt} (%) is the cumulative proportion of added biochar-C mineralised at time (t); $C_L$and $(100-C_L)$ are the proportions of labile (easily-mineralisable) and recalcitrant (slowly-mineralisable) pools in biochar-C, respectively; k_L and k_R are the mineralisation rate constants for the labile and recalcitrant pools, respectively. The Solver add-in tool in Microsoft Excel was used to estimate the model parameters by minimising the sum of the squared errors between modelled and measured values of the cumulative proportion of added biochar-C mineralised over 12 months. The mean residence time (MRT) is the inverse ($1/k_L$ or $1/k_R$) of the mineralisation rate

constant. Model parameters were obtained separately for each replication, and standard errors were calculated from four replicates.

3.2.4. Statistical analysis

Repeated measures analyses were performed for total C and biochar-C mineralisation rates separately for each temperature using a linear mixed model framework in the Genstat® 14th edition (VSN International, 2011). Each analysis consisted of fixed effects of soil and biochar treatments, time and all associated interactions, and random effects of replicate and replicate by time. To allow for correlation between repeated measures on the same units, a first order autoregressive model was fitted (giving a larger residual log-likelihood than the power model). Heterogeneity in the residual variances between time-points was included as it was deemed significant using a residual likelihood ratio test. For the cumulative (after 12 months) total C and biochar-C mineralisation, a three-way (soil, biochar and temperature) analysis of variance was performed in the Genstat® 14th edition of the log-transformed response (to remove variance heterogeneity between temperatures) with random effects of replicates. Wald-type F statistics (with Kenward-Roger adjustments) were calculated for all fixed terms and associated interactions. Where the F-statistic was significant, the means were compared using the LSD test at the 5% significance level unless stated otherwise.

3.3. Results

3.3.1. Total carbon mineralisation

Total C mineralisation rate (expressed as mg CO_2-C released per unit of total organic C per day, mg CO_2-C g^{-1} TOC day^{-1}) was initially large across all treatments and decreased with time in an exponential manner. The exception were (i) the non-amended Inceptosol at 40 °C where the total C mineralisation rate increased up to day 9 and then decreased with time, and (ii) the Vertisol at 40 °C where the rate of total C mineralisation in the 450 °C biochar amended and non-amended treatments increased between three and eight months and then decreased or stabilised (**Figure 3.1**). All main and interactive effects of biochar, soil and time on the rate of total C mineralisation at each incubation temperature were highly significant ($P < 0.001$) (**Table 3.3**). The total C mineralisation rate was consistently less (or similar, particularly at the later stages of incubation) for the biochar-amended soils than for

the correspoding non-amended soils. The only exception was the Inceptisol where the total C mineralisation rate was greater for the biochar-amended than for the non-amended soil in the first three and/or nine days of incubation. Total C mineralisation rates for the biochar-amended and non-amended soils followed the sequence: Vertisol ≤ Oxisol ≤ Entisol ≤ Inceptisol at both incubation temperatures.

Over the 12-months incubation time, the cumulative amount of total C mineralised ranged between 6.2 and 164 mg CO_2-C g^{-1} TOC and followed the sequence: Vertisol ≤ Oxisol ≤ Entisol ≤ Inceptisol across biochar and temperature treatments (**Figure 3.2**). All main and interactive effects of biochar, soil and time on total C mineralisation were highly significant ($P < 0.001$) (**Table 3.4**). The cumulative of total C mineralised was significantly larger for the 450 °C than for the 550 °C biochar-amended soil (**Table 3.S2**). The total C mineralised for the two biochar treatments was significantly less than the non-amended treatments after 12 months (**Figure 3.2**; **Table 3.S2**), with the exception of the Vertisol at 20° C where the total C mineralised was significantly greater for the 450 °C biochar-amended soil than for the non-amended soil. The cumulative of total C mineralised was significantly greater at 40 °C than at 20 °C across the biochar and soil treatments (**Figure 3.2**; **Table 3.S2**).

The $\delta^{13}C$ signatures of the CO_2 evolved from the biochar-amended and non-amended soils along the incubation time at 20 and 40° C are given in the Supporting Information (**Figure 3.S1**). These data show that the $\delta^{13}C$ signatures of the CO_2 evolved from the biochar-amended soils were more negative than from the non-amended soil throughout the incubation period. For each of the amended soils, the $\delta^{13}C$ signatures were relatively more negative for the 450° C biochar than the 550° C biochar at most stages of incubation (**Figure 3.S1**).

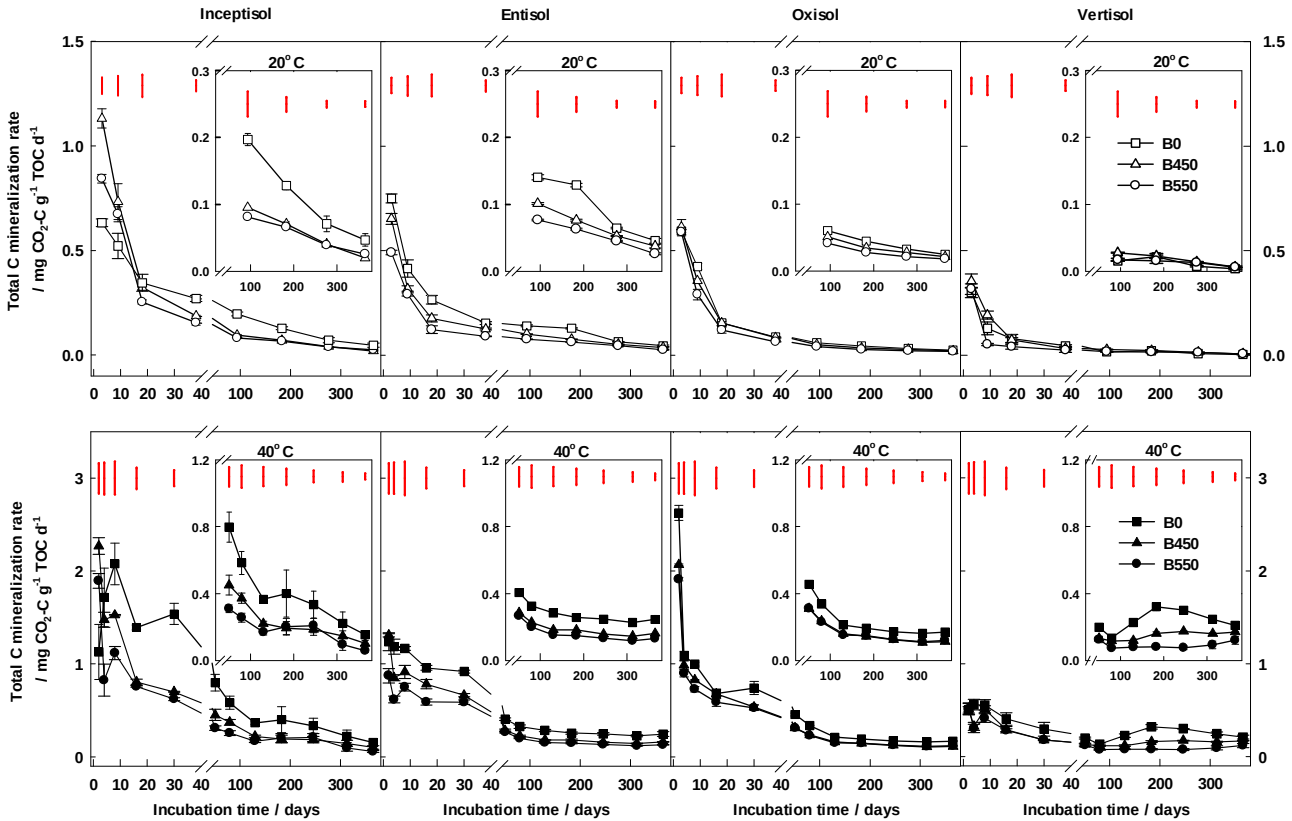

Figure 3.1. Total carbon (C) mineralisation rate (mg CO_2 emission of per gram total organic C per day, mg CO_2-C g^{-1} TOC d^{-1}) from different soil-biochar mixtures incubated at 20 °C (open symbols) and 40 °C (closed symbols) over the 12-month incubation period. Square, triangle and circle symbols represent control (without biochar), 450 and 550 °C biochar-amended soils, respectively. Error bars represent ± standard errors of the mean (n=4). Thick bars show least significant differences (at 5% level, $LSD_{0.05}$) of the interaction of soil and biochar types at different time-points for each incubation temperature.

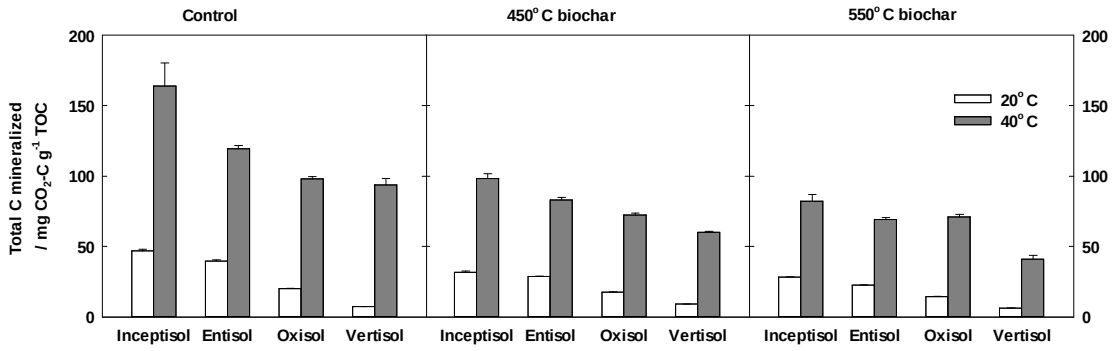

Figure 3.2. Total carbon (C) mineralised (mg CO_2 emission per gram of total organic C, mg CO_2-C g^{-1} TOC) from control (without biochar), 450 and 550 °C biochar-amended soils incubated at 20 °C (white histograms) and 40 °C (grey histograms) after 12-months incubation Error bars represent ± standard errors of the mean (n = 4).

3.3.2. Biochar carbon mineralisation

There was a rapid mineralisation rate of biochar-C up to day 3 (0.09−0.64 mg CO_2-C g^{-1} biochar-C day^{-1}) which then decreased rapidly to slow rates (0.005−0.065 mg CO_2-C g^{-1} biochar-C day^{-1}) over 12 months across all treatments (**Figure 3.3**). However, at 40 °C, the biochar-C mineralisation rate increased for the first eight days in the Inceptisol and Entisol for both biochars, and in the Vertisol for the 450° C biochar, and then decreased with time in an exponential fashion in the Inceptisol, or decreased but stabilised over time in the Entisol and the Vertisol (**Figure 3.3**). All main and interactive effects of biochar, soil and time on biochar-C mineralisation rate were highly significant ($P < 0.001$) (**Table 3.3**). Biochar-C mineralisation rates varied from significant to non-significant differences with time among the soil and biochar treatments at each of the incubation temperatures; the differences among the soil treatments were more pronounced for the 450 °C than the 550 °C biochar treatment, and also at 40 °C than 20 °C (**Figure 3.4**; **Table 3.S2**). Biochar-C mineralisation rates were slower for the 550 °C biochar than for the 450 °C biochar, and at 20 °C than 40 °C at most stages of the incubation period across all soils.

The cumulative proportion (% of added biochar-C) and amount (mg CO_2-C g^{-1} initial native SOC) of biochar-C mineralised after 12 months was significantly ($P = 0.009$) influenced by the interactive effects of soil, biochar and/or incubation

temperature treatments (**Figures 3.4 and 3.5; Table 3.4**). The proportions of the added biochar-C mineralised over 12 months varied from 0.30 to 2.71% across all treatments. At 20 °C, the proportion of biochar-C mineralised in the 450 °C biochar-amended Entisol was 1.14%, which was significantly larger than for the other soils (0.65−0.86%); the smallest proportion of biochar-C was mineralised from the Inceptisol. At 40 °C, the smallest proportion (1.47%) of biochar-C was mineralised in the 450 °C biochar-amended Oxisol; the extent of biochar-C mineralised was similar for the other three soils (2.29−2.71%). The proportion of biochar-C mineralised from the 550 °C biochar-amended soils was similar across soils at each of the incubation temperatures (0.30 to 0.42% for 20 °C and 0.97 to 1.16% at 40 °C), except for a significantly smaller proportion of biochar-C mineralised in the Vertisol than the Inceptisol at 20° C (**Figure 3.4**; **Table 3.S2**). When expressed on per unit basis of initial native SOC, the amount of biochar-C mineralised followed the sequence: Oxisol < Entisol ≤ Vertisol < Inceptisol across both biochar and both incubation temperature treatments, except for 450 °C biochar at 20 °C where the sequence was Oxisol < Vertisol < Entisol < Inceptisol (**Figure 3.5**). The proportion of the added biochar-C and amount of biochar-C mineralised (mg CO_2-C g^{-1} initial native SOC) were significantly greater (i) for the 450 °C biochar-amended soils than the 550 °C biochar-amended soils at both temperatures, and (ii) at 40 °C than 20 °C across all biochar and soil treatments (**Figures 3.4** and **Fiugre 3.5**). The extent of increase in biochar-C mineralisation with increasing temperature was smaller in the Oxisol than the other soils, particularly for the 450 °C biochar.

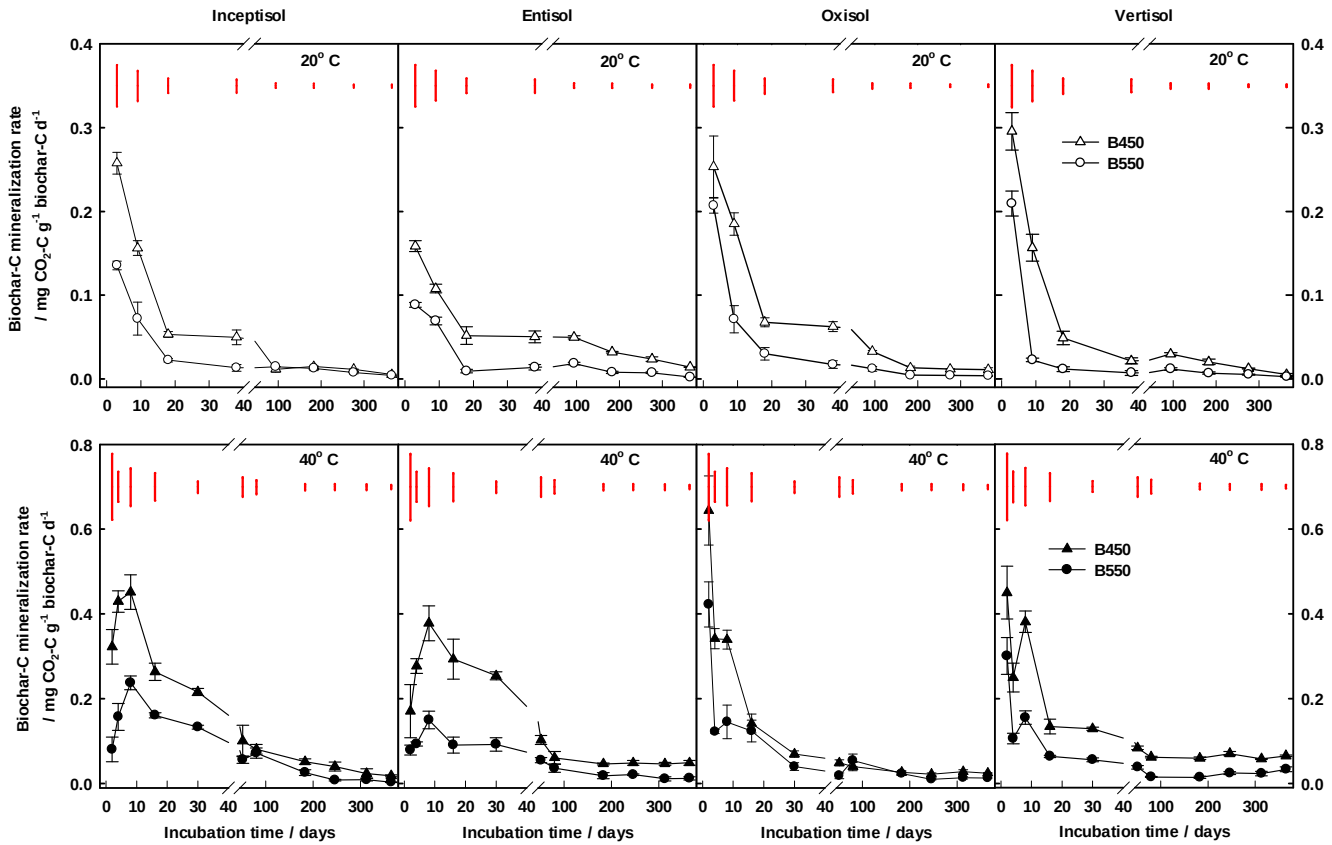

Figure 3.3. Biochar carbon (C) mineralisation rate (mg CO_2-C g^{-1} biochar-C day^{-1}) from soils amended with 450 and 550 °C biochars incubated at 20 °C (open symbols) and 40 °C (closed symbols) over 12 months incubation. Error bars represent ± standard errors of the mean (n = 4). Thick bars show least significant differences (at 5% level, $LSD_{0.05}$) of the interaction of soil and biochar types at different time-points for each incubation temperature.

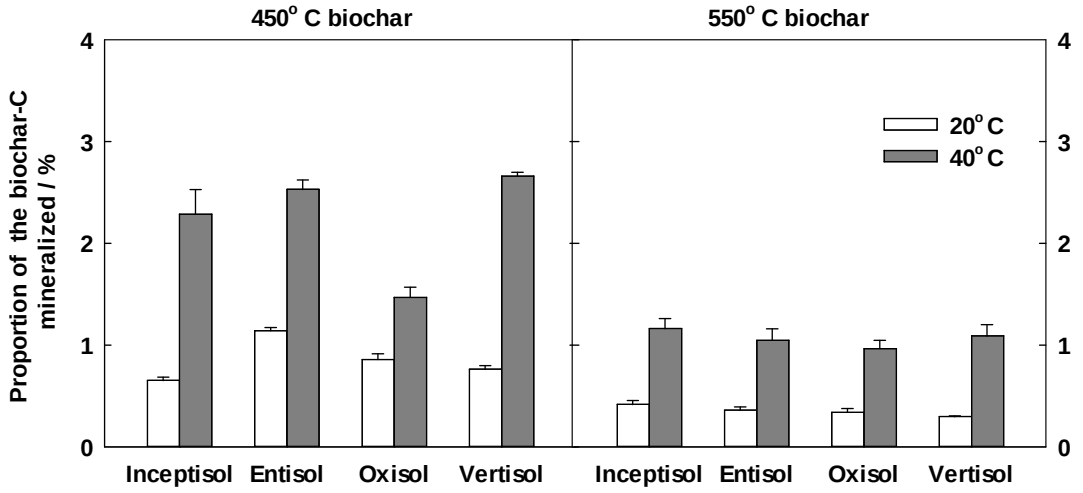

Figure 3.4. The proportion (%) of biochar carbon (C) mineralised from soils amended with 450 and 550 °C biochars incubated at 20 °C (white histograms and 40 °C (grey histograms) after 12-months incubation. Error bars represent ± standard errors of the mean (n=4).

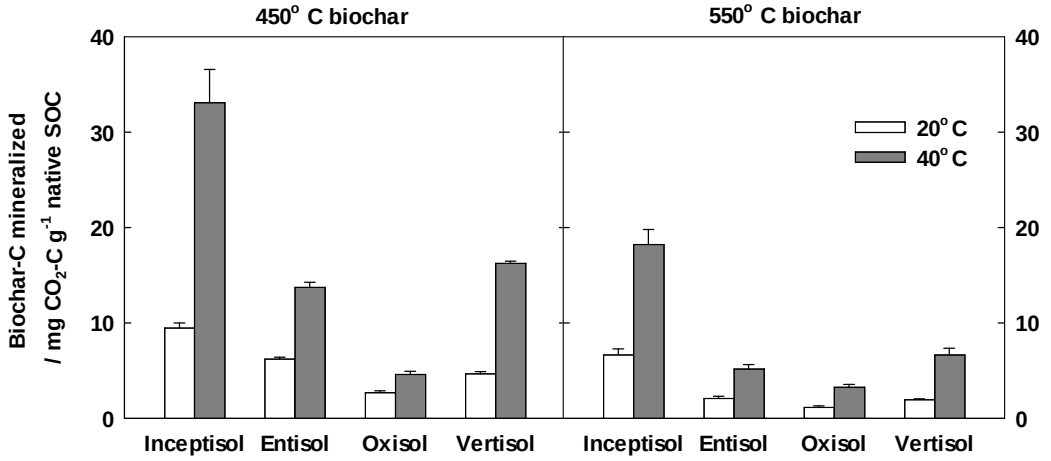

Figure 3.5. Biochar carbon (C) mineralised (mg CO_2 emission per gram of native soil organic C, mg CO_2-C g^{-1} native SOC) from soils amended with 450 and 550 °C biochars incubated at 20 °C (white histograms) and 40 °C (grey histograms) after 12-months incubation. Error bars represent ± standard errors of the mean (n = 4).

3.3.3. Mean residence time of biochar carbon in soil

The estimated MRT of recalcitrant biochar-C varied between 214 and 610 years at 20 °C and 44 and 439 years at 40 °C across soil and biochar treatments (**Table 3.2**). The model-derived labile biochar-C constituted between 0.09 and 0.70% of the total biochar-C at 20° C, with MRT of 5 to 107 days, and between 0.20 and 1.19% at 40 °C, with MRT of 9 to 45 days, across soil and biochar treatments. In general, the MRT of biochar-C increased with increasing pyrolysis temperature, and decreased with increasing incubation temperature. There was no clear pattern for the soil influence on the biochar MRT.

Table 3.2. Mean residence time of labile and recalcitrant pools of biochar carbon (C) and their proportions (%) in the four soils estimated using a two-pool exponential model fitted to the cumulative biochar-C mineralised over 12 months. B450 and B550 represent 450 and 550 °C biochar, respectively.

Soil taxonomy order	Biochar	Mean residence time[a]				Model fit (R^2)		Labile C / %	
		Labile C / days		Recalcitrant C / years					
		20 °C	40 °C	20 °C	40 °C	20 °C	40 °C	20 °C	40 °C
Inceptisol	B450	13 (±2)	33 (±5)	259 (±11)	102 (±23)	0.989-0.996	0.992-0.999	0.29 (±0.03)	1.19 (±0.20)
	B550	24 (±12)	45 (±1)	344 (±23)	439 (±82)	0.983-0.987	0.995-0.999	0.15 (±0.03)	0.82 (±0.04)
Entisol	B450	107(±16)	26 (±2)	214 (±21)	62 (±4)	0.997-0.999	0.996-0.999	0.70 (±0.07)	0.90 (±0.06)
	B550	49(±6)	29 (±3)	610 (±112)	178 (±36)	0.985-0.993	0.992-0.997	0.19 (±0.03)	0.40 (±0.02)
Oxisol	B450	24 (±1)	9 (±1)	235 (±24)	106 (±12)	0.994-0.997	0.992-0.999	0.43 (±0.02)	0.50 (±0.02)
	B550	11 (±4)	30 (±11)	579 (±60)	190 (±16)	0.984-0.996	0.980-0.997	0.17 (±0.03)	0.45 (±0.08)
Vertisol	B450	26 (±15)	11 (±1)	218 (±14)	44 (±1)	0.978-0.987	0.999	0.34 (±0.06)	0.42 (±0.01)
	B550	5 (±3)	9 (±1)	450 (±22)	126 (±20)	0.966-0.990	0.982-0.994	0.09 (±0.02)	0.20 (±0.01)

The numbers in parentheses are the standard error of the mean (n=4).
[a] The mean residence time is the inverse ($1/k_L$ or $1/k_R$) of the mineralisation rate constant.

Table 3.3. Wald F statistics for the fixed terms of incubation time, soil and biochar and their associated interactions on the tested dependent variables.

Source	Degrees of freedom / d.f.	Wald F statistic / d.f.	Denominator degrees of freedom / d.d.f	*P > F*
Total C mineralisation rate / mg CO_2-C g^{-1} TOC d^{-1}				
20 °C				
Day	7	1273.61	103.4	< 0.001
Soil	3	1347.4	85	< 0.001
Biochar	2	420.66	85	< 0.001
Day × soil	21	87.09	155.8	< 0.001
Day × biochar	14	21.52	136.9	< 0.001
Soil × biochar	6	101.82	85	< 0.001
Day × soil × biochar	42	10.43	178.4	< 0.001
40 °C				
Day	11	329.85	146.5	< 0.001
Soil	3	52.91	83.3	< 0.001
Biochar	2	231.9	83.3	< 0.001
Day × soil	33	35.15	230.4	< 0.001
Day × biochar	22	6.77	200.3	< 0.001
Soil × biochar	6	8.28	83.3	< 0.001
Day × soil × biochar	66	4.16	266.1	< 0.001
Biochar-C mineralisation rate / mg CO_2-C g^{-1} biochar-C d^{-1}				
20 °C				
Day	7	243.19	68.9	< 0.001
Soil	3	30.79	54.6	< 0.001
Biochar	1	338.09	54.6	< 0.001
Day × soil	21	9.39	100.4	< 0.001
Day × biochar	7	28.31	68.9	< 0.001
Soil × biochar	3	35.3	54.6	< 0.001
Day × soil × biochar	21	3.51	100.4	< 0.001
40 °C				
Day	10	141.41	34	< 0.001
Soil	3	56.34	53.5	< 0.001
Biochar	1	389.92	53.5	< 0.001
Day × soil	30	15.4	125.3	< 0.001
Day × biochar	10	21.43	82.9	< 0.001
Soil × biochar	3	19.56	53.5	< 0.001
Day × soil × biochar	30	2.45	125.3	< 0.001

Table 3.4. Wald F statistics for the fixed terms of soil, biochar, temperature and their associated interactions on the tested dependent variables.

Source	Degrees of freedom / d.f.	Wald F statistic / d.f.	Denominator degrees of freedom / d.d.f	*P > F*
Total C mineralised / mg CO_2-C g^{-1} TOC				
Soil	3	1048.2	69.0	< 0.001
Biochar	2	389.65	69.0	< 0.001
Temperature	1	10429.04	69.0	< 0.001
Soil × biochar	6	13.19	69.0	< 0.001
Soil × temperature	3	266.27	69.0	< 0.001
Biochar × temperature	2	28.57	69.0	< 0.001
Soil × biochar × temperature	6	13.89	69.0	< 0.001
Proportion of biochar-C mineralised / %				
Soil	3	6.54	48.0	< 0.001
Biochar	1	415.25	48.0	< 0.001
Temperature	1	691.22	48.0	< 0.001
Soil × biochar	3	7.78	48.0	< 0.001
Soil × temperature	3	7.09	48.0	< 0.001
Biochar × temperature	1	3.59	48.0	0.064
Soil × biochar × temperature	3	4.3	48.0	0.009
Biochar-C mineralised / mg CO_2-C g^{-1} native SOC				
Soil	3	304.42	45.0	< 0.001
Biochar	1	355.03	45.0	< 0.001
Temperature	1	657.5	45.0	< 0.001
Soil × biochar	3	9.51	45.0	< 0.001
Soil × temperature	3	6.6	45.0	< 0.001
Biochar × temperature	1	1.94	45.0	0.171
Soil × biochar × temperature	3	4.35	45.0	0.009

3.4. Discussion

3.4.1. Biochar carbon stability in soil

There have been some recent studies on the assessment of biochar-C stability in soil or sand mixtures (Kuzyakov et al., 2009; Nguyen & Lehmann, 2009; Nguyen et al., 2010; Zimmerman, 2010; Keith et al., 2011; Singh et al., 2012). To our knowledge, this is the first research that has focussed on improving our understanding of the stability of wood biochar, with distinct $\delta^{13}C$ signatures from that in soils, across four soils of contrasting properties at two incubation temperatures. The decrease in the fraction of total C mineralised after application of biochar to the soils, which was greater for the 550 °C biochar than the 450 °C biochar (**Figures 3.1 and 3.2**), suggests that biochar-C is relatively more recalcitrant than native organic C in the soils; this pattern has also been observed by (Cheng et al., 2008b). The proportions of biochar-C mineralised in our study across all treatments (0.30−2.71%) are similar to the range (0.4−3.0%) reported by Zimmerman (2010) also over a 12-month incubation, despite differences in biochar types, incubation media (soil compared with sand) and incubation temperature (20−40 °C compared with 32 °C). However, the proportions of biochar-C mineralised at 40 °C in our study (0.97−2.71%) are less than those reported by Nguyen et al. (2010) who reported a loss of 11−14% of oak wood biochar-C over 12-months incubation at 45 °C. As hypothesized by Singh et al. (2012), the differences in biochar-C mineralisation in Nguyen et al. (2010) and our study may be related to the use of a shorter residence time in the Daisy Reactor (about 20 minutes compared with our 40 minutes) by Nguyen et al. (2010), thus producing biochar with less intrinsic chemical recalcitrance than our biochar. Kuzyakov et al. (2009) found that 2.8−3.2% of the added biochar-C was mineralised over 12 months in a 39-month incubation study. The greater biochar-C mineralisation in the latter study than in ours study may be attributed to the grass-derived biochar, which mineralises faster than wood-derived biochars (Zimmerman, 2010). Similarly, Hilscher & Knicker (2011) reported a much faster degradation rate of char C than we did, recovering 62–65% of added C in soil after 28 months, possibly because their char was produced at low (350° C) temperature by charring biomass under oxic conditions (for 1–4 minutes) and hence having less chemical recalcitrance than in our study.

The greater C mineralisation of the 450 °C biochar than the 550 °C biochar across all soils and temperatures (**Figures 3.4 and 3.5**) can be attributed to differences in the relative proportion of alkyl and aromatic C, and the degree of condensation of aromatic C, which varies with biochar production temperature, in addition to biomass feedstock type (McBeath & Smernik, 2009; Singh et al., 2012). Cross & Sohi (2011) also found a decrease in labile (easily mineralisable) C content with increasing pyrolysis temperature. Furthermore, the degree of aromatic C condensation increases with increasing production temperature, which is related to biochar-C stability in soil (McBeath & Smernik, 2009). Several other studies have also found greater C mineralisation of low temperature biochars than of high temperature biochars (Baldock & Smernik, 2002; Zimmerman, 2010; Pereira et al., 2011).

Our results of initially high, progressively slower and then relatively stable biochar-C mineralisation over time are consistent with other temporal C mineralisation observations reported in the literature (Hamer et al., 2004; Kuzyakov et al., 2009; Zimmerman, 2010; Keith et al., 2011; Luo et al., 2011; Singh et al., 2012). This pattern of biochar-C mineralisation suggests that there are some highly labile C components in biochars, which were mineralised predominantly through biotic decomposition mechanisms (Bruun et al., 2008). We calculated that approximately 40−60% of the total biochar-C mineralised in 12 months was released within the first two months. Following the initial rapid mineralisation, there was a considerable decrease in the biochar-C mineralisation rate (**Figure 3.3**), likely due to slower decomposition of the relatively stable C components in biochars.

The MRT of biochar-C in different soils at 20 °C (214−610 years) and 40 °C (44−439 years) incubation temperatures are similar to those reported in previous studies under a range of environmental conditions (Bird et al., 1999; Kuzyakov et al., 2009). However, a short-term (120 days) study using the same biochars incubated in a Vertisol at 20° C, Keith et al. (2011) indicated a relatively short MRT (62 and 248 years) for the 450 and 550 °C biochars, respectively. These results suggest that the estimated MRT of biochars may increase further as their chemical recalcitrance increases and labile components deplete over time and after interactions with soil minerals. Clearly, longer incubation periods are required to obtain realistic estimates

of biochar-C stability (Singh et al., 2012) and to understand biochar-C stabilisation processes in mineral soils. Moreover, different models may also vary in their estimates of MRT. For example, although similar proportions (0.4−3.0%) of the added biochar-C were mineralised in our study and in Zimmerman's (2010) incubation experiment over 12 months, much larger MRT were reported in Zimmerman's study in which the half-life ranged between 10^2 and 10^7 years, than in our study. These results suggest that there is a need to further evaluate how different models vary in their ability to estimate realistically the stability and MRT of biochar in soils using long-term biochar-C mineralisation data.

3.4.2. The influence of mineralogy and native soil C on biochar carbon stability in soil

Although the soils used in this study had variation in physical, chemical and mineralogical properties (see **Table 3.1**); these variations were not systematic and did not isolate confounding variables. Nevertheless, useful information can be drawn about how soil properties may have influenced biochar-C stability in the soils. For example, when expressed as per unit native SOC, biochar-C mineralised was least in the clayey soils (Oxisol < Vertisol) followed by the sandy clay loam soil (Entisol) and greatest in the sandy soil (Inceptisol) (**Figure 3.5**). These results provide insights of the importance of clay content and mineralogy in stabilising biochar-C mineralisation in the soils. Brodowski et al. (2005) showed that oxidized biochar surfaces can chemically interact with the functional groups of clay minerals and native organic matter in soil. These interactions can decrease C mineralisation through the stabilisation of biochar-C and native SOC in organo-mineral fractions and encapsulation within the soil mineral matrix over time (Glaser et al., 2000; Brodowski et al., 2005). Mineral-organic interactions may be enhanced through accelerated mineralisation conditions in the laboratory (Liang et al. 2010; Keith et al. 2011).

Furthermore, the two clayey soils (Oxisol, Vertisol) had similar clay content (44%) but different clay mineral compositions (variable charged minerals of goethite, hematite, gibbsite and kaolinite in the Oxisol and a predominant permanently charged mineral, smectite, in the Vertisol), organic matter content (Oxisol, 4.39%; Vertisol, 2.5%) and pH (moderately acidic in the Oxisol and alkaline in the Vertisol) (**Table**

3.1). Although the soil pH was probably not ideal for soil microbes in both Oxisol and Vertisol, the large native SOC content in the Oxisol, relative to that of the Vertisol, may support greater microbial activity and biomass for biotic mineralisation of biochar-C (Keith et al., 2011). Thus, our results of less biochar-C mineralised in the Oxisol (**Figure 3.5**) can be attributed to the greater stabilising effects of variable charged minerals in the Oxisol than the permanent charged mineral (smectite) in the Vertisol.

It has been widely accepted that the association between organic matter and clay minerals involves the ligand exchange mechanism (Gu et al., 1994; Kögel-Knabner et al., 2008). The ligand exchange reactions occur between hydroxyl groups, on the surfaces of Fe and Al oxides and at the edges of phyllosilicates, and carboxyl and phenolic groups of organic matter, and these reactions may be stronger with sesquioxides than phyllosilicates (von Lützow et al., 2006). The carboxyl groups developed on biochar surfaces during its ageing in soil (Cheng et al., 2008a) may enhance the interaction of biochar surfaces with clay minerals. Moreover, the acidic pH in the Oxisol may contribute to enhanced organo-mineral association through the ligand exchange reactions (Gu et al., 1994), thus decreasing biochar mineralisation through limiting its accessibility to soil microorganisms (Santos et al., 2012). Fine clay particles may fill the pore spaces of biochar, as observed in scanning electron micrographs of the isolated biochar particles from the soils (micrographs not presented here), and consequently may limit the biotic mineralisation of biochar. The rapid decrease of biochar-C mineralisation in the first two−three weeks in the Oxisol at 40° C than in the other soils (**Figure 3.3**) suggests that interactions with the sesquioxides minerals slowed the mineralisation of the biochar-C over the incubation time. The Entisol contained illite and kaolinite and had the largest amount of calcium, which can also stabilise biochar by ligand exchange and calcium bridging between clay, native organic matter and biochar in soil; these interactions may be weaker than those occurring with sesquioxides in the Oxisol (von Lützow et al., 2006).

The native SOC content may also influence (prime) biochar-C mineralisation (Keith et al., 2011). For example, the larger proportion of the 450 °C biochar-C mineralised in the Entisol, and to some extent (non-significant at $P < 0.05$) in the Vertisol at 20 °C, may be attributed to their larger native SOC contents than in the Inceptisol (**Figure. 3.4**). Some studies have shown that biochar-C mineralisation

increases with increasing input of labile organic matter in the soil (Hamer et al., 2004; Kuzyakov et al., 2009; Keith et al., 2011; Luo et al., 2011). However, for the soils used in our study it is not possible to isolate the effect of SOC content on biochar-C mineralisation from the other confounding variables such as clay content and mineralogy, and pH. Further studies using similar soils with a clear native soil organic matter gradient are required to fully assess the role of native SOC in influencing biochar-C mineralisation.

3.4.3. The influence of incubation temperature on biochar carbon stability in soil

Our results clearly show that biochar-C mineralisation was responsive to changes in the incubation temperature across all soil-biochar treatments (**Figure 3.3, Figure 3.4** and **Figure 3.5**). There are a few distinct differences, however, in the response of biochar-C mineralisation to incubation temperature which depended on the biochar and soil treatments. The extent of increase of biochar-C mineralisation with increasing temperature was more variable for the 450° C biochar than for the 550° C biochar across different soils (**Figures 3.4** and **3.5**). The relatively smaller increase than in the other soils may have resulted from the intensification of the stabilisation effect of variable charged minerals in the Oxisol under accelerated C mineralisation conditions at 40° C (**Figures 3.4 and 3.5**). On the other hand, the greater increase in the 450° C biochar-C mineralisation in the other soils with increasing incubation temperature (**Figures 3.4 and 3.5**) could be because there was little protection from the small amount of clay in the sandy soil (Inceptisol) or limited ligand exchange reactions between biochar and permanent charged clay minerals in the Vertisol and Entisol (von Lützow et al., 2006). Other studies have also found increased biochar-C mineralisation with increasing incubation temperatures across a range of biochars (or chars) incubated in pure sand or on glass beads (Nguyen et al., 2010; Zimmermann et al., 2012). Hence, the resultant stabilisation of biochar in the sesquioxides-dominated mineral soil may negate the influence of high temperatures on biochar-C mineralisation to some extent e.g. such as those observed by Zimmermann et al. (2012) study without the presence of clay minerals.

3.5. Conclusions and implications

This study has shown that the mineralisation of biochar-C varied across soils. Biochar-clay interactions appears to have contributed more to the stabilisation of biochar-C in the variable charge soil (Oxisol) than the soils dominated by permanent charged minerals (Vertisol and Entisol) or sand (Inceptisol). Furthermore, biochar-mineral interactions may be particularly important for the stabilisation of low temperature (450 °C) biochar under accelerated mineralisation conditions at high incubation temperatures (40 °C). Our results also suggest that wood biochar produced at high temperature (550 °C) is more stable than low temperature (450 °C) biochar across all soils and incubation temperatures. From the biochar-C mineralisation results of our study and those reported in the literature, we conclude that both biochar-mineral interactions and the intrinsic chemical recalcitrance of biochar are important in determining the long-term C sequestration potential of biochar in soils.

The estimated MRT of biochars from our 12 months incubation study varied between 44 and 610 years across soil, biochar and temperature treatments. This incubation experiment was conducted under controlled laboratory conditions, the biochar-C stability (mean residence time) and the estimates reported here may vary considerably under natural field conditions.

3.6. References

Baldock, J.A., Smernik, R.J., 2002. Chemical composition and bioavailability of thermally, altered Pinus resinosa (Red Pine) wood. Organic Geochemistry 33, 1093-1109.

Barton, C.V.M., Ellsworth, D.S., Medlyn, B.E., Duursma, R.A., Tissue, D.T., Adams, M.A., Eamus, D., Conroy, J.P., McMurtrie, R.E., Parsby, J., Linder, S., 2010. Whole-tree chambers for elevated atmospheric CO_2 experimentation and tree scale flux measurements in south-eastern Australia: The Hawkesbury Forest Experiment. Agricultural and Forest Meteorology 150, 941-951.

Bird, M.I., Moyo, C., Veenendaal, E.M., Lloyd, J., Frost, P., 1999. Stability of elemental carbon in a savanna soil. Global Biogeochemical Cycles 13, 923-932.

Brodowski, S., Amelung, W., Haumaier, L., Abetz, C., Zech, W., 2005. Morphological and chemical properties of black carbon in physical soil

fractions as revealed by scanning electron microscopy and energy-dispersive X-ray spectroscopy. Geoderma 128, 116-129.

Brodowski, S., John, B., Flessa, H., Amelung, W., 2006. Aggregate-occluded black carbon in soil. European Journal of Soil Science 57, 539-546.

Brown, G., Brindley, G.W., 1980. X-ray Diffraction procedures for clay mineral identification, In: Brindley, G.W., Brown, G. (Eds.), Crystal structures of clay minerals and their Xray identification. Mineralogical Society, London, UK, pp. 305-359.

Bruun, S., Jensen, E.S., Jensen, L.S., 2008. Microbial mineralization and assimilation of black carbon: Dependency on degree of thermal alteration. Organic Geochemistry 39, 839-845.

Chapman, S.J., 1997. Carbon substrate mineralization and sulphur limitation. Soil Biology & Biochemistry 29, 115-122.

Cheng, C.H., Lehmann, J., Engelhard, M.H., 2008a. Natural oxidation of black carbon in soils: Changes in molecular form and surface charge along a climosequence. Geochimica Et Cosmochimica Acta 72, 1598-1610.

Cheng, C.H., Lehmann, J., Thies, J.E., Burton, S.D., 2008b. Stability of black carbon in soils across a climatic gradient. Journal of Geophysical Research-Biogeosciences 113, G02027.

Cheng, C.H., Lehmann, J., Thies, J.E., Burton, S.D., Engelhard, M.H., 2006. Oxidation of black carbon by biotic and abiotic processes. Organic Geochemistry 37, 1477-1488.

Cross, A., Sohi, S.P., 2011. The priming potential of biochar products in relation to labile carbon contents and soil organic matter status. Soil Biology & Biochemistry 43, 2127-2134.

Eckmeier, E., Egli, M., Schmidt, M.W.I., Schlumpf, N., Notzli, M., Minikus-Stary, N., Hagedorn, F., 2010. Preservation of fire-derived carbon compounds and sorptive stabilisation promote the accumulation of organic matter in black soils of the Southern Alps. Geoderma 159, 147-155.

FAO, 2006. World reference base for soil resources 2006, In: World Soil Resources Reports, pp. 67-100. World Soil Resources Reports No. 103. FAO, Rome.

Glaser, B., Balashov, E., Haumaier, L., Guggenberger, G., Zech, W., 2000. Black carbon in density fractions of anthropogenic soils of the Brazilian Amazon region. Organic Geochemistry 31, 669-678.

Gu, B.H., Schmitt, J., Chen, Z.H., Liang, L.Y., Mccarthy, J.F., 1994. Adsorption and desorption of natural organic-matter on iron-oxide–mechanisms and models. Environmental Science & Technology 28, 38-46.

Hamer, U., Marschner, B., Brodowski, S., Amelung, W., 2004. Interactive priming of black carbon and glucose mineralisation. Organic Geochemistry 35, 823-830.

Hilscher, A., Heister, K., Siewert, C., Knicker, H., 2009. Mineralisation and structural changes during the initial phase of microbial degradation of pyrogenic plant residues in soil. Organic Geochemistry 40, 332-342.

Hilscher, A., Knicker, H., 2011. Degradation of grass-derived pyrogenic organic material, transport of the residues within a soil column and distribution in soil organic matter fractions during a 28 month microcosm experiment. Organic Geochemistry 42, 42-54.

IBI, 2012. Standardized product definition and product testing guidelines for biochar that is used in soil. http://www.biochar-international.org/sites/default/files/Guidelines_for_Biochar_That_Is_Used_in_Soil_Final.pdf, (cited 5 March, 2013).

Kaal, J., Schneider, M.P.W., Schmidt, M.W.I., 2012. Rapid molecular screening of black carbon (biochar) thermosequences obtained from chestnut wood and rice straw: A pyrolysis-GC/MS study. Biomass & Bioenergy 45, 115-129.

Keith, A., Singh, B., Singh, B.P., 2011. Interactive priming of biochar and labile organic matter mineralization in a smectite-rich soil. Environmental Science & Technology 45, 9611-9618.

Kögel-Knabner, I., Ekschmitt, K., Flessa, H., Guggenberger, G., Matzner, E., Marschner, B., *et al.*, 2008. An integrative approach of organic matter stabilization in temperate soils: Linking chemistry, physics, and biology. Journal of Plant Nutrition and Soil Science 171, 5-13.

Kuzyakov, Y., Subbotina, I., Chen, H.Q., Bogomolova, I., Xu, X.L., 2009. Black carbon decomposition and incorporation into soil microbial biomass estimated by ^{14}C labeling. Soil Biology & Biochemistry 41, 210-219.

Lehmann, J., Gaunt, J., Rondon, M., 2006. Bio-char sequestration in terrestrial ecosystems–a review. Mitigation and Adaptation Strategies for Global Change 11, 403-427.

Lehmann, J., Rillig, M.C., Thies, J., Masiello, C.A., Hockaday, W.C., Crowley, D., 2011. Biochar effects on soil biota - A review. Soil Biology & Biochemistry 43, 1812-1836.

Liang, B.Q., Lehmann, J., Sohi, S.P., Thies, J.E., O'Neill, B., Trujillo, L., Gaunt, J., Solomon, D., Grossman, J., Neves, E.G., Luizão, F.J., 2010. Black carbon affects the cycling of non-black carbon in soil. Organic Geochemistry 41, 206-213.

Lin, Y., Munroe, P., Joseph, S., Kimber, S., Van Zwieten, L., 2012. Nanoscale organo-mineral reactions of biochars in ferrosol: an investigation using microscopy. Plant and Soil, 369-380.

Luo, Y., Durenkamp, M., De Nobili, M., Lin, Q., Brookes, P.C., 2011. Short term soil priming effects and the mineralisation of biochar following its incorporation to soils of different pH. Soil Biology & Biochemistry 43, 2304-2314.

McBeath, A.V., Smernik, R.J., 2009. Variation in the degree of aromatic condensation of chars. Organic Geochemistry 40, 1161-1168.

McBeath, A.V., Smernik, R.J., Schneider, M.P.W., Schmidt, M.W.I., Plant, E.L., 2011. Determination of the aromaticity and the degree of aromatic condensation of a thermosequence of wood charcoal using NMR. Organic Geochemistry 42, 1194-1202.

Midwood, A.J., Boutton, T.W., 1998. Soil carbonate decomposition by acid has little effect on delta ^{13}C of organic matter. Soil Biology & Biochemistry 30, 1301-1307.

Murage, E.W., Voroney, P., Beyaert, R.P., 2007. Turnover of carbon in the free light fraction with and without charcoal as determined using the ^{13}C natural abundance method. Geoderma 138, 133-143.

Nguyen, B.T., Lehmann, J., 2009. Black carbon decomposition under varying water regimes. Organic Geochemistry 40, 846-853.

Nguyen, B.T., Lehmann, J., Hockaday, W.C., Joseph, S., Masiello, C.A., 2010. Temperature sensitivity of black carbon decomposition and oxidation. Environmental Science & Technology 44, 3324-3331.

Pereira, R.C., Kaal, J., Arbestain, M.C., Lorenzo, R.P., Aitkenhead, W., Hedley, M., Macias, F., Hindmarsh, J., Macia-Agullo, J.A., 2011. Contribution to

characterisation of biochar to estimate the labile fraction of carbon. Organic Geochemistry 42, 1331-1342.

Santos, F., Torn, M.S., Bird, J.A., 2012. Biological degradation of pyrogenic organic matter in temperate forest soils. Soil Biology & Biochemistry 51, 115-124.

Singh, B.P., Cowie, A.L., Smernik, R.J., 2012. Biochar carbon stability in a clayey soil as a function of feedstock and pyrolysis temperature. Environmental Science & Technology 46, 11770-11778.

von Lützow, M., Kögel-Knabner, I., Ekschmitt, K., Matzner, E., Guggenberger, G., Marschner, B., Flessa, H., 2006. Stabilization of organic matter in temperate soils: mechanisms and their relevance under different soil conditions - a review. European Journal of Soil Science 57, 426-445.

VSN International, 2011. GenStat for Windows 14th Edition. Hemel Hempstead, UK: VSN International.

Woolf, D., Amonette, J.E., Street-Perrott, F.A., Lehmann, J., Joseph, S., 2010. Sustainable biochar to mitigate global climate change. Nature Communications 1, 56.

Zimmerman, A.R., 2010. Abiotic and microbial oxidation of laboratory-produced black carbon (biochar). Environmental Science & Technology 44, 1295-1301.

Zimmermann, M., Bird, M.I., Wurster, C., Saiz, G., Goodrick, L., Barta, J., Capek, P., Santruckova, H., Smernik, R., 2012. Rapid degradation of pyrogenic carbon. Global Change Biology 18, 3306–3316.

3.7. Supporting information

Methods for XRD and SSA analysis

For the identification of clay minerals in the experimental soils, soil samples were dispersed in dilute NaOH and the clay fraction (< 2 µm) was separated by dispersion sedimentation procedure. Dispersed clays were deposited on to ceramic tiles and the oriented clays were analysed by X-ray diffraction (XRD) following standard pretreatments (Brown & Brindley, 1980). Random powder XRD patterns were also obtained by filling the cavity of Al-holder with powdered clay fractions of the soils. X-ray diffraction patterns were obtained using a GBC MMA diffractometer (CoKα radiation at 35 kV and 28.5 mA, step size 0.02°θ and scan speed 1.0° θ per minute). The minerals in the clay fraction were estimated by comparing integrated peak areas of the minerals with the known mixtures of standard minerals.

For specific surface area and pore volume analyses of biochars, CO_2 adsorption isotherms were collected at 273K. The samples were degassed under vacuum for 12 hours at 573K before obtaining the isotherms. The analysis was done by using a Micromeritics ASAP 2020 surface area and porosity analyser.

References

Brown, G. & Brindley, G.W. 1980. X-ray Diffraction procedures for clay mineral identification. In: Crystal structures of clay minerals and their Xray identification (eds. Brindley, G.W. & Brown, G.), pp. 305-359. Mineralogical Society, London, UK.

Table 3.S1. Total organic C of initial biochar-soil treatments. B450−SOC and B550−SOC represent SOC contents for the 450 and 550 °C biochar-amended soils.

Property	**Inceptisol**	**Entisol**	**Oxisol**	**Vertisol**
WRB order	Arenosols	Calcisol	Ferralsol	Vertisol
B450 − SOC (%)	2.15 (±0.11)	3.90 (±0.21)	5.77 (±0.01)	3.63 (±0.02)
B550 − SOC (%)	2.33 (±0.13)	4.12 (±0.23)	5.84 (±0.03)	3.71 (±0.04)

The numbers in parentheses are the standard error of the mean (n=4).

Table 3.S2. Predicted means and associated LSD values for the tested dependent variables (log-transformed).

Soil	Biochar	Temperature		LSD
		20 °C	40 °C	
Total C mineralised / mg CO_2-C g^{-1} TOC				
Inceptisol	B0	3.84	5.09	0.10
	B450	3.45	4.59	
	B550	3.34	4.40	
Entisol	B0	3.68	4.78	
	B450	3.36	4.42	
	B550	3.12	4.24	
Oxisol	B0	3.00	4.58	
	B450	2.86	4.28	
	B550	2.66	4.26	
Vertisol	B0	1.97	4.54	
	B450	2.20	4.09	
	B550	1.82	3.70	
Proportion of biochar-C mineralised / %				
Inceptisol	B450	-0.43	0.81	0.22
	B550	-0.87	0.14	
Entisol	B450	0.13	0.93	
	B550	-1.04	0.03	
Oxisol	B450	-0.16	0.38	
	B550	-1.11	-0.05	
Vertisol	B450	-0.28	0.98	
	B550	-0.87	0.14	
Biochar-C mineralised / mg CO_2-C g^{-1} native SOC				
Inceptisol	B450	2.25	3.48	0.22
	B550	1.89	2.89	
Entisol	B450	1.83	2.62	
	B550	0.74	1.72	
Oxisol	B450	0.99	1.52	
	B550	0.13	1.18	
Vertisol	B450	1.54	2.79	
	B550	0.68	1.88	

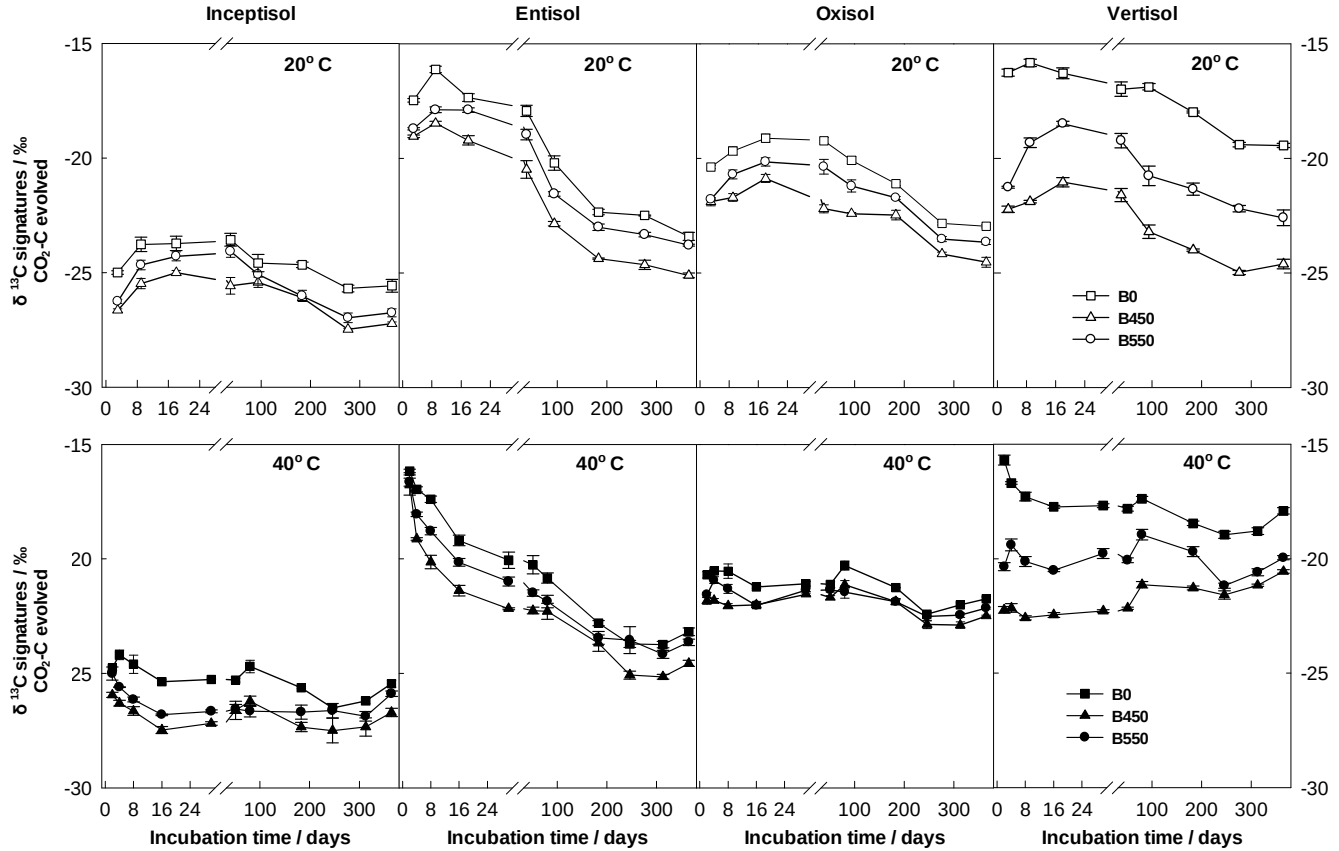

Figure 3.S1. $\delta^{13}C$ signatures (‰) of CO_2-C evolved from control (B0), 450 °C (B450) and 550 °C (B550) biochar amended soil incubated at 20 °C (open symbols) and 40 °C (closed symbols) for 12 months. Square, triangle and circle symbols represent B0, B450 and B550 treatments, respectively. Error bars represent ± standard errors of the mean (n=4).

Chapter 4: Biochar carbon stability and priming effects in four contrasting biochar-amended soils: long-term incubations at different temperatures[2]

Abstract

The aim of this work was to monitor the priming effect of biochar on native soil organic carbon (SOC) and to determine biochar-C stability over a two-year period in different soils. Two biochars, produced from δ^{13}C-depleted *Eucalyptus saligna* woody biomass (-36.4 ‰) by slow pyrolysis at 450 and 550 °C, were added to four soils (Inceptisol, Entisol, Oxisol and Vertisol) and the soil-biochar mixtures were incubated at 20, 40 and 60 °C.

The direction and magnitude of priming effect of biochar on SOC varied with soil, biochar, incubation temperature and time, ranging from -32.6 mg CO_2-C g^{-1} SOC in the 550 °C biochar amended Vertisol incubated at 60 °C to 48.3 mg CO_2-C g^{-1} SOC in the 450 °C biochar amended Inceptisol incubated at 40 °C. At 20 and 40 °C, both biochars caused positive priming of native SOC in the Inceptisol; in the other soils, biochars had either negative priming or negligible positive priming on native SOC. The 550 °C biochar caused a smaller positive (Inceptisol) or a greater negative (Entisol, Oxisol and Vertisol) priming of native SOC than the 450 °C biochar. The priming effect of biochar on native SOC changed with time; generally positive or no priming occurred during the first month, which remained positive in the Inceptisol, and shifted to negative priming with time in the Entisol, Oxisol and Vertisol. At 60 °C, positive priming was observed in the first ~6 months that changed to no priming afterwards in the Inceptisol; whereas negligible positive or negative priming occurred in the other soils in the first ~6 months that changed to positive priming in the Entisol and Oxisol, and to negative priming in the Vertisol, at the end of incubation.

[2] This chapter has been submitted to Soil Biology and Biochemistry under the title "Biochar carbon stability and priming effects in four contrasting biochar-amended soils: long-term incubations at different temperatures" in August 2013. Authors are Yunying Fang, Balwant Singh and Bhupinder Pal Singh.

The proportion of added biochar-C mineralised in soils over the two-year period was significantly ($p < 0.001$) higher for the 450 °C biochar (0.80−10.58%) than the 550 °C biochar (0.43−3.28%). The proportion of the 450 °C biochar-C mineralised was significantly ($p < 0.05$) smaller in the Oxisol and Inceptisol than in the Entisol and Vertisol across the three temperatures. In comparison, the mineralisation of 550 °C biochar-C was less affected by soil type. At 20 °C, the mean residence time (MRT) of 450 °C and 550 °C biochars in the four soils ranged from 341−454 and 732−1061 years, respectively, which is longer than the corresponding values estimated from the 1-year mineralisation data (Fang et al., 2014). At 40 and 60 °C, the MRT of both 450 °C and 550 °C biochars decreased substantially, with values ranging from 25−134 and 93−451 years, respectively. This study shows that wood biochar produced by slow pyrolysis at 550 °C can store C in soil over a century or more even at elevated temperatures. Furthermore, biochar can enhance the stabilisation of native SOC, particularly in the presence of clay and slightly increase the loss of native SOC in sandy soil.

4.1. Introduction

As the increase of atmospheric CO_2 concentration contributes greatly to global warming, there is a pressing need to capture and sequester CO_2 into long-lived plant biomass and soil organic matter pools (Lackner, 2003). Biochar is a solid elemental carbonaceous material obtained from the thermochemical conversion of biomass in an oxygen-limited environment (IBI, 2012). Biochar is a much more durable form of C than parent plant biomass or most forms of C in soil organic matter (Knicker et al., 2013; Lehmann et al., 2009; Santos et al., 2012; Zavalloni et al., 2011). Hence, the application of biochar to soil is being proposed for increasing the stable C pool and restraining the growth of atmospheric CO_2 concentration (Woolf et al., 2010; Lehmann, 2007). In addition to the C sequestration benefits (Lehmann et al., 2006), biochar application to soil has potential to generate other positive benefits, such as improving soil quality and agronomic yield (Glaser et al., 2002; Lehmann and Rondon, 2006; Liang et al., 2006; Van Zwieten et al., 2010) and reducing soil greenhouse gas emissions (Singh et al., 2010).

The addition of biochar may influence the mineralisation of organic C in soil, so called as the priming effects. If biochar increases the mineralisation of soil organic C (SOC), i.e. positive priming effect, the C sequestration benefit from biochar application to soil can be negated and conversely with the negative priming effect the C sequestration effect is increased. Wardle et al. (2008) reported the positive priming effect of wildfire charcoal on the turnover of humus litter C in boreal forests. Similarly, Luo et al. (2011) reported biochar-induced loss of organic C in a mineral soil. Besides the observations of positive priming effect of biochar on SOC mineralisation, negligible or no significant impact of biochar on CO_2 emission from soil, have also been reported (Abiven and Andreoli, 2011; Novak et al., 2010; Spokas and Reicosky, 2009; Zavalloni et al., 2011; Zimmerman et al., 2011). However, these studies have measured the total C emission from soil after biochar addition, the increased CO_2 emission may result from the biotic breakdown of labile organic C in soil or biochar (Cross and Sohi 2011), or the abiotic release of carbonate C in biochar (Jones et al., 2011). Consequently, the increased CO_2 emission from biochar-amended soil cannot be solely attributed to the positive priming effect of biochar on native SOC mineralisation. Cross and Sohi (2011) showed that the increasd CO_2 emission from soil was due to rapid mineralisation of labile components of biochar, and not due to the increased mineralisation of native SOC in the presence of biochar.
Some studies have used C isotope labelling approaches to quantify the mineralisation of biochar-C and native SOC in biochar amended soils (Farrell et al., 2013; Keith et al., 2011; Kuzyakov et al., 2009). Biochar addition to soil was observed to increase the mineralisation of added labile organic matter C (LOM-C) or native SOC (Awad et al., 2012; Farrell et al., 2013; Hamer et al., 2004; Luo et al., 2011), possibly due to enhanced microbial biomass and enzyme production. In contrast to these findings, other researchers have found no influence of biochar on native SOC mineralisation (Jones et al., 2012; Santos et al., 2012). Keith et al. (2011) reported positive priming of native SOC by biochar; however, biochar presence reduced LOM-C mineralisation (negative priming) and the magnitude of negative priming increased with increasing LOM addition rate in a Vertisol. The variable direction and magnitude of the priming effect of biochar reported in the literature may be related to variations in soil properties, including clay mineralogy, clay and native SOC contents and pH. Moreover, the direction and magnitude of priming effect of biochar on native SOC may change with incubation period. For example, a positive priming

effect of biochar on SOC was observed in the first 2−3 months (Farrell et al., 2013; Hamer et al., 2004; Luo et al., 2011), which decreased to negative priming with time (Santos et al., 2012). Besides the possible influence of soil properties and incubation time, the direction and magnitude of biochar's priming effects may change at high incubation temperatures, considering that the mineralisation of SOC and biochar generally increases with increasing temperature (Fang et al., 2014; Kirschbaum, 1995; Nguyen et al., 2010). So far there has been no research on the direct effects of incubation temperature on the priming effect of biochar in different soils.

The C sequestration benefit from biochar is linked to its stability in soil. Several studies have shown that biochar-C mineralises at a very slow rate in soils, e.g. averaged 0.1−3% applied biochar-C mineralised per year (Fang et al., 2014; Knoblauch et al., 2011; Kuzyakov et al., 2009; Liang et al., 2008; Major et al., 2010; Singh et al., 2012; Zimmerman, 2010; Zimmermann et al., 2012). The low mineralisation rate of biochar is mainly attributed to its relatively high chemical recalcitrance (McBeath and Smernik, 2009) and to some extent to its interactions with soil clay minerals and environmental conditions (Fang et al., 2014; Luo et al., 2011). Consequently, it has been demonstrated that the MRT of biochar in soils are in the range of centuries to millennia (Knicker et al., 2013; Kuzyakov et al., 2009; Major et al., 2010; Santos et al., 2012; Singh et al., 2012; Zimmerman, 2010). Incubation period seems an important factor influencing the estimates of biochar MRT since it is a function of the turnover rates of and proportion of constituent C pools in biochar (Singh et al., 2012; Zimmerman and Gao, 2013). For example, shorter MRT (62−248 years) have been reported based on the data of a 4-month incubation study (Keith et al., 2011) compared to the 1-year data (218−450 years) (Fang et al., 2014) for the same biochars incubated in a Vertisol. This could be due to distortion in the modelling data resulting from greater data points for the labile C (i.e. faster mineralisation during the earlier stages) compared to relatively recalcitrant C in biochar in shorter term studies, which may considerably underestimate the MRT of biochar-C. Therefore, long-term C mineralisation data are required to determine the realistic stability of biochar in soil.

Temperature is an important environmental factor influencing the stability of biochar-C in soil. Studies of biochar-C stability to date have been conducted in soil at or below 40 °C (Fang et al., 2014; Hilscher and Knicker, 2011a; Zimmerman, 2010),

or over glass beads at temperatures up to 60 °C (Zimmermann et al., 2012). At high incubation temperatures, biochar-C mineralisation is accelerated through relatively stronger abiotic processes than biotic processes (Zimmermann et al., 2012) and consequently the longevity of biochar is expected to be relatively short (Fang et al., 2014; Zimmermann et al., 2012). For example, in tropical savannah, where the surface soil temperature is usually above 30 °C and may reach up to 60 °C (Zimmermann et al., 2012), the estimated longevity of fire-derived char accumulating on soil surface was of decadal timescales (Bird et al., 1999; Zimmermann et al., 2012). It is possible that increased biochar-soil interactions at high incubation temperatures especially in the presence of reactive clay minerals may slow down the mineralisation of biochar-C and native SOC. Considering the potential of biochar application in tropical and sub-tropical areas for improving soil fertility and increasing soil C sequestration (Glaser et al., 2001; Lehmann and Rondon, 2006; Major et al., 2010), evaluation of biochar-C stability in soils of contrasting properties at high incubation temperatures is required.

Here, we present the result of a two-year laboratory study that used woody biochars (δ^{13}C -36.4 ‰) produced at 450 and 550 °C and incubated in four soils of contrasting properties at 20, 40 and 60 °C. The ^{13}C isotopic differences between biochar and native SOC allowed the quantification of biochar-C and native SOC mineralisation and consequently biochar-C stability and priming effect were assessed in different soils. We hypothesised that (i) the direction and magnitude of priming effect of biochar are dependent on soil type, incubation temperature and duration, and pyrolysis temperature; and (ii) the estimated MRT of biochar in soil will increase with increasing incubation period.

4.2. Materials and methods

4.2.1. Biochars and soils

A δ^{13}C-depleted woody biomass from *Eucalyptus saligna* saplings that had been grown under an elevated CO_2 environment for 2 years (Barton et al., 2010) was used to produce biochars. Biochars were produced by slow pyrolysis at a heating rate of 5−10 °C/min from 20 to 450 °C or 20 to 550 °C, which was followed by holding at 450 or 550 °C for 40 min (Daisy Reactor at Pacific Pyrolysis, Australia).

Surface (0−15 cm) soils were taken from four agricultural fields in Australia (Fang et al., 2014). The experimental soils included a sandy soil − Inceptisol, a sandy clay loamy soil − Entisol, and two clayey soils – an Oxisol and a Vertisol. Properties of the soils and biochars have been described earlier (Fang et al., 2014); the most relevant properties of soils and biochars are shown in **Table 4.1**.

Table 4.1. Some relevant properties of the soils and biochars used in the incubation experiment.

Soil type	pH (1:5 H_2O)	Sand (%)	Silt (%)	Clay (%)	Organic carbon (%)	Inorganic carbon (%)	$\delta^{13}C$ (‰)	Dominant clay minerals
Inceptisol	5.70 (±0.01)	97.5 (±0.1)	1.2 (±0.1)	1.3 (±0.1)	0.95 (±0.02)	−	-28.17 (±0.02)	Kaolinite,
Entisol	8.77 (±0.01)	66.3 (±0.1)	12.2 (±0.2)	21.5 (±0.4)	2.53 (±0.09)	6.01 (±0.06)	-14.08 (±0.01)	Illite, kaolinite
Oxisol	5.65 (±0.01)	24.3 (±2.0)	31.6 (±1.4)	44.1 (±0.6)	4.39 (±0.02)	−	-21.35 (±0.01)	Goethite, gibbsite, kaolinite, hematite, anatase
Vertisol	7.89 (±0.01)	27.3 (±0.7)	28.5 (±0.8)	44.2 (±0.1)	2.25 (±0.04)	−	-17.32 (±0.01)	Smectite, kaolinite
450 °C biochar	8.64 (±0.05)	−	−	−	67.40 (±0.20)	−	-36.34 (±0.01)	−
550 °C biochar	9.96 (±0.01)	−	−	−	73.19 (±0.14)	−	-36.53 (±0.02)	−

The number in the parentheses are the standard error of the mean (n=4).

4.2.2. Laboratory incubation

To investigate the priming effects of biochar on native SOC of the four soils, equivalent to 300 g oven-dried basis and < 2 mm soil fractions were separately mixed with the 450 °C biochar (B450) or the 550 °C biochar (B550) at 20 g kg^{-1} soil (dry weight basis). The incubation experiment is described in detail in Fang et al. (2014). Briefly, the soil-biochar mixtures and control soils were supplied with a microbial inoculum and a nutrient solution, and then the samples were incubated at 20±1 °C, 40±1 °C or 60±1 °C. Soil moisture was periodically monitored and maintained at 70% of the maximum water holding capacity of each soil. Each treatment was replicated four times. The CO_2 evolved was trapped in NaOH and the traps were periodically replaced between 12 and 22 times across different incubation temperatures over the two-year period.

4.2.3. Mineralisation of biochar-C and native SOC

The total soil C mineralised (mg kg^{-1} soil) at each sampling time was determined by titrating a known volume of the trap solution against 0.1 M HCl, using phenolphthalein as the indicator. To determine the $\delta^{13}C$ signature of trapped CO_2-C, a 10 ml aliquot of the CO_2 trap solution was mixed with 10 ml of 1.25 M $SrCl_2$ to precipitate $SrCO_3$. The $\delta^{13}C$ analysis of precipitates was done by an isotope ratio mass spectrometer (IRMS; Delta V, Thermo Finnigan) as described by Keith et al. (2011). The $\delta^{13}C$ signatures (‰) of CO_2-C evolved from control and biochar treatments are shown in Appendix 5.

The proportion of biochar-derived CO_2-C ($C_{Biochar}$ (%)) in the total CO_2-C evolved was determined using a two-pool ^{13}C isotopic mixing model (Kuzyakov and Bol, 2006), as given below:

$$C_{Biochar}\,(\%) = \frac{(\delta_T{}^{13}CO_2 - \delta_C{}^{13}CO_2)}{(\delta_B{}^{13}CO_2 - \delta_C{}^{13}CO_2)} \times 100 \qquad (4.1)$$

where $\delta_T{}^{13}CO_2$ is the $\delta^{13}C$ value of the total CO_2-C evolved from biochar-soil mixtures, $\delta_C{}^{13}CO_2$ is the $\delta^{13}C$ value for the CO_2-C evolved from the same soil but without biochar amendment, and $\delta_B{}^{13}C$ is the ^{13}C isotopic composition of fresh biochar. The proportion of native soil C mineralised was determined by subtracting the proportion of CO_2-C derived from biochar from 100. The amounts of biochar-C

and native SOC mineralised were then calculated and normalised to per gram of added biochar-C and initial native SOC, respectively.

4.2.4. Priming effect

The priming effect (PE) of native SOC induced by biochar was calculated as follows (Kuzyakov and Bol, 2006):

$$PE = C_{B,SOC} - C_{SOC} \quad (4.2)$$

Where, $C_{B,SOC}$ is the amount (mg kg^{-1} soil) of CO_2-C evolved from soil in the presence of biochar and C_{SOC} is the amount (mg kg^{-1} soil) of CO_2-C evolved from soil without biochar (i.e. control soil). The primed native SOC mineralisation was normalised to per gram of initial native SOC.

4.2.5. Biochar and native SOC's mean residence time

A two-pool exponential model was fitted to the time series of cumulative proportion of C mineralised from biochar or native SOC over the 2-year incubation period to estimate their MRT.

$$C_{min}(t) = C_1 \times \left(1 - e^{-k_1 t}\right) + C_2 \times (1 - e^{-k_2 t}) \quad (4.3)$$

Where $C_{min}(t)$ is the cumulative amount of C mineralised (%); and t is the incubation time (days). The parameters, C_1 and C_2, represent the proportion (%) of the labile and recalcitrant C pools in biochar-C or native SOC, respectively; k_1 and k_2 are the mineralisation rate constants for the labile and recalcitrant pools, respectively. It was assumed that $C_1 + C_2 = 100\%$ for the added biochar-C or native SOC mineralised. The parameters, C_1, C_2, k_1 and k_2, were estimated using a nonlinear least-squares curve fitting in SigmaPlot 12.0 by minimising the sum of the squared errors between the modelled and measured values of cumulative C mineralised over the two-year period. The parameters were estimated separately for each replication, and standard errors were calculated from the derived values of four replicates. The MRT is the inverse of the mineralisation rate constant ($1/k_1$ or $1/k_2$).

4.2.6. Statistical analysis

For the cumulative amount of total C and biochar-C mineralised, a three-way (soil, biochar and temperature) analysis of variance was performed using Genstat® 14th edition (VSN International, 2011) of the log-transformed response (to remove

variance heterogeneity between temperatures) with random effects of replicates. For the priming effect, a three-way (soil, biochar and temperature) analysis of variance was performed. Where the F-statistic was significant, the means were compared using the LSD test at the 5% significance level unless stated otherwise.

4.3. Results

4.3.1. Mineralisation of total soil carbon

Over the 2-year incubation period, the cumulative amount of total C mineralised (i.e. biochar + native SOC), expressed as mg CO_2-C released per unit of total organic C (TOC), ranged between 10.3 and 365 mg CO_2-C g^{-1} TOC (**Figure 4.1** and **Figure 4.S1**). The total C mineralised followed the sequence: Vertisol ≤ Oxisol ≤ Entisol ≤ Inceptisol for both biochar-amended and non-amended soils at 20, 40 °C and non-amended soils at 60 °C. For biochar-amended soils at 60 °C the total C was mineralised in the sequence: Vertisol < Inceptisol < Entisol ≈ Oxisol. The total C mineralised from soils amended with the two biochars was significantly smaller than the non-amended treatments; the only exception was the Vertisol at 20 °C where the total C mineralised was significantly greater for the 450 °C biochar-amended soil than the non-amended soil. Overall, the cumulative amount of total C mineralised from the biochar treatments followed the trend: control ≤ 450 °C biochar ≤ 550 °C biochar in each soil. The total C mineralised was significantly ($p < 0.001$) highest at 60 °C, followed by 40 °C, and the lowest at 20 °C. When the total C mineralised was expressed in different unit, i.e. mg CO_2-C kg^{-1} soil (Figure 4.S5), the sequence of total C mineralised from the biochar-amended and non-amended soils changed to the following order: Vertisol < Inceptisol < Oxisol ≤ Entisol at 20 °C; and Inceptisol < Vertisol < Entisol < Oxisol at 40 and 60 °C.

All main and interactive effects of time, biochar and soil on the total C mineralisation rate at each incubation temperature were significant ($p < 0.001$) over the two years incubation period (see Supporting Information 4.7; **Table 4.S1**). Total C mineralisation rates were fast initially across all treatments, which then decreased to slow rates in an exponential manner over 12 months (Fang et al. 2014); the rates continuously remained slow at 20 and 40 °C, or continued to decrease to slower rates

at 60 °C, between 12 and 24 months after incubation. Overall, total C mineralisation rates ranged from 0.006−0.05, 0.04−0.25 and 0.05−0.33 mg CO_2-C g^{-1} TOC d^{-1} at 20, 40 and 60 °C, respectively, in the 12 to 24 months period (**Figure 4.S2**). Generally, total C mineralisation rates were slower for the biochar-amended soils than the corresponding non-amended soils at 20 °C, 40 °C and 60 °C. During the 12 to 24 month incubation period, total C mineralisation rates were not significantly different between soils and biochar treatments at each incubation temperature.

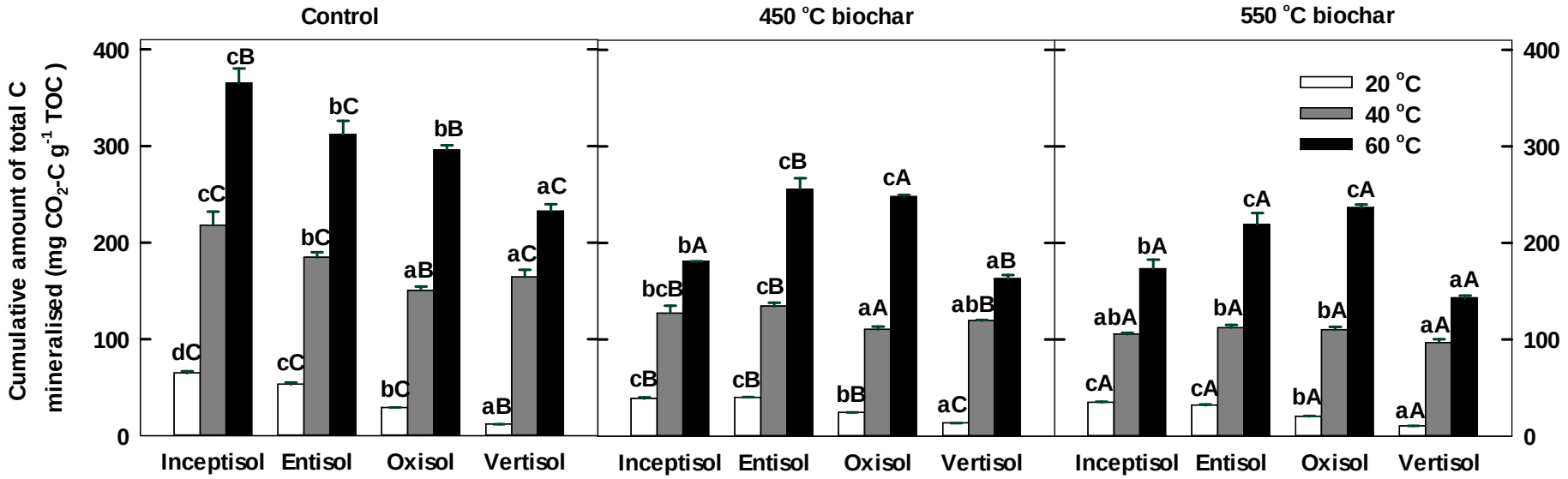

Figure 4.1. Cumulative amounts of total carbon (C) mineralised (mg CO_2-C g^{-1} TOC) from control (without biochar), 450 and 550 °C biochar-amended soils at 20 °C (white columns), 40 °C (grey columns) and 60 °C (black columns) over the 2-year of incubation period. Error bars represent standard error of the means (n = 4). Small letters compare significant differences among soils for each of the biochar or control treatments at each incubation temperature. Capital letters compare significant differences among control, 450 and 550 °C biochar treatments for each of the soil types at each incubation temperature.

4.3.2. Priming effect of biochar on native SOC

The cumulative priming effect of biochars on native SOC mineralisation (mg CO_2-C g^{-1} SOC) after 2 years of incubation was significantly ($p = 0.004$) influenced by the main effects of soil, and the interactive effects of soil, temperature and biochar (**Table 4.2**). The two biochars resulted in a significantly ($p = 0.004$) different priming effect on native SOC mineralisation at 20 and 40 °C, with generally a lower priming effect for the 550 °C biochar than the 450 °C biochar. However, there was no clear pattern in the priming effect for the two biochars at 60 °C.

At 20 and 40 °C, both biochars produced a positive priming effect on native SOC mineralisation over the whole incubation period in the Inceptisol. Whereas, in the Entisol, Oxisol and Vertisol, both biochars had a negligible priming effect in the initial few months and then negative priming effect from the 550 °C biochar, with the exception of the Vertisol at 20 °C (**Figure 4.2**). Overall, the priming effect was less positive (in the Inceptisol) or more negative (in the Entisol, Oxisol and Vertisol) from the 550 °C biochar than the 450 °C biochar at 20 and 40 °C. In the Inceptisol, the positive priming effect from both biochars levelled off at 6 months after incubation with a maximum value of about 20 and 40 mg CO_2-C g^{-1} SOC at 20 °C and 40 °C, respectively. In the Entisol, the 450 °C biochar had a small priming effect with values ranging from -1.83 to 1.07 mg CO_2-C g^{-1} SOC at 20 °C and -4.75 to 3.75 mg CO_2-C g^{-1} SOC at 40 °C. The 550 °C biochar produced negligible negative priming in the first 6 weeks and then the negative priming increased (-7.22 to -18.45 mg CO_2-C g^{-1} SOC) over the remaining incubation period at 20 and 40 °C. In the Oxisol at 20 °C, there was a small positive or negative priming from the 450 °C biochar, and a significant negative priming from the 550 °C biochar; whereas at 40 °C, the negative priming became greater (-5.46 to -10.89 mg CO_2-C g^{-1} SOC) with time from both 450 and 550 °C biochars over the two-year incubation period. In the Vertisol at 20°C, both biochars showed a negligible negative or positive priming effect, ranging from -0.67 to 5.61 mg CO_2-C g^{-1} SOC. At 40 °C, initially there was negligible priming from both biochars, which became strongly negative and reached to a maximum value at 12 months (-12.45 to -35.50 mg CO_2-C g^{-1} SOC). Afterwards, the negative priming from the 450 °C biochar was reversed to a slightly positive priming and the negative from the 550 °C biochar continued but with a decreased intensity towards the end of incubation period.

The priming effect of biochars on native SOC mineralisation showed a different behaviour over time at 60 °C, compared to 20 and 40 °C (**Figure 4.2**). In the Inceptisol, the initial positive priming effect was greater for the 550 °C biochar than the 450 °C biochar, which reached to a maximum value on day 80, and then decreased to negligible negative or positive priming for the remaining incubation period. In the Entisol and the Oxisol, small negative priming occurred in the first 6 to 12 months, which was reversed to positive priming with time for both biochars. In the Vertisol, after almost no priming effect during the first 3 months, both biochars produced negative priming at 5 months, which was continued and then plateaued after 12 months. The negative priming effect was greater from the 450 °C biochar than 550 °C biochar at 60 °C in the Vertisol (**Figure 4.2**). The cumulative priming effect of biochars on native SOC mineralisation expressed as per kg soil was shown in Figure 4.S6.

Table 4.2. Statistical significance of the effects of soil, biochar and temperature treatments and their interactions on and total C, biochar-C mineralised, proportion of biochar-C mineralised and priming effect over the 2-year incubation period.

Treatment effect	Total C mineralised	Biochar-C mineralised	Proportion of biochar-C mineralised	Priming of biochar on native SOC
Soil (S)	***	***	***	***
Biochar (B)	***	***	***	ns
Temperature	***	***	***	ns
S × B	***	***	***	ns
S × T	***	***	***	***
B × T	***	*	ns	*
S × B × T	***	0.003	0.003	0.004

* $p < 0.05$; *** $p \leq 0.001$; ns, not significant.

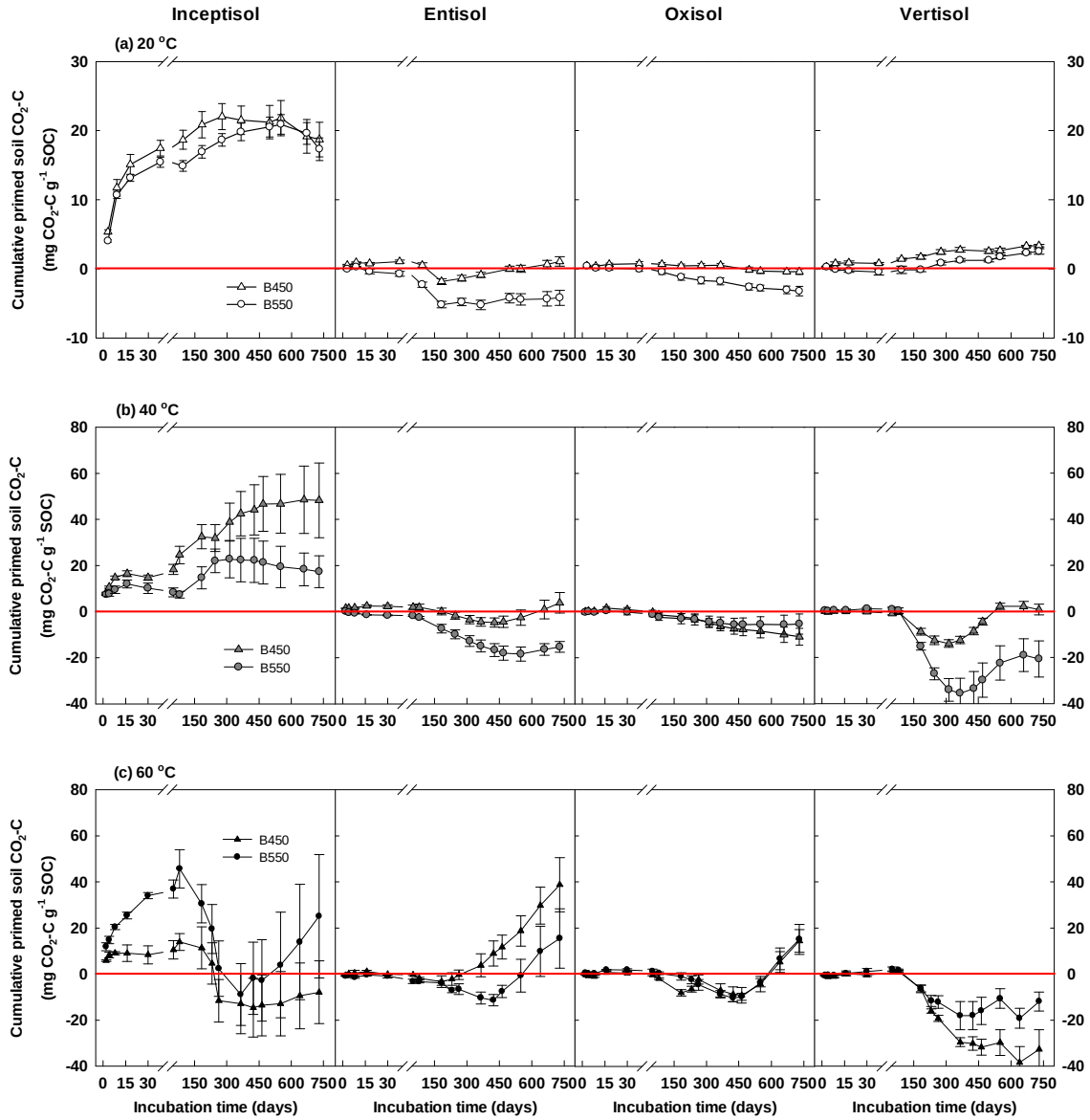

Figure 4.2. Cumulative amounts of primed native SOC (mg CO_2-C g^{-1} native SOC) in soils induced by the addition of 450 °C biochar (triangle) and 550 °C biochar (circle) at 20 °C (empty symbols), 40 °C (grey symbols) and 60 °C (dark symbols) over the 2-year of incubation period. Error bars represent standard error of the means (n = 4).

4.3.3. Biochar-C mineralisation

The proportion of added biochar-C mineralised at two years was significantly ($p = 0.003$) influenced by the main effects of soil and temperature and the interactive effects of soil, biochar and temperature treatments (**Table 4.2**). The proportions of biochar-C mineralised over the two-year incubation period varied from 0.43 to 10.58% across all treatments. The mineralisation of biochar-C increased with increasing incubation temperatures across the four soils and for both biochars (**Figure 4.3**). The proportion of biochar-C mineralised from the 450 °C biochar was significantly ($p < 0.001$) greater than from the 550 °C biochar. At 20 °C, the proportion of biochar-C mineralised in the 450 °C biochar-amended Entisol remained significantly greater (1.50%) than the other soils (0.80−1.09%), and the smallest proportion of biochar-C was mineralised from the Inceptisol after the two-year of incubation. At 40 °C, the proportion of biochar-C mineralised in the 450 °C biochar was significantly greater in the Vertisol (5.19%) than in the Entisol (4.20%); and a significantly smaller proportion of 450 °C biochar-C was mineralised in the Oxisol (2.94%) and Inceptisol (3.03%). At 60 °C, the proportion of 450 °C biochar-C mineralised was the greatest in the Vertisol (10.58%), followed by the Entisol (8.18%), and much smaller mineralisation occurred in the Inceptisol (5.84%) or Oxisol (5.38%). The proportion of 550 °C biochar-C mineralised (0.43 to 0.52%) was similar across the four soils at 20 °C. However, the proportion of biochar-C mineralised from the 550 °C biochar at 40 and 60 °C was greatest in the Vertisol compared to the other soils, with 2.63 and 3.28% mineralised, respectively, cf. 1.40−1.54% at 40 °C and 2.31−3.18% at 60 °C (**Figure 4.3**).

When expressed on per unit basis of the initial native SOC, the biochar-C mineralised from both biochars after the 2-year of incubation period at 40 and 60 °C followed the sequence: Oxisol < Entisol < Vertisol < Inceptisol (**Figure 4.3**). At 20 °C, the mineralisation sequence was Oxisol < Vertisol ≤ Entisol < Inceptisol, which is similar to the sequence observed from the first year of incubation data (Fang et al., 2014).

A time series of the cumulative fraction of added biochar-C mineralised and the biochar-C mineralisation rates are shown in the Supporting Information (**Figure S3** and **Figure 4.S4**). The cumulative fraction of added biochar-C mineralised was greater for the 450 °C biochar than the 550 °C biochar throughout the incubation

(**Figure S3**). All main and interactive effects of time, biochar and soil on the biochar-C mineralisation rate at each incubation temperature were significant ($p < 0.001$) over the two years incubation period (**Table 4.S1**). The mineralisation rate of biochar-C at 20 and 40 °C in the first year have been discussed in Fang et al. (2014). In the second year, biochar-C mineralisation rates for the 450 °C biochar were mostly higher at 60 °C than 40 °C across the soils, but for the 550 °C biochar there was no significant difference between 40 and 60 °C at most stages of incubation across all soils. Biochar-C mineralisation rates for both biochars were the lowest at 20 °C across the four soils (**Figure S4**).

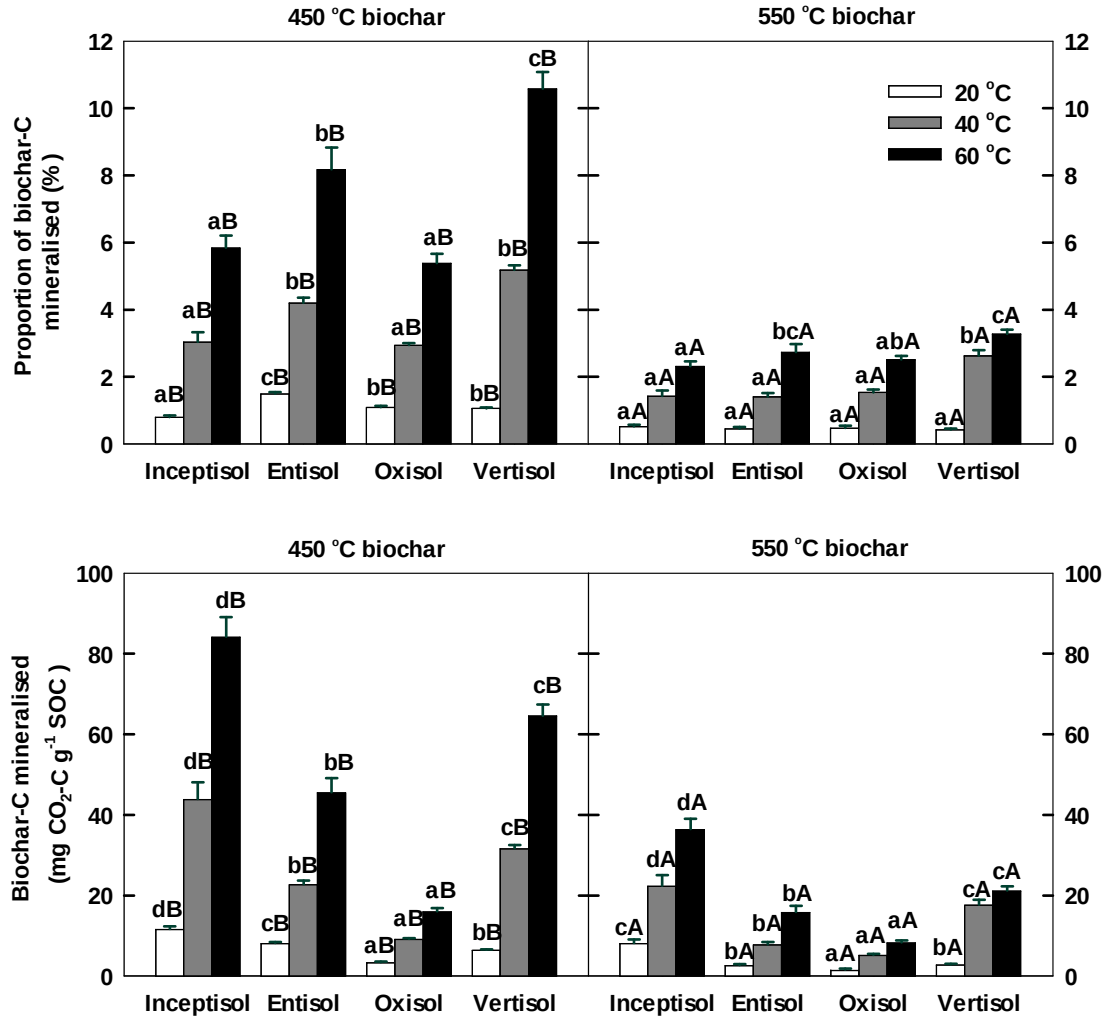

Figure 4.3. The proportions (%) and cumulative amounts of biochar carbon (C) mineralised (mg CO_2-C g^{-1} biochar-C) from soils amended with 450 °C and 550 °C biochars at 20 °C (white columns), 40 °C (grey columns) and 60 °C (dark columns)

over the 2-year of incubation period. Error bars represent standard error of the means (n = 4). Small letters compare significant differences among soils for each of the biochar at each of the incubation temperature. Capital letters compare significant differences between the two biochars at each temperature and within each soil.

4.3.4. Mean residence time of biochar-C and SOC

The MRT of labile and recalcitrant C of biochar and native SOC was estimated using a two-pool exponential model and the results are presented in **Table 4.3** and **Table 4.4**. The MRT of recalcitrant C in the biochars varied between 341 and 1061 years at 20 °C, 41 and 451 years at 40 °C and 25 and 127 years at 60 °C across the soil and biochar treatments (**Table 4.3**). The model-derived labile biochar-C ranged between 0.14 and 3.27% of the total biochar-C across all treatments. The MRT of labile biochar-C ranged between 2 and 147 days and did not show any systematic trend across the treatments (**Table 4.3**).

The MRT of the recalcitrant fraction in the native SOC was shorter than that of the biochar-C and it decreased with increasing incubation temperature (*cf*. **Table 4.3** and **Table 4.4**). At 20 °C, the MRT of recalcitrant C in native SOC was the greatest in the Vertisol (240 years), followed by Oxisol (94 years), Entisol (71 years) and Inceptisol (54 years). At 40 and 60 °C, the MRT of recalcitrant C in native SOC varied between 12−16 years, and 7−21 years, respectively (**Table 4.4**). Model predicted labile SOC constituted between 0.92 and 33.2% of the total SOC across all treatments and it increased with increasing incubation temperature. The MRT of the model estimated labile SOC varied from 16 to 298 days across all treatments (**Table 4.4**).

Table 4.3. Mean residence time (MRT) of labile and recalcitrant pools of biochar carbon, and the proportion of model-derived labile biochar-C in the four soils. The parameters were estimated using a two-pool exponential model fitted to the biochar-C mineralisation data over the 2-year incubation period. B450 and B550 represent the biochars produced at 450 and 550 °C, respectively.

	Soil	Labile C (days)			Recalcitrant C (years)			Labile C (%) in biochar		
		20 °C	40 °C	60 °C	20 °C	40 °C	60 °C	20 °C	40 °C	60 °C
B450	Inceptisol	24 (±4)	45 (±6)	114 (±15)	454 (±33)	134 (±18)	77 (±10)	0.39 (±0.04)	1.45 (±0.19)	3.27 (±0.32)
	Entisol	147 (±21)	24 (±3)	38 (±15)	372 (±39)	60 (±3)	28 (±3)	0.96 (±0.10)	0.85 (±0.05)	1.15 (±0.28)
	Oxisol	35 (±4)	6 (±1)	2 (±1)	341 (±10)	84 (±1)	45 (±4)	0.53 (±0.04)	0.39 (±0.05)	0.45 (±0.15)
	Vertisol	43 (±20)	8 (±1)	104 (±8)	345 (±47)	41 (±1)	25 (±2)	0.46 (±0.08)	0.33 (±0.02)	3.03 (±0.07)
B550	Inceptisol	82 (±20)	52 (±5)	31 (±9)	992 (±220)	451 (±71)	127 (±23)	0.31 (±0.04)	0.92 (±0.07)	0.66 (±0.19)
	Entisol	78 (±4)	58 (±24)	61 (±23)	1061 (±166)	246 (±21)	102 (±25)	0.26 (±0.03)	0.54 (±0.09)	0.78 (±0.23)
	Oxisol	15 (±5)	29 (±10)	2 (±1)	768 (±151)	185 (±2)	94 (±4)	0.19 (±0.03)	0.43 (±0.07)	0.25 (±0.04)
	Vertisol	27 (±14)	5 (±1)	81 (±25)	732 (±99)	93 (±7)	97 (±13)	0.15 (±0.03)	0.14 (±0.01)	1.29 (±0.28)

$R^2 > 0.95$; the numbers in parentheses are the standard error of the mean (n=4).

Table 4.4. Mean residence time (MRT) of labile and recalcitrant C pools of native SOC, and the proportion of model-derived labile native SOC in the four soils. The parameters were estimated using a two-pool exponential model fitted to the SOC mineralisation data over the 2-year incubation period.

Soil	Labile C (days)			Recalcitrant C (years)			Labile C (%)		
	20 °C	40 °C	60 °C	20 °C	40 °C	60 °C	20 °C	40 °C	60 °C
Inceptisol	78 (±15)	77 (±24)	213 (±14)	57 (±6)	17 (±2)	20 (±3)	3.01 (±0.26)	11.49(±2.56)	33.23 (−)
Entisol	99 (±8)	41 (±6)	100 (±11)	73 (±6)	12 (±1)	9 (±1)	2.67 (±0.07)	3.96 (±0.43)	13.35 (±0.82)
Oxisol	23 (±2)	36 (±2)	108 (±21)	94 (±1)	16 (±1)	7 (±1)	0.92 (±0.03)	3.93 (±0.11)	8.78 (±1.31)
Vertisol	16 (±1)	298 (±117)	179 (±34)	241 (±9)	18 (±4)	12 (±1)	0.34 (±0.04)	5.88 (±1.98)	9.68 (±1.57)

$R^2 > 0.99$; the numbers in parentheses are the standard error of the mean (n=4).

4.4. Discussion

4.4.1. Priming effect of biochar on native SOC mineralisation

Soil properties may influence the biochar induced priming of native SOC. The direction and magnitude of priming of native SOC was different for the four soils, with generally positive priming in the sandy soil (Inceptisol), and negative or negligible positive priming in the other soils. The observation of positive priming of native SOC in the Inceptisol is consistent with earlier studies where a significant increase of organic C mineralisation has been reported after the addition of biochar in sand or sandy soils (Awad et al., 2012; Farrell et al., 2013; Hamer et al., 2004). The positive priming of native SOC in the Inceptisol could be attributed to the addition of small amount of labile C in the biochar which increased soil microbial activities (Farrell et al., 2013), the so called co-metabolic effect (Hamer et al., 2004). Moreover, the stabilisation of SOC and biochar-C through organo-mineral associations (Fang et al., 2014; von Lützow et al., 2006) in the Inceptisol was expected to be minimal due to its low clay content (1.3%). The positive priming from biochar in the Inceptisol may also be related to relatively greater lability of native organic C for microorganisms, as suggested by the shorter MRT (57 years) for the recalcitrant C fraction in this soil relative to the other soils (73−241 years) at 20 °C.

In soils containing adequate clay content (> 20%), stabilisation or a decrease of native SOC mineralisation in the presence of biochar may occur through biochar induced organo-mineral interactions; this paradigm seems to be supported in our study by observations of negative priming from biochar in a sandy clay loam (Entisol) or clayey soils i.e. Oxisol and Vertisol (**Figure 4.2**). Complexation of organic matter with dissolved minerals and on variable charged surfaces, e.g. Fe and Al oxides, and edges of kaolinite and 2:1 clay minerals via ligand exchange reactions can result in the formation of strong organo-mineral associations (Gu et al., 1994; von Lützow et al., 2006). Cation bridging by Ca^{2+} between permanent charged minerals (e.g. smectite and illite) and organic functional groups in the Vertisol and Entisol can be an important mechanism for SOC stabilisation in these soils (von Lützow et al., 2006). Previous studies have suggested that “aged” biochar may facilitate interactions between native SOC and clay and/or dissolved minerals in soils through the mechanisms of complexation reactions, ligand exchange or cation bridging, thus

stabilising native SOC (Brodowski et al., 2006; Cheng et al., 2008; Hilscher et al., 2009; Joseph et al., 2010). The interaction of biochar with native organic matter and clay minerals during ageing may also enhance soil aggregation, possibly mediated by enhanced biological activity (Brodowski et al., 2006; Herath et al., 2013; Liang et al., 2010). However, it is not yet clear to what extent biochar could increase soil aggregation over the duration of this study (2 years).

In our study, the results of greater positive priming from the 450 °C biochar than the 550 °C biochar, especially at 20 and 40 °C (**Figure 4.2**), are consistent with the results of earlier studies, attributing this phenomenon to the greater co-metabolic effect of lower-temperature biochars (Luo et al., 2011; Zimmerman et al., 2011). We observed more labile C in the 450 °C biochar amended soils than the 550 °C biochar amended soils in our MRT modelling results (**Table 4.3**). The above results could also partly be due to the greater specific surface area (228 and 191 m^2 g^{-1}, respectively) and pore volume (67.5 and 57.2% of the total, respectively) of the 550 °C biochar than the 450 °C biochar, which could have caused greater physical and chemical interactions with native SOC and soil minerals in the higher-temperature biochar treatment than the lower-temperature biochar treatment (Kasozi et al., 2010).

As the dynamics of priming effect of biochar on native SOC was followed over time in this study, this provided useful information for interpreting the differences across treatments along an ageing continuum. The priming effect of biochar continued throughout the incubation period, albeit the direction and magnitude changed over time, which may be the result of several interacting factors, such as changes in microbial activity and composition, and the extent of biochar-induced mineral protection and sorption of organic matter on biochar. Initially, the positive priming effect occurred across the soils, biochar and temperature treatments. Some researchers have suggested that this additional CO_2 emission is an "apparent positive priming" effect within the first few days after the organic C application, which is linked to the accelerated turnover of native microbial biomass C rather than from the accelerated mineralisation of native SOC (Blagodatskaya and Kuzyakov, 2008; De Nobili et al., 2001; Perelo and Munch, 2005; Wu et al., 1993). As mentioned above, the small proportion of labile C in biochar can accelerate the activity of soil microorganisms that respond specifically to this substrate (Lehmann

et al., 2011). The accelerated activity of microorganisms can then enhance the mineralisation of native SOC ("real positive priming"), as a result of co-metabolism and higher enzyme production (Blagodatskaya and Kuzyakov, 2008). Furthermore, with time, the real positive priming may predominate relative to the apparent positive priming, which is generally induced immediately following the addition of labile organic matter (Kuzyakov, 2010).

The negative priming occurred over time in the soils containing significant clay minerals but levelled off after 6−18 months, or the negative priming switched to positive priming in some cases, e.g. Entisol and Vertisol at 40 °C after 18 months. These results indicate that the factors contributing to the priming effect may change during prolonged incubation. For example, the sorption capacity of biochar may decrease with ageing (Martin et al., 2012), which could occur due to the blocking of the biochar external surface during the adsorption process (Pignatello et al., 2006). The reversal of negative priming to either no priming or positive priming may also occur due to the shift in microbial community structure degrading relatively recalcitrant C in the soil (Anderson et al., 2011) following the depletion of relatively labile C components in soil and biochar. Gram positive bacteria, known users of recalcitrant C (Bird et al., 2011; Santos et al., 2012) may increase in community size relative to other microbial groups. Furthermore, fungi, the major decomposers of aromatic compounds (Kabuyah et al., 2012), were observed to increase in size in the presence of aged biochar (Zimmermann et al., 2012). Microbial enzyme activities may also shift to degrade relatively recalcitrant C forms, for example, Zimmermann et al. (2012) found 'aromatic transformation' enzymes in the presence of 1-year aged biochar. Such shifts in microbial communities and their enzymes to relatively recalcitrant C forms may have contributed to the change in direction of priming of native SOC from biochar after the 24 months of incubation. Further research is warranted to test the hypothesis about shifts in microbial communities and their enzymes to alter the priming effects of biochar.

Microbial activity may increase with increasing incubation temperature from 20 and 40 °C which can lead to the increased organic C mineralisation. However, the incubation temperature did not significantly influence the biochar priming effect. This could partly be due to stabilisation of native SOC by sorption on to biochar (Pignatello et al., 2006) and/or to a possible increase in biochar induced organo-

mineral interactions with increasing incubation temperature. At 60 °C, the additional cumulative release of CO_2-C after a 2-year period in the Inceptisol, Entisol and Oxisol may be attributed to the abiotic effect, such as the increased solubility and degradation of humic substances at high temperature, instead of "positive priming". By comparison, the negative priming effect of biochar on native SOC was sustained in the Vertisol at 60 °C, possibly because of less solubility or relatively more recalcitrant nature of native SOC in the Vertisol compared to the other soils.

4.4.2. Biochar-C mineralisation in soil

Consistent with the results of our 1-year incubation study (Fang et al., 2014), the C stability of the 450 °C biochar produced varied with soil properties across the three incubation temperatures over the 2-year period. Clay mineralogy was hypothesised to play an important role in influencing biochar-C stability as biochar functional groups interact with mineral fractions (Cusack et al., 2012; Hilscher and Knicker, 2011b; Joseph et al., 2010). Biochar-C mineralisation (mg^{-1} CO_2-C g^{-1} native SOC) was significantly higher in the sandy soil (Inceptisol) than in the sandy clay loam soil (Entisol) or the clayey soils (Oxisol < Vertisol) at 20 °C, thus highlighting the role of clay content and clay mineralogy in stabilising biochar. Biochar-C mineralised (% of added C in biochar) across the Inceptisol, Entisol and Vertisol was similar up to 12-month. However, in this 2-year study, the results clearly showed that a smaller proportion of added biochar-C was mineralised in the relatively SOC-poor Inceptisol than in the Entisol and Vertisol across all temperatures. These results highlight the importance of native SOC content, among other confounding soil properties, in altering the mineralisation of biochar-C.

Similar to the results of 1-year incubation study (Fang et al., 2014), the C stability of biochar produced at higher temperature (550 °C) was less affected by soil properties. Similarly, Steinbeiss et al. (2009) found no difference in the stability of a considerably high temperature (850 °C) biochar in two soils (forest and arable soils). The C stability was greater for biochar produced at 550 °C than at 450 °C pyrolysis temperature across the three incubation temperatures, which is similar to the conclusion drawn from the 1-year data (Fang et al., 2014). Pyrolysis at lower temperatures may result in lower aromatic C and higher labile C components in biochar (Ameloot et al., 2013; McBeath et al., 2011), and therefore the higher

biochar-C mineralisation in lower temperature biochars than higher temperature biochars (Singh et al., 2012).

The mineralisation of biochar-C continued to increase from 12 to 24 months and it was 23−46%, 23−157% and 30−137% times higher than the corresponding values observed in the first 12 months at 20, 40 and 60 °C, respectively, across all biochar and soil treatments (Fang et al., 2014). The C mineralised from 12 to 24 months was higher than, or equal to, that observed in the first 12 months in certain biochar-soil treatment combinations at high incubation temperatures (40 or 60 °C), for example, the 550 °C biochar-Vertisol-40 °C, 550 °C biochar-Oxisol-60 °C, and 450 °C biochar-Oxisol-40 and 60 °C. The rapid biochar-C mineralisation of biochar in the second year indicates that biochar-C may not necessarily stabilise at high incubation temperatures. Consistent with our finding, Zimmermann et al. (2012) also reported rapid biochar-C mineralisation in an aged biochar (11-year old) at high (30−50 °C) incubation temperatures and there was no significant difference in the degradation rate of the 11-year and 1-year aged biochar. Furthermore, the increased biochar-C mineralisation with increasing incubation temperatures could be caused by the increased abiotic than biotic oxidation of biochar-C (Zimmermann et al., 2012).

The MRT of the recalcitrant fraction of C in the biochars at 20 °C (341−1061 years), 40 °C (41−451 years), and 60 °C (25−127 years) across the soils agreed well with previous studies employing incubation temperatures ranging from 22 °C to 60 °C (Bird et al., 1999; Kuzyakov et al., 2009; Singh et al., 2012; Zimmermann et al., 2012). The MRT of the biochars increased for the 2-year data compared to the 1-year data at 20 °C; however similar MRT values were observed for the two data sets at 40 °C (*cf*. Fang et al., 2014). These results indicate that longer incubation periods may be needed for obtaining a more realistic estimate of the biochar-C stability, particularly at lower temperatures (Singh et al., 2012).

4.5. Summary and implications for C sequestration in soil

Mineralisation of native SOC in a sandy soil (Inceptisol) was stimulated by biochar addition. On the other hand, in a sandy clayey loam (Entisol) and clayey soils (Oxisol and Vertisol), mineralisation of native SOC was generally suppressed in the presence of biochar. Our results suggest that over the two years incubation period, the

interaction between biochar, native SOC and clay minerals will result in an overall increased stabilisation of native SOC in clayey soils. The 550 °C biochar resulted in greater stabilisation of native SOC than the 450 °C biochar at 20 and 40 °C. Our study has shown that biochar can persist in soil over a few centuries to millennia timescales with a mean annual temperature of 20 °C. However, at elevated temperatures (40 or 60 °C), which may be experienced in tropical environments at certain times and especially in surface soil, only the biochars produced at a higher pyrolysis temperature (e.g. 550 °C) may persist for more than 100 years. Whereas, a lower temperature biochar (e.g. 450 °C biochar) may degrade in soils over decadal scales to just over a century at elevated temperatures with only minimal role of clay minerals or other soil properties in enhancing biochar-C stability. Considering the above two benefits of the 550 °C biochar application to the mineral soils (i.e. greater native SOC stabilisation as well as biochar-C stability), wood biochar produced by slow pyrolysis at 550 °C may be more effective for C sequestration in soil, relative to that produced at 450 °C.

4.6. References

Abiven, S., Andreoli, R., 2011. Charcoal does not change the decomposition rate of mixed litters in a mineral cambisol: a controlled conditions study. Biology and Fertility of Soils 47, 111-114.

Ameloot, N., De Neve, S., Jegajeevagan, K., Yildiz, G., Buchan, D., Funkuin, Y.N., Prins, W., Bouckaert, L., Sleutel, S., 2013. Short-term CO_2 and N_2O emissions and microbial properties of biochar amended sandy loam soils. Soil Biology & Biochemistry 57, 401-410.

Anderson, C.R., Condron, L.M., Clough, T.J., Fiers, M., Stewart, A., Hill, R.A., Sherlock, R.R., 2011. Biochar induced soil microbial community change: Implications for biogeochemical cycling of carbon, nitrogen and phosphorus. Pedobiologia 54, 309-320.

Awad, Y.M., Blagodatskaya, E., Ok, Y.S., Kuzyakov, Y., 2012. Effects of polyacrylamide, biopolymer, and biochar on decomposition of soil organic matter and plant residues as determined by ^{14}C and enzyme activities. European Journal of Soil Biology 48, 1-10.

Barton, C.V.M., Ellsworth, D.S., Medlyn, B.E., Duursma, R.A., Tissue, D.T., Adams, M.A., Eamus, D., Conroy, J.P., McMurtrie, R.E., Parsby, J., Linder, S., 2010. Whole-tree chambers for elevated atmospheric CO_2 experimentation and tree scale flux measurements in south-eastern Australia: The Hawkesbury Forest Experiment. Agricultural and Forest Meteorology 150, 941-951.

Bird, J.A., Herman, D.J., Firestone, M.K., 2011. Rhizosphere priming of soil organic matter by bacterial groups in a grassland soil. Soil Biology & Biochemistry 43, 718-725.

Bird, M.I., Moyo, C., Veenendaal, E.M., Lloyd, J., Frost, P., 1999. Stability of elemental carbon in a savanna soil. Global Biogeochemical Cycles 13, 923-932.

Blagodatskaya, E., Kuzyakov, Y., 2008. Mechanisms of real and apparent priming effects and their dependence on soil microbial biomass and community structure: critical review. Biology and Fertility of Soils 45, 115-131.

Brodowski, S., John, B., Flessa, H., Amelung, W., 2006. Aggregate-occluded black carbon in soil. European Journal of Soil Science 57, 539-546.

Cheng, C.H., Lehmann, J., Engelhard, M.H., 2008. Natural oxidation of black carbon in soils: Changes in molecular form and surface charge along a climosequence. Geochimica Et Cosmochimica Acta 72, 1598-1610.

Cheng, C.H., Lehmann, J., Thies, J.E., Burton, S.D., Engelhard, M.H., 2006. Oxidation of black carbon by biotic and abiotic processes. Organic Geochemistry 37, 1477-1488.

Cross, A., Sohi, S.P., 2011. The priming potential of biochar products in relation to labile carbon contents and soil organic matter status. Soil Biology & Biochemistry 43, 2127-2134.

Cusack, D.F., Chadwick, O.A., Hockaday, W.C., Vitousek, P.M., 2012. Mineralogical controls on soil black carbon preservation. Global Biogeochemical Cycles 26, GB2019.

De Nobili, M., Contin, M., Mondini, C., Brookes, P.C., 2001. Soil microbial biomass is triggered into activity by trace amounts of substrate. Soil Biology & Biochemistry 33, 1163-1170.

Fang, Y., Singh, B., Singh, B.P., Krull, E., 2014. Biochar carbon stability in four contrasting soils. European Journal of Soil Science, 65, 60–71.

Farrell, M., Kuhn, T.K., Macdonald, L.M., Maddern, T.M., Murphy, D.V., Hall, P.A., Singh, B.P., Baumann, K., Krull, E.S., Baldock, J.A., 2013. Microbial

utilisation of biochar-derived carbon. Science of the Total Environment, in press.

Glaser, B., Haumaier, L., Guggenberger, G., Zech, W., 2001. The 'Terra Preta' phenomenon: a model for sustainable agriculture in the humid tropics. Naturwissenschaften 88, 37-41.

Glaser, B., Lehmann, J., Zech, W., 2002. Ameliorating physical and chemical properties of highly weathered soils in the tropics with charcoal - a review. Biology and Fertility of Soils 35, 219-230.

Gu, B.H., Schmitt, J., Chen, Z.H., Liang, L.Y., Mccarthy, J.F., 1994. Adsorption and desorption of natural organic-matter on iron-oxide–mechanisms and models. Environmental Science & Technology 28, 38-46.

Hamer, U., Marschner, B., Brodowski, S., Amelung, W., 2004. Interactive priming of black carbon and glucose mineralisation. Organic Geochemistry 35, 823-830.

Herath, H.M.S.K., Camps-Arbestain, M., Hedley, M., 2013. Effect of biochar on soil physical properties in two contrasting soils: An Alfisol and an Andisol. Geoderma 209-210, 188-197.

Hilscher, A., Heister, K., Siewert, C., Knicker, H., 2009. Mineralisation and structural changes during the initial phase of microbial degradation of pyrogenic plant residues in soil. Organic Geochemistry 40, 332-342.

Hilscher, A., Knicker, H., 2011a. Carbon and nitrogen degradation on molecular scale of grass-derived pyrogenic organic material during 28 months of incubation in soil. Soil Biology & Biochemistry 43, 261-270.

Hilscher, A., Knicker, H., 2011b. Degradation of grass-derived pyrogenic organic material, transport of the residues within a soil column and distribution in soil organic matter fractions during a 28 month microcosm experiment. Organic Geochemistry 42, 42-54.

IBI, 2012. Standardized product definition and product testing guidelines for biochar that is used in soil. http://www.biochar-international.org/sites/default/files/Guidelines_for_Biochar_That_Is_Used_in_Soil_Final.pdf, (cited 5 March, 2013).

Jones, D.L., Murphy, D.V., Khalid, M., Ahmad, W., Edwards-Jones, G., DeLuca, T.H., 2011. Short-term biochar-induced increase in soil CO_2 release is both biotically and abiotically mediated. Soil Biology & Biochemistry 43, 1723-1731.

Jones, D.L., Rousk, J., Edwards-Jones, G., DeLuca, T.H., Murphy, D.V., 2012. Biochar-mediated changes in soil quality and plant growth in a three year field trial. Soil Biology & Biochemistry 45, 113-124.

Joseph, S.D., Camps-Arbestain, M., Lin, Y., Munroe, P., Chia, C.H., Hook, J., van Zwieten, L., Kimber, S., Cowie, A., Singh, B.P., Lehmann, J., Foidl, N., Smernik, R.J., Amonette, J.E., 2010. An investigation into the reactions of biochar in soil. Australian Journal of Soil Research 48, 501-515.

Kabuyah, R.N.T.M., van Dongen, B.E., Bewsher, A.D., Robinson, C.H., 2012. Decomposition of lignin in wheat straw in a sand-dune grassland. Soil Biology & Biochemistry 45, 128-131.

Kasozi, G.N., Zimmerman, A.R., Nkedi-Kizza, P., Gao, B., 2010. Catechol and humic acid sorption onto a range of laboratory-produced black carbons (biochars). Environmental Science & Technology 44, 6189-6195.

Keith, A., Singh, B., Singh, B.P., 2011. Interactive priming of biochar and labile organic matter mineralization in a smectite-rich soil. Environmental Science & Technology 45, 9611-9618.

Kirschbaum, M.U.F., 1995. The temperature dependence of soil organic matter decomposition, and the effect of global warming on soil organic C storage. Soil Biology & Biochemistry 27, 753-760.

Knicker, H., Gonzalez-Vila, F.J., Gonzalez-Vazquez, R., 2013. Biodegradability of organic matter in fire-affected mineral soils of Southern Spain. Soil Biology & Biochemistry 56, 31-39.

Knoblauch, C., Maarifat, A.A., Pfeiffer, E.M., Haefele, S.M., 2011. Degradability of black carbon and its impact on trace gas fluxes and carbon turnover in paddy soils. Soil Biology & Biochemistry 43, 1768-1778.

Kuzyakov, Y., 2010. Priming effects: Interactions between living and dead organic matter. Soil Biology & Biochemistry 42, 1363-1371.

Kuzyakov, Y., Bol, R., 2006. Sources and mechanisms of priming effect induced in two grassland soils amended with slurry and sugar. Soil Biology & Biochemistry 38, 747-758.

Kuzyakov, Y., Subbotina, I., Chen, H.Q., Bogomolova, I., Xu, X.L., 2009. Black carbon decomposition and incorporation into soil microbial biomass estimated by ^{14}C labeling. Soil Biology & Biochemistry 41, 210-219.

Lackner, K.S., 2003. A guide to CO_2 sequestration. Science 300, 1677-1678.

Lehmann, J., 2007. A handful of carbon. Nature 447, 143-144.

Lehmann, J., Czimczik, C., Laird, D., Sohi, S., 2009. Stability of biochar in soil, In: Lehmann, J., Joseph, S. (Eds.), Biochar for Environmental Management: Science and Technology. Earthscan London, pp. 183-205.

Lehmann, J., Gaunt, J., Rondon, M., 2006. Bio-char sequestration in terrestrial ecosystems–a review. Mitigation and Adaptation Strategies for Global Change 11, 403-427.

Lehmann, J., Rillig, M.C., Thies, J., Masiello, C.A., Hockaday, W.C., Crowley, D., 2011. Biochar effects on soil biota - A review. Soil Biology & Biochemistry 43, 1812-1836.

Lehmann, J., Rondon, M., 2006. Bio-char soil management on highly weathered soils in the humid tropics. Biological Approaches to Sustainable Soil Systems 113, 517-530.

Liang, B., Lehmann, J., Solomon, D., Kinyangi, J., Grossman, J., O'Neill, B., Skjemstad, J.O., Thies, J., Luizao, F.J., Petersen, J., Neves, E.G., 2006. Black carbon increases cation exchange capacity in soils. Soil Science Society of America Journal 70, 1719-1730.

Liang, B., Lehmann, J., Solomon, D., Sohi, S., Thies, J.E., Skjemstad, J.O., Luizao, F.J., Engelhard, M.H., Neves, E.G., Wirick, S., 2008. Stability of biomass-derived black carbon in soils. Geochimica Et Cosmochimica Acta 72, 6069-6078.

Liang, B.Q., Lehmann, J., Sohi, S.P., Thies, J.E., O'Neill, B., Trujillo, L., Gaunt, J., Solomon, D., Grossman, J., Neves, E.G., Luizão, F.J., 2010. Black carbon affects the cycling of non-black carbon in soil. Organic Geochemistry 41, 206-213.

Luo, Y., Durenkamp, M., De Nobili, M., Lin, Q., Brookes, P.C., 2011. Short term soil priming effects and the mineralisation of biochar following its incorporation to soils of different pH. Soil Biology & Biochemistry 43, 2304-2314.

Major, J., Lehmann, J., Rondon, M., Goodale, C., 2010. Fate of soil-applied black carbon: downward migration, leaching and soil respiration. Global Change Biology 16, 1366-1379.

Martin, S.M., Kookana, R.S., Van Zwieten, L., Krull, E., 2012. Marked changes in herbicide sorption-desorption upon ageing of biochars in soil. Journal of Hazardous Materials 231, 70-78.

McBeath, A.V., Smernik, R.J., 2009. Variation in the degree of aromatic condensation of chars. Organic Geochemistry 40, 1161-1168.

McBeath, A.V., Smernik, R.J., Schneider, M.P.W., Schmidt, M.W.I., Plant, E.L., 2011. Determination of the aromaticity and the degree of aromatic condensation of a thermosequence of wood charcoal using NMR. Organic Geochemistry 42, 1194-1202.

Nguyen, B.T., Lehmann, J., Hockaday, W.C., Joseph, S., Masiello, C.A., 2010. Temperature sensitivity of black carbon decomposition and oxidation. Environmental Science & Technology 44, 3324-3331.

Novak, J.M., Busscher, W.J., Watts, D.W., Laird, D.A., Ahmedna, M.A., Niandou, M.A.S., 2010. Short-term CO_2 mineralization after additions of biochar and switchgrass to a Typic Kandiudult. Geoderma 154, 281-288.

Perelo, L.W., Munch, J.C., 2005. Microbial immobilisation and turnover of ^{13}C labelled substrates in two arable soils under field and laboratory conditions. Soil Biology & Biochemistry 37, 2263-2272.

Pignatello, J.J., Kwon, S., Lu, Y., 2006. Effect of natural organic substances on the surface and adsorptive properties of environmental black carbon (char): Attenuation of surface activity by humic and fulvic acids. Environmental Science & Technology 40, 7757-7763.

Santos, F., Torn, M.S., Bird, J.A., 2012. Biological degradation of pyrogenic organic matter in temperate forest soils. Soil Biology & Biochemistry 51, 115-124.

Singh, B.P., Cowie, A.L., Smernik, R.J., 2012. Biochar carbon stability in a clayey soil as a function of feedstock and pyrolysis temperature. Environmental Science & Technology 46, 11770-11778.

Singh, B.P., Hatton, B.J., Singh, B., Cowie, A.L., Kathuria, A., 2010. Influence of biochars on nitrous oxide emission and nitrogen leaching from two contrasting soils. Journal of Environmental Quality 39, 1224-1235.

Spokas, K.A., Reicosky, D.C., 2009. Impacts of sixteen different biochars on soil greenhouse gas production. Annals of Environmental Science 3, 179-193.

Steinbeiss, S., Gleixner, G., Antonietti, M., 2009. Effect of biochar amendment on soil carbon balance and soil microbial activity. Soil Biology & Biochemistry 41, 1301-1310.

Van Zwieten, L., Kimber, S., Morris, S., Chan, K.Y., Downie, A., Rust, J., Joseph, S., Cowie, A., 2010. Effects of biochar from slow pyrolysis of papermill waste on agronomic performance and soil fertility. Plant and Soil 327, 235-246.

von Lützow, M., Kögel-Knabner, I., Ekschmitt, K., Matzner, E., Guggenberger, G., Marschner, B., Flessa, H., 2006. Stabilization of organic matter in temperate soils: mechanisms and their relevance under different soil conditions - a review. European Journal of Soil Science 57, 426-445.

VSN International, 2011. GenStat for Windows 14th Edition. Hemel Hempstead, UK: VSN International.

Wardle, D.A., Nilsson, M.C., Zackrisson, O., 2008. Fire-derived charcoal causes loss of forest humus. Science 320, 629-629.

Woolf, D., Amonette, J.E., Street-Perrott, F.A., Lehmann, J., Joseph, S., 2010. Sustainable biochar to mitigate global climate change. Nature Communications 1, 56.

Wu, J., Brookes, P.C., Jenkinson, D.S., 1993. Formation and destruction of microbial biomass during the decomposition of glucose and ryegrass in soil. Soil Biology & Biochemistry 25, 1435-1441.

Zavalloni, C., Alberti, G., Biasiol, S., Delle Vedove, G., Fornasier, F., Liu, J., Peressotti, A., 2011. Microbial mineralization of biochar and wheat straw mixture in soil: A short-term study. Applied Soil Ecology 50, 45-51.

Zimmerman, A.R., 2010. Abiotic and microbial oxidation of laboratory-produced black carbon (biochar). Environmental Science & Technology 44, 1295-1301.

Zimmerman, A.R., Gao, B., 2013. The stability of biochar in the environment, In: Ladygina, N., Rineau, F. (Eds.), Biochar and Soil Biota. CRC Press, pp. 1-40.

Zimmerman, A.R., Gao, B., Ahn, M.Y., 2011. Positive and negative carbon mineralization priming effects among a variety of biochar-amended soils. Soil Biology & Biochemistry 43, 1169-1179.

Zimmermann, M., Bird, M.I., Wurster, C., Saiz, G., Goodrick, L., Barta, J., Capek, P., Santruckova, H., Smernik, R., 2012. Rapid degradation of pyrogenic carbon. Global Change Biology 18, 3306–3316.

4.7. Supporting Information

Statistical analysis

Repeated measures analyses were performed for TOC and biochar-C mineralisation rates using a linear mixed model framework in Genstat® 14th edition (VSN International, 2011). Each analysis consisted of fixed effects of soil, biochar, temperature, time and all associated interactions, and random effects of replicate and replicate by time. Separate repeated measures analysis of soil C mineralisation rate was conducted for each temperature. To allow for correlation between repeated measures on the same units, a first order autoregressive model was fitted. Heterogeneity in the residual variances between time-points was included as it was deemed significant using a residual likelihood ratio test.

References

VSN International, 2011. GenStat for Windows 14th Edition. Hemel Hempstead, UK: VSN International.

Table 4.S1. Statistical significance of the effects of time, soil and biochar treatments and their interactions on and total C and biochar-C mineralisation rate over the 2-year incubation period.

Treatment effect	Total C mineralisation rate	Biochar-C mineralisation rate
Time (T)	***	***
Soil (S)	***	***
Biochar (B)	***	***
T × S	***	***
T × B	***	***
S × B	***	***
T × S × H	***	***

* $p < 0.05$; *** $p \leq 0.001$; ns, not significant.

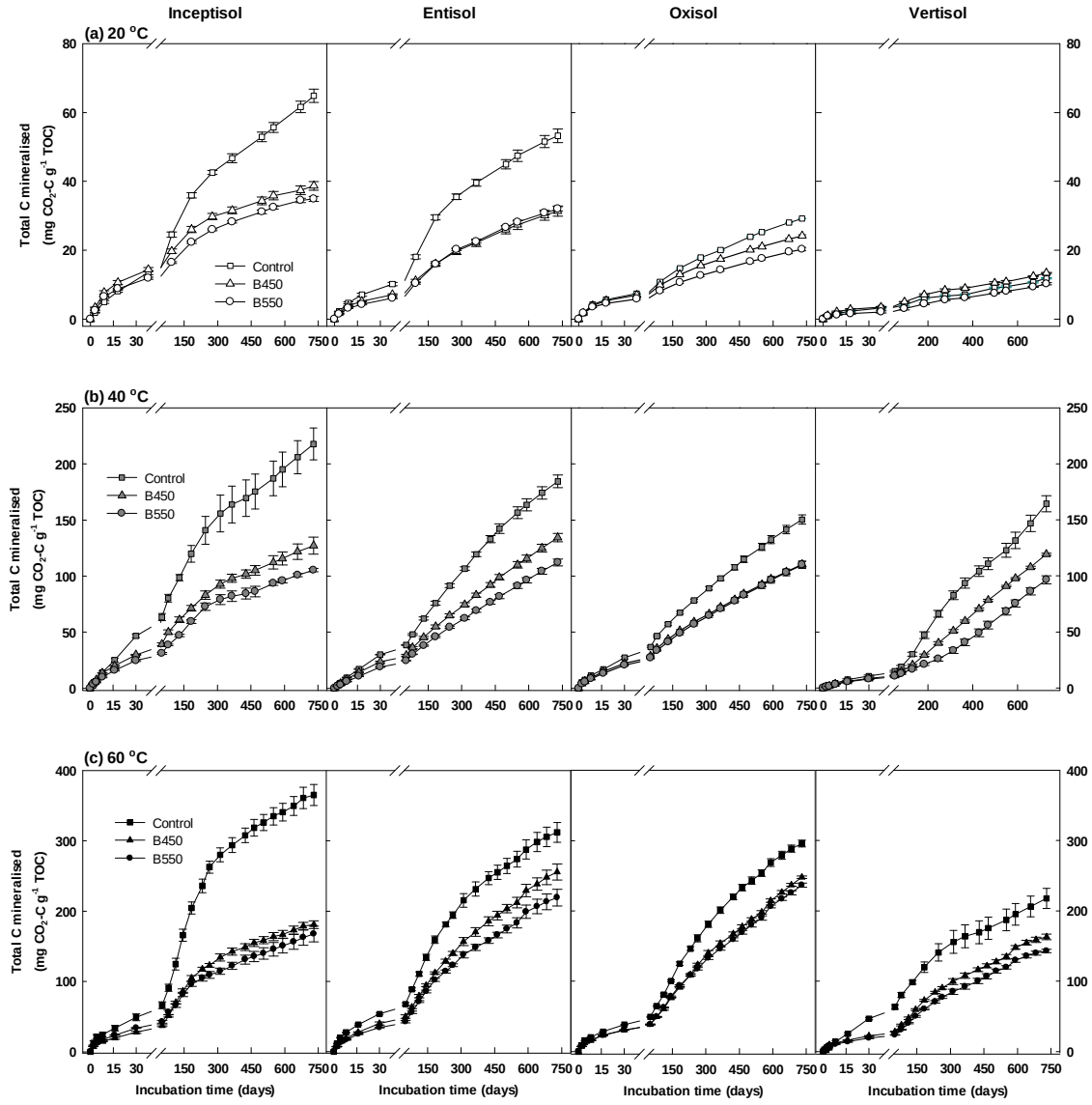

Figure 4.S1. Cumulative amounts of total carbon (C) mineralised (mg CO_2-C g^{-1} TOC) from control (without biochar), 450 and 550 °C biochar-amended soils incubated at 20, 40 and 60 °C after the two years incubation period. Square, triangle, circle symbols represent control, 450 and 550 °C biochar, respectively. Error bars represent standard error of the means (n = 4).

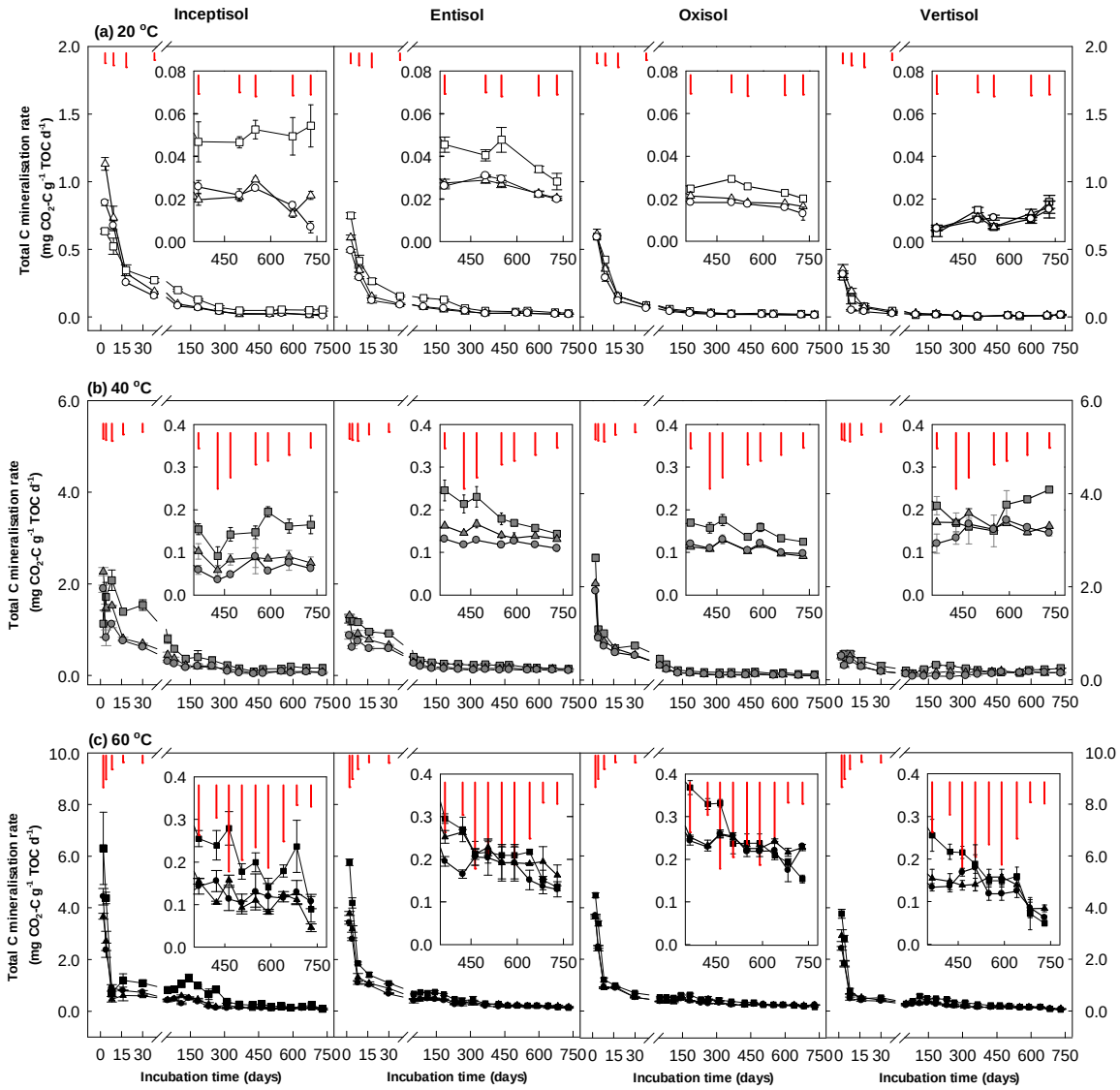

Figure 4.S2. Total carbon (C) mineralisation rate (mg CO_2-C g^{-1} TOC d^{-1}) from control (without biochar), 450 and 550 °C biochar-amended soils incubated at 20, 40 and 60 °C after the two years incubation period. Square, triangle, circle symbols represent control, 450 and 550 °C biochar, respectively. Error bars represent standard error of the means (n = 4).

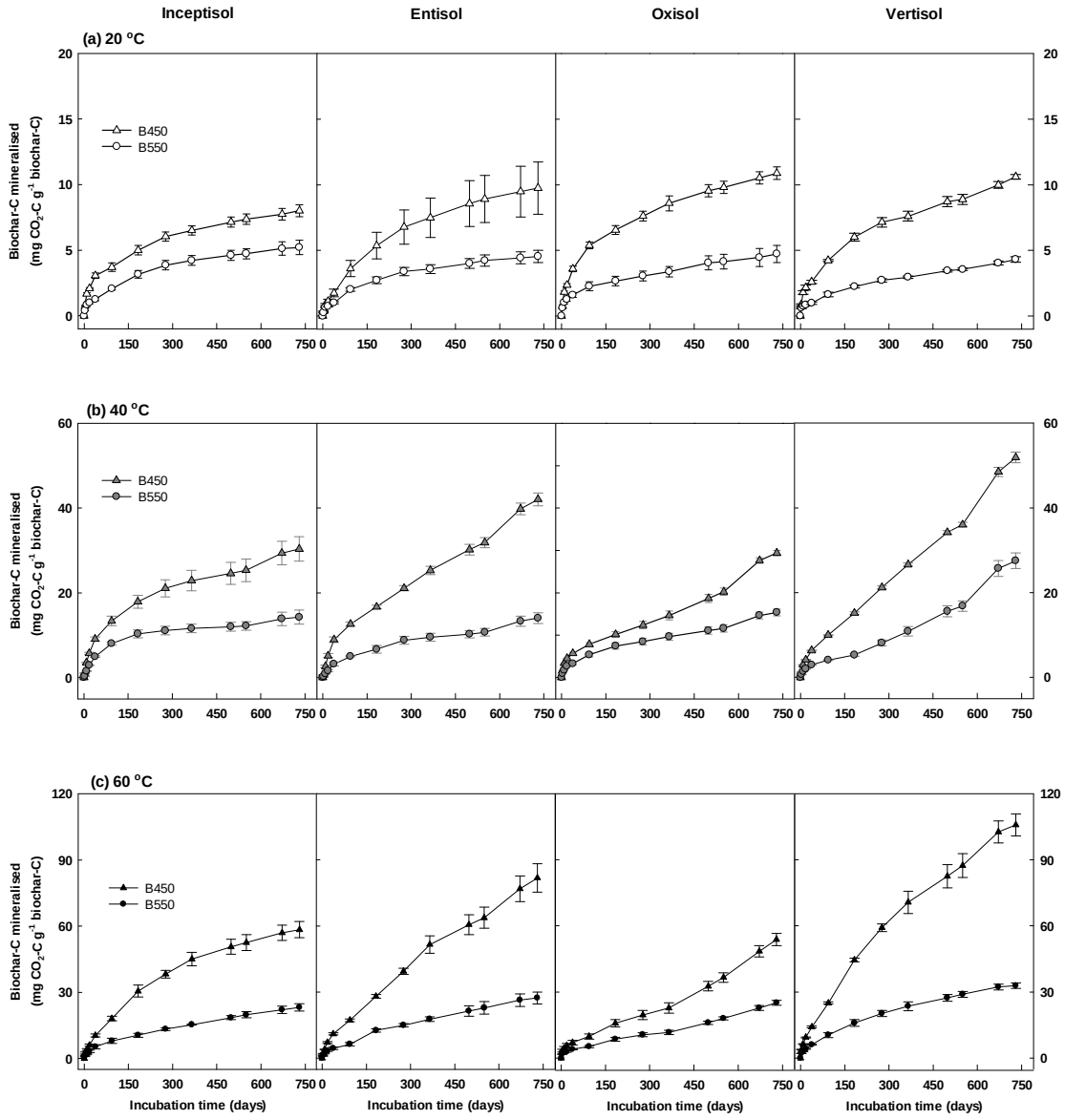

Figure 4.S3. Cumulative amount of biochar carbon (C) mineralised (mg CO_2-C g^{-1} biochar-C) from soils amended with 450 °C biochar (triangle symbol) and 550 °C biochar (circle symbol) at 20, 40 and 60 °C over two years incubation period. Error bars represent standard error of the means (n = 4).

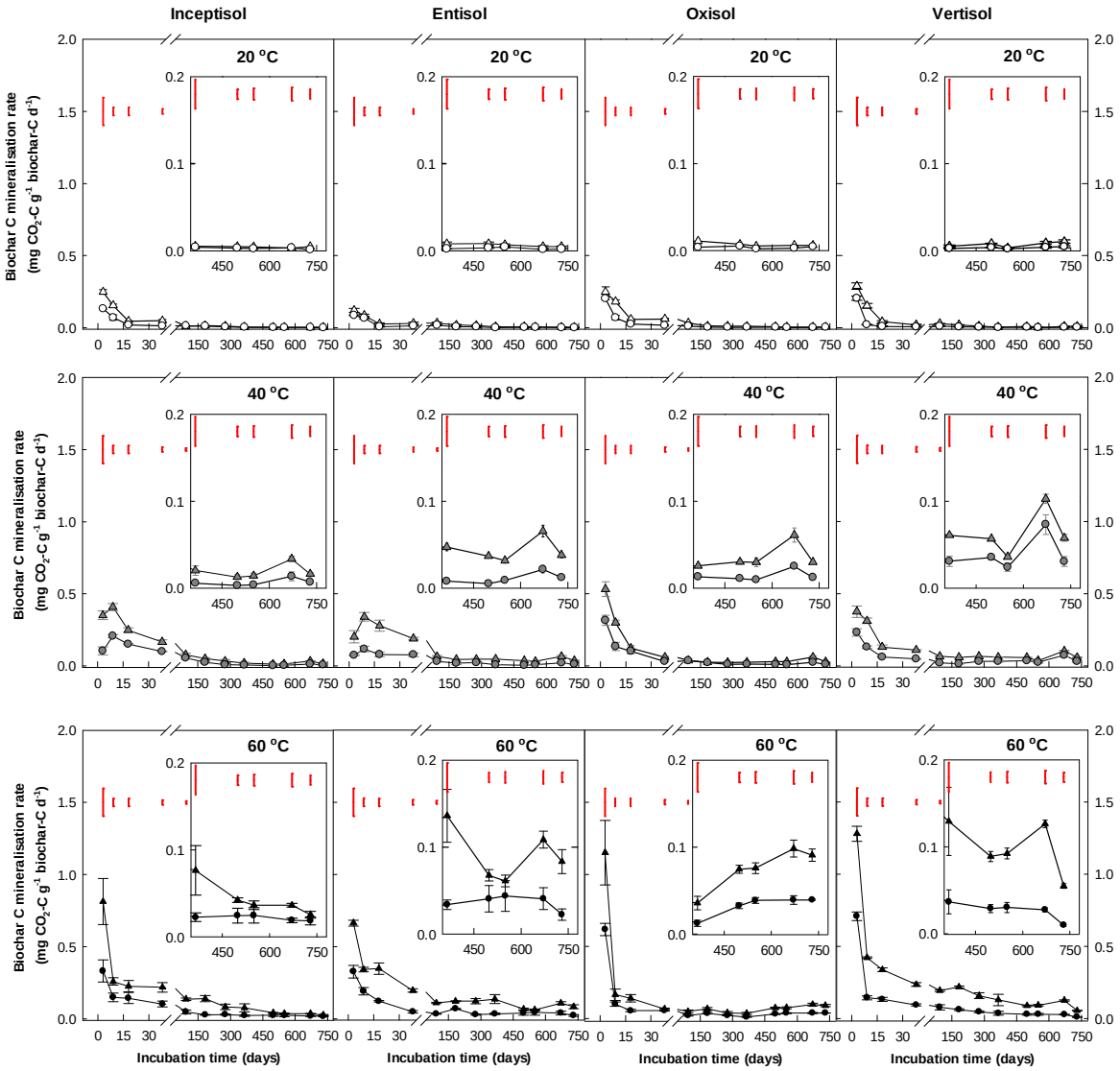

Figure 4.S4. Biochar carbon (C) mineralisation rate (mg CO_2-C g^{-1} biochar-C d^{-1}) from soils amended with 450 °C biochar (triangle symbol) and 550 °C biochar (circle symbol) at 20 40 and 60 °C over the two years incubation period. Error bars srepresent standard error of the means (n=4). Thick bars show least significant differences (at 5% level, $LSD_{0.05}$) of the interaction of soil and biochar types at different time-points.

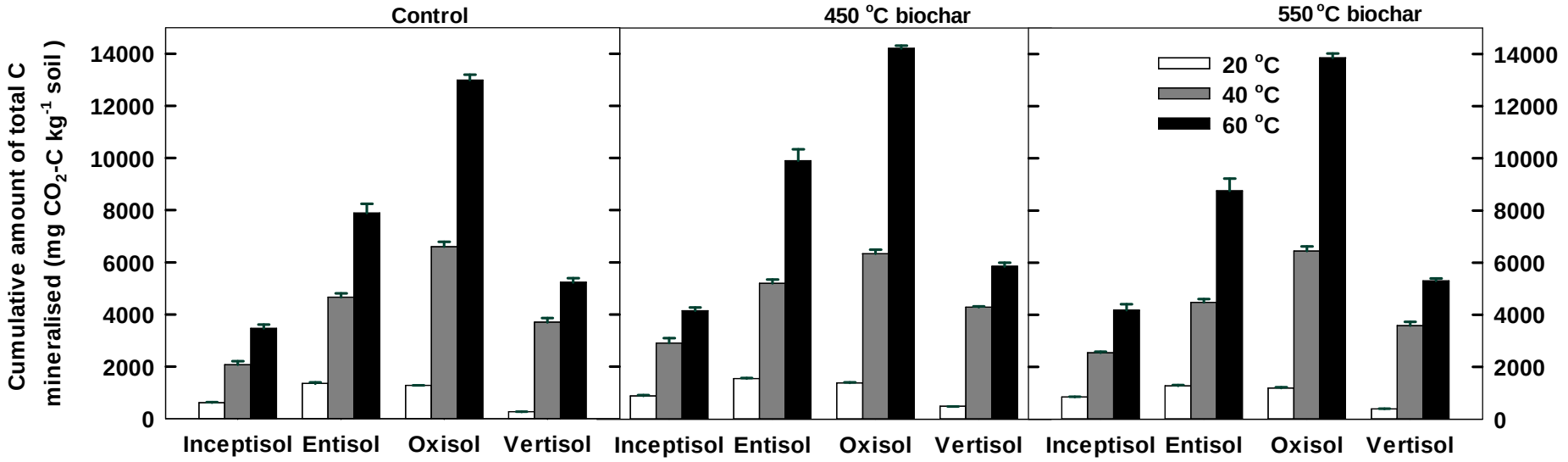

Figure 4.S5. Cumulative amounts of total carbon (C) mineralised (mg CO_2-C kg^{-1} soil) from control (without biochar), 450 and 550 °C biochar-amended soils at 20 °C (white columns), 40 °C (grey columns) and 60 °C (black columns) over the 2-year of incubation period. Error bars represent standard error of the means (n = 4).

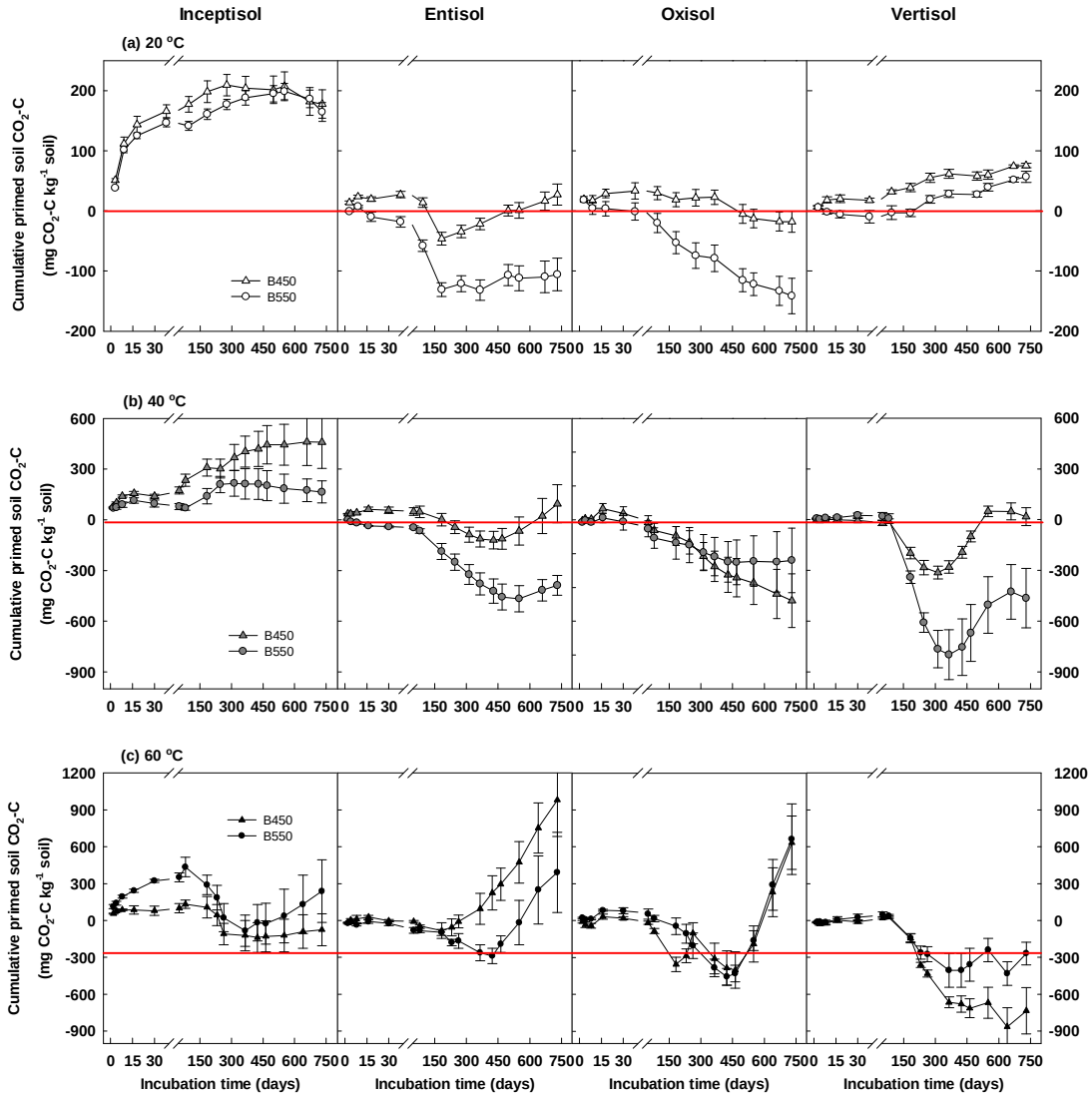

Figure 4.S6. Cumulative amounts of primed native SOC (mg CO_2-C kg^{-1} soil) in soils induced by the addition of 450 °C biochar (triangle) and 550 °C biochar (circle) at 20 °C (empty symbols), 40 °C (grey symbols) and 60 °C (dark symbols) over the 2-year of incubation period. Error bars represent standard error of the means (n = 4).

Chapter 5: Temperature sensitivity of biochar and native carbon mineralisation in biochar-amended soils[3]

Abstract

Temperature sensitivity of biochar-C in soil is not well understood. To acquire this information, we incubated two $\delta^{13}C$-depleted (–36 ‰) wood biochars produced at 450 and 550 °C, under controlled laboratory conditions at 20, 40 and 60 °C in four contrasting soils (Inceptisol, Entisol, Oxisol and Vertisol). The respired CO_2 and associated $\delta^{13}C$ were analysed periodically (12–22 times) over two years. The temperature sensitivity of biochar-C and native SOC mineralisation was computed as: (i) averaged Q_{10} (Q_{10a}) for the whole (2-year) time series using a temperature-incorporated mineralisation model to estimate a temperature scaling function for the exponential Q_{10} model; (ii) instantaneous Q_{10} (Q_{10i}) by using a time series of C mineralisation rates for a simple Q_{10} model; and (iii) cumulative Q_{10} (Q_{10c}) by using cumulative C mineralised for a simple Q_{10} model.

The mineralisation rates of biochar-C and native SOC increased with increasing temperature and their sensitivities to temperature were significantly ($p < 0.001$) affected by soil type. For example, biochar-C Q_{10a} was the greatest (also for native SOC) in the Vertisol (2.74–2.77), followed by Inceptisol (2.47–2.66) and Entisol (2.39–2.45), and the smallest in the Oxisol (1.93–2.20) for the 20−40 °C range. Biochar and native SOC Q_{10a} were the smallest in the Vertisol for the 40−60 °C range. Biochar-C Q_{10a} was not influenced by biochar type (450 or 550 °C). The presence of biochar decreased Q_{10a} of native SOC in the Entisol, Vertisol and Inceptisol, but this influence did not occur in the Oxisol, especially at 20−40 °C. The temperature sensitivity of biochar-C (Q_{10a} and Q_{10c}) and SOC (Q_{10a} and Q_{10i}) decreased with increasing incubation temperatures. The Q_{10i} values of biochar-C and SOC increased with time at 20−40 °C. Even though biochar-C was more stable than native SOC (based on their mineralisation rate constants), the $Q_{10a,}$ Q_{10c} and Q_{10i}

[3] This chapter has been submitted to Agriculture, Ecosystems & Environment under the title "Temperature sensitivity of biochar and native carbon mineralisation in biochar-amended soils" in June 2013. Authors are Yunying Fang, Bhupinder Pal Singh and Balwant Singh. This paper has been revised and resubmitted to Agriculture, Ecosystems & Environment in August 2013.

values for biochar-C were either smaller or similar to that of native SOC. In conclusion, soil characteristics can alter the temperature sensitivity of biochar-C. Furthermore, biochar can decrease the temperature sensitivity of native SOC mineralisation and consequently enhance C sequestration in soil under climate warming.

5.1. Introduction

An accelerated decomposition of soil organic carbon (SOC), especially of the stable forms of carbon (C), by increasing temperature is of considerable significance to the C balance in soils and the global C cycle. The temperature sensitivity of soil C mineralisation, referred to as Q_{10}, is defined as the rate of increase in soil CO_2 emission with a 10 °C increase in temperature (Kirschbaum, 1995). Q_{10} is an important parameter to evaluate the feedback intensity between CO_2 emission and global warming (Luo et al., 2001; Zhou et al., 2009). Q_{10} may change with changes in chemical recalcitrance of organic matter, organo-mineral interactions and environmental conditions, and consequently alter the responses of SOC to global warming (Conant et al., 2008a; Craine et al., 2010; Davidson and Janssens, 2006; Wagai et al., 2013; Zimmermann et al., 2012b).

Soil organic carbon (SOC) is generally partitioned into labile and relatively stable SOC pools based on their turnover rates (Dungait et al., 2012; Krull et al., 2003; Paustian et al., 1992). Labile SOC pools are chemically less recalcitrant C, which turns over in months (Krull et al., 2003). Stable SOC pools are either chemically more recalcitrant or stabilised through protection by and within the soil mineral matrix, with turnover times in the range of several years to centuries (Dungait et al., 2012). It has been reported that the stable SOC pools are more sensitive to changes in temperature than the labile SOC pools (Conant et al., 2008b; Ghee et al., 2013; Haddix et al., 2011; Knorr et al., 2005). However, there are conflicting reports of similar temperature sensitivity of labile and stable SOC pools (Fang et al., 2005) or smaller temperature sensitivity of stable SOC pools than labile SOC pools (Liski et al., 1999). These contradictions indicate a high degree of mechanistic uncertainty. More recently, Wagai et al. (2013) reported that the temperature sensitivity of organic C mineralisation increased with increasing aromaticity of the light, mineral-free, organic C fractions in soil, thus supporting an

enzyme kinetic theory for the relationship of C quality and temperature sensitivity in the mineral-free organic fraction (Bosatta and Ågren, 1999; Davidson and Janssens, 2006). However, Wagai et al. (2013) did not find the temperature sensitivity of organic C to be related to the C quality indices of bulk soil or with the C molecular structure of bulk organic fraction, possibly due to the protective effect of the soil mineral matrix. Similarly, Giardina and Ryan (2000) found that the decomposition of whole SOC was not sensitive to temperature changes in mineral soils. The organo-mineral interactions in mineral soils may decrease the organic C accessibility to microbes for decomposition (Mikutta et al., 2006; Torn et al., 1997) and consequently confound the relationship between C quality and temperature sensitivity of SOC mineralisation (Davidson and Janssens, 2006; Kirschbaum, 2006). Furthermore, the temperature sensitivity of organic C mineralisation in soil usually decreases with increasing temperature (Kirschbaum, 1995; Suseela et al., 2012). Other environmental conditions may also play roles in the variation of temperature sensitivity (Davidson and Janssens, 2006). For example, Suseela et al. (2012) reported an effect of soil moisture on Q_{10}, with a decrease in Q_{10} under drought conditions.

Biochar is a solid material obtained from thermochemical conversion of biomass in an oxygen-limited environment (IBI, 2012) and is purposely produced for application to agricultural soil as an amendment (Lehmann and Joseph, 2009). Due to its predominantly aromatic C structures at temperature exceeding 400 °C (McBeath et al., 2011), biochar may degrade at a slower rate than other forms of C in soil. Hence conversion of biomass to biochar is proposed for long-term C storage and mitigate climate change (Lehmann et al., 2009). For example, less than 0.1 to 3% of the added biochar-C was mineralised per year across biochars produced at contrasting production temperatures or using different feedstocks, with the estimated mean residence time (MRT) ranging from a century to several millennia (Knoblauch et al., 2011; Kuzyakov et al., 2009; Singh et al., 2012; Zimmerman, 2010). Furthermore, biochar may stabilise native SOC (Keith et al., 2011; Liang et al., 2010), through physical and chemical interactions between biochar, native SOC and soil minerals (Fang et al., 2014; von Lützow et al., 2006). However, there is a lack of knowledge about the temperature sensitivity of biochar-C mineralisation (Nguyen et al., 2010), particularly in soils of contrasting characteristics, and also it is not known

if the presence of biochar could alter the temperature sensitivity of native SOC. In studies without the presence of clay minerals, the temperature sensitivity of biochar decomposition was found to decrease with increasing incubation temperature (Nguyen et al., 2010; Zimmermann et al., 2012a). Moreover, the temperature sensitivity of biochar-C mineralisation was also found to increase with increasing pyrolysis temperature, i.e. increased degree of condensation (McBeath et al., 2011; Nguyen et al., 2010).

Most studies of temperature sensitivity of SOC decomposition have been conducted to simulate temperature conditions of common occurrence in temperate areas, i.e. < 30 °C (Conant et al., 2008a; Fang et al., 2005; Kirschbaum, 1995; Wagai et al., 2013). There is a limited understanding of temperature sensitivity of biochar-C and native SOC mineralisation in biochar-amended soils in sub-tropical or tropical environments, where ground surface temperatures are mostly over 30 °C and may reach up to 60 °C during summer season (Zimmermann et al., 2012a). The objective of this study was to determine the temperature sensitivity of biochar-C mineralisation in soils of contrasting characteristics at temperature observed in typical sub-tropical and tropical conditions. We also assessed the influence of biochar on the temperature sensitivity of native SOC mineralisation. We conducted incubation studies at 20, 40 and 60 °C for up to two years and estimated the mineralisation rate constants of C in the 450 and 550 °C biochars and of native SOC to characterise their potential stability in different soils. The hypotheses we proposed were that (i) the temperature sensitivity of biochar-C and native SOC will vary across soils of contrasting properties, (ii) the 550 °C biochar will have a greater Q_{10} than the 450 °C biochar, and similarly biochar-C, owing to its high chemical recalcitrance, will have greater Q_{10} than native SOC, and (iii) the presence of biochar-C will influence native SOC temperature sensitivity.

5.2. Materials and methods

5.2.1. Biochars and soils

Two biochars were produced at 450 and 550 °C by slow pyrolysis (5−10 °C/min heating rate and 40 min residence time in a Daisy Reactor at Pacific Pyrolysis,

Australia) of δ^{13}C-depleted woody biomass of *Eucalyptus saligna* trees. The trees had been grown under an elevated CO_2 environment for two years (Barton et al., 2010). Chemical properties of biochars and associated analytical methods used for their characterisation are given in Fang et al. (2014). The relevant properties of biochars are $pH_{1:5\ water}$ 8.64, organic C 67.4%, δ^{13}C -36.3‰, H/C ratio 0.62 and ash content 3% for the 450 °C biochar, and $pH_{1:5\ water}$ 9.96, organic C 73.2%, δ^{13}C -36.5‰, H/C ratio 0.49 and ash content 7% for the 550 °C biochar.

Four contrasting agricultural soils, i.e. Inceptisol ($pH_{1:5\ water}$ 5.70, organic C 0.95%, δ^{13}C -28.2‰, clay content 1.3% and water holding capacity 21% (wt wt^{-1})); Entisol ($pH_{1:5\ water}$ 8.77, organic C 2.53%, δ^{13}C -14.1‰, clay content 21.5% and water holding capacity 39% (wt wt^{-1})); Oxisol ($pH_{1:5\ water}$ 5.65, organic C 4.39%, δ^{13}C -21.4‰, clay content 44% and water holding capacity 50% (wt wt^{-1})); and Vertisol ($pH_{1:5\ water}$ 7.89, organic C 2.25%, δ^{13}C -17.3‰, clay content 44% and water holding capacity 52% (wt wt^{-1})) were used in this study. The water holding capacity of the soils was determined after freely draining saturated soil for 24 h. Further details about chemical properties of the soils and associated analytical methods are given in Fang et al. 2014.

5.2.2. Laboratory incubation

The biochars and soils were ground to < 2 mm for the incubation experiment. The incubation experiment details are described in Fang et al. (2014). Briefly, the two biochars were separately mixed with each of the four soils (300 g oven-dry) at 2% (w/w); a non-amended control soil was also included. The biochar-soil mixtures were incubated in sealed plastic jars at 20, 40 and 60 °C for up to two years. Each treatment was replicated four times. The biochar-soil mixtures were adjusted at 70% water holding capacity of each soil, which was maintained by adding water periodically throughout the incubation duration. The CO_2 traps were changed at day 3, 9, 18, 38, 94, 183, 276, 365, 498, 550, 671 and 730 for the 20 °C incubation experiment, and at day 2, 4, 8, 16, 30, 51, 80, 130, 183, 246, 313, 365, 428, 469, 550, 591, 659 and 730 for the 40 °C incubation experiment, and at day 2, 4, 8, 16, 30, 51, 80, 112, 144, 183, 231, 263, 311, 365, 423, 463, 505, 550, 591, 640, 683 and 730 for the 60 °C incubation experiment. The sampling intervals were varied for the different temperatures because of the expected differences in the CO_2 emission rates at the

three temperatures. The traps were analysed for total CO_2-C and $\delta^{13}C$, as described in Fang et al. 2014.

5.2.3. Mineralisation of biochar-C and native SOC

The total C mineralised (mg kg^{-1} soil) at each sampling time from the biochar-amended and control soils was determined by titrating a 1 mL aliquot of the CO_2 trap solution against 0.1 M HCl, using phenolphthalein as the indicator. To determine the $\delta^{13}C$ signature of the trapped CO_2-C, a 10 mL aliquot of the CO_2 trap solution was mixed with 10 mL of 1.25 M $SrCl_2$ to precipitate the trapped CO_2 as $SrCO_3$. The detail of $\delta^{13}C$ analysis has been described by Keith et al. (2011). The $\delta^{13}C$ signatures (‰) of CO_2-C evolved from control and biochar treatments are shown in Appendix 5.

The proportion of biochar-derived CO_2-C ($C_{Biochar}$ (%)) in the total CO_2-C produced from the soils was determined using a two-pool ^{13}C isotopic mixing model (Keith et al., 2011). Using the proportions of biochar or native SOC-derived, the amounts of biochar-C or native SOC mineralised were calculated from total C mineralised (mg kg^{-1} soil) in the biochar-amended soils. The amounts of biochar-C and native SOC mineralised were then normalised to per gram of added biochar-C and initial native SOC, respectively.

The rates of C mineralised from biochar and native SOC sources were calculated from the amounts of CO_2-C released between the two sampling time points and then dividing them by number of days (Kuzyakov et al., 2009). Linear interpolation was done to determine mineralisation rates at the same incubation time for different temperatures.

5.2.4. Temperature sensitivity of biochar-C and native SOC

The temperature sensitivity of biochar-C and native SOC mineralisation at different temperature ranges was computed as: (i) averaged Q_{10} (Q_{10a}) over the whole incubation period using a temperature-incorporated mineralisation model to estimate a temperature scaling factor for the exponential Q_{10} function; (ii) instantaneous Q_{10} (Q_{10i}) by using a time series of observed C mineralisation rates for a simple Q_{10} function; and (iii) cumulative Q_{10} (Q_{10c}) by using cumulative C mineralised for a simple Q_{10} model. The following calculations were performed on the data for each replicate soil in turn.

To determine the Q_{10a} of biochar-C and native SOC mineralisation, firstly, the cumulative biochar-C and SOC mineralisation over time was fitted to a temperature-incorporated two-pool exponential model (Kätterer et al., 1998; Reichstein et al., 2000), as given below:

$$C_{min}(t, T) = C_1 \times \left(1 - e^{-r(T)\, k_1 t}\right) + C_2 \times \left(1 - e^{-r(T) k_2 t}\right) \quad (5.1)$$

Where C_{min} (t, T) is the cumulative proportion of added biochar-C mineralised (mg C g^{-1} biochar-C) [or the cumulative fraction of native SOC mineralised (mg C g^{-1} SOC)] as a function of temperature (T) and time (t); r(T) is a temperature scaling function, relating mineralisation rate at temperature T to the rate at reference temperature T_{ref}. This approach assumes that both rate constants (k_1, k_2) are equally affected by temperature (Kätterer et al., 1998; Reichstein et al., 2000), The r(T) at T in Equation 5.1 was estimated using a nonlinear least-squares curve fitting by minimising the sum of the squared errors between modelled and measured values of cumulative C mineralised in SigmaPlot 12.0. The values of the other parameters, i.e. C_1, C_2, k_1, k_2 in Equation 5.1 were obtained by fitting a two-pool exponential model (Equation 5.2) in SigmaPlot 12.0, as described above, to the time series of cumulative C mineralised at T_{ref} (Kätterer et al., 1998; Reichstein et al., 2000).

$$C_{min}(t) = C_1 \times \left(1 - e^{-k_1 t}\right) + C_2 \times \left(1 - e^{-k_2 t}\right) \quad (5.2)$$

Where C_{min} (t) is the cumulative biochar-C mineralised (mg C g^{-1} biochar-C) or the cumulative fraction of native SOC mineralised (mg C g^{-1} SOC); and t is the incubation time (days). The parameters, C_1 and C_2, represent the proportion (% of added biochar-C, or mg C g^{-1} native SOC) of the labile and recalcitrant C pools in biochar-C or native SOC, respectively, at T_{ref}; and k_1 and k_2 are the mineralisation rate constants for the labile and recalcitrant pools, respectively, at T_{ref}. It is assumed $C_1 + C_2 = 100\%$ for the added biochar-C mineralised, or 1000 mg CO_2-C g^{-1} SOC for native SOC mineralised. An example of calculation has shown in Appendix 4.

The Q_{10a} values for the 20–40 °C or 40–60 °C temperature range were then determined by the common exponential Q_{10} model (Reichstein et al., 2000). T_{ref} was 20 °C and 40 °C for estimating Q_{10a} at 20–40 °C and 40–60 °C, respectively.

$$Q_{10a} = r(T)^{\frac{10}{T - T_{ref}}} \quad (5.3)$$

A time series of the Q_{10i} values of the instantaneous mineralisation rates of biochar and native SOC were determined by the following simple Q_{10} function (Kirschbaum, 1995):

$$Q_{10i}(t) = \left(\frac{R_{t,T_2}}{R_{t,T_1}}\right)^{\frac{10}{T_2 - T_1}} \quad (5.4)$$

Where R_t is the C mineralisation rate at incubation time t. T_1 and T_2 are the two incubation temperatures, i.e. 20 and 40 °C, or 40 and 60 °C, respectively.

The cumulative C mineralisation data (after one and two years, or between one and two years) were used to calculate Q_{10c}. The Q_{10c} values of biochar and native SOC were determined by the following simple Q_{10} function equation (Nguyen et al., 2010):

$$Q_{10c} = \left(\frac{R_2}{R_1}\right)^{\frac{10}{T_2 - T_1}} \quad (5.5)$$

where, R_1 and R_2 is cumulative C loss (% of initial C concentration) at temperature T_1 and T_2. T_1 and T_2 are the incubation temperatures, i.e. 20 and 40 °C, or 40 and 60 °C, respectively.

Q_{10c} were calculated from cumulative C mineralisation from a certain period of time (one year, two years or between one and two years), differing from Q_{10a} which is an averaged temperature sensitivity for the whole (2-year) time series incorporating a temperature scaling function for the exponential Q_{10} model (Equations 5.1 and 5.3).

5.2.5. Statistical analysis

Repeated measures analyses were performed for biochar-C and SOC mineralisation rates and instantaneous Q_{10} (Q_{10i}) of biochar and SOC using a linear mixed model framework in Genstat® 14th edition (VSN International, 2011). Each analysis consisted of fixed effects of soil, biochar, temperature, time and all associated interactions, and random effects of replicate and replicate by time. To allow for correlation between repeated measures on the same units, a first order autoregressive model was fitted (giving a higher residual log-likelihood than the power model). Heterogeneity in the residual variances between time-points was included as it was deemed significant using a residual likelihood ratio test. For Q_{10a} of biochar-C and

native SOC, a three-way (soil, biochar and temperature) analysis of variance was performed in Genstat® 14th edition. Where the F-statistic was significant, the means were compared using the LSD test at the 5% significance level unless stated otherwise.

5.3. Results

5.3.1. Carbon mineralisation

Biochar-C: Biochar-C mineralisation rates were initially high across all soil and temperature treatments (0.09–1.28 mg C g^{-1} biochar-C d^{-1}) and then decreased in an exponential manner to small values (0.01–0.22 mg C g^{-1} biochar-C d^{-1}) with time (**Figure 5.1**). The mineralisation rates were significantly ($p < 0.001$) influenced by incubation temperature, soil type, biochar type, time, and their interactive effects (**Table 5.1**). Both the mineralisation rate and the cumulative biochar-C mineralised increased with increasing incubation temperatures in all soils for both biochars (**Figure 5.1** and **Figure 5.S1**). After the initial flush of CO_2 emission (first 2 to 3 weeks), biochar-C mineralisation rates ranged from 0.01−0.05, 0.02−0.10 and 0.01−0.22 mg C g^{-1} biochar-C d^{-1}, at 20, 40 and 60 °C, respectively. Biochar-C mineralisation rates for the 450 and 550 °C biochars were initially (in the first week) the greatest in the Oxisol and the Vertisol, at all three incubation temperatures, and then decreased rapidly in first two weeks of incubation.

At 20 °C, the cumulative fraction (mg CO_2-C g^{-1} biochar-C) of 450 °C biochar-C mineralised over two years followed the trend: Inceptisol ≤ Entisol ≤ Oxisol ≈ Vertisol (**Figure 5.S1**). At 40 and 60 °C, the cumulative fraction of 450 °C biochar-C mineralised was the greatest in the Vertisol and the smallest in the Oxisol and Inceptisol. The cumulative fraction of 550 °C biochar-C mineralised from the four soils was similar at 20 °C, greater in the Vertisol than the other soils at 40 °C, and greater in the Vertisol and Entisol than in the Inceptisol and Oxisol at 60 °C. Biochar-C mineralisation (both rate and cumulative fraction) was greater for the 450 °C than the 550 °C biochar across the soil and incubation temperature treatments over the whole incubation period (**Figure 5.1** and **Figure 5.S1**). The extent of increase in biochar-C mineralisation with increasing incubation temperature was greater in the

Vertisol for the 450 °C biochar, and in the Vertisol and Entisol for the 550 °C biochar, than the other soils (**Figure 5.1** and **Figure 5.S1**).

Table 5.1. Statistical significance of the effects of incubation time, soil, biochar and temperature treatments and their interactions on biochar-C and native SOC mineralisation rates, and temperature sensitivity parameters (Q_{10i}, Q_{10a}) over the 2-year incubation period.

Treatment effect	Biochar-C mineralisation rate	SOCmineralisation rate	Biochar Q_{10i}	SOC Q_{10i}	Biochar Q_{10a}	SOC Q_{10a}
Time (T)	***	***	***	***	–	–
Soil (S)	***	***	***	***	***	***
Biochar (B)	***	***	*	***	ns	***
Temperature (Tm)	***	***	***	***	***	***
T × S	***	***	***	***	–	–
T ×B	***	***	*	***	–	–
S × B	***	***	ns	***	*	***
T × Tm	***	***	***	***	–	–
S × Tm	***	***	***	***	***	***
B ×Tm	***	***	ns	***	ns	***
T × S × B	***	***	ns	***	–	–
T × S × Tm	***	***	***	***	–	–
T× B × Tm	***	***	*	***	–	–
S × B × Tm	***	***	***	***	ns	***
T × S × B × Tm	***	***	***	***	–	–

* $p < 0.05$; *** $p \leq 0.001$; ns, not significant.

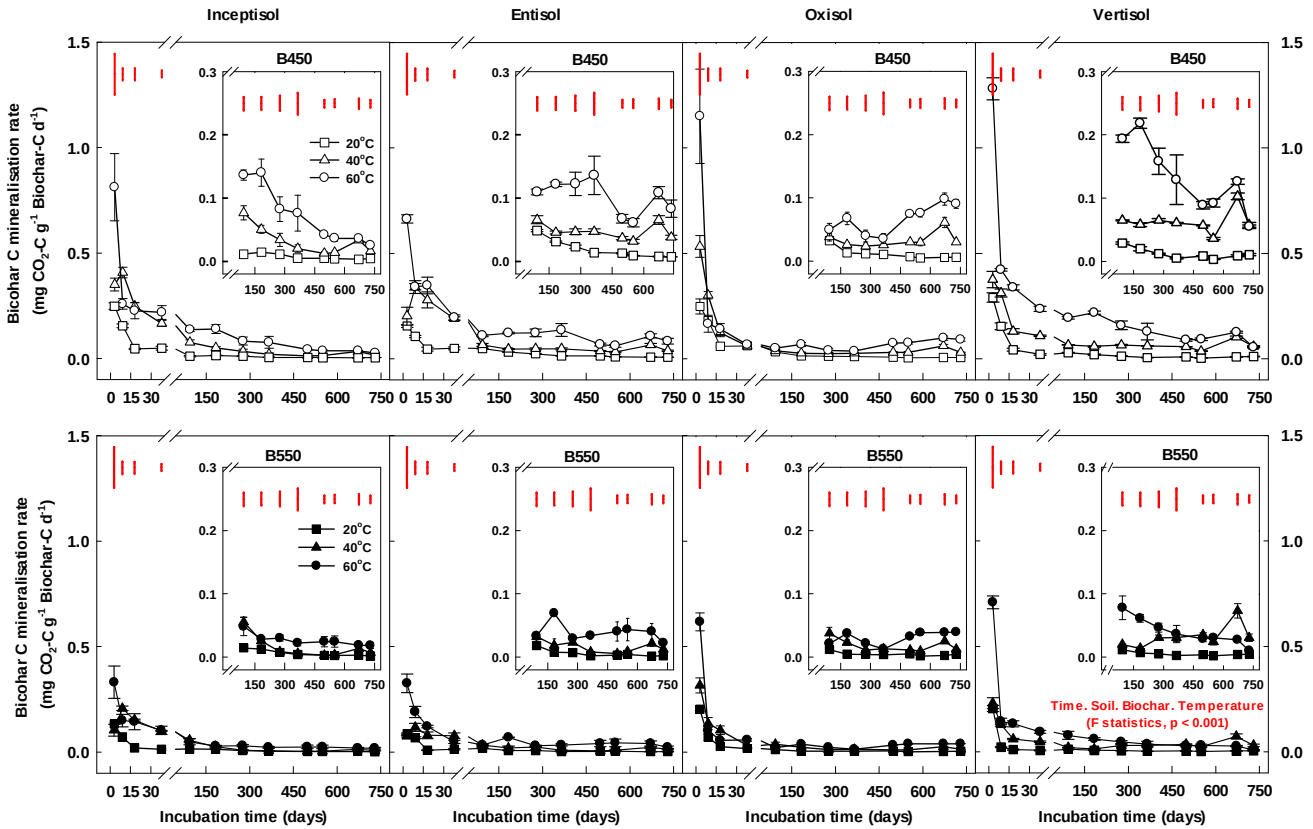

Figure 5.1. Biochar carbon (C) mineralisation rate (mg CO_2-C g^{-1} biochar-C d^{-1}) for 450 and 550 °C biochar-amended soils at 20 °C (square), 40 °C (triangle) and 60 °C (circle) over the 2-year incubation period. Empty and black filled symbols represent 450 °C biochar (B450) and 550 °C biochar (B550), respectively. The insets show the biochar-C mineralisation rate from 94 days after incubation with an expanded *y*-axis scale for clarity. Error bars represent ± standard errors of the mean (n=4). Red bars show least significant differences (at 5% level, LSD0.05) across biochar, soil and incubation temperature treatments at different time-points.

Native SOC: The mineralisation rate of native SOC in biochar-amended and control (non-amended) treatments was initially (up to day 3) great across all soil and temperature treatments (0.30−10.85 mg CO_2-C g^{-1} SOC d^{-1}) and decreased to small values (0.01−1.10 mg CO_2-C g^{-1} SOC d^{-1}) in an exponential manner with time (**Figure 5.3**). Like biochar-C, the mineralisation rates of native SOC in the biochar-amended and control treatments were significantly ($p < 0.001$) influenced by incubation temperature, soil type, biochar type, time, and their interactive effects (**Table 5.1**). Native SOC mineralisation (both rate and cumulative fraction) increased with increasing incubation temperature across all soil and biochar treatments (**Figure 5.2** and **Figure 5.S2**); the extent of increase was generally larger for temperature increase from 20 to 40 °C than from 40 to 60 °C. The rates and cumulative fractions of native SOC mineralised over time across the biochar and temperature treatments followed the sequence: Vertisol ≤ Oxisol ≤ Entisol ≤ Inceptisol (**Figure 5.2** and **Figure 5.S2**). In the Inceptisol, the rates of native SOC mineralisation were greater for the 450 °C and/or 550 °C biochar-amended soils than the control soils at several stages during the first few weeks at all three incubation temperatures. However, for the other soils, the rates of native SOC mineralisation at different times during incubation were generally similar in the biochar-amended and the control treatments.

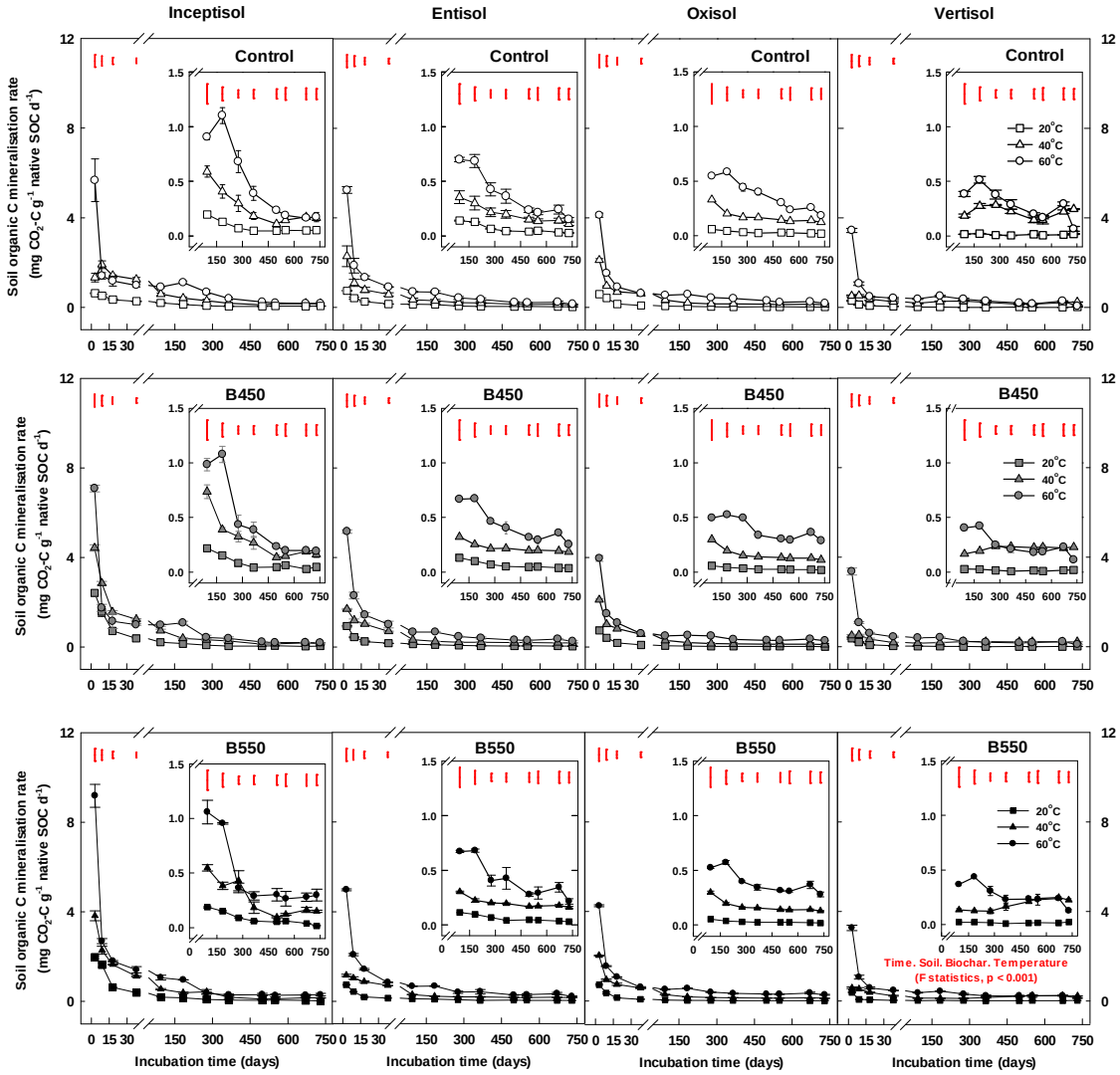

Figure 5.2. Native soil organic carbon (SOC) mineralisation rate (mg CO_2-C g^{-1} SOC d^{-1}) from control, 450 and 550 °C biochar-amended soils at 20 °C (square), 40 °C (triangle) and 60 °C (circle) over the 2-year incubation period. Empty, grey filled and black filled symbols represent control, 450 °C biochar (B450) and 550 °C biochar (B550), respectively. The insets show the native SOC mineralisation rate from 94 days after incubation with an expanded *y*-axis scale for clarity. Error bars represent ± standard errors of the mean (n=4). Red bars show least significant differences (at 5% level, $LSD_{0.05}$) across biochar, soil and incubation temperature treatments at different time-points.

5.3.2. Temperature coefficient (Q_{10})

Biochar-C: The Q_{10a} and Q_{10c} values of biochar-C mineralisation were significantly affected by the main effects of temperature and soil type, and the interactive effects

of soil, biochar, and/or temperature (**Table 5.1** and **Table 5.S1).** The Q_{10a} values of biochar-C mineralisation for both biochars were greater for the low temperature range 20−40 °C than the high temperature range 40−60 °C. The Q_{10a} values ranged from 1.93−2.77 and 1.31−1.79 (Q_{10c} from 1.65−2.44 and 1.10−1.43) at 20−40 °C and 40−60 °C, respectively (**Table 5.2** and **Table 5.S2**). For the 20−40 °C range, the smallest Q_{10a} value occurred in the Oxisol (1.93 and 2.20 for the 450 and 550 °C biochars, respectively) and the greatest value was observed in the Vertisol (2.77 and 2.74 for the 450 and 550 °C biochars, respectively). The Q_{10a} values in the Inceptisol across both biochars (2.47–2.66) were similar to that in the Entisol (2.39–2.45) (**Table 5.2**). Similarly, the Q_{10c} values were the greatest for both biochars in the Vertisol (**Table 5.S2**). In the 40−60 °C range, the Q_{10a} values for the 450 °C biochar were smaller in the Oxisol (1.38), and greater in the Inceptisol (1.79), than the other three soils. The Q_{10a} values for the 550 °C biochar among the soils were in the order of Entisol ≈ Inceptisol > Oxisol ≈ Vertisol (**Table 5.2**). At 40−60 °C, Q_{10c} values of both biochars showed no difference between soil treatments. The Q_{10c} was smaller in the first year of incubation (1.31−1.88) than in the second year (1.72−3.93) across biochar and soil type (**Table 5.S4**). In general, the Q_{10a} and Q_{10c} values of the 450 °C biochar were similar to that of the 550 °C biochar, when comparing across the soils within each incubation temperature range (**Table 5.2** and **Table 5.S2**), although there were some exceptions in the case of Q_{10a} values. These exceptions are: (i) the Q_{10a} value for the 450 °C biochar was significantly smaller than the 550 °C biochar in the Oxisol (20–40 °C) and Entisol (40–60 °C), and (ii) the Q_{10a} value for the 450 °C biochar-amended Vertisol (40–60 °C) was significantly greater than the 550 °C biochar amended Vertisol (**Table 5.2**).

The Q_{10i} values of biochar-C were significantly affected by the main effects of temperature range, soil type, biochar type, time and also by their interactive effects in most cases (**Table 5.1**). The Q_{10i} values across the treatments were highly variable over the incubation period and ranged between 0.91 and 4.55 for the 20−40 °C range, which is greater than calculated (i.e. between 0.58 and 2.90) for the 40−60 °C range (**Figure 5.3**). At 20−40 °C, the Q_{10i} values for both biochars increased with time particularly in the Vertisol; the increasing trend with time was more variable in the other soils. On the other hand, at 40−60 °C, the Q_{10i} values for both biochars decreased with time in the Vertisol, but showed no clear trend in the other soils. The

Q_{10i} values for both biochars were greater in the Vertisol at 20−40 °C and smaller in the Vertisol at 40−60 °C, mainly in the later stages of incubation, than the other soils (**Figure 5.3**). There was no significant difference in the Q_{10i} values between the 450 and 550 °C biochars across different temperature ranges, times or soils (**Figure 5.3**; **Table 5.1**).

Table 5.2. Averaged temperature sensitivity (Q_{10a}) of biochar-C mineralisation over the 2-year incubation period for the two temperature ranges. Small letters compare significant differences between the soils for each biochar at each of the temperature range. ($LSD_{0.05}$ = 0.25)

Soil	20−40 °C		40−60 °C	
	B450	B550	B450	B550
Inceptisol	2.66 (±0.16) c	2.47 (±0.15) b	1.79 (±0.08) b	1.61 (±0.05) b
Entisol	2.39 (±0.06) b	2.45 (±0.12) b	1.53 (±0.06) ab	1.79 (±0.12) b
Oxisol	1.93 (±0.04) a	2.20 (±0.09) a	1.38 (±0.05) a	1.31 (±0.05) a
Vertisol	2.77 (±0.33) c	2.74 (±0.08) b	1.60 (±0.04) ab	1.32 (±0.04) a

The numbers in parentheses are the standard error of the mean (n=4).

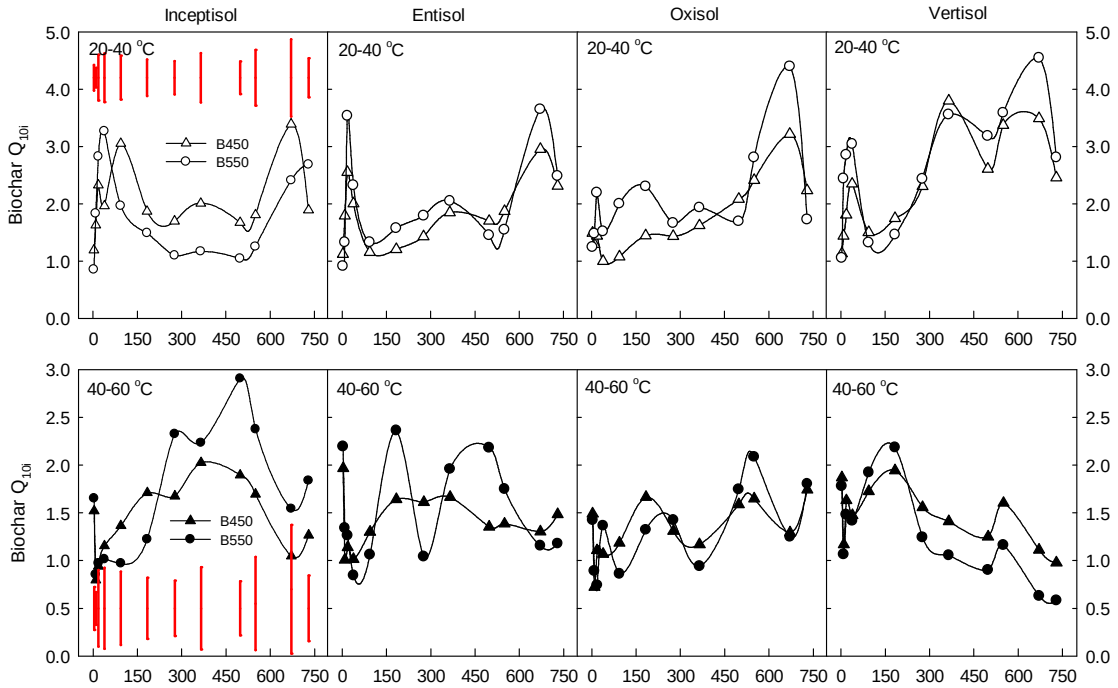

Figure 5.3. Time series of the instantaneous Q_{10} (Q_{10i}) of biochar-C mineralisation rates observed within two temperature ranges, i.e. 20−40 °C and 40−60 °C, during two years of incubation. Triangle and circle symbols represent 450 °C biochar (B450) and 550 °C biochar (B550), respectively. Red bars show least significant differences (at 5% level, $LSD_{0.05}$) across biochar, soil and temperature treatments at different time-points.

Native SOC: The Q_{10a} and Q_{10c} values for native SOC mineralisation in the biochar-amended and control treatments were significantly influenced by temperature range, soil type, biochar type and their interactive effects (**Table 5.1** and **Table 5.S3**). The Q_{10a} and Q_{10c} values of native SOC mineralisation were greater for the 20−40 °C range than the 40−60 °C range across all soil and biochar treatments (**Table 5.3** and **Table 5.S3**). For the 20−40 °C range, the Q_{10a} and Q_{10c} values for native SOC across the treatments were significantly greater in the Vertisol than the other soils, and the smallest values were observed in the Entisol or Inceptisol (**Table 5; 5S3**). On the other hand, at 40−60 °C, the Q_{10a} and Q_{10c} values for native SOC across the biochar treatments were significantly smaller in the Vertisol than the other soils. The greatest Q_{10a} values were observed in the Inceptisol for the control and 550 °C biochar treatments and in the Oxisol for the 450 °C biochar treatment. Relative to their

respective controls, in the 20−40 °C range, the SOC Q_{10a} values were significantly smaller in the 450 and 550 °C biochar-amended Entisol and Vertisol and in the 550 °C biochar-amended Inceptisol only. The SOC Q_{10c} was significantly smaller in the biochar-amended Vertisol only, relative to the control. For the 40−60 °C range, the SOC Q_{10a} values were significantly smaller in the 450 °C biochar-amended Inceptisol, relative to the control, but the presence of 450 or 550 °C biochar did not significantly affect the SOC Q_{10a} values between the other soils (**Table 5.3)**. The Q_{10c} was smaller in the first year of incubation (1.66−3.64) than in the second year (1.71−3.96) across biochar and soil type (**Table 5.S5**).

The Q_{10i} values of native SOC were also significantly influenced by the main effects of time, soil, biochar, temperature and their interactive effects (**Table 5.1**). After the first 18 days, the Q_{10i} values were greater for the 20−40 °C range than the 40−60 °C range across all soil and biochar treatments (**Figure 5.4**). For the 20−40 °C range, the Q_{10i} values of native SOC in the biochar-amended and control Vertisol consistently increased with time throughout from 1.14 to 3.70; in the Inceptisol, Entisol and Oxisol, the Q_{10i} values were small initially (1.24−1.88), and then increased and stabilised with time in the range of 1.65−2.35. On the other hand, in the 40−60 °C range, the Q_{10i} values of native SOC decreased rapidly across all biochar and soil treatments for up to 38 days and then stabilised in the Inceptisol, Entisol and Oxisol, but continued to decrease in an exponential manner in the Vertisol (**Figure 5.4**). For the 20−40 °C range, after the first month, the Q_{10i} values of native SOC among the soils followed the trend: Inceptisol ≈ Entisol < Oxisol < Vertisol across the biochar treatments. In comparison, for the 40−60 °C range, the Q_{10i} values of native SOC were similar among the soils, but became smaller in the Vertisol than the other soils towards the end of incubation. For the 20−40 °C range, the native SOC Q_{10i} values were consistently smaller in the 450 °C biochar and/or 550 °C biochar-amended Inceptisol and Vertisol than the corresponding control, while at 40−60 °C, only the 550 °C biochar-amended Vertisol had greater native SOC Q_{10i} values than the corresponding control or the 450 °C biochar amended treatment (**Figure 5.4**).

Table 5.3. Averaged temperature sensitivity (Q_{10a}) of native soil organic C (SOC) mineralisation over the 2-year incubation period for the two temperature ranges. Small letters compare significant differences among the soils for each biochar at each of the temperature range. Capital letters compare significant differences between biochar treatments for each soil at each of the temperature range. ($LSD_{0.05}$ =0.18)

Soil	20−40 °C			40−60 °C		
	Control	B450	B550	Control	B450	B550
Inceptisol	2.65 (±0.13) abB	2.62 (±0.10) bB	2.35(±0.09) aA	1.85 (±0.03) cB	1.47 (±0.04) bA	1.72 (±0.09) bB
Entisol	2.57 (±0.04) aB	2.32 (±0.03) aA	2.31 (±0.02) aA	1.50 (±0.04) bA	1.61 (±0.03) bcA	1.56 (±0.05) abA
Oxisol	2.83 (±0.04) bA	2.79 (±0.04) bA	2.97 (±0.05) bA	1.66 (±0.02) bcA	1.75 (±0.02) cA	1.69 (±0.01) bA
Vertisol	4.61 (±0.12) cC	4.01 (±0.03) cB	3.44 (±0.14) cA	1.30 (±0.03) aA	1.22 (±0.01) aA	1.37 (±0.02) aA

The numbers in parentheses are the standard error of the mean (n=4).

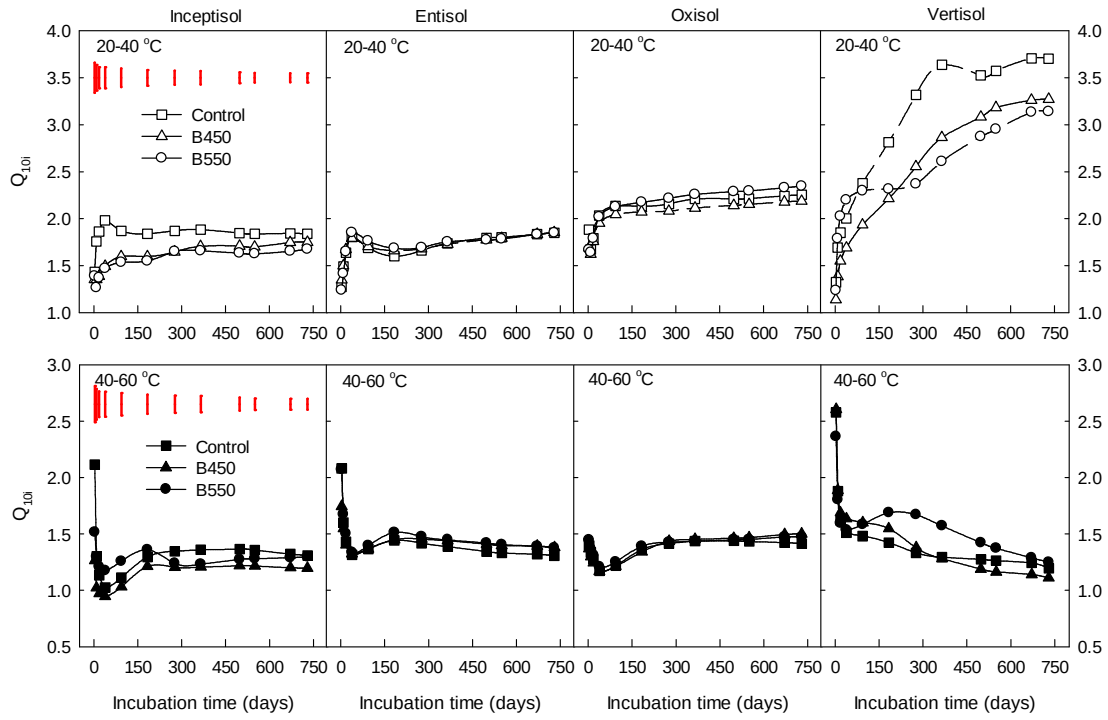

Figure 5.4. Time series of the instantaneous Q_{10} (Q_{10i}) of native soil organic C (SOC) mineralisation rates observed within two temperature ranges, i.e. 20−40 °C and 40−60 °C, during two years of incubation. Square, triangle and circle symbols represent control, 450 °C biochar (B450) and 550 °C biochar (B550), respectively. Red bars show least significant differences (at 5% level, $LSD_{0.05}$) across biochar, soil and temperature treatments at different time-points.

5.4. Discussion

There has been a recent study on the assessment of temperature sensitivity (Q_{10}) of biochar-C in response to increasing incubation temperature in a sand-biochar mixture (Nguyen et al., 2010). To our knowledge, this is the first study that has assessed biochar-C temperature sensitivity in soils of contrasting properties and the influence that biochar may have on the temperature sensitivity of native SOC mineralisation.

As expected, we found that the mineralisation rates of both biochar-C and native SOC increased with increasing temperature (Davidson and Janssens, 2006; Nguyen et al., 2010; Trumbore et al., 1996). Across all biochars and soils, the ranges for Q_{10} (Q_{10a}) values for biochar (1.93−2.77) and native SOC (2.31−4.61) at 20−40°C are wider than the reported values (1.0−3.0) in the literature at similar temperatures

(Kätterer et al., 1998; Kirschbaum, 1995; Nguyen et al., 2010). The Q_{10i} values of biochar-C fluctuated widely with time, i.e. between 0.91 and 4.55 at 20−40 °C, and between 0.58 and 2.90 at 40−60 °C, possibly due to relatively large variance in very small C mineralisation rates of the biochars (**Figure 5.1**). In contrast, the Q_{10i} values of native SOC had relatively stable trends over time and fluctuated within relatively narrow ranges with time, i.e. between 1.14 and 3.70 at 20−40 °C, and between 0.95 and 2.60 at 40−60 °C, across all biochar and soil treatments. The relatively wider ranges of Q_{10i} and Q_{10a} values in our study for biochar-C or native SOC (c.f. the values reported in literature) was due to their greater and smaller values observed in the Vertisol, at 20−40 °C and 40−60 °C, respectively, than the other soils.

The greater temperature sensitivity (Q_{10a}, Q_{10i}) of native SOC mineralisation for the lower temperature range (20−40 °C) than the higher temperature range (40−60 °C) in our study is consistent with other studies (Kirschbaum, 1995; Nguyen et al., 2010; Suseela et al., 2012). The smaller Q_{10} of biochar-C and native SOC in the high temperature range possibly results from decreased soil microbial activity (Zimmermann et al., 2012a). Also, abiotic oxidation may increase with increasing temperature (Zimmermann et al., 2012a), including the volatilisation of organic compounds. Additionally, the loss of C by abiotic oxidation may be less temperature sensitive than the loss of C by biotic processes.

5.4.1. Q_{10} and organic C quality

Soil organic matter and biochar are comprised of organic C constituents of different labilities, which are likely to mineralise at different rates at different temperatures, and therefore the Q_{10i} is expected to change with time (**Figure 5.3** and **Figure 5.4**). Initially, the high C mineralisation may be attributed to the most labile C fractions (Haddix et al., 2011), which seem to be depleted faster at 40 °C than 20 °C (**Figure 5.1** and **Figure 5.2**). Consequently, the larger mineralisation of SOC at 40 °C than 20 °C caused the SOC Q_{10i} to increase initially (up to 38 days) in the 20−40 °C range. On the other hand, the most labile C fraction seems to have mineralised rapidly at 60 °C (e.g. in the first 3 days), leading to a greater decrease in the C mineralisation rate with time at 60 °C relative to 40 °C (**Figure 5.2**). This may have led to a rapid decrease in SOC Q_{10i} (up to 38 days) in the 40−60 °C range. The biochar Q_{10i} also

showed similar trends to that of SOC Q_{10i} but the variability was large for the biochar Q_{10i} (**Figure 5.3**).

The increase of biochar or SOC Q_{10i} with time in the 20−40 °C temperature range (**Table 5.2** and **Table 5.3**) agrees with the finding by Conant et al. (2008a), who observed that the Q_{10} of SOC (Q_{10}: 1.7−3.3) was smaller at the beginning of incubation than at the later stage (Q_{10}: 2.4−4.9) at 25−35 °C. Similarly, the Q_{10c} was smaller in the first year of incubation than in the second year across biochar and soil type (**Table 5.S4** and **Table 5.S5**). According to the enzyme kinetic theory, the temperature sensitivity of recalcitrant-C is greater than labile-C, as more activation energy and reaction steps are needed for the decomposition of recalcitrant-C (Bosatta and Ågren, 1999; Davidson and Janssens, 2006). Some researchers confirmed this theory and found greater Q_{10} for more recalcitrant-C than labile-C pool in soils (Craine et al., 2010; Fierer et al., 2006; Knorr et al., 2005; Leifeld and Fuhrer, 2005). Consistent with this theory, we observed an increase in Q_{10i} for biochar or native SOC at 20−40 °C with time but not at 40−60 °C. This may due to decreased microbial and enzyme activities at 60 °C (Zimmermann et al., 2012a), and hence the C quality-temperature relationship may not be valid to explain the change of Q_{10i} in the 40−60 °C range.

Biochar type did not significantly influence the temperature sensitivity of biochar-C mineralisation (**Table 5.1** and **Table 5.S1**), although these biochars possessed different C stability as shown by their mineralisation rate constants (**Table 5.S6**). Furthermore, the temperature sensitivity was similar for the two biochars, or smaller for the 450 °C biochar than the 550 °C biochar, across most combinations of biochar and soil treatments (**Table 5.2**). Similarly, Nguyen et al. (2010) found that the temperature sensitivity of higher-temperature biochars (600 °C) was only slightly greater than the lower-temperature (350 °C) biochars. Furthermore, although biochar-C seems to be more stable than native SOC (as indicated by their mineralisation rate constants, see **Table 5.S6 and Table 5.S7)**, Q_{10a} of biochar-C was either smaller or similar to native SOC (**Table 5.2, Table 5.3, Table 5.S2 and Table 5.S3**). These data suggests that the theory of greater temperature sensitivity for relatively recalcitrant material (such as biochar) may not hold true when degrading in mineral soil. These results could imply greater storage potential of biochar-C in mineral soil under warming conditions.

5.4.2. Biochar-C mineralisation, Q_{10} and soil effect

Different Q_{10a} or Q_{10c} values of biochar-C for the four soils (**Table 5.1** and **Table 5.S1)** indicate that soil characteristics may have influenced the temperature sensitivity of biochar-C. For example, the smallest Q_{10a} of biochar-C was observed in the Oxisol and the greatest Q_{10a} or Q_{10c} in the Vertisol (**Table 5.2** and **Table 5.S2**). Both soils had similar high clay content (44%), however, the compositions of clay minerals were different, i.e. Fe and Al oxides in the Oxisol and smectite in the Vertisol. Consequently different physico-chemical stabilisation mechanisms may have occurred to significantly affect the temperature sensitivity of biochar-C in these two soils. It has been shown that biochar develops acidic functional groups during oxidation in soil and this process generates acidity around biochar (Cheng et al., 2008; Hilscher and Knicker, 2011). The smaller biochar Q_{10} in the Oxisol may be attributed to the stabilisation of biochar-C mineralisation via ligand exchange between functional groups on biochar surface, native organic matter and sesquioxides in the Oxisol (Gu et al., 1995; von Lützow et al., 2006). The acidic soil pH (5.65) in the Oxisol may have further enhanced the surface complexation reactions (Gu et al., 1995). The complexation of organic matter with Fe and Al oxides may decrease mineralisation of organic matter in soil (Zech et al., 1997) and hence its temperature sensitivity. Furthermore, organic matter in soil, including biochar, may be protected from mineralisation through entrapment within aggregates (Herath et al., 2013; Pronk et al., 2012). Such processes (i.e. organo-mineral complexation and aggregation) may be expected to occur at a relatively faster rate in the Oxisol (acidic pH) containing high native organic matter content and variable charge minerals than in the alkaline soils containing permanent charge minerals (Reichert et al., 2009). On the other hand, the greatest biochar Q_{10} in the Vertisol could be due to weaker interactions between limited carboxyl functional groups of biochar and the permanent charged mineral − smectite in the Vertisol. At higher incubation temperatures, the negatively-charged functional groups in biochar increase over time (Chapter 6; Cheng and Lehmann, 2009) and thus further decrease the weak interactions between biochar and the negative charges of smectites. The greater biochar Q_{10} in the Entisol than the Oxisol (**Table 5.2**) may also be attributed to the relatively weak interaction between biochar functional groups and kaolinite or illite and cation (Ca^{2+}) bridging (Schulten and Leinweber, 2000; Turchenek and

Oades, 1979; von Lützow et al., 2006). The Inceptisol had very low clay content (1.3%) and hence a minimal chemical interaction between clay and biochar would be expected in this soil. This may be the reason for the greater biochar Q_{10} in the Inceptisol than the Oxisol and the Entisol. There were other factors such as organic C content and pH that differed among the soils and may have confounded the effect of clay content and mineralogy on biochar Q_{10}. Further studies using soils of contrasting clay mineralogy but similar clay and SOC contents are required to isolate the mineral composition effects on biochar temperature sensitivity.

Our study has also shown that the soil effect on biochar temperature sensitivity may vary when Q_{10} values are estimated by different methods. For example, Q_{10c} of biochar had no significant difference between the Inceptisol, Entisol and Oxisol (except for the biochar 450 °C where Oxisol ≈ Entisol < Inceptisol in the 20−40 °C range) (**Table 5.2**). Since Q_{10c} was calculated from the cumulative C loss over the whole incubation period, the time effect was not considered. Consequently, the same Q_{10c} values were observed in the Inceptisol, Entisol and Oxisol, although the greatest biochar-C mineralisation rate occurred initially in the Oxisol, which decreased faster with time than the values observed for the Inceptisol and the Entisol.

5.4.3. Biochar influence on Q_{10} of native SOC

Biochar has large microporosity and specific surface area (191 and 228 $m^2\ g^{-1}$ for the 450 and 550 °C biochar, respectively), and these properties may play an important role in both physically and chemically interactions of biochar with native SOM and soil minerals. Although native SOM molecules may not be very soluble in the incubated systems without the addition of labile organic matter, mobile organic compounds may form during mineralisation. The mobile organic compounds may physical or chemical bound with biochar, thereby protecting organic compounds from microbial attack. However, according to the theory proposed by Pignatello et al. (2006), SOM molecules may become more flexible and slowly access interior pores in biochar with increasing incubation temperature and thus limit accessibility to soil microorganisms. Furthermore, biochar has been reported to increase the stability of macro-aggregates in a 10-month incubation study (Herath et al., 2013). Thus, it can be postulated that the stabilisation of native SOC may occur from one or more of the processes suggested above and may explain the smaller Q_{10a} values of native SOC

observed in the presence of biochar in the Inceptisol, Entisol and Vertisol for the 20−40 °C range. On the other hand, the addition of biochar did not significantly decrease native SOC temperature sensitivity in the Oxisol. This could be due to the presence of a large amount of variable charged minerals (goethite, gibbsite, hematite and kaolinite) and SOC may already have been well protected by chemical interaction with these minerals. Additionally, the ratio of biochar-C and native SOC was the lowest in the Oxisol compared to the other soils.

5.5. Conclusions and implications for carbon sequestration

This 2-year incubation study shows that increased soil temperature can accelerate the mineralisation of both biochar-C and native SOC in soils of contrasting properties. The temperature sensitivity of biochar-C was influenced by soil characteristics. The smallest Q_{10} for biochar in the Oxisol is possibly related to stronger organo-biochar-mineral interactions due to the presence of a significant proportion of variable charged minerals. As such, biochar application to Oxisol is a promising approach for C sequestration even in increasing temperature scenarios. Our results suggest that the presence of biochar may play an important role in decreasing native SOC temperature sensitivity, possibly through enhanced physical and chemical protection via surface complexation and cation bridging reactions.

Being a relatively recalcitrant C type, the temperature sensitivity of biochar-C mineralisation was expected to be greater than native SOC according to the kinetic theory; however, in our study biochar-C Q_{10a} (1.31−2.77) was smaller or the same as the native SOC Q_{10a} (1.30−4.61). This is possibly due to the influence of organo-mineral interactions, which decrease the 'intrinsic' biochar-C Q_{10} values. The smaller Q_{10} for the biochar-C than the native SOC suggests a high C sequestration potential of biochar even under warming conditions and especially in clayey soils.

5.6. References

Barton, C.V.M., Ellsworth, D.S., Medlyn, B.E., Duursma, R.A., Tissue, D.T., Adams, M.A., Eamus, D., Conroy, J.P., McMurtrie, R.E., Parsby, J., Linder, S., 2010. Whole-tree chambers for elevated atmospheric CO2 experimentation and tree scale flux measurements in south-eastern Australia: The Hawkesbury Forest Experiment. Agricultural and Forest Meteorology 150, 941-951.

Bosatta, E., Ågren, G.I., 1999. Soil organic matter quality interpreted thermodynamically. Soil Biology & Biochemistry 31, 1889-1891.

Cheng, C.H., Lehmann, J., 2009. Ageing of black carbon along a temperature gradient. Chemosphere 75, 1021-1027.

Cheng, C.H., Lehmann, J., Engelhard, M.H., 2008. Natural oxidation of black carbon in soils: Changes in molecular form and surface charge along a climosequence. Geochimica Et Cosmochimica Acta 72, 1598-1610.

Conant, R.T., Drijber, R.A., Haddix, M.L., Parton, W.J., Paul, E.A., Plante, A.F., Six, J., Steinweg, J.M., 2008a. Sensitivity of organic matter decomposition to warming varies with its quality. Global Change Biology 14, 868-877.

Conant, R.T., Steinweg, J.M., Haddix, M.L., Paul, E.A., Plante, A.F., Six, J., 2008b. Experimental warming shows that decomposition temperature sensitivity increases with soil organic matter recalcitrance. Ecology 89, 2384-2391.

Craine, J.M., Fierer, N., McLauchlan, K.K., 2010. Widespread coupling between the rate and temperature sensitivity of organic matter decay. Nature Geoscience 3, 854-857.

Davidson, E.A., Janssens, I.A., 2006. Temperature sensitivity of soil carbon decomposition and feedbacks to climate change. Nature 440, 165-173.

Dungait, J.A.J., Hopkins, D.W., Gregory, A.Z., Whitmore, A.P., 2012. Soil organic matter turnover is governed by accessibility not recalcitrance. Global Change Biology 18, 1781–1796.

Fang, C.M., Smith, P., Moncrieff, J.B., Smith, J.U., 2005. Similar response of labile and resistant soil organic matter pools to changes in temperature. Nature 436, 881-881.

Fang, Y., Singh, B., Singh, B.P., Krull, E., 2014. Biochar carbon stability in four contrasting soils. European Journal of Soil Science, 65, 60–71.

Fierer, N., Colman, B.P., Schimel, J.P., Jackson, R.B., 2006. Predicting the temperature dependence of microbial respiration in soil: A continental-scale analysis. Global Biogeochemical Cycles 20, GB3026.

Ghee, C., Neilson, R., Hallett, P.D., Robinson, D., Paterson, E., 2013. Priming of soil organic matter mineralisation is intrinsically insensitive to temperature. Soil Biology & Biochemistry 66, 20-28.

Giardina, C.P., Ryan, M.G., 2000. Evidence that decomposition rates of organic carbon in mineral soil do not vary with temperature. Nature 404, 858-861.

Gu, B.H., Schmitt, J., Chen, Z., Liang, L.Y., Mccarthy, J.F., 1995. Adsorption and desorption of different organic-matter fractions on iron-oxide. Geochimica Et Cosmochimica Acta 59, 219-229.

Haddix, M.L., Plante, A.F., Conant, R.T., Six, J., Steinweg, J.M., Magrini-Bair, K., Drijber, R.A., Morris, S.J., Paul, E.A., 2011. The role of soil characteristics on temperature sensitivity of soil organic matter. Soil Science Society of America Journal 75, 56-68.

Herath, H.M.S.K., Camps-Arbestain, M., Hedley, M., 2013. Effect of biochar on soil physical properties in two contrasting soils: An Alfisol and an Andisol. Geoderma 209-210, 188-197.

Hilscher, A., Knicker, H., 2011. Carbon and nitrogen degradation on molecular scale of grass-derived pyrogenic organic material during 28 months of incubation in soil. Soil Biology & Biochemistry 43, 261-270.

IBI, 2012. Standardized product definition and product testing guidelines for biochar that is used in soil. http://www.biochar-international.org/sites/default/files/Guidelines_for_Biochar_That_Is_Used_in_Soil_Final.pdf, (cited 5 March, 2013).

Kätterer, T., Reichstein, M., Andrén, O., Lomander, A., 1998. Temperature dependence of organic matter decomposition: a critical review using literature data analyzed with different models. Biology and Fertility of Soils 27, 258-262.

Keith, A., Singh, B., Singh, B.P., 2011. Interactive priming of biochar and labile organic matter mineralization in a smectite-rich soil. Environmental Science & Technology 45, 9611-9618.

Kirschbaum, M.U.F., 1995. The temperature dependence of soil organic matter decomposition, and the effect of global warming on soil organic C storage. Soil Biology & Biochemistry 27, 753-760.

Kirschbaum, M.U.F., 2006. The temperature dependence of organic-matter decomposition - still a topic of debate. Soil Biology & Biochemistry 38, 2510-2518.

Knoblauch, C., Maarifat, A.A., Pfeiffer, E.M., Haefele, S.M., 2011. Degradability of black carbon and its impact on trace gas fluxes and carbon turnover in paddy soils. Soil Biology & Biochemistry 43, 1768-1778.

Knorr, W., Prentice, I.C., House, J.I., Holland, E.A., 2005. Long-term sensitivity of soil carbon turnover to warming. Nature 433, 298-301.

Krull, E.S., Baldock, J.A., Skjemstad, J.O., 2003. Importance of mechanisms and processes of the stabilisation of soil organic matter for modelling carbon turnover. Functional Plant Biology 30, 207-222.

Kuzyakov, Y., Subbotina, I., Chen, H.Q., Bogomolova, I., Xu, X.L., 2009. Black carbon decomposition and incorporation into soil microbial biomass estimated by 14C labeling. Soil Biology & Biochemistry 41, 210-219.

Lehmann, J., Czimczik, C., Laird, D., Sohi, S., 2009. Stability of biochar in the soil, In: Lehmann, J., Joseph, S. (Eds.), Biochar for Environmental Management: Science and Technology. Earthscan, London, pp. 183-205.

Lehmann, J., Joseph, S., 2009. Biochar for environmental management: Science and technology. Earthscan, London.

Leifeld, J., Fuhrer, J., 2005. The temperature response of CO_2 production from bulk soils and soil fractions is related to soil organic matter quality. Biogeochemistry 75, 433-453.

Liang, B.Q., Lehmann, J., Sohi, S.P., Thies, J.E., O'Neill, B., Trujillo, L., Gaunt, J., Solomon, D., Grossman, J., Neves, E.G., Luizão, F.J., 2010. Black carbon affects the cycling of non-black carbon in soil. Organic Geochemistry 41, 206-213.

Liski, J., Ilvesniemi, H., Makela, A., Westman, C.J., 1999. CO2 emissions from soil in response to climatic warming are overestimated - The decomposition of old soil organic matter is tolerant of temperature. Ambio 28, 171-174.

Luo, Y.Q., Wan, S.Q., Hui, D.F., Wallace, L.L., 2001. Acclimatization of soil respiration to warming in a tall grass prairie. Nature 413, 622-625.

McBeath, A.V., Smernik, R.J., Schneider, M.P.W., Schmidt, M.W.I., Plant, E.L., 2011. Determination of the aromaticity and the degree of aromatic condensation of a thermosequence of wood charcoal using NMR. Organic Geochemistry 42, 1194-1202.

Mikutta, R., Kleber, M., Torn, M.S., Jahn, R., 2006. Stabilization of soil organic matter: Association with minerals or chemical recalcitrance? Biogeochemistry 77, 25-56.

Nguyen, B.T., Lehmann, J., Hockaday, W.C., Joseph, S., Masiello, C.A., 2010. Temperature sensitivity of black carbon decomposition and oxidation. Environmental Science & Technology 44, 3324-3331.

Paustian, K., Parton, W.J., Persson, J., 1992. Modeling soil organic matter in organic-amended and nitrogen-fertilized long-term plots. Soil Science Society of America Journal 56, 476-488.

Pignatello, J.J., Kwon, S., Lu, Y., 2006. Effect of natural organic substances on the surface and adsorptive properties of environmental black carbon (char): Attenuation of surface activity by humic and fulvic acids. Environmental Science & Technology 40, 7757-7763.

Pronk, G.J., Heister, K., Ding, G.C., Smalla, K., Kogel-Knabner, I., 2012. Development of biogeochemical interfaces in an artificial soil incubation experiment; aggregation and formation of organo-mineral associations. Geoderma 189, 585-594.

Reichert, J.M., Norton, L.D., Favaretto, N., Huang, C.H., Blume, E., 2009. Settling Velocity, Aggregate Stability, and Interrill Erodibility of Soils Varying in Clay Mineralogy. Soil Science Society of America Journal 73, 1369-1377.

Reichstein, M., Bednorz, F., Broll, G., Kätterer, T., 2000. Temperature dependence of carbon mineralisation: conclusions from a long-term incubation of subalpine soil samples. Soil Biology & Biochemistry 32, 947-958.

Schulten, H.R., Leinweber, P., 2000. New insights into organic-mineral particles: composition, properties and models of molecular structure. Biology and Fertility of Soils 30, 399-432.

Singh, B.P., Cowie, A.L., Smernik, R.J., 2012. Biochar carbon stability in a clayey soil as a function of feedstock and pyrolysis temperature. Environmental Science & Technology 46, 11770-11778.

Suseela, V., Conant, R.T., Wallenstein, M.D., Dukes, J.S., 2012. Effects of soil moisture on the temperature sensitivity of heterotrophic respiration vary seasonally in an old-field climate change experiment. Global Change Biology 18, 336-348.

Torn, M.S., Trumbore, S.E., Chadwick, O.A., Vitousek, P.M., Hendricks, D.M., 1997. Mineral control of soil organic carbon storage and turnover. Nature 389, 170-173.

Trumbore, S.E., Chadwick, O.A., Amundson, R., 1996. Rapid exchange between soil carbon and atmospheric carbon dioxide driven by temperature change. Science 272, 393-396.

Turchenek, L.W., Oades, J.M., 1979. Fractionation of organo-mineral complexes by sedimentation and density techniques. Geoderma 21, 311-343.

von Lützow, M., Kögel-Knabner, I., Ekschmitt, K., Matzner, E., Guggenberger, G., Marschner, B., Flessa, H., 2006. Stabilization of organic matter in temperate soils: mechanisms and their relevance under different soil conditions - a review. European Journal of Soil Science 57, 426-445.

VSN International, 2011. GenStat for Windows 14th Edition. Hemel Hempstead, UK: VSN International.

Wagai, R., Kishimoto-Mo, A.W., Yonemura, S., Shirato, Y., Hiradate, S., Yagasaki, Y., 2013. Linking temperature sensitivity of soil organic matter decomposition to its molecular structure, accessibility, and microbial physiology. Global Change Biology 19, 1114-1125.

Zech, W., Senesi, N., Guggenberger, G., Kaiser, K., Lehmann, J., Miano, T.M., Miltner, A., Schroth, G., 1997. Factors controlling humification and mineralization of soil organic matter in the tropics. Geoderma 79, 117-161.

Zhou, T., Shi, P.J., Hui, D.F., Luo, Y.Q., 2009. Global pattern of temperature sensitivity of soil heterotrophic respiration (Q_{10}) and its implications for carbon-climate feedback. Journal of Geophysical Research-Biogeosciences 114, G02016.

Zimmerman, A.R., 2010. Abiotic and microbial oxidation of laboratory-produced black carbon (biochar). Environmental Science & Technology 44, 1295-1301.

Zimmermann, M., Bird, M.I., Wurster, C., Saiz, G., Goodrick, L., Barta, J., Capek, P., Santruckova, H., Smernik, R., 2012a. Rapid degradation of pyrogenic carbon. Global Change Biology 18, 3306–3316.

Zimmermann, M., Leifeld, J., Conen, F., Bird, M.I., Meir, P., 2012b. Can composition and physical protection of soil organic matter explain soil respiration temperature sensitivity? Biogeochemistry 107, 423-436.

5.7. Supporting Information

Table 5.S1. Statistical significance of the effects of incubation time, soil, biochar, temperature treatments and their interactions on biochar-C and native SOC temperature sensitivity parameters (Q_{10c}) over the 2-year incubation period.

Treatment effect	Biochar Q_{10c}	SOC Q_{10c}
Soil (S)	***	***
Biochar (B)	ns	*
Temperature (Tm)	***	***
S × B	ns	***
S × Tm	***	***
B ×Tm	ns	***
S × B × Tm	*	***

* $p < 0.05$; *** $p \leq 0.001$; ; ns, not significant.

Table 5.S2. Biochar Q_{10c} (± standard errors) over the 2-year incubation period for the two temperature ranges. Small letters compare significant differences between the soils for each biochar at each of the temperature range.

Soil	20−40 °C		40−60 °C	
	B450	B550	B450	B550
Inceptisol	1.95±0.14 b	1.67±0.14 a	1.40±0.09 a	1.35±0.05 a
Entisol	1.68±0.05 a	1.78±0.12 a	1.39±0.05 a	1.40±0.08 a
Oxisol	1.65±0.03 a	1.86±0.19 a	1.35±0.04 a	1.28±0.03 a
Vertisol	2.21±0.02 b	2.44±0.03 b	1.43±0.03 a	1.10±0.04 a

Table 5.S3. SOC Q_{10c} (± standard errors) over the 2-year incubation period for the two temperature ranges. Small letters compare significant differences between the soils for each biochar at each of the temperature range. Capital letters compare significant differences between biochar treatments for each soil at each of the temperature range.

Soil	20−40 °C			40−60 °C		
	Control	B450	B550	Control	B450	B550
Inceptisol	1.84±0.08 aA	1.75±0.05 aA	1.68±0.04 aA	1.31±0.04 abA	1.20±0.06 aA	1.30±0.06 aA
Entisol	1.85±0.05 aA	1.85±0.03 aA	1.85±0.03 aA	1.31±0.05 abA	1.38±0.02 bA	1.38±0.01 abA
Oxisol	2.25±0.03 bA	2.19±0.03 bA	2.35±0.04 bA	1.41±0.02 bA	1.50±0.03 bA	1.47±0.03 bA
Vertisol	3.70±0.07 cB	3.27±0.02 cA	3.14±0.10 cA	1.19±0.02 aA	1.11±0.02 aA	1.25±0.04 aA

Table 5.S4. Biochar Q_{10c} (± standard errors) in the first and second year of incubation.

		20−40 °C		40−60 °C	
Soil	Treatment	1st year	2nd year	1st year	2nd year
Inceptisol	B450	1.88±0.15	2.26±0.24	1.42±0.10	1.36±0.10
	B550	1.67±0.11	1.72±0.31	1.20±0	1.97±0.21
Entisol	B450	1.49±0.03	2.18±0.12	1.43±0.03	1.35±0.09
	B550	1.65±0.15	2.22±0.07	1.38±0.10	1.44±0.07
Oxisol	B450	1.31±0.06	2.53±0.16	1.25±0.10	1.47±0.10
	B550	1.73±0.19	2.22±0.27	1.11±0.07	1.53±0.04
Vertisol	B450	1.87±0.03	2.93±0.17	1.63±0.05	1.18±0.04
	B550	1.86±0.08	3.35±0.10	1.48±0.03	0.78±0.02

Table 5.S5. Native SOC Q_{10c} (± standard errors) in the first and second year of incubation.

Soil	Treatment	20−40 °C		40−60 °C	
		1st year	2nd year	1st year	2nd year
Inceptisol	Control	1.88±0.10	1.71±0.04	1.36±0.06	1.18±0.11
	B450	1.71±0.03	1.94±0.15	1.21±0.05	1.17±0.08
	B550	1.66±0.06	1.75±0.04	1.23±0.05	1.54±0.12
Entisol	Control	1.74±0.03	2.15±0.11	1.39±0.04	1.13±0.07
	B450	1.73±0.02	2.13±0.05	1.44±0.02	1.28±0.03
	B550	1.75±0.04	2.06±0.04	1.45±0.01	1.25±0.02
Oxisol	Control	2.21±0.02	2.35±0.07	1.44±0.01	1.37±0.02
	B450	2.11±0.02	2.36±0.04	1.45±0.02	1.59±0.05
	B550	2.26±0.01	2.55±0.11	1.44±0.02	1.54±0.06
Vertisol	Control	3.64±0.09	3.80±0.22	1.29±0.04	1.05±0.03
	B450	2.86±0.06	3.96±0.19	1.28±0.01	0.91±0.04
	B550	2.61±0.11	3.77±0.16	1.57±0.09	0.98±0.04

Table 5.S6. Parameters of a, k_1, k_2 from two-pool exponential model for biochar (R^2: 0.920−0.999).

Soil	Treatment	a (%)			k_1 ($\times 10^{-2}$ d^{-1})			k_2 ($\times 10^{-5}$ d^{-1})		
		20°C	40°C	60°C	20°C	40°C	60°C	20°C	40°C	60°C
Inceptisol	B450	0.39	1.45	3.27	4.4	2.3	0.9	0.6	2.2	3.7
	B550	0.31	0.92	0.66	1.6	2.0	3.7	0.3	0.7	2.4
Entisol	B450	0.96	0.85	1.15	0.7	4.3	5.0	0.8	4.6	10.3
	B550	0.26	0.54	0.78	1.3	2.5	3.7	0.3	1.1	3.2
Oxisol	B450	0.53	0.39	0.45	2.9	18.3	83.6	0.8	3.3	6.2
	B550	0.19	0.43	0.25	9.9	5.2	51.2	0.4	1.5	2.9
Vertisol	B450	0.46	0.33	3.03	3.7	13.8	1.0	0.8	6.6	11.4
	B550	0.15	0.14	1.29	11.8	20.5	2.7	0.4	3.0	2.9
SE		0.03−0.10	0.01−0.33	0.07−0.32	0.1−7.7	0.2−2.9	0.1−41.9	0.02−0.1	0.02−0.4	0.1−0.5

Table 5.S7. Parameters of a, k_1, k_2 from two-pool exponential model for native SOC (R^2: 0.974−0.999).

Soil	Biochar	a (mg CO_2 g^{-1} SOC)			k_1 ($\times 10^{-2}$ d^{-1})			k_2 ($\times 10^{-5}$ d^{-1})		
		20°C	40°C	60°C	20°C	40°C	60°C	20°C	40°C	60°C
Inceptisol	Control	3.42	114.93	332.28	1.4	1.7	0.5	4.9	16.6	13.3
	B450	4.94	115.27	248.94	3.2	2.1	0.7	5.8	24.6	22.8
	B550	2.98	120.63	178.17	3.3	1.6	1.5	6.5	18.5	42.1
Entisol	Control	26.73	39.59	133.5	1.0	2.6	1.0	3.8	23.5	32.2
	B450	20.52	35.10	85.9	1.6	3.9	2.5	4.9	23.3	48.6
	B550	18.54	34.07	85.2	1.3	3.2	3.9	4.4	20.3	45.3
Oxisol	Control	9.23	39.28	87.77	4.4	2.8	1.0	2.9	16.8	36.9
	B450	9.97	39.24	39.00	4.9	3.1	6.2	2.7	15.0	46.1
	B550	8.67	36.28	44.34	5.5	3.2	4.7	2.5	16.3	45.1
Vertisol	Control	3.42	51.56	96.82	6.3	0.5	0.6	1.1	18.6	23.3
	B450	4.94	63.57	55.35	6.7	0.04	1.5	1.4	22.7	23.3
	B550	2.98	16.15	57.41	13.9	0.02	1.5	1.5	18.9	26.3
SE		0.23 −0.78	1.15 −25.58	5.18 −21.52	0.1 −7.1	0.01 −3.9	0.4 −6.2	0.03 −0.5	0.4 −3.6	1.7 −8.7

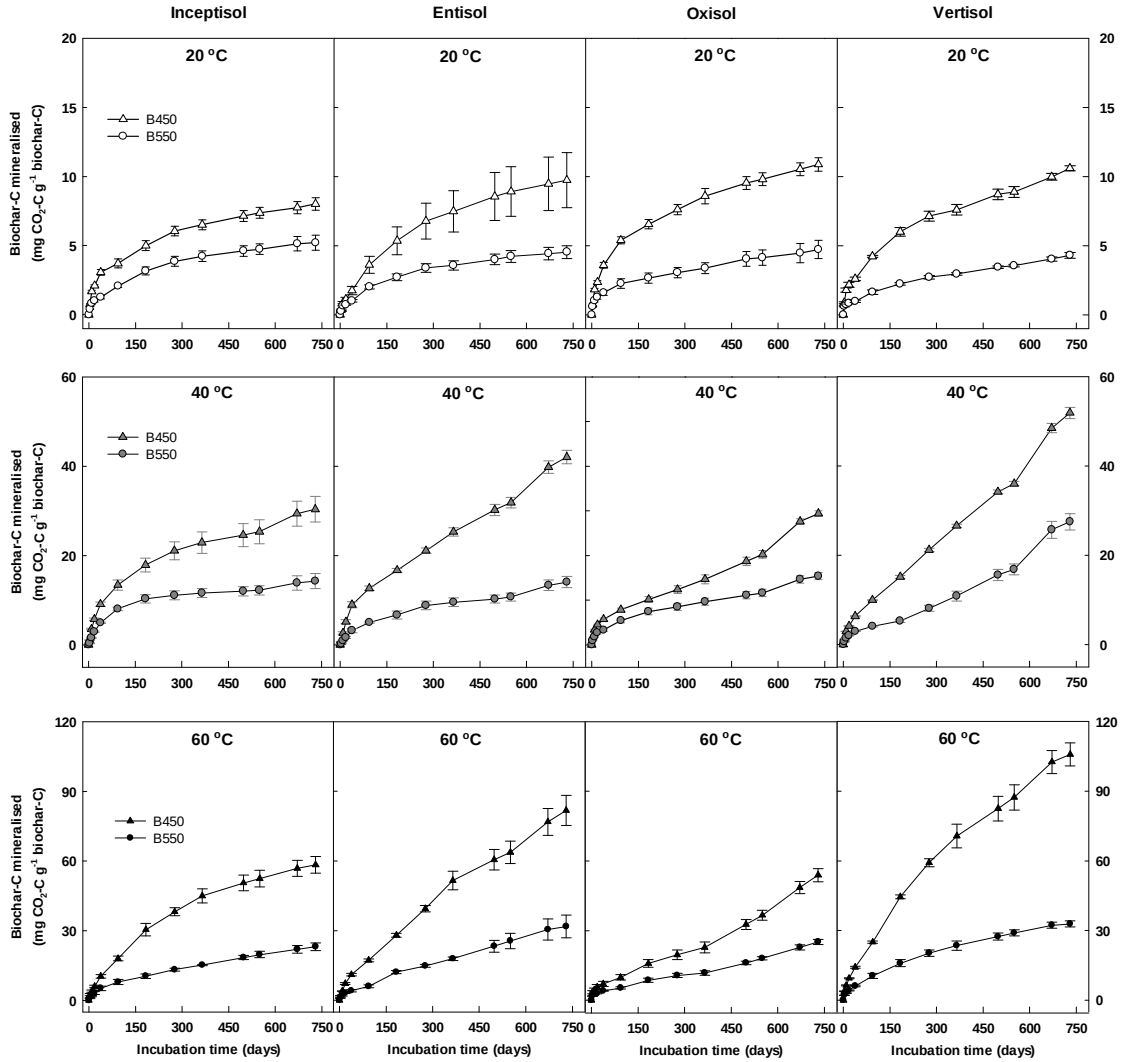

Figure 5.S1. Total biochar carbon (C) mineralised (mg CO_2-C g^{-1} biochar-C) from 450 and 550 °C biochar-amended soils at 20 °C (empty), 40 °C (grey filled) and 60 °C (black filled) over the 2-year incubation period. Error bars represent ± standard errors of the mean (n=4).

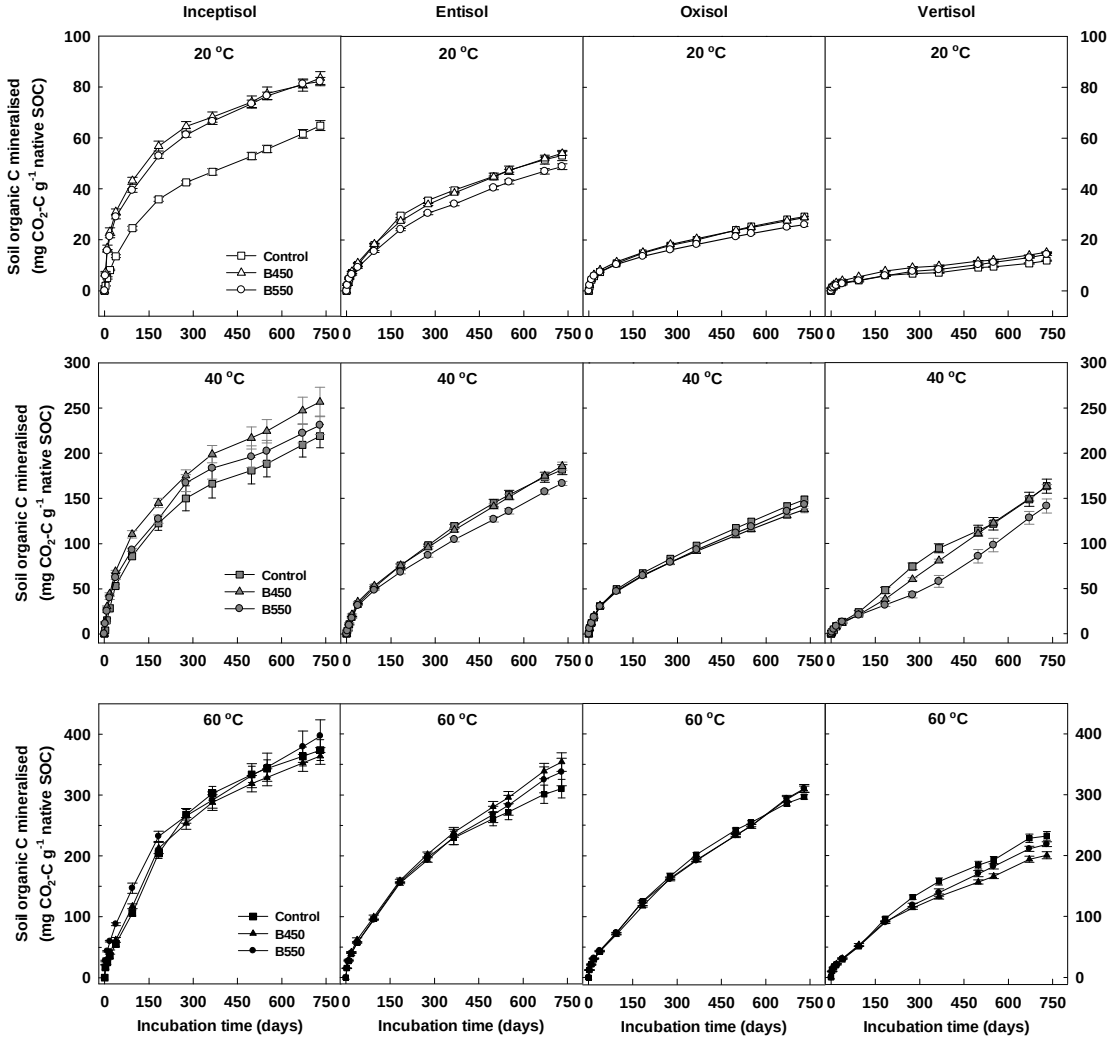

Figure 5.S2. Total native soil organic carbon (C) mineralised (mg CO_2-C g^{-1} SOC) from control (without biochar), 450 and 550 °C biochar-amended soils at 20 °C (empty), 40 °C (grey filled) and 60 °C (black filled) over the 2-year incubation period. Error bars represent ± standard errors of the mean (n=4).

Chapter 6: Application of NEXAFS spectroscopy and XPS for the characterisation of carbon functional groups of aged biochars in soils

Abstract

Biochar stability is crucial for the long-term carbon (C) storage in soils. However, some proportion of biochar-C is mineralised in soil with ageing, particularly at high temperatures. The oxidation of biochar leads to the development of surface functional groups on biochar, which increases biochar's reactivity and may contribute to the cation exchange capacity of soil. In this study, C functional groups of a number of relevant organic C compounds and the light fraction (< 1.8 g cm^{-3}) of natural soil and soil amended with biochars (fresh and aged for 1 and 2 years at 20, 40 and 60 °C) were determined using near-edge X-ray absorption fine structure (NEXAFS) spectroscopy and X-ray photoelectron spectroscopy (XPS) techniques. The spectra of biochar and light fraction of the control and biochar amended soils showed two distinct peaks at ~285.1 and 288.5 eV, which were attributed to the C1s-$\pi^*_{C=C}$ transitions of aromatic C (and protonated and alkylated aromatic C) and C1s-$\pi^*_{C=O}$ transitions of carboxylic C, carboxyamide C and carbonyl C. The proportion of aromatic C and the aromaticity index (aromatic C/carboxyl and amide C) were substantially greater in the light fraction of the biochar amended soils than the corresponding light fraction of the unamended soils. The proportion of aromatic C was much higher in the light fraction of the B550 amended soils than in the corresponding B450 amended light fraction of the WA (Inceptisol) and NSW (Oxisol) soils. The proportion of aromatic C in the light fraction of biochar amended soils did not show any change after for 12 months at various temperatures. Consistent with the NEXFAS results, XPS analysis also showed the dominance of aromatic C and protonated and alkylated aromatic C in the light fraction of the biochar amended WA soil. The proportion of functional groups obtained from the XPS analysis did not show any consistent trend for the ground samples. However, the proportion of carboxyl groups in the hand-picked biochar samples increased with increasing ageing time, and similarly there was some increase in carboxyl groups with increasing

incubation temperature. NEXAFS and XPS techniques show good potential for the characterisation of C rich fraction isolated from natural soil and soil amended with biochar. The limited data suggest that much longer ageing time will be needed for the development of significant amount of carboxyl groups on biochar surfaces.

6.1. Introduction

'Natural biochar' is ubiquitous in soils worldwide and exists as a continuum of biomass combustion products such as char or charcoal, and soot, which are collectively referred to as black C (Schmidt and Noack, 2000). Char in soil mainly results from biomass burning and wild fires, and its subsequent accumulation or aeolian transport over centuries (Kuhlbusch and Crutzen, 1995). More recently, there has been growing interest in the soil application of biochar for long-term C storage and other multiple benefits. Biochar has the potential to increase soil C, reduce greenhouse gas emissions, improve soil properties, enhance agricultural productivity, and effectively absorb hazardous organic compounds and heavy metals in soil (Lehmann, 2007a,b; Namgay et al., 2010; Singh et al., 2010; Yu et al., 2009; Kookana et al., 2011). Like char, biochar comprises highly aromatic and chemically stable components of C, along with some easily degradable aliphatic structures (Lehmann, 2007a,b). Biomass type and pyrolysis conditions, such as heating temperature, heating rate and conditions, determine the C forms within biochars particles (Czimczik et al., 2002; Keiluweit et al., 2010; McBeath et al., 2009; 2011). Furthermore soil environmental conditions determine the stability of biochar in soils (Cheng et al., 2006; 2008; Keith et al., 2011; Fang et al., 2014). However, determination of changes in the molecular structure and chemical properties of biochars applied to soil remains a major challenge.

Although biochar contains a significant proportion of recalcitrant C, some of the biochar-C applied to soil is mineralised and certain conditions, such as high soil temperature and moisture, may facilitate rapid abiotic and biotic oxidation of biochar in soil (Cheng et al., 2006; 2008; Keith et al., 2011; Liang et al., 2006). The creation of surface functional groups on biochar is important for its increased reactivity and contribution to the cation exchange capacity of soils (Liang et al., 2006). Furthermore, the increased interaction of biochar with clay minerals in soils and consequent

entrapment within newly formed aggregates may increase the stability and longevity of biochar in soil (Glaser et al., 2000; Brodowski et al., 2005).

The structure of biochar has been described as condensed aromatic rings which forms clusters as thermal degradation proceeds (Preston and Schmidt, 2006). However, Knicker et al. (2008) proposed a different model that describes biomass-derived black carbon as a mixture of heat-altered biopolymers which forms small clusters with a high degree of substitution with N, O and S groups. Despite the differing views about changes in the chemical structure during black carbon or biochar formation, there is a general agreement that proportion of aromatic carbon increases with increasing heat treatment temperature (McBeath et al., 2011). It has been suggested that non-linearity exists in the phase transitions and degree of aromaticity in the heat-induced transformation of plant biomass (Keiluweit et al., 2010). It is thus important to characterize chemical structure of biochar produced at different temperatures in order to evaluate their stability in soils.

Considerable research has been conducted to understand the mineralisation of biochar-C in soils (Hamer et al., 2004; Cheng et al., 2006; 2008; Liang et al., 2008; Zimmerman, 2010; Keith et al., 2011). However, little is known about the C functional groups in biochars aged in soils under different conditions. Spectroscopic techniques including solid-state 13C nuclear magnetic resonance (NMR), X-ray photoelectron and Fourier-transform infrared (FTIR) have been widely used for the characterisation and monitoring of biochar in soils (McBeath et al., 2011; Cheng et al., 2006; 2008; Liang et al., 2008). Among the spectroscopic methods, NMR spectroscopy has been most commonly used for the structural characterisation of black carbon and biochar in soils (Baldock and Smernick, 2002; Czimczik et al. 2002; McBeath et al., 2011). However, the technique has some drawbacks, such as the poor detection limit of biochar-C with cross polarization 13C NMR, poor signal to noise ratio for biochars produced at high temperatures, loss of NMR signal in the presence of paramagnetic and ferromagnetic minerals (Freitas et al., 1999; 2002; Hedges et al., 2000; Begaudeau et al., 2012).

Near-edge X-ray absorption fine structure (NEXAFS) spectroscopy is an element specific technique that has been successfully employed for the characterisation of heterogeneous and complex environmental C materials. NEXAFS

has been used in conjunction with scanning transmission X-ray microscopy (STXM) for determining nanoscale spatial heterogeneity of organic C in black carbon particles, and characterizing surface functional groups of black carbon in Anthroposols from Brazil (Schumächer et al., 2005; Lehmann et al., 2005; Liang et al., 2006, 2008). Keilweit et al. (2010) employed C-NEXAFS to relate C speciation to the degree of structural order in biochar produced at charring temperature ranging from 100 to 700 °C. Heymann et al. (2011) characterized a range of C rich materials including black carbon reference materials, environmental matrices and potential interfering materials using C-NEXAFS.

X-ray photoelectron spectroscopy (XPS) is a surface specific technique (depth of analysis < 10 nm) and it provides quantitative analyses of all elements, except for H and He (Briggs and Seah, 1990). Additionally, the local environment of atoms can affect the binding energy of certain core electrons, such as C_{1s} electrons, which allows the identification and estimation of relative abundance of different species of an element. It has been used for the characterisation of surface functional groups and to determine the change in element composition of biochar with ageing (Cheng and Lehmann, 2009; Cheng et al., 2006; Lin et al., 2012; Nguyen et al., 2009). For example, Cheng et al. (2006) observed oxidation of C groups and formation of carboxylic C in black carbon particles incubated at high incubation temperature (70 °C). Similarly, Nguyen et al. (2009) reported an increase of O content and a decrease of C content on biochar surface or entire particles after decades of ageing in soil.

The recent published work suggests that both XPS and NEXAFS are ideally suited for characterising C functional groups of soil organic carbon (SOC) and biochar. The specific objectives of the research were (i) to investigate the chemistry of C of the light fraction of unamended and biochar amended soils after ageing at different temperatures; and (ii) to identify changes in the molecular structure of biochar-C (and native organic C) with ageing in contrasting soils at three temperatures. A number of reference organic compounds relevant to soils and two original biochar were also analysed in order to compare the performance of the beamline and to identify the C functional groups. We hypothesised that the proportion of carboxylic carbon will increase on biochar after ageing in soils, and the

increasing incubation temperature will further increase the development of carboxylic functional groups.

6.2. Materials and Methods

6.2.1. Biochar and reference samples

We analysed light fraction isolated from four contrasting soils soon after mixing (day 0) and ageing for 1 year and 2 years at 20 °C, 40 °C and 60 °C. The four soils are referred to as NSW (an Oxisol), WA (an Inceptisol), QLD (a Vertisol), and SA (an Entisol) soil in this chapter; the description of the experimental soils and the two biochars are given elsewhere (Fang et al., 2014). Native soil organic carbon (SOC) was also isolated from the four soils without any biochar amendment. Biochar and native SOC were isolated from the four soils by a density separation procedure after dispersing the soils and soil-biochar mixtures in sodium polytungstate solution, 1.8 g cm^{-3} (Golchin et al., 1994). The aged biochars were obtained by incubating two biochars, produced from a woody biomass by slow pyrolysis at 450 °C (B450) and 550 °C (B550), with four contrasting soils from Australia at 70% water holding capacity and at three temperatures, i.e. 20 °C, 40 °C and 60 °C, for up to 2 years. The experimental details for the incubation experiment have been previously described by Fang et al. (2014).

Fifteen reference compounds of C (analytical grade reagents), sourced from the Agricultural Chemistry Laboratory at the University of Sydney, were included in the C 1s-NEXAFS analysis.

6.2.2. Near edge X-ray absorption fine structure spectroscopy

Carbon 1s-NEXAFS spectra were obtained at the soft X-ray spectroscopy beamline of the Australian Synchrotron in Melbourne (Cowie et al., 2010). The beam was operational in top-up mode at the time of analysis and the storage ring beam current ranged between 150 and 200 mA. The soft X-ray beamline is equipped with a plane grating monochromator that is capable of providing between 10^{11} and 10^{12} photons s^{-1}/200mA at the K-edge of the required element with a resolving power better than 10^4. The photon energy for C 1s-NEXAFS was calibrated using photoemission of the

gold 4f7/2 peak at 83.96 eV that was obtained from a reference foil available on the standard manipulator.

Ground samples of the reference compounds and isolated SOC and SOC and biochar-C fractions were mounted on to the sample disc using a double-sided adhesive carbon tape. The samples were loaded into a vacuum chamber (2×10^{-10} mbar) for the analysis. C(1s) K-edges spectra were obtained in the 275–315 eV range using a step size of 0.1 eV and the dwell time of 0.5 sec. The spot size of the beam under operating conditions was approximately 0.75×0.50 mm. No deterioration in the signal was observed in repeated measurements (up to five) at a spot with the dwell time of 0.5 sec.

The NEXAFS signal was simultaneously recorded in Fluorescence yield (FLY), total electron yield (TEY) and auger electron yield (AEY) modes. The AEY signal was recorded using a SPECS Phoibos 150 Hemispherical Analyser positioned at an angle of 45° with respect to the beam. Spectra were normalised using I_0 reference gold foil prior to peak assignments and peak fitting. The reference gold foil spectra were previously normalised using argon sputtered clean gold surface; and all raw AEY, FEY and I_0 data were also corrected for the dark current and normalised to correctly produce the C spectra of the samples. Background correction and normalisation of NEXFAS spectra was done using Athena 0.8.056 (Ravel and Newville, 2005). An example spectrum at different stages of correction is presented in the supporting information (**Figure 6.S1).**

The fine structure in the C-NEXAFS region ranges between 283 and 290 eV, and above 290 eV transitions tend to be very broad and overlaps with absorption edges (Cody et al., 1998) therefore we have only considered the main C1s-π^* and 1s-3p/σ^* valence transitions in the 284−290 eV range for discussion.

In order to evaluate the changes in surface functional groups of biochars, semi-quantitative analysis of NEXAFS spectra was done by peak deconvolution using Whooskha, a MatLab based software program. Peak positions were assigned based on the published data and the details are given in **Table 6.1**. The number of peaks in a fit was kept the same within a data set (i.e. mixture of a particular soil and biochar type) and attempts were made to fit the data with as few peaks as possible

(**Figure 6.S2**). All peaks were fitted to Gaussian function, except for the NEXAFS step edge where an arctangent step function was used. We expect 1−3% errors in the relative proportion of various functional groups derived from Gaussian function using the procedure.

6.2.3. X-ray photoelectron spectroscopy

XPS analysis was conducted using an ESCALAB250Xi (Thermo Scientific, UK) spectrometer with a monochromatic Al Kα radiation (energy 1486.68 eV) at 164W (10.8 mA and 15.2kV) and a spot size approximately 0.5 mm in diameter. A finely ground powder or hand-picked biochar or soil organic carbon particles were fixed onto a metallic samples holder using a double-sided non-conducting tape. During analysis vacuum was maintained < 2×10^{-8} kPa. Survey scans were obtained covering a binding energy range from 0 to 1350 eV with the pass-energy of 100 eV, and for elemental region (C, N and O) scans we used 20 eV pass energy and a 0.1 step size. The binding energy was calibrated against the 4f7/2 line of gold at 83.96 eV, the Ag 3d5 line of silver at 368.21 eV and the 2p3 line of copper at 932.62 eV (Seah, 2003). For C, binding energy was corrected relative to C 1s line at 285.0 eV for adventitious hydrocarbon.

XPS spectra were analysed and deconvoluted using the Gaussian-Lorentzian sum function with 30% Gaussian-Lorentzian value to optimise the spectra using software Avantage (Thermo Scientific). A Shirley background correction was carried out to remove background noise (Briggs and Seah, 1990). Atomic ratios of Al, Si, C, N, and O were calculated from the peak areas of the Al(2p), Si(2p), C(1s), N(1s) and O(1s), respectively. The elemental composition of the relevant elements was then calculated using the atomic ratio and atomic weight of the individual element. The elemental analysis was used to make comparison for a given set of samples and not to derive the absolute composition of the samples.

The XPS analysis was done only for the light fraction isolated from the WA soil with and without the addition of the B450. The light fraction was separated from the soil and soil-biochar mixture immediately after mixing (Day 0) and after incubation in the soils for 1 and 2 years at 20, 40 and 60 °C. The samples were analysed after hand grinding the light fraction into fine powder to determine the composition and

functional groups of C and N of the bulk samples, and hand-picked particles from the light fraction were analysed to observe the surfaces (~ 10 nm) of biochar and native SOC particles.

6.3. Results and discussion

6.3.1. NEXAFS spectroscopy of reference C compounds

It should be pointed out that a dip at approximately 291.2 eV is an artefact of the normalisation procedure resulting from the C contamination on gold and it persisted in some of the spectra despite correction being made with argon sputtered clean gold surface (e.g. **Figure 6.3B, Figure 6.5A,B**).

NEXAFS spectra, peak positions and chemical structures of the reference compounds are presented in **Figure 6.1 and Table 6.2**. Carbohydrates are structural components of cell wall of most microorganisms and plants. The two carbohydrates, L-Arabinose (an aldopentose) and L-Rhamnose (6-deoxyaldohexose), showed a very sharp peak close to 289.5 eV and another sharp peak at 288.6 eV, which was present on the shoulder of the large peak and less obvious in case of L-Arabinose (**Table 6.2; Fig 6.1A**). The 289.45 eV peak has been attributed to 1s-3p/σ* transitions of C-OH groups (O-alkyl) in monosaccharides (Solomon et al., 2009), and similar band has been reported in 1s-3p/σ* transitions of alcohols and other hydoxylated linked C species (Ishi and Hitchcock, 1988; Cody et al., 2009). A less distinct and much smaller band was present at 288.62 eV in the spectrum of L-Rhamnose, probably due to C1s-1s-π* transition. Additional sharp peaks at 286.80 eV in the spectrum of L-Arabinose and 287.59 eV in the L-Rhamnose spectrum could be due to 1s-π* transition of C-O group and 1s-3p/σ* transition of C-H group, respectively. Despite the similarities in the main features of the spectra for L-Arabinose and L-Rhamnose with the published data, multiple peaks, in the 290-300 eV region, observed by Solomon et al. (2009) did not occur in our spectra, and instead a broad peak, with maximum at ~294 eV, was observed.

Gallic acid (a phenolic acid) showed sharp peaks at 285.06, 287.58, and 288.54 eV and slightly less intense peaks at 286.08, 286.78 eV (**Table 6.1; Figure 1B**). The 285.06 eV peak may be assigned to The C1s-π* transitions from C atoms

connected to O atoms (C-OH) in the aromatic ring of gallic acid (Francis and Hitchcock, 1992; Hitchcock et al., 1992; Robin et al., 1988; Cody et al., 1998). The spectral features at 286.08, 286.78 and 287.58 eV are also associated with C1s-π* transitions corresponding to C1s-$\pi^*_{C\text{-}OH}$ transitions and the energy positions are modified by OH substituents in phenol (Francis and Hitchcock, 1992). The sharp absorption band at 288.54 eV is attributed to the C1s-π* transition of carboxylate C (COOH), and the high energy shift has been attributed to the electron withdrawing nature of oxygen (Cody et al., 1998).

Vanillin (a phenolic aldehyde) spectrum showed some similarity with gallic acid with intense peak at 288.60 eV and a peak at ~287.60 eV which could be assigned to C1s-π*transitions of carboxylate C and C1s-π* transitions from C atoms connected to OH as before. The peak at 292.69 eV may be due to C1s-$\pi^*_{C\text{-}H}$ transitions from the methoxy group (–O–CH_3) in vanillin (Francis and Hitchcock, 1992).

The sharp peaks at 288.75 and 288.58 eV in the spectra (**Figure 6.1B**) of citric and benzoic acids, respectively, may be assigned to C1s-$\pi^*_{C=O}$ transitions of carboxylate C (Cody et al., 1998; Kuznetsova et al., 2001). In benzoic acid the broad peak at 285.06 eV possibly arise from C1s-$\pi^*_{C=C}$ transitions of C bonds (C=C) in the aromatic ring structure (Cody et al., 1998; Solomon et al., 2009).

Adenine is a purine where six-membered rings are attached to five membered rings; it is an integral part of deoxyribonucleic acid (DNA), ribonucleic acid (RNA), and adenosine triphosphate (ATP). In the NEXAFS spectrum of adenine, two very sharp peaks at 287.54 and 286.90 eV (**Table 6.2; Figure 6.1C**) were assigned to structural C-N_x species and a small broad peak at 284.89 eV was attributed to $\pi^*_{C=C}$ transition (Samuel et al., 2006). The C1s-$\pi^*_{C=C}$ transitions from the ring structure of adenine also contributed to the main two peaks at 287.54 and 286.90 eV (Solomon et al., 2009). Similar to Samuel et al. (2006), we did not observe the intense peak at 288.70 eV that was reported by Solomon et al. (2009) for the C1s-$\pi^*_{C=C}$ transitions of C=C-NH and C=C-NH_X species.

Amino acids are a important component of soil organic matter; forming up to 50% of the organic nitrogen in soils and 90% of the soil N exist in the organic form.

The essential feature of the structure of amino acids is the presence of amine ($-NH_2$) and carboxylic (-COOH) functional groups that are attached to a saturated C atom, C (Kaznacheyev et al., 2002). All six amino acids analysed in this study showed a strong peak close to 288.8 eV (288.74-288.80 eV; **Table 6.2, Figure 6.1D**), which is consistent with the published literature on the C K-edge NEXAFS of amino acids and the peak has been attributed to C1s-$\pi^*_{C=O}$ transitions of carboxyl/carbonyl, COOH/COO-, groups in amino acids (Boese et al., 1997; Buckley and Besley, 2011; Cooper et al., 2004; Kaznacheyev et al., 2002; Solomon et al., 2009). The distinct peak at 285.16 eV in the phenylalanine spectrum is most likely due to the C1s-$\pi^*_{C=C}$ transition of aromatic side chain of phenylalanine (Cooper et al., 2004; Solomon et al., 2009). A low intensity peak at 287.80 eV in the phenylalanine has been assigned to the C1s-π^*_{C-H} and Rydberg excitations (Kaznacheyev et al., 2002). In the histidine spectrum, a very strong peak at 287.13 eV was also attributed to the C1s-π^*_{C-H} and Rydberg excitations (Kaznacheyev et al., 2002; Solomon et al., 2007). The high energy peaks at approximately 289.38 and 289.58 eV in arginine and lysine, respectively have been attributed to C1s-$\pi^*_{C=N}$ transitions; according to Kaznacheyev et al. (2002), C in this bonding is bonded to three N atoms and hence the peak from the C1s-$\pi^*_{C=N}$ transition appears above that of a C 1s(COO^-) group.

6.3.2. NEXAFS spectroscopy of biochars and the light fractions of soil and soil aged with biochars

The NEXAFS spectra of the two biochars (B450 and B550) are quite similar to each other and to the wood char spectrum presented by Heymann et al. (2011). The biochar spectra have two distinct peaks at 285.18 and 288.45 eV (**Figure 6.2; Table 6.3**).The first peak (285.18 eV) can be attributed to the C1s-$\pi^*_{C=C}$ transitions of aromatic C, and protonated and alkylated aromatic C; and the peak at 288.45 eV probably represents C1s-$\pi^*_{C=O}$ transitions of carboxylic C, carboxyamide C and carbonyl C (Samuel et al., 2006; Francis and Hitchcock, 1992; Hitchcock et al., 1992; Hitchcock and Ishii, 1987; Robin et al., 1988; Cody et al., 1998). The deconvolution procedure identified four additional peaks in the spectra of both biochars at 286.48 (C1s-$\pi^*_{C\text{-}OH,\ C=O}$), 287.40 (1s-3p/$\sigma^*_{C-H}$), 289.83 (C1s-$\pi^*_{C-O}$) and 290.62 (C1s-$\pi^*_{C=O}$) eV; the position of these peaks is within the ranges of the suggested functional groups (**Table 6.1**). Based on the peak area, the proportion of aromatic C (G2) was

slightly greater in B550 biochar than B450 biochar, which is expected as aromatic condensation in biochar increases with increasing heat treatment temperature (McBeath and Smernik, 2009; McBeath et al., 2011). Contrary to this, the aromaticity index (aromatic carbon (G2)/carboxyl and amide carbon (G6)) was marginally greater for B450 than B550. All in all, the differences in the C 1s NEXFAS spectra of the two biochars were negligible. Although aromatic condensation increases with increasing heat treatment temperature in the 200−1000°C, the increase is rapid in the low temperature range and reached > 89% at 400°C (McBeath et al., 2011); therefore, it is possible to observe similar spectra for the two biochars produced at 450 and 550 °C.

NEXAFS spectra and the peak data for the light density fraction of the unamended four soils and biochar amended soils are presented in **Figures 6.3−6.7** and **Tables 6.4−6.7**. Similar to the biochar spectra, two distinct peaks at ~285.1 and 288.5 eV (**Figures 6.3−6.7**) were present in all samples. However, the intensity of the aromatic (285.1 eV) peak was smaller and of the carboxylic C (and carboxyamide C and carbonyl C) peak at 288.5 eV was larger than in the biochar spectra. In the SA samples, an additional peak at 290.35 eV was observed, which was attributed to the C1s-$\pi^*_{C=O}$ transitions of carbonate (Gilbert et al., 2011) in the soil (**Figure 6.6**). Calcite was identified from the X-ray diffraction analysis of the soil, and chemical analysis showed that 6.0% inorganic C was present in this soil (Fang et al., 2014). In addition to the C peaks, two peaks at approximately 297.4 and 300 eV were present in the SA and Qld spectra and more prominent in the SA sample (**Figures 6.5** and **Figures 6.6**). These peaks correspond to L3 (K-L_3-2p3/2) and L2 (K-L_2-2p3/2) edges of potassium. Potassium peaks originated from the presence of illite in the clay fraction of these two soils and its proportion was greater in the clay fraction of the SA soil than in the Qld soil (Fang et al., 2014).

In all soil and soil-biochar samples 5−6 Gaussian peaks were fitted, and the main difference among the soils was in the resolution of O-alkyl (G7) and carbonyl (G8) peaks, these peaks were resolved in the WA and NSW soils only (**Tables 6.4−6.7**). The functional groups of C represented by the peaks are described in the **Table 6.1** and the peak positions agree well with the published data on SOC and biochar-C (Heymann et al., 2011; Keiluweit et al., 2012; Klebber et al. 2011;

Lehmann et al., 2009; Liang et al., 2006; Schäfer et al., 2005; Schumacher et al., 2005; Solomon et al., 2005). The proportion of aromatic C (proportion of G2) and the aromaticity index (aromatic C/carboxyl and amide C, G2/G7; Kleber et al., 2011) were substantially greater in the light fraction of the biochar amended soils than the corresponding light fraction of the unamended soil; the difference was minimal in the case of SA soil (**Table 6.7**) where problems were encountered in separating the light fraction from the biochar amended soils and biochar recovery was very poor. The proportion of aromatic carbon also increased in the control soils (i.e. without biochar addition) in most of the samples after ageing for one year at different temperatures (**Tables 6.4−6.7**). The laboratory incubation results show that a substantial portion of the native soil C was mineralised in the 12-month period (0.7−6.8% of the total C mineralised at 20°C, 5.8−19.9% at 40°C and 13.3−30.3% at 60°C), which might have increased the proportion of aromatic C in the residual native SOC. The proportion of aromatic C in the light fraction of biochar amended soils did not show any consistent trend; however, there was some tendency in the data toward an increase in the aromaticity index for the aged samples at various temperatures (**Tables 6.4−6.7**). There are two possible reasons for no observed changes in the proportion of aromatic C in biochar amended light fractions, firstly a small proportion of the biochar-C was mineralised (0.34−7.07% of the total biochar-C) during the 12-month incubation period, which did not produce any observable change in the C functional groups of biochar-C. Secondly, the mixing of native soil C with the biochar-C in the light fraction masked any difference in the aromatic C of the original and aged biochar samples, considering that there was a consistent and substantial increase in the aromatic C in the native SOC after ageing. The incubation temperature also did not produce any consistent change in the proportion of C functional groups, and the same two reasons perhaps apply in these results as well.

In the two soils (WA and NSW), where the light fraction of both B450 and B550 amended soils were analysed, the proportion of aromatic C (G2) and the aromaticity index were much higher in the light fraction of the B550 amended soils than the corresponding B450 amended light fraction (**Figure 6.7; Table 6.4** and **Table 6.5**). These results are consistent with our C mineralisation data from the incubation experiment, which showed a significantly lower biochar-C mineralisation from the B550 amended soils (0.34−1.52%) than the corresponding B450 amended

soils (0.65−7.07%). The modelling results from 2-year mineralisation data predict much longer residence time for B550 (344−579 years) than B450 (218−259 years) in these soils (Fang et al., 2014). It has reported in number of previous studies that the proportion of aromatic C in biochar or black carbon increases with increasing pyrolysis temperatures (Czimczik et al., 2002; Keiluweit et al., 2010; McBeath and Smernik, 2011).

6.3.3. XPS of aged biochar samples

Normalised concentrations of C, O, Si, Al and N in the light fraction are presented in the **Table 6.8**. Minor amounts of Mg, P, Na, Ca and W were also observed in some of the samples, Na and W being residual from the sodium polytungstate used in the density fractionation procedure and Mg, P and Ca being present in small amounts in SOC and the biochar (**Figure 6.S3**). There was no consistent trend in the C content, except being generally higher in hand-picked biochar particles than the ground biochar and native SOC particles. All samples contained substantial amounts of Si and Al; the atomic ratio of Al/Si is < 1.0 in all samples, which suggests the presence of both kaolinite (Al/Si ~1.0) and quartz. The two minerals were identified from the X-ray diffraction analysis of the clay fraction of the WA soil (Fang et al., 2014). Oxygen content appears to have increased with ageing in all light fractions; however, due to the presence of quartz and kaolinite it is not possible to unambiguously attribute this to the oxidation of C groups of biochar. Nitrogen content was similar for the ground SOC and biochar samples; however, the N content of hand-picked biochar samples was greater than the ground SOC and biochar samples.

The C1s peak was deconvoluted into four peaks – representing C-C/C-H, aromatic C (284.81−285.03 eV), C-O, aromatic C (286.42−286.73 eV), C=O, ketone C, 287.81−288.03 eV and COO, carboxylic C (288.60−289.55 eV) (Proctor and Sherwood, 1982). The proportion of C functional groups in the ground samples of the light fractions isolated from the WA soil (i.e. native SOC) and soil treated with biochar did not show any obvious trend (**Table 6.9**). In both group of samples, the dominant C functional groups were C-C/C-H and C-O; and C=O and COO groups were less than 10%. These results are consistent with the XPS results of black carbon powdered samples reported by Cheng et al. (2006). The C1s-XPS spectra of the light

fraction of native SOC (isolated from the control soil) and the original biochar (B450) were quite different to each other. The biochar spectrum showed a much greater proportion of C-C/C-H group than the native SOC, whereas the other C groups (C-O, C=O and COO) were present in greater proportion in the native SOC than the biochar. The proportion of COO group progressively increased slightly in the hand-picked aged biochar samples (1 and 2 years), which suggests limited oxidation of C groups on the surface of biochar particles (**Table 6.9**). Similar observations were also made by Cheng et al. (2006) and Joseph et al. (2010) for black carbon and biochar samples. We observed the presence of COO group in the original biochar unlike Joseph et al. (2010), who reported the absence of COO group in a fresh green waste biochar.

The deconvolution of N 1s spectra of most samples was done into (i) N in organic matrix possibly associated with proteins and amino acids (400.03−400.89 eV), and (ii) quaternary N and/or -NO groups (401.73−402.77 eV) (Abe and Watanbe, 2004). However, in the original biochar samples N 1s peaks existed into (i) aromatic amine, purine and imidazome C (C=N) with bonding energy between 399.04 and 399.35 eV, and (ii) N in the organic matrix similar to the other samples (400.86−400.89 eV). It is expected that in the wood biochar produced at 450°C most of the nitrogen will exit in the form of 'black nitrogen', where heteroaromatic N structures are formed during the pyrolysis process (Knicker, 2007; 2010). Most of the N existed in organic matrix and approximately < 10% in quaternary N and/or -NO groups. There was no consistent trend in the proportion of N functional groups of native SOC and biochar samples with ageing at different temperatures, which is expected as N bound in hetrocyclic compounds is considered to be chemically stable (Leinweber and Schulten, 2000).

6.4. Conclusions

The spectral features and peak positions observed for the relevant organic compounds were consistent with the published literature. Similarly, spectral features of biochars and the light fractions of soil and soil amended with the biochars were consistent with the limited published data. The aromatic C peaks were substantially larger in the biochars than the native SOC or native SOC mixed with biochars. The proportion of aromatic C in the control soil (without biochar) increased with ageing

and increased incubation temperature. The light fraction of the soil amended with the high temperature biochar (B550) showed a greater proportion of the aromatic C than the corresponding samples from the corresponding low temperature biochar (B450). After one year ageing, we did not observe any consistent change in the C functional group of light fraction separated from biochar amended soils, possibly the mixing of native soil C with the biochar-C in the light fraction masked any difference in the aromatic C between the fresh and aged biochar samples. XPS results of the ground samples also did not show any difference in C groups between fresh and aged light fractions of the WA soil. However, the XPS analysis of hand-picked biochar samples showed increased oxidation with increasing ageing time and the increasing incubation temperature.

Both NEXAFS and XPS are useful techniques for the characterisation of native SOC and biochar-C. However, due to the similarities in the spectral features of the biochar and native C it is difficult to determine the changes in biochar-C with ageing in soils. In the future studies, hand-picked biochar samples representing a range of particle sizes should be analysed using both NEXAFS and XPS to determine their C functional groups. There are substantial overlaps between the peaks of various C groups in the spectra of both NEXAFS and XPS, and thus there are limitations in the quantitative analysis of the data.

6.5. References

Abe, T., Watanabe, A., 2004. X-ray photoelectron spectroscopy of nitrogen functional groups in soil humic acids. Soil Science 169, 35-43.

Baldock, J.A., Smernik, R.J., 2002. Chemical composition and bioavailability of thermally, altered Pinus resinosa (Red Pine) wood. Organic Geochemistry 33, 1093-1109.

Begaudeau, K., Morizet, Y., Florian, P., Paris, M., Mercier, J.C., 2012. Solid-state NMR analysis of Fe-bearing minerals: implications and applications for Earth sciences. European Journal of Mineralogy 24, 535-550.

Boese, J., Osanna, A., Jacobsen, C., Kirz, J., 1997. Carbon edge XANES spectroscopy of amino acids and peptides. Journal of Electron Spectroscopy and Related Phenomena 85, 9-15.

Briggs, D., Seah, M., 1990. Practical surface analysis, Second edition, Volume 1, Auger and X-ray Photoelectron Spectroscopy. John Wiley & Sons Chichester, England.

Brodowski, S., Amelung, W., Haumaier, L., Abetz, C., Zech, W., 2005. Morphological and chemical properties of black carbon in physical soil fractions as revealed by scanning electron microscopy and energy-dispersive X-ray spectroscopy. Geoderma 128, 116-129.

Buckley, M.W., Besley, N.A., 2011. A theoretical study of the near edge X-ray absorption fine structure of amino acids and proteins. Chemical Physics Letters 501, 540-546.

Cheng, C.H., Lehmann, J., 2009. Ageing of black carbon along a temperature gradient. Chemosphere 75, 1021-1027.

Cheng, C.H., Lehmann, J., Engelhard, M.H., 2008. Natural oxidation of black carbon in soils: Changes in molecular form and surface charge along a climosequence. Geochimica Et Cosmochimica Acta 72, 1598-1610.

Cheng, C.H., Lehmann, J., Thies, J.E., Burton, S.D., Engelhard, M.H., 2006. Oxidation of black carbon by biotic and abiotic processes. Organic Geochemistry 37, 1477-1488.

Cody, G.D., Ade, H., Wirick, S., Mitchell, G.D., Davis, A., 1998. Determination of chemical-structural changes in vitrinite accompanying luminescence alteration using C-NEXAFS analysis. Organic Geochemistry 28, 441-455.

Cody, G.D., Brandes, J., Jacobsen, C., Wirick, S., 2009. Soft X-ray induced chemical modification of polysaccharides in vascular plant cell walls. Journal of Electron Spectroscopy and Related Phenomena 170, 57-64.

Cooper, G., Gordon, M., Tulumello, D., Turci, C., Kaznatcheev, K., Hitchcock, A.R., 2004. Inner shell excitation of glycine, glycyl-glycine, alanine and phenylalanine. Journal of Electron Spectroscopy and Related Phenomena 137, 795-799.

Cowie, B.C.C., Tadich, A., Thomsen, L., 2010. The Current Performance of the Wide Range (90-2500eV) Soft X-ray Beamline at the Australian Synchrotron.

Sri 2009: The 10th International Conference on Synchrotron Radiation Instrumentation 1234, 307-310.

Czimczik, C.I., Preston, C.M., Schmidt, M.W.I., Werner, R.A., Schulze, E.D., 2002. Effects of charring on mass, organic carbon, and stable carbon isotope composition of wood. Organic Geochemistry 33, 1207-1223.

Fang, Y., Singh, B., Singh, B.P., Krull, E., 2014. Biochar carbon stability in four contrasting soils. European Journal of Soil Science, 65, 60–71.

Francis, J.T., Hitchcock, A.P., 1992. Inner-Shell Spectroscopy of Para-Benzoquinone, Hydroquinone, and Phenol - Distinguishing Quinoid and Benzenoid Structures. Journal of Physical Chemistry 96, 6598-6610.

Freitas, J.C.C., Bonagamba, T.J., Emmerich, F.G., 1999. 13C high-resolution solid-state NMR study of peat carbonization. Energy & Fuels 13, 53-59.

Freitas, J.C.C., Passamani, E.C., Orlando, M.T.D., Emmerich, F.G., Garcia, F., Sampaio, L.C., Bonagamba, T.J., 2002. Effects of ferromagnetic inclusions on 13C MAS NMR spectra of heat-treated peat samples. Energy & Fuels 16, 1068-1075.

Gilbert, P.U.P.A., Young, A., Coppersmith, S.N., 2011. Measurement of c-axis angular orientation in calcite (CaCO3) nanocrystals using X-ray absorption spectroscopy. Proceedings of the National Academy of Sciences of the United States of America 108, 11350-11355.

Glaser, B., Balashov, E., Haumaier, L., Guggenberger, G., Zech, W., 2000. Black carbon in density fractions of anthropogenic soils of the Brazilian Amazon region. Organic Geochemistry 31, 669-678.

Golchin, A., Oades, J.M., Skjemstad, J.O., Clarke, P., 1994. Study of Free and Occluded Particulate Organic-Matter in Soils by Solid-State C-13 Cp/Mas Nmr-Spectroscopy and Scanning Electron-Microscopy. Australian Journal of Soil Research 32, 285-309.

Hamer, U., Marschner, B., Brodowski, S., Amelung, W., 2004. Interactive priming of black carbon and glucose mineralisation. Organic Geochemistry 35, 823-830.

Hedges, J.I., Eglinton, G., Hatcher, P.G., Kirchman, D.L., Arnosti, C., Derenne, S., Evershed, R.P., Kogel-Knabner, I., de Leeuw, J.W., Littke, R., Michaelis, W., Rullkotter, J., 2000. The molecularly-uncharacterized component of nonliving organic matter in natural environments. Organic Geochemistry 31, 945-958.

Heymann, K., Lehmann, J., Solomon, D., Schmidt, M.W.I., Regier, T., 2011. C 1s K-edge near edge X-ray absorption fine structure (NEXAFS) spectroscopy for characterizing functional group chemistry of black carbon. Organic Geochemistry 42, 1055-1064.

Hitchcock, A.P., Ishii, I., 1987. Carbon K-Shell Excitation-Spectra of Linear and Branched Alkanes. Journal of Electron Spectroscopy and Related Phenomena 42, 11-26.

Hitchcock, A.P., Urquhart, S.G., Rightor, E.G., 1992. Inner-shell spectroscopy of benzaldehyde, terephthalaldehyde, ethyl benzoate, terephthaloyl chloride, and phosgene - models for core excitation of poly (ethylene-terephthalate). Journal of Physical Chemistry 96, 8736-8750.

Ishii, I., Hitchcock, A.P., 1988. The oscillator-strengths for C1s and O1s excitation of some saturated and unsaturated organic alcohols, acids and esters. Journal of Electron Spectroscopy and Related Phenomena 46, 55-84.

Joseph, S.D., Camps-Arbestain, M., Lin, Y., Munroe, P., Chia, C.H., Hook, J., van Zwieten, L., Kimber, S., Cowie, A., Singh, B.P., Lehmann, J., Foidl, N., Smernik, R.J., Amonette, J.E., 2010. An investigation into the reactions of biochar in soil. Australian Journal of Soil Research 48, 501-515.

Kaznacheyev, K., Osanna, A., Jacobsen, C., Plashkevych, O., Vahtras, O., Agren, H., Carravetta, V., Hitchcock, A.P., 2002. Innershell absorption spectroscopy of amino acids. Journal of Physical Chemistry A 106, 3153-3168.

Keiluweit, M., Bougoure, J.J., Zeglin, L.H., Myrold, D.D., Weber, P.K., Pett-Ridge, J., Kleber, M., Nico, P.S., 2012. Nano-scale investigation of the association of microbial nitrogen residues with iron (hydr)oxides in a forest soil O-horizon. Geochimica Et Cosmochimica Acta 95, 213-226.

Keiluweit, M., Nico, P.S., Johnson, M.G., Kleber, M., 2010. Dynamic molecular structure of plant biomass-derived black carbon (biochar). Environmental Science & Technology 44, 1247-1253.

Keith, A., Singh, B., Singh, B.P., 2011. Interactive priming of biochar and labile organic matter mineralization in a smectite-rich soil. Environmental Science & Technology 45, 9611-9618.

Kleber, M., Nico, P.S., Plante, A.F., Filley, T., Kramer, M., Swanston, C., Sollins, P., 2011. Old and stable soil organic matter is not necessarily chemically

recalcitrant: implications for modeling concepts and temperature sensitivity. Global Change Biology 17, 1097-1107.

Knicker, H., 2007. How does fire affect the nature and stability of soil organic nitrogen and carbon? A review. Biogeochemistry 85, 91-118.

Knicker, H., 2010. "Black nitrogen" - an important fraction in determining the recalcitrance of charcoal. Organic Geochemistry 41, 947-950.

Knicker, H., Hilscher, A., Gonzalez-Vila, F.J., Almendros, G., 2008. A new conceptual model for the structural properties of char produced during vegetation fires. Organic Geochemistry 39, 935-939.

Kookana, R.S., Sarmah, A.K., Van Zwieten, L., Krull, E., Singh, B., 2011. Biochar application to soil: Agronomic and environmental benefits and unintended consequences. Advances in Agronomy, 112, 103-143.

Kuhlbusch, T.A.J., Crutzen, P.J., 1995. Toward a global estimate of black carbon in residues of vegetation fires representing a sink of atmospheric CO2 and a source of O2. Global Biogeochemical Cycles 9, 491-501.

Kuznetsova, A., Popova, I., Yates, J.T., Bronikowski, M.J., Huffman, C.B., Liu, J., Smalley, R.E., Hwu, H.H., Chen, J.G.G., 2001. Oxygen-containing functional groups on single-wall carbon nanotubes: NEXAFS and vibrational spectroscopic studies. Journal of the American Chemical Society 123, 10699-10704.

Lehmann, J., 2007. Bio-energy in the black. Frontiers in Ecology and the Environment 5, 381-387.

Lehmann, J., 2007. A handful of carbon. Nature 447, 143-144.

Lehmann, J., Brandes, J., Fleckenstein, H., Jacobsen, C., Solomon, D., Thieme, J., 2009. Synchrotron-based near-edge X-ray spectroscopy of natural organic matter in soils and sediments. In: , In: Senesi, N., Xing, P., Huang, P.M. (Eds.), Biophysico- Chemical Processes Involving Natural Nonliving Organic Matter in Environmental Systems. IUPAC Series on Biophysico-Chemical Processes in Environmental Systems Wiley, NJ, pp. 729-781.

Lehmann, J., Liang, B.Q., Solomon, D., Lerotic, M., Luizao, F., Kinyangi, J., Schafer, T., Wirick, S., Jacobsen, C., 2005. Near-edge X-ray absorption fine structure (NEXAFS) spectroscopy for mapping nano-scale distribution of organic carbon

forms in soil: Application to black carbon particles. Global Biogeochemical Cycles 19, GB1013.

Leinweber, P., Schulten, H.R., 2000. Nonhydrolyzable forms of soil organic nitrogen: Extractability and composition. Journal of Plant Nutrition and Soil Science-Zeitschrift Fur Pflanzenernahrung Und Bodenkunde 163, 433-439.

Liang, B., Lehmann, J., Solomon, D., Kinyangi, J., Grossman, J., O'Neill, B., Skjemstad, J.O., Thies, J., Luizao, F.J., Petersen, J., Neves, E.G., 2006. Black Carbon increases cation exchange capacity in soils. Soil Science Society of America Journal 70, 1719-1730.

Liang, B., Lehmann, J., Solomon, D., Sohi, S., Thies, J.E., Skjemstad, J.O., Luizao, F.J., Engelhard, M.H., Neves, E.G., Wirick, S., 2008. Stability of biomass-derived black carbon in soils. Geochimica Et Cosmochimica Acta 72, 6069-6078.

Lin, Y., Munroe, P., Joseph, S., Kimber, S., Van Zwieten, L., 2012. Nanoscale organo-mineral reactions of biochars in ferrosol: an investigation using microscopy. Plant and Soil 357, 369-380.

McBeath, A.V., Smernik, R.J., 2009. Variation in the degree of aromatic condensation of chars. Organic Geochemistry 40, 1161-1168.

McBeath, A.V., Smernik, R.J., Schneider, M.P.W., Schmidt, M.W.I., Plant, E.L., 2011. Determination of the aromaticity and the degree of aromatic condensation of a thermosequence of wood charcoal using NMR. Organic Geochemistry 42, 1194-1202.

Namgay, T., Singh, B., Singh, B.P., 2010. Influence of biochar application to soil on the availability of As, Cd, Cu, Pb, and Zn to maize (Zea mays L.). Australian Journal of Soil Research 48, 638-647.

Nguyen, B.T., Lehmann, J., Kinyangi, J., Smernik, R., Riha, S.J., Engelhard, M.H., 2009. Long-term black carbon dynamics in cultivated soil. Biogeochemistry 92, 163-176.

Preston, C.M., Schmidt, M.W.I., 2006. Black (pyrogenic) carbon: a synthesis of current knowledge and uncertainties with special consideration of boreal regions. Biogeosciences 3, 397-420.

Proctor, A., Sherwood, P., 1982. XPS studies of carbon fibre surface Surface and Interface Analysis 4, 213.

Ravel, B., Newville, M., 2005. ATHENA, ARTEMIS, HEPHAESTUS: data analysis for X-ray absorption spectroscopy using IFEFFIT. Journal of Synchrotron Radiation 12, 537-541.

Robin, M.B., Ishii, I., Mclaren, R., Hitchcock, A.P., 1988. Fluorination effects on the inner-shell spectra of unsaturated molecules. Journal of Electron Spectroscopy and Related Phenomena 47, 53-92.

Samuel, N.T., Lee, C.Y., Gamble, L.J., Fischer, D.A., Castner, D.G., 2006. NEXAFS characterization of DNA components and molecular-orientation of surface-bound DNA oligomers. Journal of Electron Spectroscopy and Related Phenomena 152, 134-142.

Schäfer, T., Buckau, G., Artinger, R., Kim, J.I., Geyer, S., Wolf, M., Bleam, W.F., Wirick, S., Jacobsen, C., 2005. Origin and mobility of fulvic acids in the Gorleben aquifer system: implications from isotopic data and carbon/sulfur XANES. Organic Geochemistry 36, 567-582.

Schmidt, M.W.I., Noack, A.G., 2000. Black carbon in soils and sediments: Analysis, distribution, implications, and current challenges. Global Biogeochemical Cycles 14, 777-793.

Schumacher, M., Christl, I., Scheinost, A.C., Jacobsen, C., Kretzschmar, R., 2005. Chemical heterogeneity of organic soil colloids investigated by scanning transmission X-ray microscopy and C-1s NEXAFS microspectroscopy. Environmental Science & Technology 39, 9094-9100.

Seah, M. P. 2003. Surface Analysis by Auger and X-ray Photoelectron Spectroscopy. In: Surface Analysis by Auger and X-ray Photoelectron Spectroscopy (Eds D. Briggs and J. T. Grant), pp. 345-375. IM Publications and Surface Spectra Limited, Chichester, ISBN: 1 901019047.Singh, B., Singh, B.P., Cowie, A.L., 2010. Characterisation and evaluation of biochars for their application as a soil amendment. Australian Journal of Soil Research 48, 516-525.

Solomon, D., Lehmann, J., Kinyangi, J., Liang, B.Q., Heymann, K., Dathe, L., Hanley, K., Wirick, S., Jacobsen, C., 2009. Carbon (1s) NEXAFS spectroscopy of biogeochemically relevant reference organic compounds. Soil Science Society of America Journal 73, 1817-1830.

Solomon, D., Lehmann, J., Kinyangi, J., Liang, B.Q., Schafer, T., 2005. Carbon K-edge NEXAFS and FTIR-ATR spectroscopic investigation of organic carbon speciation in soils. Soil Science Society of America Journal 69, 107-119.

Yu, X.Y., Ying, G.G., Kookana, R.S., 2009. Reduced plant uptake of pesticides with biochar additions to soil. Chemosphere 76, 665-671.

Zimmerman, A.R., 2010. Abiotic and microbial oxidation of laboratory-produced black carbon (biochar). Environmental Science & Technology 44, 1295-1301.

Table 6.1. Peak assignments for the C(1s) NEXAFS spectra based on the published literature (Cody et al., 1998; Francis and Hitchcock, 1992; Heymann et al., 2011; Kaznacheyev et al., 2002; Keiluweit et al., 2012; Klebber et al. 2011; Lehmann et al., 2009; Schäfer et al., 2005; Schumacher et al., 2005; Solomon et al., 2005).

Energy range (eV)	Transition	Bond and C form	Deconvolution curve*
283.0-284.5	1s-π*	C=O, quinine C	G1
284.0-285.5	1s-π*	C=C, aromatic C; C-H, protonated and alkylated aromatic C; carbonyl substituted aryl C	G2
286.0-287.4	1s-π*	C-OH, phenolic C, C=O, ketonic C; R-(C=O)-R'; C=N, C-N, N-substituted aromatic C	G4
287.0-287.8	1s-3p/σ*	C-H, aliphatic C of CH_3, CH_2 and CH nature	G5
288.0-288.8	1s-π*	COOH, carboxylic C; COO, carboxyamide; C=O carbonyl C	G6
289.0-289.5	1s-π*	C-O, O-alkyl C	G7
290.0-290.5	1s-π*	C=O, carbonyl, carboxyl substituted aromatic	G8

*Based on the notation used by Keiluweit et al., 2012

Table 6.2. C1s-NEXAFS spectral peaks of structurally different reference carbon compounds used in the study.

Compound	Chemical structure	Photon energy (eV)						
L-Rhamnose	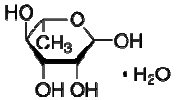	-	-	-	287.59	288.62	289.46	-
L-Arabinose	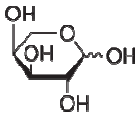	-	286.80	-	-	288.6*	289.45	294.07
Chitin	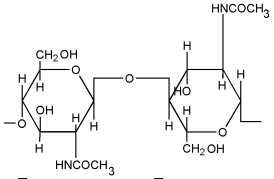	285.21	-	-	-	288.56	289.54	-
Pectin	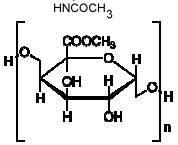	-	286.78	-	-	288.76	289.49	-
Gallic acid	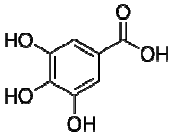	285.06	286.08	286.78	287.58	288.54	-	-
Citric acid	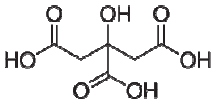	-	-	-	287.04*	288.75	-	-
Vanillin	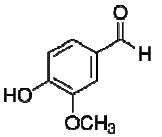	-	-	-	287.63*	288.60	-	292.69

Benzoic acid	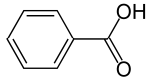	285.06	-	-	-	288.58	-	-
Adenine	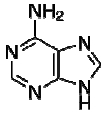	284.89	286.90	-	287.54	-	-	-
DL-Phenylalanine	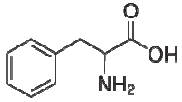	285.16	-	-	287.80*	288.80	-	-
L-Histidine	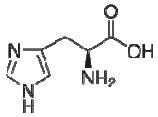	-	-	-	287.13	288.75	-	-
L-Arginine	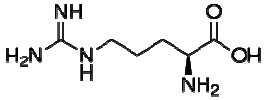	-	-	-	-	288.74	289.38	-
L-Glutamic acid	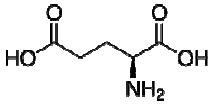	-	-	-	-	288.84	-	290.18
L-Alanine	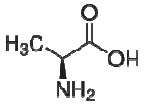	-	-	-	-	288.80	-	-
L-Lysine		-	-	-	-	288.80	289.58	-

*peak is not very clear.

Table 6.3. The energy position and relative proportion of functional groups in C 1s NEXAFS spectra of the two biochars, B450 and B550, as determined by Gaussian peak deconvolution.

Biochar	Photon energy (eV)						Aromaticity index*
	285.18	286.48	287.40	288.45	289.83	290.62	
	G2	G4	G5	G6	G7	G8	
B450	26.1	7.9	14.5	11.2	36.4	3.8	0.7
B550	26.8	7.3	14.9	12.1	32.7	6.2	0.6

*Aromaticity index = G2/G6, following Keiluweit et al. (2012)

Table 6.4. The energy position and relative proportion of functional groups in the C 1s NEXAFS spectra of the light density fraction (1.8 g cm^{-3}) of the WA soil, and soil amended with biochars, WA450 is the soil amended with the 450 °C biochar and WA550 is the soil amended with the 550 °C biochar. The light fraction was separated immediately after mixing biochar (Day 0) with the soil and after ageing for 1 year in soil at three temperatures, i.e. 20, 40 and 60 °C. Gaussian peak numbers correspond to the C functional described in Table 6.1.

Soil / biochar	Time	Temp. (°C)	Photon energy (eV)						Aromaticity index*
			285.27	286.57	287.57	288.49	289.56	290.65	
			G2	G4	G5	G6	G7	G8	
WA0	Day 0	−	7.3	3.9	16.5	12.7	50.8	8.8	0.6
	1 year	20	9.6	4.6	13.5	12.1	52.1	8.2	0.8
	1 year	40	9.3	6.0	12.8	11.9	50.5	9.6	0.8
	1 year	60	10.5	4.8	14.0	11.8	51.3	7.5	0.9
WA450	Day 0	−	15.1	4.0	16.2	10.3	48.7	5.7	1.5
	1 year	20	16.9	7.0	13.8	10.9	48.6	2.7	1.5
	1 year	40	−	−	−	−	−	−	−
	1 year	60	19.5	7.0	13.3	11.6	46.0	2.7	1.7
WA550	Day 0	−	21.0	4.3	16.1	12.1	40.6	5.9	1.7
	1 year	20	20.1	3.3	19.3	12.9	37.0	7.5	1.6
	1 year	40	20.5	4.6	18.9	11.2	37.9	6.9	1.8
	1 year	60	21.6	6.5	14.7	14.5	38.0	4.6	1.5

*Aromaticity index = G2/G6, following Keiluweit et al. (2012)

Table 6.5. The energy position and relative proportion of functional groups in the C 1s NEXAFS spectra of the light density fraction (1.8 g cm^{-3}) of the NSW soil, and soil amended with biochars, NSW450 is the soil amended with the 450 °C biochar and NSW550 is the soil amended with the 550 °C biochar. The light fraction was separated immediately after mixing biochar (Day 0) with the soil and after ageing for 1 year in soil at three temperatures, i.e. 20, 40 and 60 °C. Gaussian peak numbers correspond to the C functional described in Table 6.1.

Soil / biochar	Time	Temp. (°C)	Photon energy (eV)					Aromaticity index*
			285.15	286.81	287.64	288.55	289.75	
			G2	G4	G5	G6	G7	
NSW0	Day 0	−	7.9	6.1	11.6	22.6	51.7	0.3
	1 year	20	9.2	8.4	10.2	21.3	50.8	0.4
	1 year	40	9.4	7.9	11.7	24.5	46.5	0.4
	1 year	60	11.1	8.2	12.9	22.5	45.3	0.5
NSW450	Day 0	−	22.8	8.3	8.8	33.4	26.7	0.7
	1 year	20	21.1	8.5	10.4	28.8	31.1	0.7
	1 year	40	19.8	13.1	5.3	23.1	38.7	0.9
	1 year	60	19.5	10.0	8.0	26.7	35.9	0.7
NSW550	Day 0	−	26.5	11.6	6.1	33.3	22.5	0.8
	1 year	20	27.3	11.3	6.2	36.8	18.4	0.7
	1 year	40	25.6	13.2	5.4	31.7	24.1	0.8
	1 year	60	21.2	10.4	6.5	35.5	26.4	0.6

*Aromaticity index = G2/G6, following Keiluweit et al. (2012)

Table 6.6. The energy position and relative proportion of functional groups in the C 1s NEXAFS spectra of the light density fraction (1.8 g cm^{-3}) of the Qld soil, and soil amended with biochars, Qld450 is the soil amended with the 450 °C biochar and Qld550 is the soil amended with the 550 °C biochar. The light fraction was separated immediately after mixing biochar (Day 0) with the soil and after ageing for 1 year in soil at three temperatures, i.e. 20, 40 and 60 °C. Gaussian peak numbers correspond to the C functional described in Table 6.1.

Soil	Time	Temp. (°C)	Photon energy (eV)					Aromaticity index*
			285.19	286.52	287.35	288.50	290.05	
			G2	G4	G5	G6	G8	
Qld 0	Day 0	−	11.7	3.7	11.4	27.9	45.2	0.4
	1 year	20	7.8	7.9	9.6	37.2	37.6	0.2
	1 year	40	15.0	6.5	9.1	33.0	36.5	0.5
	1 year	60	10.0	4.9	12.6	20.8	51.8	0.5
Qld 450	Day 0	−	23.0	7.9	7.4	30.5	31.2	0.8
	1 year	20	22.5	10.5	7.5	32.9	26.7	0.7
	1 year	40	20.2	11.6	6.4	25.9	35.9	0.8
	1 year	60	20.3	10.8	7.7	24.8	36.3	0.8

*Aromaticity index = G2/G6, following Keiluweit et al. (2012)

Table 6.7. The energy position and relative proportion of functional groups in the C 1s NEXAFS spectra of the light density fraction (1.8 g cm^{-3}) of the SA soil, and soil amended with biochars, SA450 is the soil amended with the 450 °C biochar and SA550 is the soil amended with the 550 °C biochar. The light fraction was separated immediately after mixing biochar (Day 0) with the soil and after ageing for 1 year in soil at three temperatures, i.e. 20, 40 and 60 °C. Gaussian peak numbers correspond to the C functional described in Table 6.1.

Soil	Time	Temp. (°C)	Photon energy (eV)						Aromaticity index*
			285.18	286.71	287.57	288.50	289.84	290.45	
			G2	G4	G5	G6	G7	G8	
SA0	Day 0	−	8.3	6.4	10.2	16.2	57.2	1.7	0.5
	1 year	20	7.9	5.5	11.1	16.4	55.3	3.9	0.5
	1 year	40	10.4	8.9	7.9	17.0	47.3	8.6	0.6
	1 year	60	8.8	5.5	12.4	14.3	54.4	4.7	0.6
SA450	Day 0	−	13.2	6.3	10.7	15.9	51.4	2.6	0.8
	1 year	20	11.7	7.2	10.2	16.5	52.4	2.0	0.7
	1 year	40	14.7	8.0	10.2	17.3	47.5	2.3	0.9
	1 year	60	13.7	7.4	10.0	15.9	50.7	2.3	0.9

*Aromaticity index = G2/G6, following Keiluweit et al. (2012)

Table 6.8. XPS derived element composition of the B450 biochar and the light fraction fraction (< 1.8 g cm^{-3}) of the WA soil and WA amended with 450 °C biochar. The light fraction was isolated from the soil and soil-biochar mixtures immediately after mixing (Day 0) and after incubation for 1 and 2 years at 20, 40 and 60 °C.

Sample		O1s	C1s	N1s	Si2p	Al2p	C/N	Al/Si (atomic)
			Ground powder- WA soil (no biochar)					
Day 0	-	36.6	37.9	2.7	15.0	7.9	14.3	0.55
1-year	20 °C	29.6	59.6	2.3	4.7	3.8	25.9	0.85
	40 °C	29.3	59.5	2.6	5.7	3.0	22.6	0.54
	60 °C	39.9	31.9	2.6	16.1	9.5	12.4	0.62
2-year	20 °C	40.8	33.0	2.4	15.2	8.5	13.5	0.58
	40 °C	36.7	40.4	2.6	12.6	7.6	15.3	0.62
	60 °C	41.2	27.8	2.4	18.1	10.4	11.4	0.60
			Ground powder-WA soil amended with 450 °C biochar					
Day 0	-	34.4	49.8	2.5	9.2	4.1	19.9	0.46
1-year	20 °C	34.5	47.9	2.4	9.9	5.3	19.7	0.56
	40 °C	33.8	51.3	2.0	7.9	5.0	25.8	0.66
	60 °C	32.3	52.3	2.8	7.4	5.2	18.7	0.73
2-year	20 °C	41.2	30.8	2.1	15.9	10.0	14.5	0.66
	40 °C	40.1	31.4	2.3	16.5	9.8	13.8	0.62
	60 °C	34.7	43.6	1.9	12.8	7.1	23.4	0.58
			Hand-picked intact particles-WA soil amended with 450 °C biochar					
1-year	40 °C	30.4	57.1	3.1	5.7	3.7	18.2	0.67
2-year	20 °C	38.2	49.3	4.1	6.2	2.2	11.9	0.37
	40 °C	35.5	57.2	3.9	2.7	0.7	14.9	0.29
	60 °C	38.6	52.5	3.7	4.2	1.1	14.2	0.27

Table 6.9. Atom ratio of carbon (C1s) and nitrogen (N 1s) obtained from the XPS spectra of the 450 °C biochar and the light fraction of native soil organic carbon and/or aged 450 °C biochar isolated from the WA soil. The light fraction was isolated from the soil and soil-biochar mixtures immediately after mixing (Day 0) and after incubation for 1 and 2 years at 20, 40 and 60 °C.

Sample		C-C/C-H	C-O	C=O	O=C-O	N in organic matrix	Quaternary N and/or -NO groups
Ground powder-control (no biochar)							
Day 0	-	64.3	22.6	8.0	5.1	88.2	11.8
1 year	20 °C	66.1	20.8	7.5	5.5	92.8	7.2
	40 °C	63.5	23.1	7.9	5.5	92.1	7.9
	60 °C	57.0	28.7	9.0	5.3	94.1	5.9
2 year	20 °C	51.4	33.4	8.8	6.3	92.8	7.2
	40 °C	59.3	27.4	8.6	4.7	91.5	8.5
	60 °C	59.1	28.0	6.4	6.6	95.5	4.5
Ground powder-450 °C biochar							
	Original	83.4	10.4	3.6	2.6	64.1	35.9*
Day 0	-	65.8	21.4	6.6	6.2	96.1	3.9
1 year	20 °C	66.5	21.7	6.9	4.9	86.9	13.1
	40 °C	66.0	22.0	6.8	5.2	91.1	8.9
	60 °C	69.6	19.3	6.1	5.0	89.7	10.3
2 year	20 °C	55.8	30.4	7.5	6.3	92.5	7.5
	40 °C	57.5	28.9	8.0	5.6	91.1	8.9
	60 °C	63.0	23.8	7.9	5.4	90.4	9.6
Particle-control							
Day 0	-	51.4	31.1	11.0	6.4	90.0	10.0
Particle-450 °C biochar							
	Original	76.2	16.1	4.7	3.0	69.9	30.1*
1-year	20 °C	57.3	27.3	7.9	7.5	91.8	8.2
	40 °C	64.6	22.3	7.5	5.7	92.8	7.2
	60 °C	55.0	27.5	8.2	9.3	94.0	6.0
2-year	20 °C	55.3	30.0	5.5	9.2	91.0	9.0
	40 °C	62.5	22.6	6.9	8.1	94.0	6.0
	60 °C	58.3	26.7	5.5	9.4	93.7	6.3

*In biochar samples the peak is assigned to aromatic amine, purine and imidazome C (C=N) with bonding energy between 399.04 and 399.35 eV.

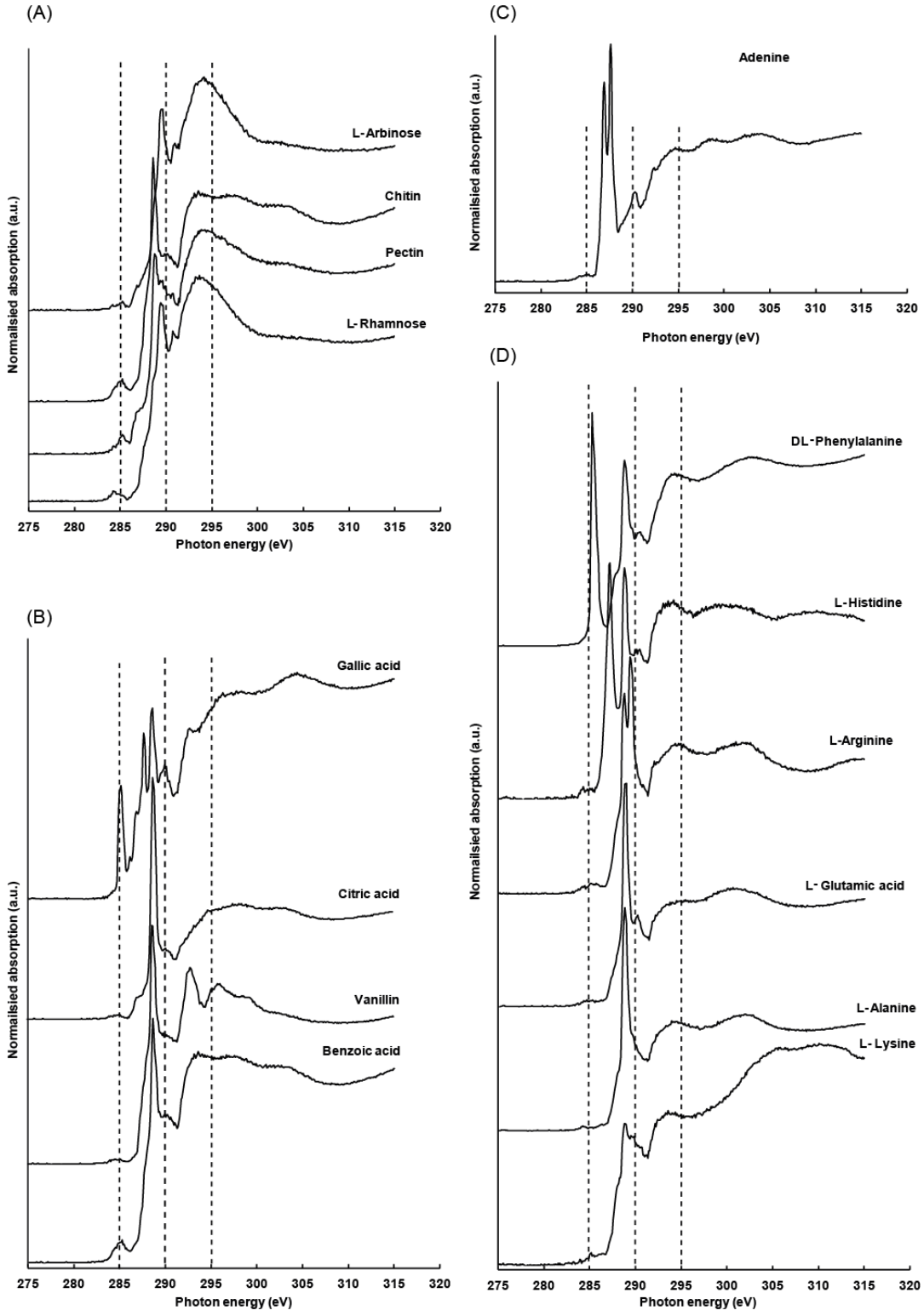

Figure 6.1. C 1s-NEXAFS spectra of the reference C compounds used in the study. (A) L-Arabinose, chitin, pectin and L-Rhamnose; (B) Gallic acid, citric acid, vanillin and benzoic acid; (C) Adenine; and (D) DL-Phenylalanine, L-Histidine, L-Arginine, L-Glutamic acid, L-Alanine and L-Lysine. The dotted lines at 285, 290 and 295 eV are given to assist in comparing the peak positions.

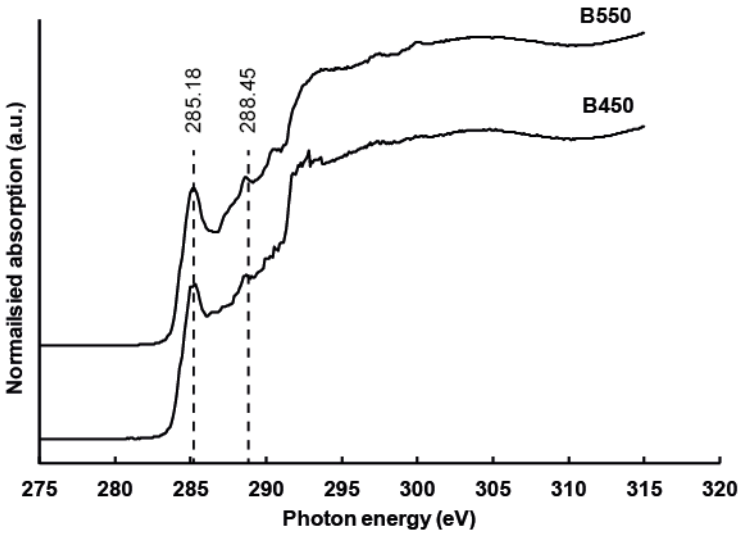

Figure 6.2. C 1s-NEXAFS spectra of the two original biochar samples, B450 is the Eucalyptus wood biochar produced at 450 °C and B550 is the Eucalyptus wood biochar produced at 550 °C.

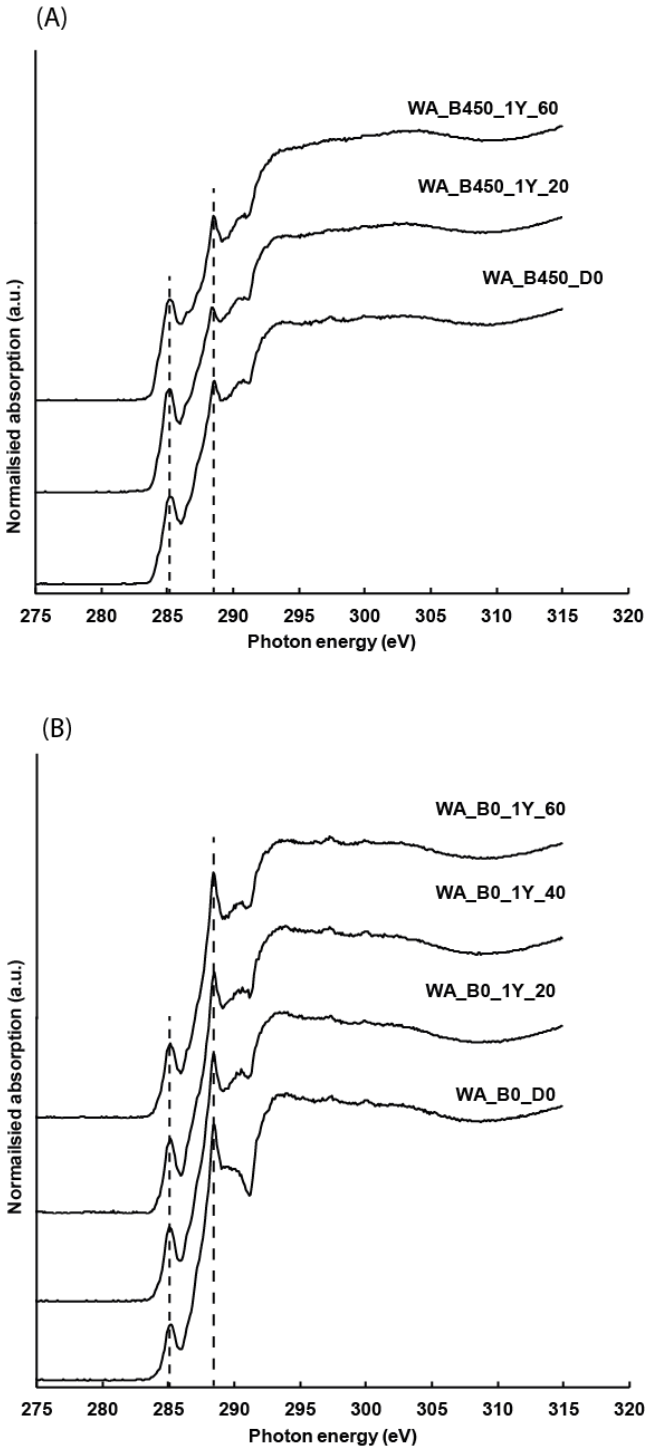

Figure 6.3. C 1s-NEXAFS spectra of the light fraction of the control WA soil and the WA soil treated with B450 biochar after incubation at different time and temperatures. WA_B0_D0 = WA soil without biochar on the first day; WA_B0_1Y_20 is the WA soil without biochar aged for 1 year at 20 °C, and similarly after ageing for 1 year at 40 °C (WA_B0_1Y_40) and 60 °C (WA_B0_1Y_60). WA_B450_D0 = WA soil amended with 450 °C biochar and the light fraction isolated soon after mixing; WA_B450_1Y_20 is the WA soil with biochar ageing for 1 year at 20 °C, and similarly after ageing for 1 year at 60 °C (WA_B450_1Y_60).

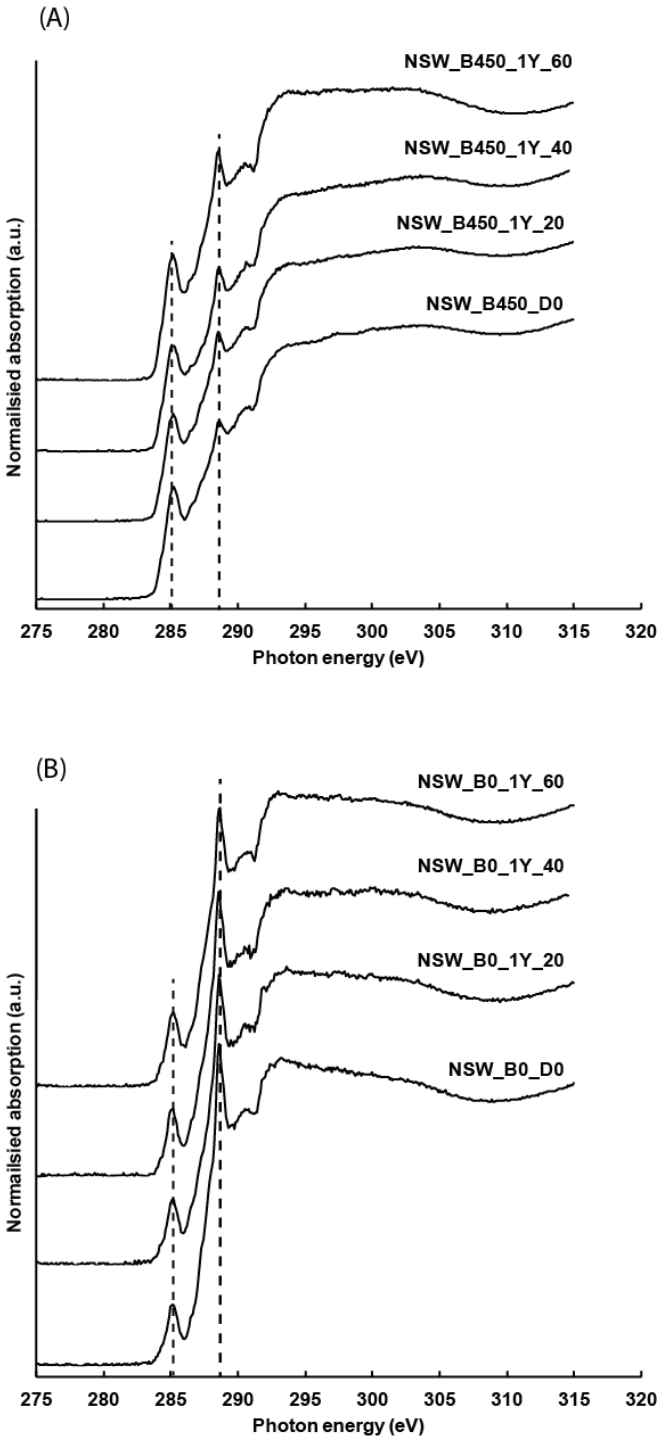

Figure 6.4. C 1s-NEXAFS spectra of the light fraction of the control NSW soil and the NSW soil treated with B450 biochar after incubation at different time and temperatures. NSW_B0_D0 = NSW soil without biochar on the first day; NSW_B0_1Y_20 is the NSW soil without biochar aged for 1 year at 20 °C, and similarly after ageing for 1 year at 40 °C (NSW_B0_1Y_40) and 60 °C (NSW_B0_1Y_60). NSW_B450_D0 = NSW soil amended with 450 °C biochar and the light fraction isolated soon after mixing; NSW_B450_1Y_20 is the NSW soil with biochar ageing for 1 year at 20 °C, and similarly after ageing for 1 year at 40 °C (NSW_B450_1Y_40 WA) and 60 °C (NSW_B450_1Y_60).

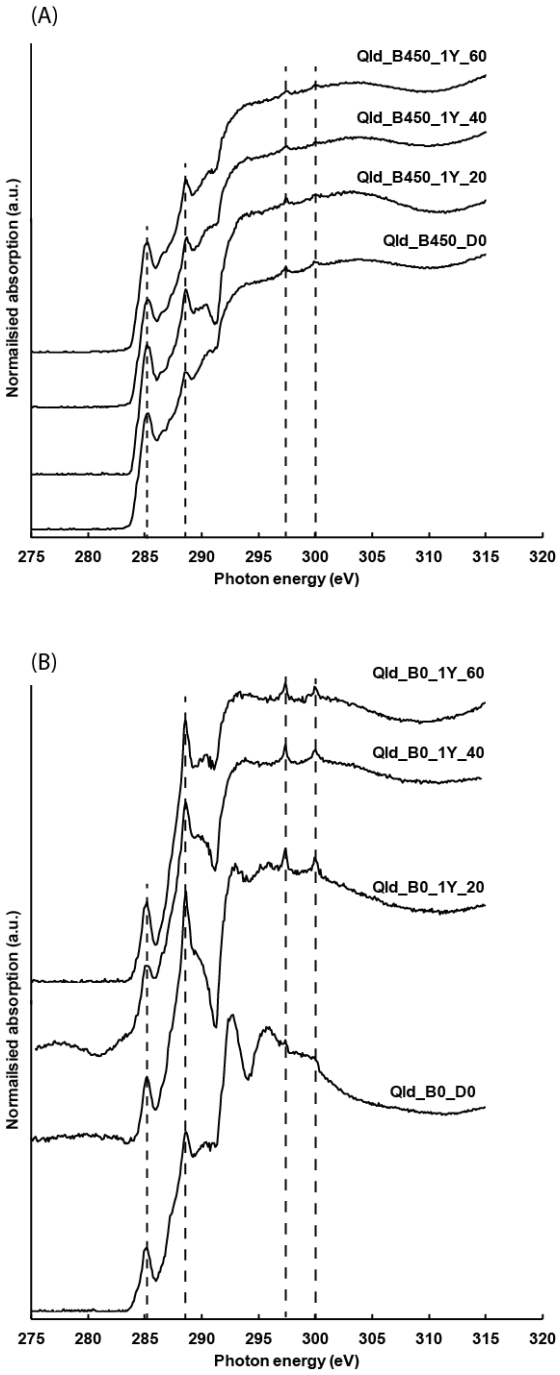

Figure 6.5. C 1s-NEXAFS spectra of the light fraction of the control Qld soil and the Qld soil treated with B450 biochar after incubation at different time and temperatures. Qld_B0_D0 = Qld soil without biochar on the first day; Qld_B0_1Y_20 is the Qld soil without biochar aged for 1 year at 20 °C, and similarly after ageing for 1 year at 40 °C (Qld_B0_1Y_40) and 60 °C (Qld_B0_1Y_60). Qld_B450_D0 = Qld soil amended with 450 °C biochar and the light fraction isolated soon after mixing; Qld_B450_1Y_20 is the Qld soil with biochar ageing for 1 year at 20 °C, and similarly after ageing for 1 year at 40 °C (Qld_B450_1Y_40) and 60 °C (Qld_B450_1Y_60).

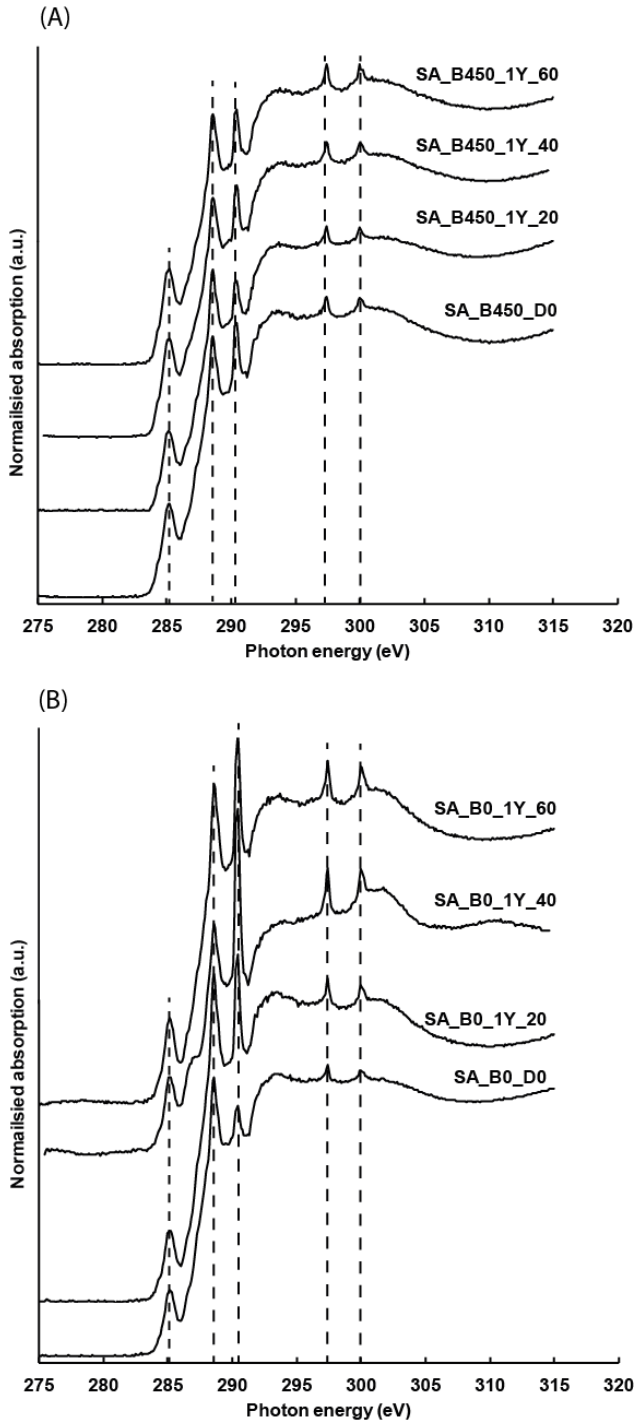

Figure 6.6. C 1s-NEXAFS spectra of the light fraction of the control SA soil and the SA soil treated with B450 biochar after incubation at different time and temperatures. SA_B0_D0 = NSW soil without biochar on the first day; SA_B0_1Y_20 is the NSW soil without biochar aged for 1 year at 20 °C, and similarly after ageing for 1 year at 40 °C (SA_B0_1Y_40) and 60 °C (SA_B0_1Y_60). SA_B450_D0 = NSW soil amended with 450 °C biochar and the light fraction isolated soon after mixing; SA_B450_1Y_20 is the SA soil with biochar ageing for 1 year at 20 °C, and similarly after ageing for 1 year at 40 °C (SA_B450_1Y_40 and 60 °C (NSW_B450_1Y_60).

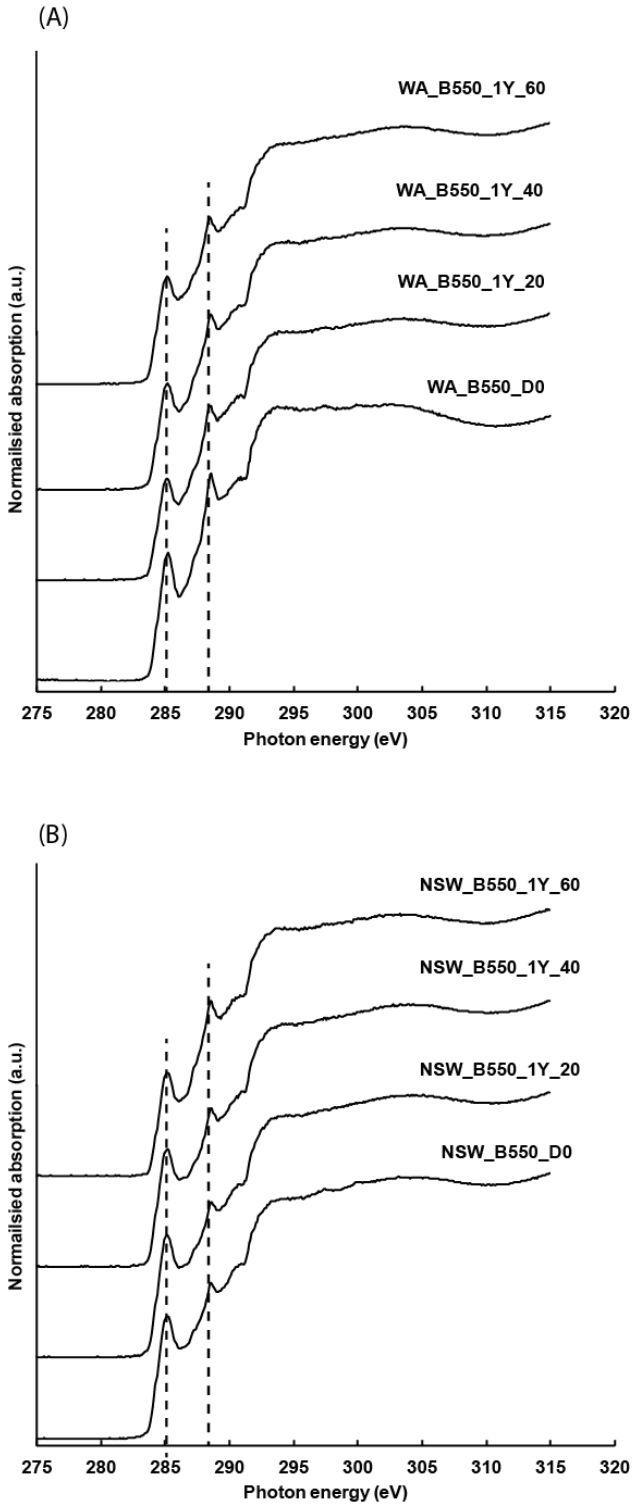

Figure 6.7. C 1s-NEXAFS spectra of the light fraction of the NSW and WA soils amended with B550 biochar after incubation at different time and temperatures. NSW_B550_D0 = NSW soil amended with 550 °C biochar and the light fraction isolated soon after mixing; NSW_B550_1Y_20 is the NSW soil with biochar ageing for 1 year at 20 °C, and similarly after ageing for 1 year at 40 °C (NSW_B550_1Y_40 WA) and 60 °C (NSW_B550_1Y_60), and similar notation for the Qld soil.

6.6. Supporting Information

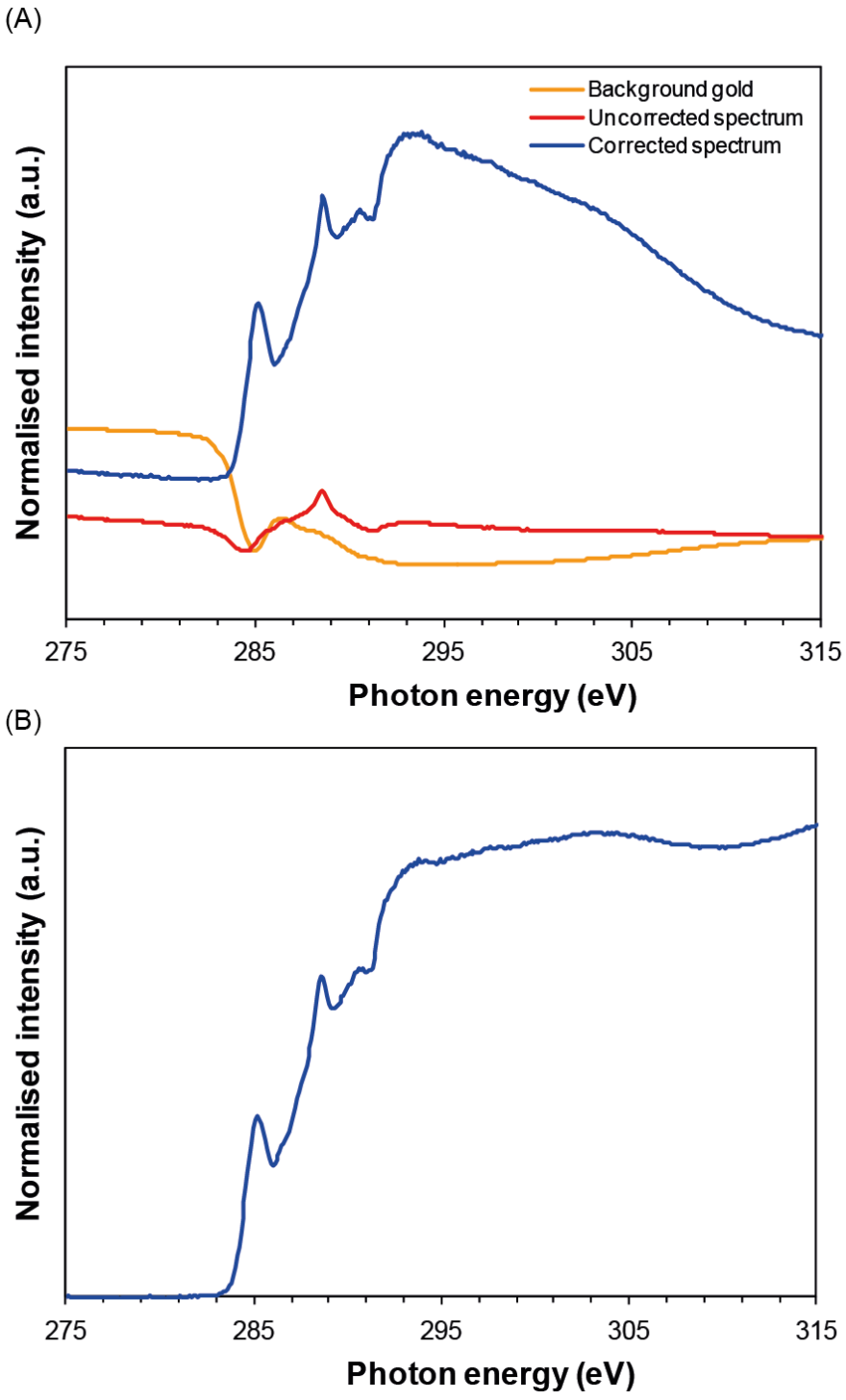

Figure 6.S1. (A) Gold (sputtered) spectrum, uncorrected and corrected spectra (auger electron yield, AEY) of the light fraction of carbon isolated from 450 °C biochar treated soil after one of incubation at 20 °C in a Vertisol (Qld soil); and (B) is the corrected spectrum after background correction and normalisation.

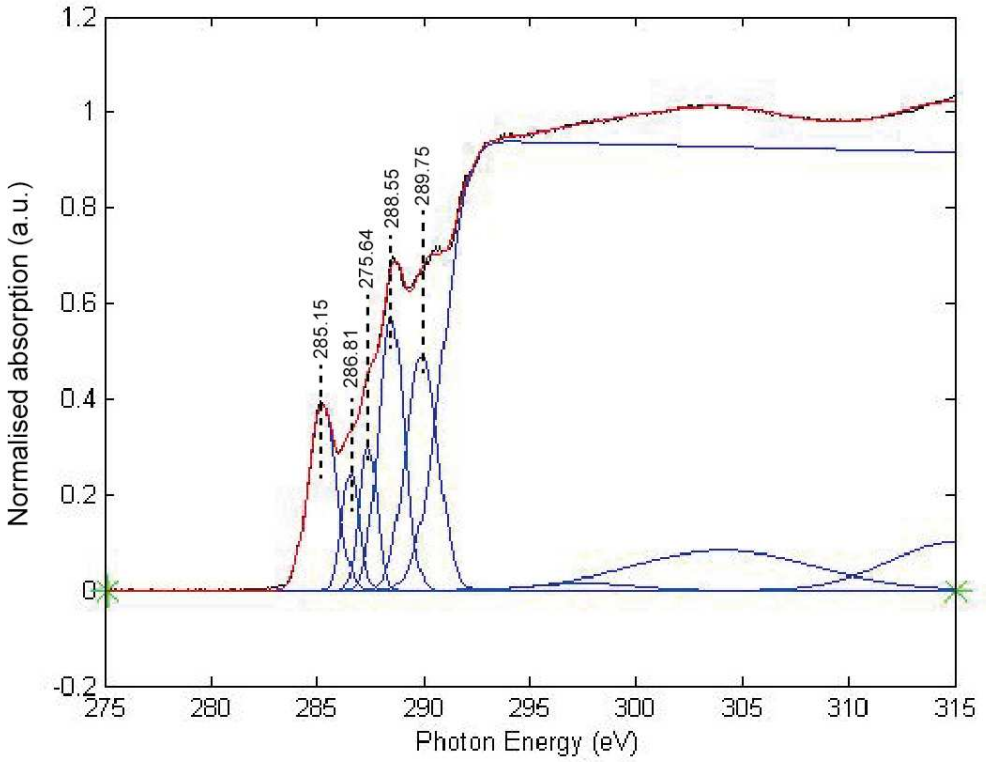

Figure 6.S2. An illustration of the Gaussian and arctangent functions used for the spectral deconvolution of C 1s NEXAFS of the light fraction of soil and soil-biochar samples. The black and red lines represent the original and fitted spectrum, respectively. The blue lines are for the fitted peaks and the peak positions are indicated in the text.

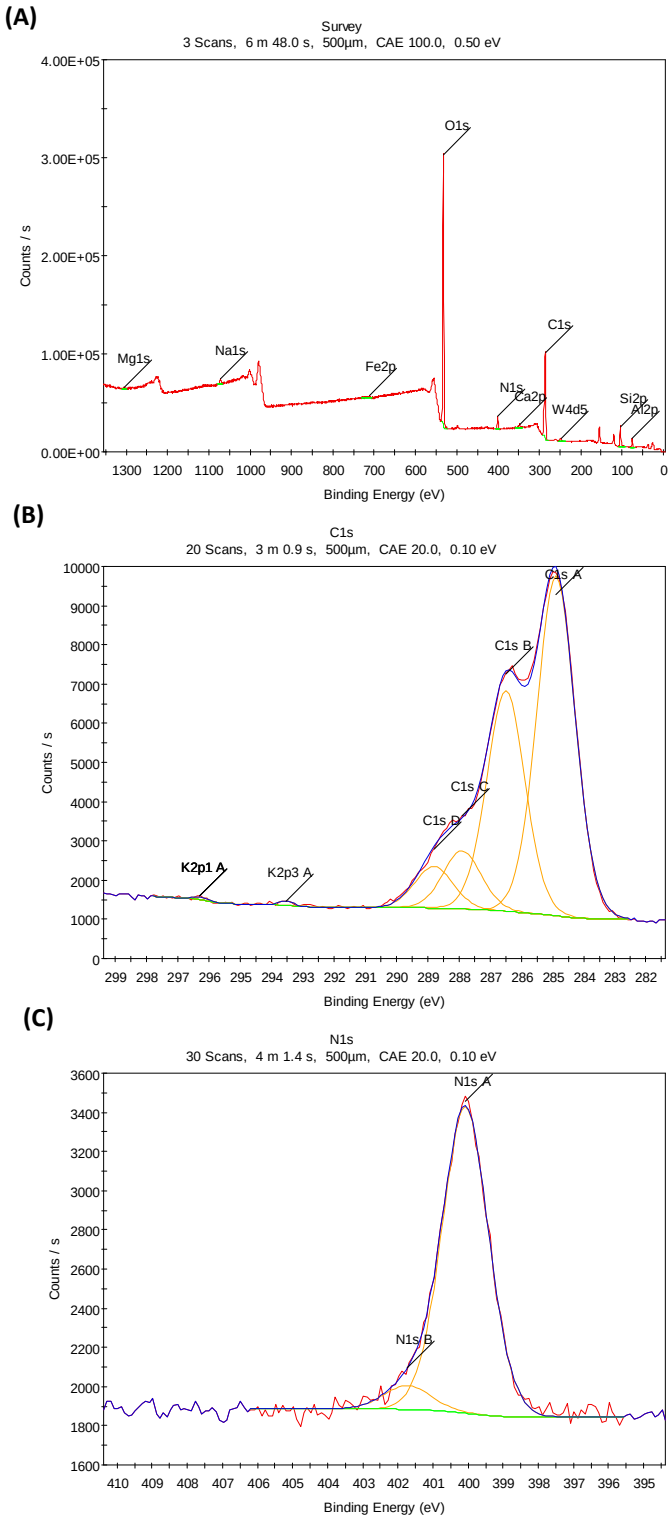

Figure 6.S3. (A) Survey scan of the light fraction (< 1.8 g cm^{-3}) of the WA soil (an Inceptisol) showing peaks of major elements; (B) the high-resolution spectrum for the C region of the same sample showing the four deconvoluted peaks of C 1s at 284.89 (C-C/C-H), 286.49 (C-O), 287.89 (C=O) and 288.79 eV (O=C-O); and (C) the high-resolution spectrum for the N region of the same sample showing the two deconvoluted peaks of N 1s at 400.1 and 402.03 eV.

Chapter 7: A long-term study of interactive priming of biochar and labile carbon mineralisation in a Vertisol

Abstract

Added biochar and labile organic matter (LOM) in soil may interactively prime carbon (C) mineralisation. However, the direction and persistence of the interactive priming effects over a relatively longer period remain unknown. A 2.1-year incubation study was conducted using two δ^{13}C-depleted biochars produced at 450 and 550 °C from *Eucalyptus saligna*, extending the results beyond 4 months (Keith et al., 2011). Each of the biochars (at 2%, w/w) in combination with sugarcane residue (at 0, 1, 2 or 4% w/w) were mixed with a smectite-rich soil.

Our results show that the magnitude and direction of interactive priming of biochar-C and sugarcane residue (source of LOM) C mineralisation observed at the end of the 4-month incubation were generally sustained over the remaining 2.1 years. Overall, the positive priming effect of LOM on biochar-C mineralisation and the negative priming effect of biochar on LOM-C mineralisation increased with increasing LOM application rate. The mean residence times (MRT) of biochars estimated from the 2.1-year data was greater than those estimated from the 4-month incubation data. The MRT of the 450 °C and 550 °C biochars in the absence of added LOM were 713 and 978 years, respectively. The MRT of the 450 °C and 550 °C biochars decreased to 314–322 and 567–643 years, respectively, in the presence of different levels of LOM. Over the 2.1-years, between 0.6 and 1.7% of the biochar-C was mineralised across the biochar and LOM treatments, and between 54 and 65% of the biochar-C mineralisation occurred in the first 4-months of incubation. The proportion of C mineralised for the 450 °C biochar was significantly ($p < 0.001$) greater than the 550 °C biochar. Terminal restriction fragment length polymorphism (T-RFLP) analysis showed that increasing rate of LOM addition changed bacterial and fungal community structures in soil. For example, in the 4% LOM treatment, the fungal community structure was significantly different to the control and the other LOM treatments (1 and 2%). However, the addition of biochar did not affect the microbial community structures in the soil. In conclusion, although the input of LOM

produced a positive priming effect on biochar-C mineralisation with increasing LOM rates in the Vertisol, biochar can still persist in the soil in the range of a few centuries.

7.1. Introduction

Biochar application to soil has been advocated as a mean of long-term C storage in a terrestrial ecosystem to counter the effects of rising levels of atmospheric carbon dioxide (Glaser et al., 2001; Lehmann and Joseph, 2009; Woolf et al., 2010). The C storage benefits of biochar would be increased if there is a negative priming effect of biochar on native soil C.

Previous studies have shown different priming effects, i.e. positive, negative or no effect of biochar on the mineralisation of native soil organic carbon (SOC) or added LOM (Cross and Sohi, 2011; Farrell et al., 2013; Hamer et al., 2004; Keith et al., 2011; Luo et al., 2011; Zimmerman et al., 2011). The positive priming of biochar has been linked to the co-metabolic effect of a small proportion of labile C in biochars, enhancing the growth of microbial communities and therefore accelerating organic C mineralisation in soil (Farrell et al., 2013; Hamer et al., 2004; Luo et al., 2011). Keith et al. (2011) found a positive priming effect of biochar on LOM-C applied at 1% (wt/wt) in a smectite soil, and the positive priming was changed to negative priming when the LOM application rate increased from 1% to 2 or 4% (wt/wt). The negative priming effect of biochar on LOM-C mineralisation may result from (i) increased organo-mineral chemical interactions with the co-addition of biochar and LOM in a mineral soil (Brodowski et al., 2006) and/or (ii) improved aggregate stability (Herath et al., 2013). Furthermore, some of the dissolved LOM may be physically entrapped within the pore structure of biochar (Pignatello et al., 2006). Hence, LOM may be chemically and physically protected against biotic decomposition in the biochar-amended mineral soil. On the other hand, the addition of LOM in soil may positively prime the mineralisation of labile C components in biochar in a relatively short-term (Hamer et al., 2004; Keith et al., 2011; Kuzyakov et al., 2009; Luo et al., 2011), or there may be no significant effect on aged biochar-C (Liang et al., 2010). Keith et al. (2011) found that the positive priming effect of LOM on biochar-C mineralisation was time dependent at low application rates of LOM (1 and 2%) during a 4-month incubation period whereas the positive priming of biochar was sustained at high application rate of LOM (4%) over the same period. It is

possible that the biochar-induced physico-chemical interactions may also stabilise biochar-C mineralisation over time in organo-mineral fractions (Keith et al. 2011). The above results suggest that the direction and magnitude of interactive priming effects may change due to the depletion of labile C in biochar with time or with increasing LOM addition rate. Over a longer term period, the factors (such as organo-mineral interaction, sorption of LOM on biochar, and microbial activity and/or structure) contributing to interactive priming effect may change further, and consequently, the direction and magnitude of interactive priming may also change with time. Therefore, it is necessary to assess the interactive priming effect of biochar and LOM input in soil over a longer-term period, to gain a better understanding of the mechanisms and the C sequestration potential of biochar in soil.

An increase in the activity of microorganisms and associated enzymes in the presence of biochar was considered to be the main reason for the occurrence of positive priming effect in soils (Kuzyakov et al., 2000). The LOM addition rate or composition may influence the microbial community and consequently the interactive priming effects. For example, the easily available carbon (glucose) was found to increase bacterial growth rates accompanied by decreased fungal growth rates, whereas complex carbon (cellulose) was observed to increase both bacterial and fungal growth rates (Meidute et al., 2008). Similarly, Rousk and Baath (2007) reported an increased bacterial and fungal growth with the addition of alfalfa and barley straw in soil. Acosta-MartÃnez and Harmel (2006) reported an increased bacterial and fungal populations with poultry litter application at rates higher than 6.7 t ha^{-1}. However, very little is known about changes in microbial community with the addition of LOM and their likely influence on the interactive priming effects in biochar-amended soil. This study has made an attempt to provide some insights into this knowledge gap.

Biochar generally has a high stability in soil (Fang et al., 2014; Kuzyakov et al., 2009; Singh et al., 2012), however, it can be degraded by both abiotic and biotic processes (Cheng et al., 2006; Knicker et al., 2013; Zimmerman, 2010). The biological degradation of biochar may be the dominant process for degrading biochar-C in soils at temperature below 40 °C (Zimmermann et al., 2012). On the other hand, biochar serves as a habitat for microbes and increases soil microbial biomass (Kolb et al., 2009; Lehmann et al., 2011; O'Neill et al., 2009; Pietikäinen et

al., 2000; Warnock et al., 2007). In some cases, the total microbial biomass remains unchanged (Farrell et al., 2013; Steinbeiss et al., 2009), while microbial structure may shift to an increased proportion fungal communities (Steinbeiss et al., 2009). Farrell et al. (2013) found an increased gram positive bacteria biomass, which are recognised to utilise biochar as a C source (Farrell et al., 2013; Santos et al., 2012). These studies were conducted over a short-term period (months) and the significant shift of microbial community structure could be due to the labile-C in biochar (Farrell et al., 2013). However, with the depletion of labile-C fraction over time, the difference in microbial community in the absence and presence of biochar may not exist.

This incubation experiment, a continuation of the short-term (4-month) study (Keith et al., 2011) and an extension to analyse microbial community structure at the termination of the incubation experiment, was conducted over a 2.1-year period. The specific aims of the study were to: (i) measure the biochar-C mineralisation and the interactive priming effect of sugarcane residue (LOM)-C and biochar-C mineralisation over a longer term in a clayey soil; and (ii) evaluate the effect of LOM and biochar treatments on microbial community structure in the soil after the long-term incubation. The hypotheses of the research were that the negative priming effect of biochar on LOM-C mineralisation will change over a longer term period and the presence of LOM will decrease the biochar-C stability. Furthermore, biochar and LOM presence over a longer term will change the microbial community structure in the soil.

7.2. Material and methods

7.2.1. Biochar, organic matter and soil incubation experiment

The detailed procedures and relevant properties of soil, biochar and sugarcane residue have been described by Keith et al. (2011) and are presented in the Appendix 6. Briefly, biochars, sugarcane residue and the clayey soil (Vertisol) were homogenously mixed and incubated in the dark at 20 ± 1 °C in the laboratory over a 2.1-year period. Biochars were produced at 450 and 550 °C from δ^{13}C-depleted *Eucalyptus saligna* wood biomass. The smectite dominant soil used for the incubation experiment had a $pH_{1:5H2O}$ 8.10; organic C and clay content of 0.45% and

53%, respectively. The biochars were applied at rates of 0 or 2% (w/w) and the sugarcane residue was added at rates of 0, 1, 2 or 4% (w/w) to 200 g soil (oven-dried basis). All treatments were replicated three times. A nutrient solution and a microbial inoculum were added to each treatment and the moisture content was adjusted to 60% of soil water holding capacity. The CO_2 evolved from the soil and soil-biochar mixtures was continuously trapped in NaOH solution. The CO_2 traps were replaced after 240, 310, 430, 506, 630 and 758 days of incubation; the earlier traps were replaced after 1, 2, 5, 8, 13, 20, 30, 44, 65, 90, and 120 days (Keith et al., 2011).

7.2.2. Mineralisation of biochar, mean residence time and priming effect

The total C mineralised (mg kg^{-1} soil) in treatments was determined by titrating a known volume of the CO_2 trap solution against 0.1 M HCl, using phenolphthalein as the indicator. To quantify the proportion of CO_2 derived from biochar or sugarcane residue (LOM) + native soil C, the trap solution was precipitated with $SrCl_2$, and a $SrCO_3$ precipitate was obtained for $\delta^{13}C$ analysis (see chapter 3). From the $\delta^{13}C$ data the proportion of CO_2 derived from biochar was determined by a two end-member mixing model (Keith et al., 2011).

$$C_{\text{Biochar}}\,(\%) = \frac{(\delta_T{}^{13}CO_2 - \delta_{SLOM}{}^{13}CO_2)}{(\delta_B{}^{13}CO_2 - \delta_{SLOM}{}^{13}CO_2)} \times 100 \qquad (7.1)$$

where $\delta_T{}^{13}CO_2$ is the $\delta^{13}C$ value of total CO_2-C evolved from biochar and LOM amended soil, $\delta_{SLOM}{}^{13}CO_2$ is the $\delta^{13}C$ value for the CO_2-C evolved from LOM amended or non-amended soil and $\delta_B{}^{13}C$ is the ^{13}C isotopic value of the fresh biochars (−36.3‰ and −36.4‰ for the 450 and 550 °C biochar, respectively).

Using the proportion of CO_2-C derived from biochar, the proportion and amount of soil + LOM-C mineralised was determined. Due to the similar $\delta\,^{13}C$ values of soil (−14.3‰) and LOM (−12.7‰), the quantity of C mineralised from soil C and LOM-C was indistinguishable.

Biochar-C mineralisation data were fitted to the two-pool exponential model to estimate the MRT of biochar-C in the soil (Equation 3.2 in Chapter 3).

The priming effect of biochar-C (i.e. changes in native soil C or soil + LOM-C mineralised induced by biochar) on native soil C ± LOM-C (PE^{B}_{SLOM}) was calculated as:

$$PE^{B}_{SLOM} = C_{B,SLOM} - C_{SLOM} \quad (7.2)$$

where, $C_{B,SLOM}$ is the amount (mg kg^{-1} soil) of soil or soil + LOM-C mineralised from biochar-amended soil and C_{SLOM} is the amount (mg kg^{-1} soil) of soil or soil + LOM-C mineralised from control soil (without biochar).

The priming effect of LOM (i.e. changes in biochar-C mineralisation induced by LOM addition) on biochar-C (PE^{SLOM}_{B}) was determined as:

$$PE^{SLOM}_{B} = C_{B,SLOM} - C_{B} \quad (7.3)$$

where $C_{B,SLOM}$ is the amount (mg kg^{-1} soil) of biochar-C mineralised from biochar-amended soil in the presence of LOM and C_B is the amount (mg kg^{-1} soil) of biochar-C mineralised from biochar-amended soil in the absence of LOM.

7.2.3. Terminal restriction fragment length polymorphism (T-RFLP) analysis

DNA extractions: Soil DNA was extracted from 0.25 g soil samples using the MoBio Powersoil® DNA Isolation Kit (MO BIO Laboratories, Inc.) and following the protocol provided by the supplier. Purified soil DNA was stored at −20 °C. The amounts of extracted DNA were qualitatively assessed on a 1.0% agarose gel run at 220 V for 20 min and stained with ethidium bromide.

The DNA extractions were tested for suitability for PCR by 16S rRNA gene amplification. Initial PCR amplification was performed using F27 (AGAGTTTGATCMTGGCTCAG) and R1492 (TACGGTTACCTTGTTACGACTT) primers in a total volume of 15 µl, containing 8.9 µl Milli-Q water, 3 µl PCR Reaction buffer (5 × MyTaq™ Red DNA Polymerase, BIOLINE), 0.5 µl F27 (10 µM), 0.5 µl R1492 (10 µM), 0.1 µl Taq and 2 µl extracted DNA as the template. After initial denaturation at 95 °C for 5 min, the reactions were cycled 35 times at 95 °C for 30 s, 60 °C for 30 s, and 72 °C for 1 min with a final elongation step at 72 °C for 5 min in an S1000 Touch™ Thermal Cycler (Bio-Rad). PCR products were visualized on 1.5% *agarose* gels stained with ethidium bromide (Sigma), using

ChemiDoc™ MP (Bio-Rad). Any extractions that yielded insufficient DNA were re-extracted.

T-RFLP analysis: T-RFLP analysis of bacterial and fungal communities was carried out by targeting 16S rRNA genes and internal transcribed spacer (ITS) genes, respectively, using primers labelled at the 5′ end with 5-carboxyfluorescein (FAM) or VIC. For bacterial communities, T-RFLP was performed with labelled primers 338 F-FAM (ACWCCTACGGGWGGCWGC) and 1050R-NED (AYCTCACGRCACGAGCTGAC). Fluorescently labelled primers were synthesised by Life Technologies. The PCR program described above was used in a total volume of 30 μl, containing 17.8 μl Milli-Q water, 6 μl PCR Reaction buffer (5 × MyTaq™ Red DNA Polymerase, BIOLINE), 1 μl F27 (10 μM), 1 μl R1492 (10 μM), 0.2 μl Taq and 4 μl extracted DNA as the template. The thermocycling program included an initial denaturation step at 95 °C for 5 min followed by 35 cycles of denaturation step at 95 °C for 30 s, annealing step at 60 °C for 30 s, elongation step at 72 °C for 1 min, and a final 7 min elongation step at 72 °C. Fungal community analysis was done with ITS1-VIC (TCCGTAGGTGAACCTGCGG) and ITS4-VIC (TCCTCCGCTTATTGATATGC) primers, under the same conditions, but using a temperature of 47 °C in the annealing step. PCR products were checked by 1.5% agarose gels described as above. PCR products (40-55 μl) were purified by ethanol precipitation. In each PCR product, 0.1 volumes of 3 M sodium acetate (pH 5.2) and 2 volumes of absolute ethanol were added, and they were incubated for 30 min at room temperature. The supernatant was discarded after centrifugation at 12,000 *g* for 20 min and the precipitates washed with 70% ethanol. To dissolve the DNA precipitate, 15 μl of Milli-Q water was added. The purified DNA concentration was between 100 and 200 ng μl^{-1}. The purified PCR product was digested with 0.25 μl of restriction enzyme *Hha I* (bacteria) or *Taq I* (fungi), 0.25μl of BSA, 2.5 μl of 10 × NEB buff 4, and 7 μl of Milli-Q water. The bacterial DNA samples were incubated at 37 °C overnight. The restriction enzyme was inactivated by incubation at 65 °C (*Hha I*) or 80 °C (*Taq I*) for 20 min. Bacterial and fungal DNA samples were combined and T-RFLP chromatogram was generated by the Australian Genome Research Facility (AGRF).

7.2.4. Statistical analysis

Cumulative total C and biochar-C, MRT, and interactive priming effect of LOM and biochar, were analysed with the two-way (sugarcane residue and biochar) analysis of variance performed in Genstat® 14th edition (VSN International, 2011). Repeated measures analyses were performed for total C and biochar-C mineralisation rates using a linear mixed model framework in Genstat® 14th edition (Fang et al., 2014). Each analysis consisted of fixed effects of LOM, biochar, time and all associated interactions, and random effects of replicate, and replicate and time. To allow for correlation between repeated measures on the same units, a first order autoregressive model was fitted (giving a higher residual log-likelihood than the power model). Heterogeneity in the residual variances between time-points was included as it was deemed significant using a residual likelihood ratio test. Where the F-statistic was significant, the means were compared using the LSD test at the 5% significance level unless stated otherwise.

T-RFLP data was analysed using the T-REX analysis pipeline (Culman et al., 2009). The same settings were used for both bacteria and fungi. Noise filtering (determining true peaks from background noise) was performed using the approach developed by Abdo et al. (2006). Briefly, true peaks were identified by an iterative approach where peaks whose height area exceeded the standard deviation computed over all peaks (with a standard deviation multiplier of 1.1). T-RFs were aligned using the T-align algorithm (Smith et al., 2005) with a clustering threshold of 0.5 and allowing for more than one peak to be classified as a single T-RF. Data matrices were constructed in T-REX using peak presence or absence and relativised peak height and peak area. Additive main effects and multiplicative interaction analysis (AMMI) was performed within T-REX, and non-metric MDS (using the Bray-Curtis measure of dissimilarity) was performed using the PAST software package (Hammer et al., 2001).

7.3. Results

7.3.1. Total C mineralisation

Over the 2.1 years of incubation, total C mineralisation (CO_2-C produced on per unit of total C) increased significantly ($p < 0.001$) with increasing LOM application rates (**Table 7.1**). In the 0% LOM treatment, approximately 45% of the total C mineralised over the total experimental period, i.e. 2.1 years, occurred

between 4 and 25 months. In comparison, in the 1, 2 and 4% of LOM treatments only 16−23% of the total C was mineralised over the same period. The presence of biochar significantly ($p < 0.001$) decreased the total C mineralised on per unit total C basis during the incubation period. Total C mineralisation (mg CO_2-C g^{-1} soil C) was the greatest in the control, followed by the 450 °C biochar, and the smallest in the 550 °C biochar treatments (**Figure 7.1**).

Total C mineralisation rates (CO_2-C g^{-1} soil C d^{-1}) were significantly ($p < 0.001$) affected by the main effects of LOM, biochar, time, and the interactive effects of LOM, biochar and time during the 2.1-year incubation period (**Table 7.1**). Total C mineralisation rate decreased with time, for example, from 0.30 mg CO_2-C g^{-1} soil C d^{-1} at 4-month to 0.05 mg CO_2-C g^{-1} soil C d^{-1} at 2.1-year for 4% LOM in the 450 °C biochar treatments (**Figure 7.2**). Total C mineralisation rate significantly ($p < 0.001$) increased with increasing application rates of the LOM. The presence of biochar significantly decreased total C mineralisation rates. However, total C mineralisation rates in different treatments were not affected by the interactive effects of LOM and biochar (**Table 7.1**).

Table 7.1. Statistical significance of the effects of incubation time, LOM and biochar treatments and their interactions on the mineralisation rate of total C and biochar-C, the amount of total C and biochar-C mineralised, mean residence time (MRT) and the interactive priming effects of LOM and biochar-C.

Treatment effect	Total C mineralisation rate	Biochar-C mineralisation rate	Total C mineralised	Biochar-C mineralised	MRT	Priming of LOM on biochar-C	Priming of biochar on LOM-C
Time (T)	***	***	–	–	–	–	–
LOM (L)	***	***	***	*	***	***	*
Biochar (B)	***	***	***	***	***	ns	ns
T × L	***	***	–	–	–	–	–
T × B	***	***	–	–	–	–	–
L × B	ns	*	***	ns	ns	ns	ns
T × L × B	***	ns	–	–	–	–	–

* $p < 0.05$; *** $p \leq 0.001$; ns, not significant.

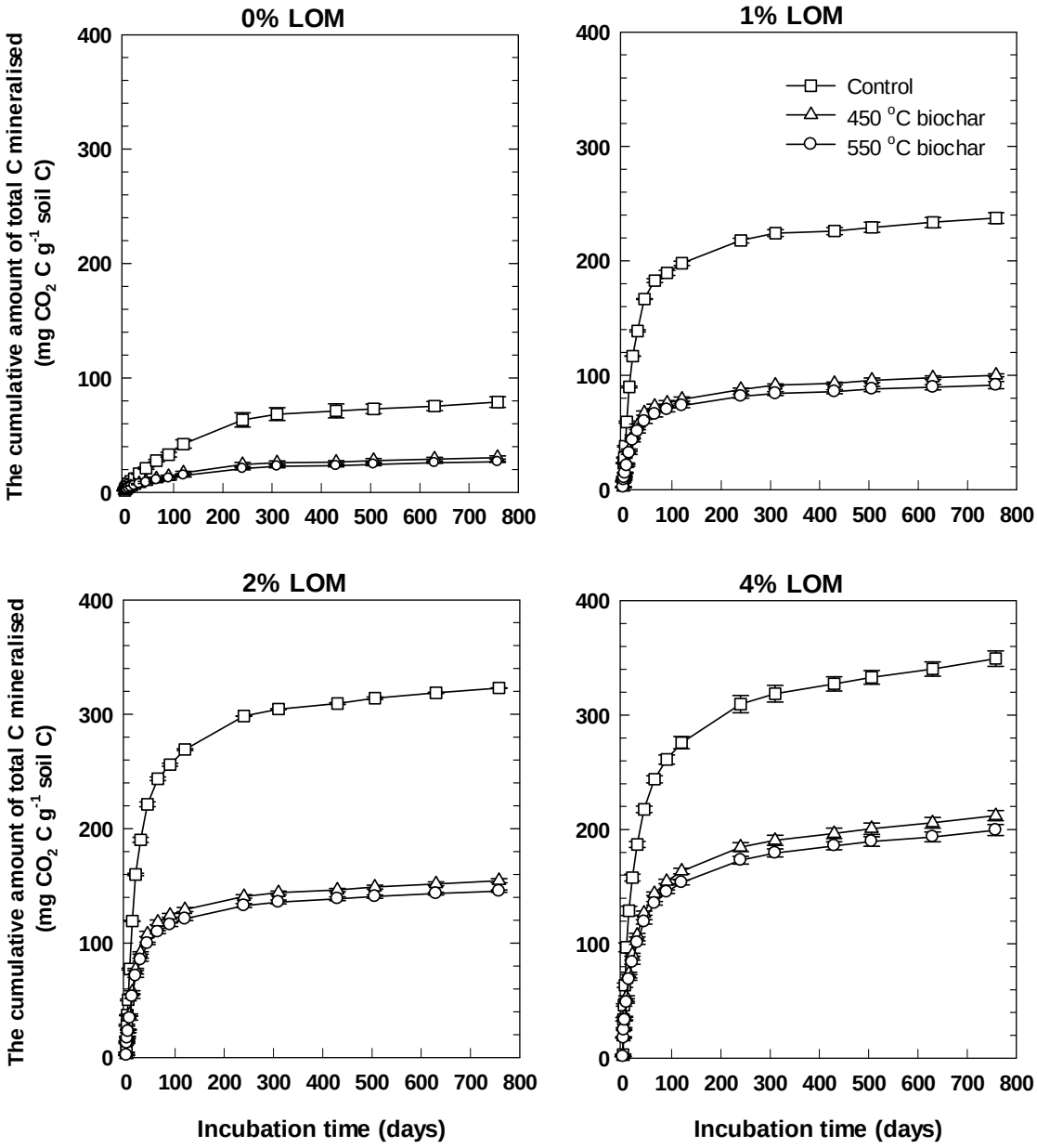

Figure 7.1. The cumulative amount of total C mineralised (mg CO_2-C g^{-1} soil C) from soil mixed with the LOM (0, 1, 2 or 4 %) and biochars (450 °C or 550 °C) over the 2.1-year incubation period. Square, triangle and circle represent the control (i.e. no biochar), 450 °C biochar and 550 °C biochar treatments, respectively. Error bars represent the standard errors of the mean (n = 3).

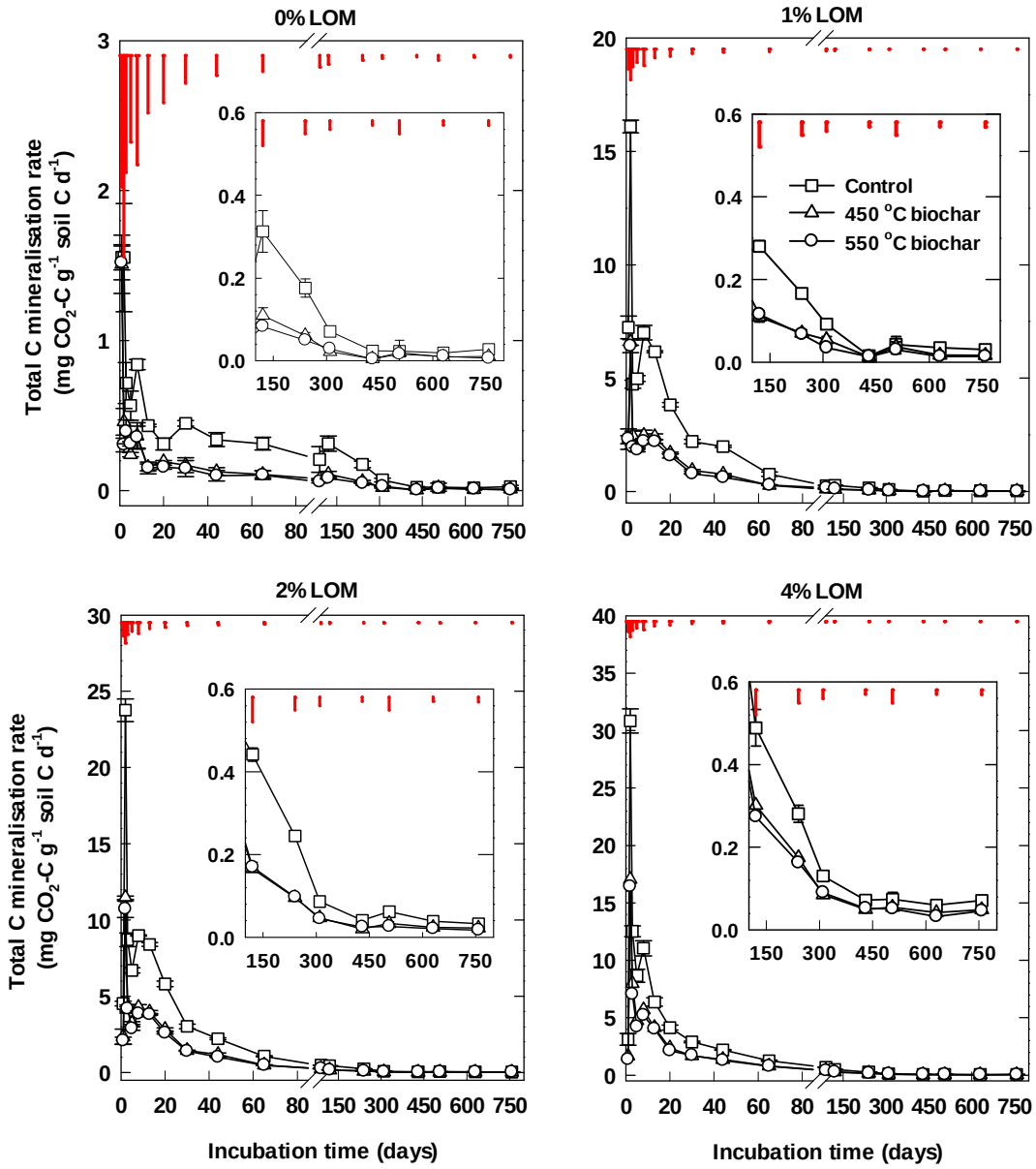

Figure 7.2. Total C mineralisation rate (mg CO_2-C g^{-1} soil C d^{-1}) from soil mixed with the LOM (0, 1, 2 or 4 %) and biochars (450 or 550 °C) during the 2.1-year incubation period. Square, triangle and circle represent the control (i.e. no biochar), 450 °C biochar and 550 °C biochar treatments, respectively. Error bars represent the standard errors of the mean (n = 3). The insets show the total C mineralisation rate from the day-120 with an expanded *y*-axis scale. Red thick bars show least significant differences (at 5% level, $LSD_{0.05}$) of the interaction of biochar and LOM at different time-points.

7.3.2. Biochar-C mineralisation

Over the 2.1 years of incubation, the proportion of biochar-C mineralised ranged between 0.6 and 1.7% of the applied biochar-C across all treatments. The proportion of C mineralised in the 450 and 550 °C biochar in the native soil (i.e. 0% LOM treatment) was 1.3% and 0.7%, respectively. In the presence of LOM (1, 2 and 4%), between 1.2 and 1.7% for the 450 °C biochar, and between 0.6 and 1.0% for the 550 °C biochar, of the added biochar-C was mineralised (**Figure 7.3**). Increasing LOM application rate did not significantly increase the biochar-C mineralisation. Of the total biochar-C mineralised, between 35 and 46% was mineralised during 4 to 25 months period. Within each LOM treatment, the amount of biochar-C mineralised from the 450 °C biochar was 1.7 to 2.2 times greater than that observed for the 550 °C biochar treatments.

Biochar-C mineralisation rate decreased with time and it was significantly ($p < 0.001$) affected by the main effects of the LOM, biochar, time and the interactive effects of LOM and time, and biochar and time during the 2.1-year incubation period (**Table 7.1**). Biochar-C mineralisation rates varied from significant to non-significant in the LOM and biochar treatments with time and were relatively smaller at 4 to 25 month than at 0 to 4 month, ranging from 0.01 to 0.59 mg CO_2-C kg^{-1} soil d^{-1} (**Figure 7.4**).

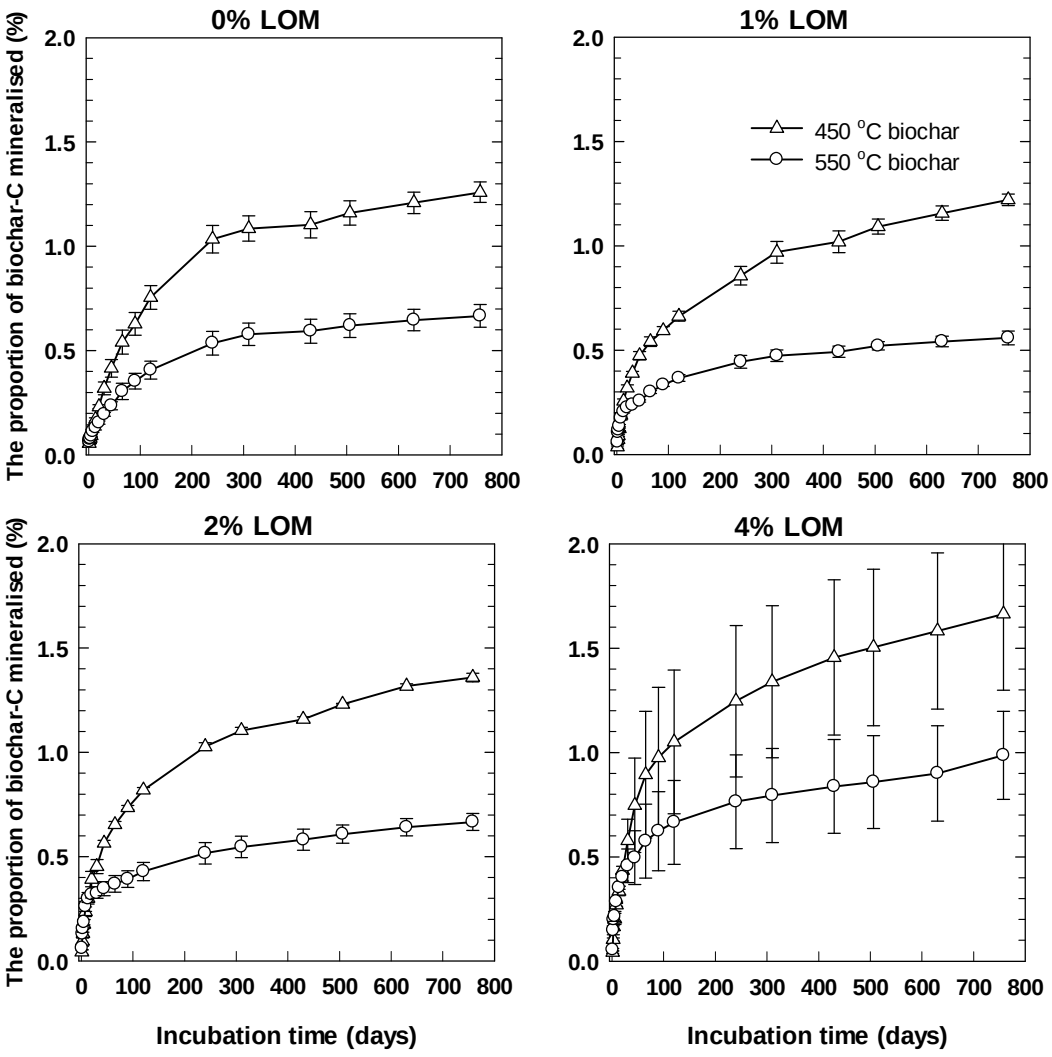

Figure 7.3. The proportion (%) of the applied biochar carbon (C) mineralised from different combination treatments of the LOM (0, 1, 2 or 4 %) and biochars (450 or 550 °C) during the 2.1-year period. Triangle and circle represent the 450 and 550 °C biochar, respectively. Error bars represent the standard errors of the mean (n = 3).

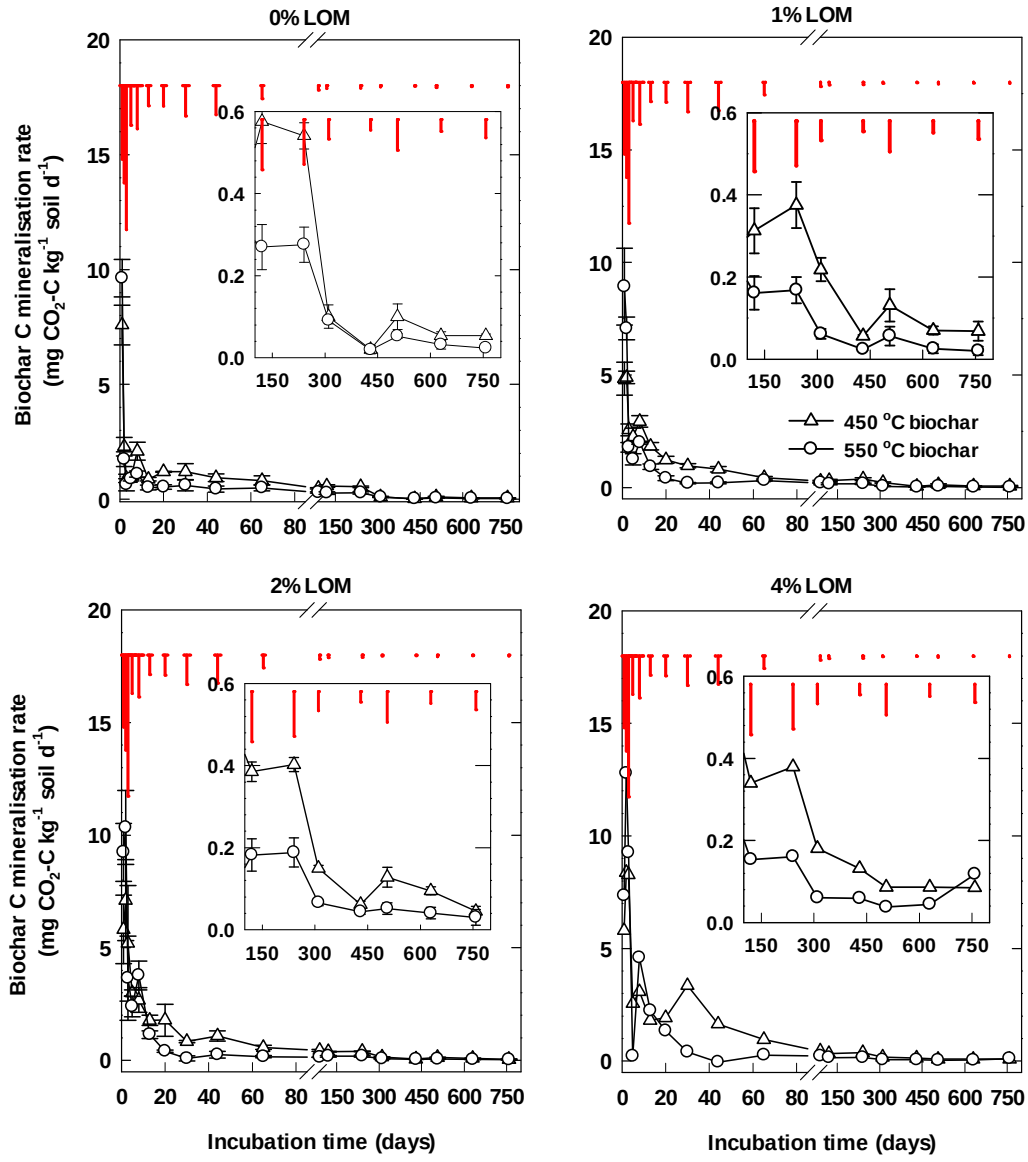

Figure 7.4. Biochar-C mineralisation rate (mg CO_2-C kg^{-1}soil d^{-1}) during the 2.1-year incubation period. Soil was mixed with the LOM (0, 1, 2 or 4 %) and biochars (450 or 550 °C). Triangle and circle represent the 450 and 550 °C biochar, respectively. Error bars represent standard errors of the mean (n = 3). The insets show the biochar-C mineralisation rate from the day-120 with an expanded *y*-axis scale. Thick red bars show least significant differences (at 5% level, $LSD_{0.05}$) of the interaction of biochar and LOM at different time-points.

The estimated MRT of the biochars based on the 2.1-year incubation data were much higher (**Table 7.2**) than those obtained from the 4-month incubation period data (Keith et al., 2011; Appendix 6). The MRT of the 450 and 550 °C biochar was 314−713 and 567−978 years, respectively, across different LOM treatments

(**Table 7.2**). This is compared to MRT of 62−112 and 100−248 years estimated from the mineralisation data over the 4-month incubation period. The MRT of both biochars was significantly ($p < 0.001$) higher in the control soil (i.e. with no LOM addition) than in the LOM treatments. The LOM application rates ranging from 1 to 4%, however, did not significantly affect the MRT of both biochars. The MRT of the labile biochar-C varied between 1 and 4 days across the biochar and LOM treatments, and the proportion of labile C in biochar ranged from 0.28 to1.03% of the total biochar-C.

The proportion of CO_2 (%) evolved from the biochar decreased with increasing LOM application rates (**Figure 7.5**), ranging from 17−33%, 6−20%, 5−15% and 2−8% for 0, 1, 2 and 4% LOM treatments, respectively. For each of the LOM application rates, the proportion of CO_2 evolved was greater from the 450 °C biochar than the 550 °C biochar treatment.

Table 7.2. The mean residence time (± standard errors) of the labile and recalcitrant pools of biochar-C estimated using a two-pool exponential model fitted to the biochar-C mineralisation data over the 2.1-year incubation period. The small letters indicate significant difference between the LOM application rates for each biochar, and the capital letters indicate significant the differences between the two biochars at each LOM application rate. ($LSD_{0.05} = 268$)

Treatments		Mean residence time		Labile pool (%)
Biochar	**LOM (%)**	**Labile (days)**	**Resistant (years)**	
450 °C	0	1±0	713±51 aA	0.97±0.07
450 °C	1	2±0	322±14 bA	0.63±0.05
450 °C	2	1±0	321±28 bA	0.77±0.04
450 °C	4	1±1	314±37 bA	1.03±0.41
550 °C	0	2±1	978±212 aA	0.45±0.09
550 °C	1	4±0	643±68 bB	0.28±0.01
550 °C	2	3±0	585±82 bA	0.35±0.04
550 °C	4	2±1	567±48 bA	0.62±0.22

$R^2 > 0.93$

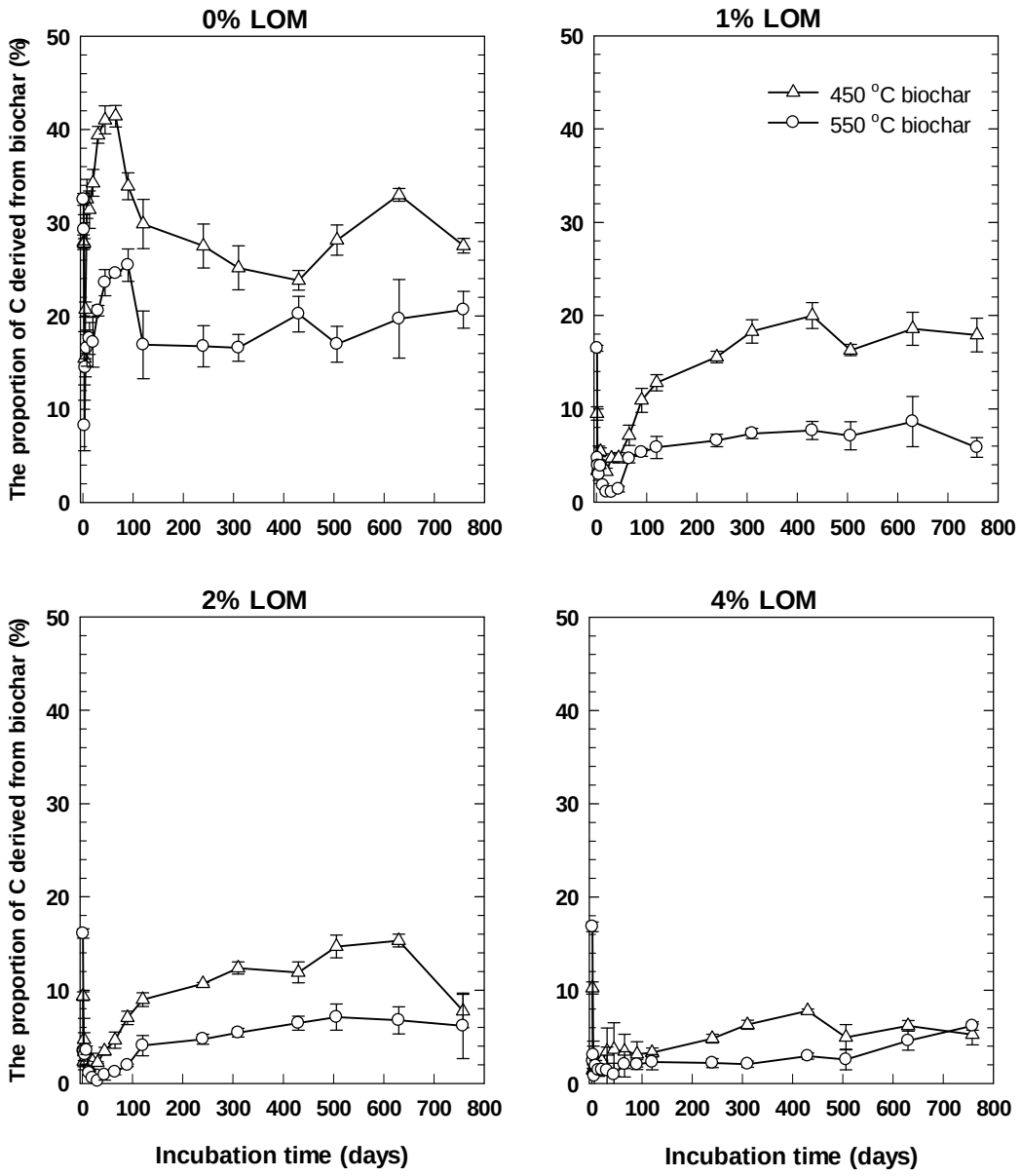

Figure 7.5. The proportion (%) of C mineralised derived from biochars in different combination treatments of the LOM (0, 1, 2 or 4 %) and biochars (450 or 550 °C) during the 2.1-year incubation period. Triangle and circle represent the 450 °C biochar and 550 °C biochar treatment, respectively. Error bars represent standard errors of the mean (n = 3).

7.3.3. Interactive priming effect of biochar and LOM mineralisation

The magnitude and direction of the priming effect of LOM on biochar-C mineralisation was variable with the increasing LOM application rates, biochar treatment and time (**Figure 7.6**). After the initial (over 4-month) positive priming of biochar-C that increased with increasing LOM input; there was a negative priming at about 4-month for the 1% LOM treatment, which remained negative for both

biochars until the termination of the experiment. The positive priming of biochar-C in the 2% LOM treatment changed to no priming for the 450 and 550 °C biochar after approximately 6 months of incubation. After the 6 months, the no priming effect of LOM on biochar changed to positive priming in the case of 450 °C biochar and remained close to no priming for the 550 °C biochar treatment. For the 4% LOM treatments, the positive priming of biochar-C was sustained for the two biochars over the whole incubation period; however, the uncertainty was quite large in the measurements. In term of the biochar treatments, there was no significant difference in the priming effect of LOM on biochar-C mineralisation between the 450 and 550 °C biochars.

The direction and magnitude of priming were different for the lower (≤ 1%) and higher (≥ 2%) application rate of LOM. In the 0% and 1% LOM treatments, the biochars showed a positive priming effect on the LOM-C mineralisation + native soil C mineralisation over time (**Figure 7.7**), whereas for the 2 and 4% LOM treatments, the negative priming effect sustained over the whole incubation period. The negative priming effect was enhanced when the LOM application rate was increased from 2% to 4%. Since native soil C content (0.45%) was small, the priming effect may be mainly attributed to LOM-C mineralisation, particularly at 4% LOM rate. The magnitude of the priming effect of biochar on the native SOC and/or LOM-C mineralisation was relatively stable from 4 to 25 months in all treatments, except for the 1% LOM treatment where the negative priming effect was changed to positive priming after 10 months and 18 months in the 450 and 550 °C biochar, respectively. There was no significant difference in the priming effect of the 450 and 550 °C biochar on the native soil C and LOM-C mineralisation.

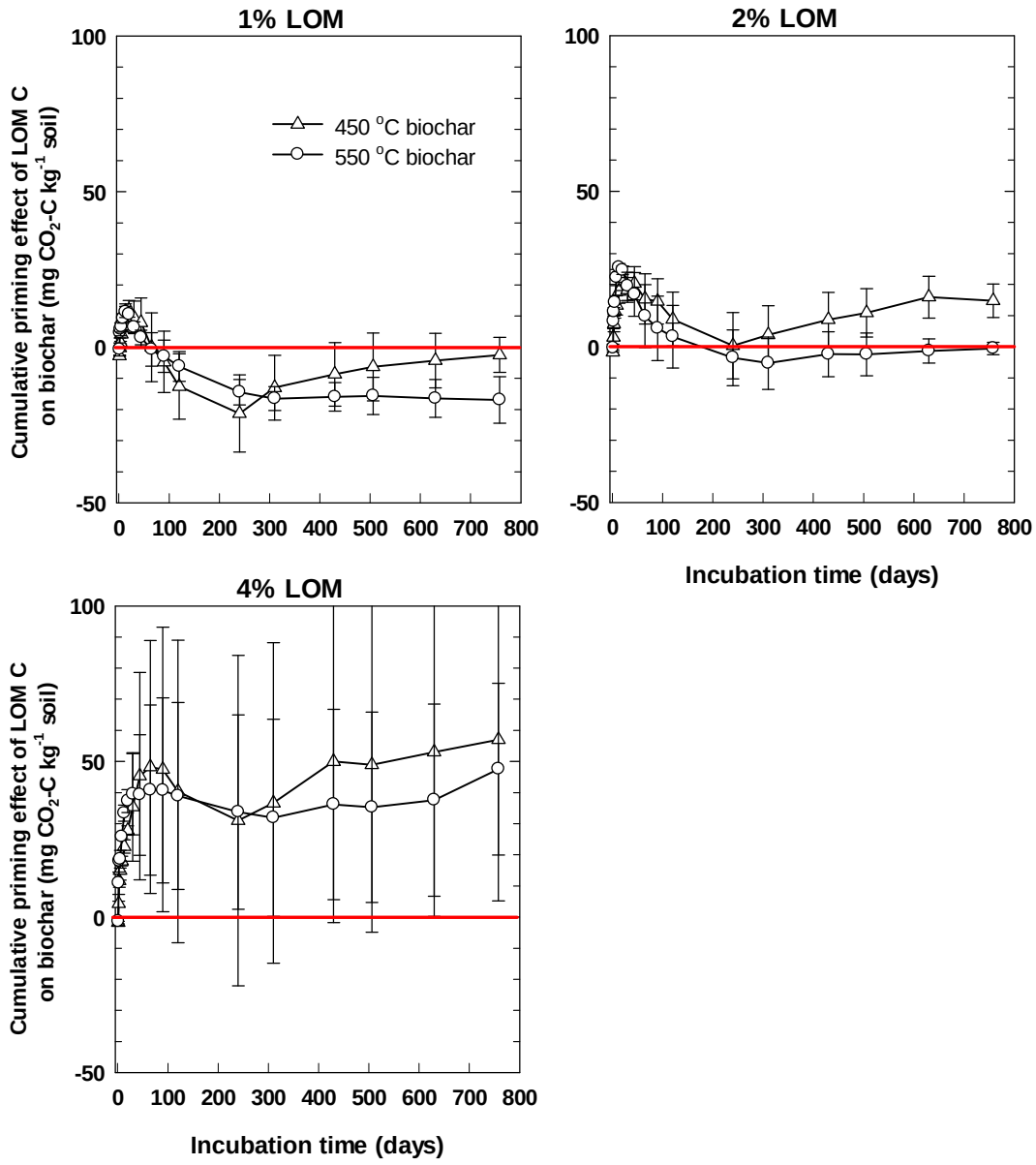

Figure 7.6. The cumulative priming effect of the LOM on the mineralisation of biochar-C during the 2.1-year incubation period. Triangle and circle represent the 450 and 550 °C biochar treatment, respectively. Error bars represent the standard error of the mean (n = 3).

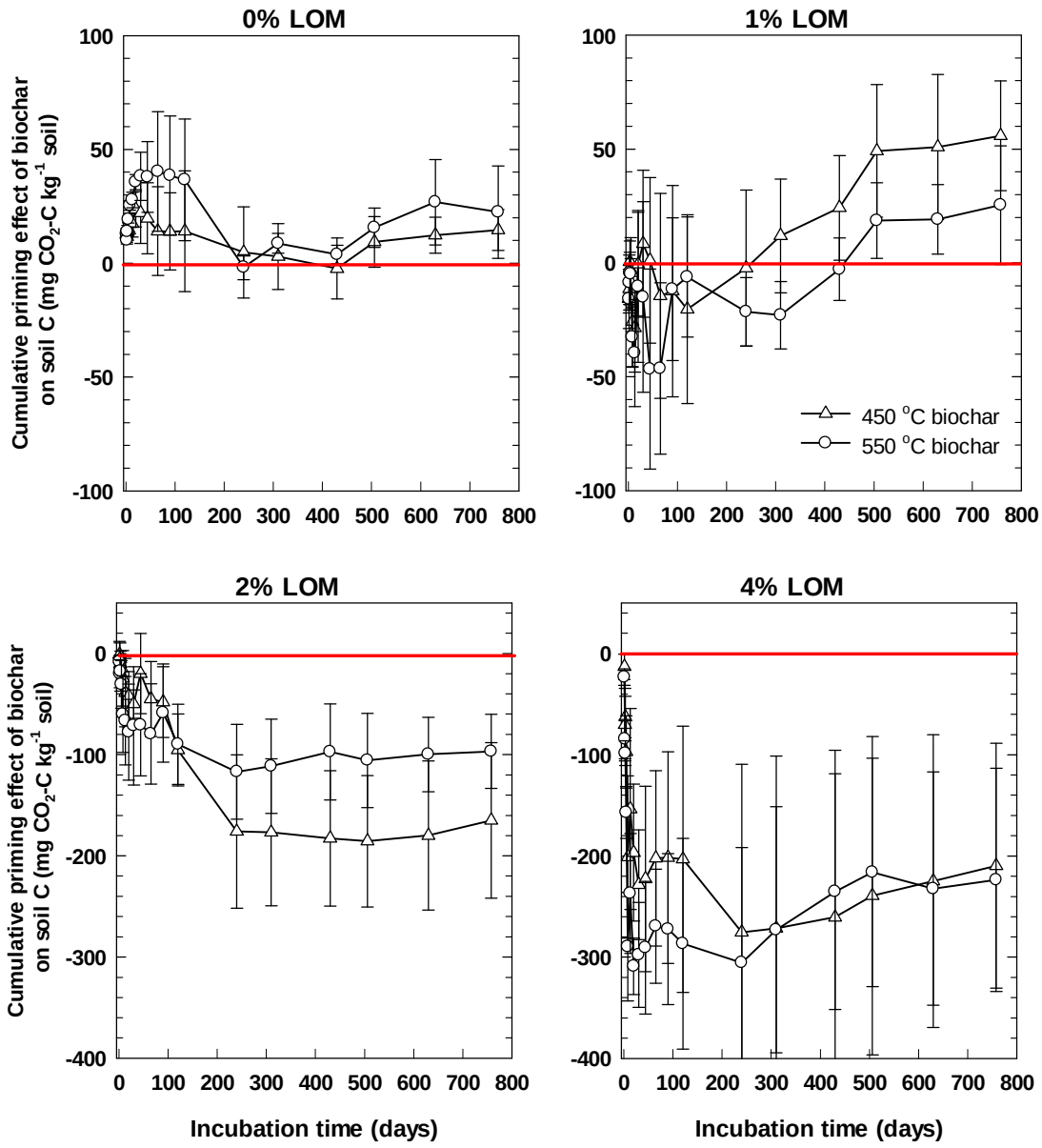

Figure 7.7. The cumulative priming effect of the biochars on the mineralisation of native soil carbon or native soil C plus LOM-C, during the 2.1-year incubation period. Triangle and circle represent the 450 and 550 °C biochar treatment, respectively. Error bars represent the standard error of the mean (n = 3).

7.3.4. Effect of biochar and LOM on microbial community structure

Table 7.3 shows the main characteristics of T-RFLP datasets of all samples with different combination of LOM and biochar treatments. Bacterial and fungal T-RFLP analysis yielded a total of 443 and 226 distinct T-RFs, respectively. T-RF richness

was higher for bacteria than fungi, with average at 131.3 and 67.7, respectively. Beta diversity was 3.2 and 2.4 in bacterial and fungal T-RFs, respectively.

Table 7.3. Characteristics of T-RFLP datasets of all samples with different combination of LOM and biochar treatments**.**

	Total T-RFs	**Richness (range)**	**Beta diversity**	**% empty data cells**
Bacteria	443	131.3 (64,185)	3.2	76.1
Fungi	226	67.7 (30,111)	2.4	70.1

The cluster analysis of the T-RFs in each sample resulted in a dendogram that revealed clustering, or similarity, between the bacterial communities associated with different treatments. The cluster analysis of peak height in bacterial and fungal communities revealed three and two main clusters, respectively. However, there was no clear pattern for different biochar and LOM treatments in the clusters (see Appendix 7). Each cluster was comprised of communities from different LOM and biochar treatments or replications. The cluster analysis of peak appearance and absence in bacterial and fungal communities showed no obvious cluster. Non-metric MDS analysis of the microbial community structure showed that there were no significant differences between LOM rates and biochar treatments (see Appendix 7).

Additive main effects and multiplicative interaction (AMMI) measures variation caused by the interaction between T-RFs and treatments, it can tease out trends in the data that are otherwise masked by T-RF variability. **Table 7.4** shows the distribution of variation within the T-RFLP datasets from ANOVA. Bacteria had the main effects variation of 58.8% and 80.4% in binary and peak height, respectively. The interaction effects were 41.2% and 19.6% in binary and peak height, respectively. In contrast, fungal communities had the main effects variation of 77.1% and 77.8% and the interaction effects of 22.9% and 25.2% in binary and peak height, respectively. The main source of variation in the dataset was due to variation in T-RF diversity between samples. This is a typical characteristic of T-RFLP datasets and has the potential to mask trends in the dataset resulting from differences between experimental treatments. In the **Table 7.4**, it can be seen that for interaction effects a high signal to noise ratio was obtained when using peak height data and this effect was diminished in the binary (presence/absence) data. Hence, peak height data was used for all subsequent analyses.

Table 7.4. The variation (%) in T-RFLP datasets as determined by the analysis of variance.

	Main Effects (%)			Interaction effects (%)		
Target	Total	T-RFs	Environments	Total	Signal	Noise
Bacteria						
Binary	58.8	57.8	1.0	41.2	8.2	33.0
Height	80.4	80.4	0	19.6	14.0	5.6
Fungi						
Binary	77.1	75.5	1.6	22.9	3.1	19.8
Height	74.8	74.8	0	25.2	20.3	4.9

The values are percentages based on the three T-RFLP data types: binary (presence/absence), height (relativised peak height) and area (relativised peak area). The main and interaction effects make up the two main sources of variation within the T-RFLP dataset. The main effects are a subtotal for the T-RFs and Environments. Similarly, the interaction effects are a subtotal for both interaction signal and interaction noise.

The community structures of bacteria, based on T-RFLP analysis, are displayed using AMMI (**Figure 7.8a**). The bacterial community shift did not respond to the addition of biochar but responded to the addition of LOM. The addition of LOM led to a bacterial community shift along IPC 1 which explained 69.0% of the variance. The bacterial community showed a significant shift with the addition of LOM relative to the treatments without LOM addition (i.e. 0% LOM).

The community structures of fungi using AMMI are displayed in **Figure 7.8b**. In the 0% LOM treatments and original soil, we could not extract DNA for fungal T-RFLP analysis. The first two principal components (IPC 1 and 2) explained 85.8% and 6.91% variance, respectively. The fungal community shift did not respond to the biochar addition. The addition of LOM significantly affected the community structures of fungi in terms of IPC 1. The fungal community structures were significantly changed when the LOM application rate was increased to 4%.

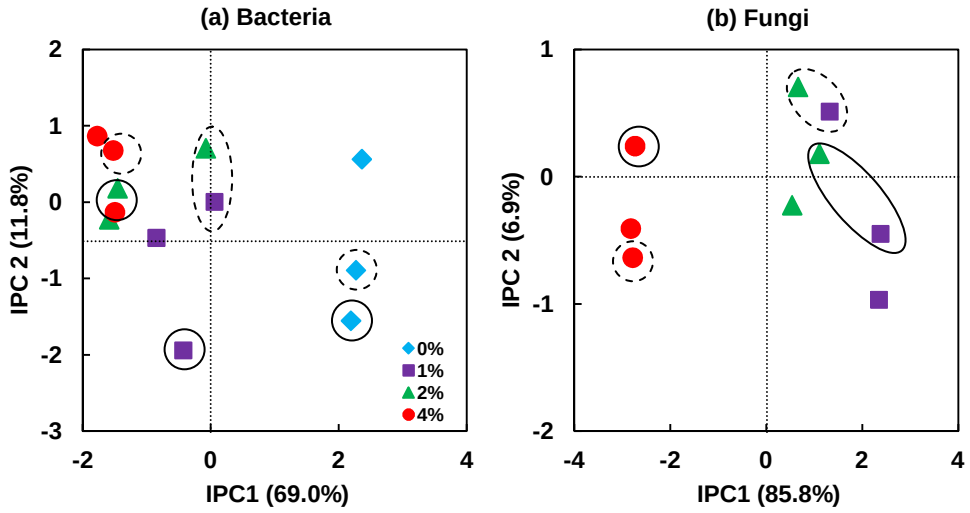

Figure 7.8. The ordinations of T-RFLP profiles with double-centred principle components. The AMMI analysis of (a) bacterial communities and (b) fungal communities, present in the soil with 0, 1, 2 or 4% LOM and biochar treatments. Symbols with non-circles, dotted line circled and solid line circled represent no biochar, the 450 and 550 °C biochar treatment, respectively.

7.4. Discussion

7.4.1. Biochar-C mineralisation and mean residence time

The proportion of wood biochars C mineralised over 2.1-year period (0.6−1.7%) was similar to that of the plant-based biochars (400 and 550 °C) over 2-year (0.4−1.4%) incubated in the same Vertisol (Singh et al., 2012). Moreover, the proportion of biochar-C mineralised in the present study was also similar to that of the same wood biochars C mineralised (0.4−1.5%) in different soils (Vertisol, Inceptisol, Entisol and Oxisol) over the 2-year incubation period (Chapter 4).

To the best of our knowledge, this is the first long-term study that has provided the information on the MRT of wood biochar-C in soil supplemented with different levels of LOM. The longer MRT of biochar in the control (0% LOM) than in the presence of LOM treatments (1, 2, and 4%) (**Table 7.2**) suggests that the input of plant-derived C (such as plant litter or root exudates) could reduce the longevity of biochar-C under natural field conditions and it should be considered in estimating the MRT of biochars. Despite the decrease in the MRT of biochar-C, the MRT of

biochar-C was still over several hundred years. The two end-member mixing model assumes that the $\delta^{13}C$ values of CO_2 evolved from soil C + LOM in the biochar-amended soil to be the same as to the control treatment (soil C + LOM without biochar). However, LOM has a slightly enriched $\delta^{13}C$ values (-12.7‰) than soil C (-14.3‰). Thus in a scenario where biochar presence would increase LOM contribution to the respired CO_2, the model will underestimate the extent of biochar-C mineralisation. This pattern will be reversed if biochar presence would decrease LOM contribution to the respired CO_2. Assuming 5–6% variation in the LOM contribution to the respired CO_2 in the presence of biochar, biochar-C mineralisation may vary by 3% relative to a scenario where no impact of biochar on LOM contribution was considered in the two-end member mixing model (see Table A6.2. in Appendix 6).

The duration of the incubation period influences the estimates of biochar MRT, which is indicated by much longer MRT of both biochars (314−713 years for the 450 °C biochar, and 567−978 years for the 550 °C biochar) in this study (2.1-year) compared to the estimates obtained from the short-term biochar-C mineralisation results reported earlier (62−112 years for the 450 °C biochar, and 100−248 years for the 550 °C biochar) (Keith et al., 2011). Similarly, Singh et al. (2012) also showed that the MRT values of biochars increased from 47−1054 to 87−1982 years with increasing incubation period from 6-months to 2-years. The MRT values estimated from shorter incubation data are likely to be biased towards labile C components, whereas data from longer incubation experiments include more data points that may better represent the recalcitrant C component of biochar. Thus, the inclusion of additional data points with longer incubation time is likely to provide more robust estimates of biochar MRT than estimated from shorter incubation periods.

7.4.2. The priming effect of biochar on LOM mineralisation

In agreement with the data from the short-term study (Keith et al., 2011) and the study using an aged biochar-amended soil (Liang et al., 2008), our results show that over a longer incubation period, there was a negative priming effect of biochar on LOM-C mineralisation, which increased with the increasing application rate of LOM. The negative priming effect may be attributed to several reasons. Firstly, biochar has a pore structure with large surface area which can absorb LOM (Lehmann et al., 2005; Miura et al., 2007; Pignatello et al., 2006). But the adsorption capacity of

biochar to LOM may decrease with time due to the pore blockage by organic matter (Kwon and Pignatello, 2005). This may lead to a plateau in the magnitude of the negative priming effect as observed after 4 months. Secondly, the presence of biochar and LOM can promote interactions between biochar, organic matter and soil minerals, leading to the formation of relatively stable organo-mineral entities, therefore protecting organic matter in soil from microbial attack (Brodowski et al., 2006; Liang et al., 2010). Likewise, the surface oxygen functional groups on biochar (i.e. carboxyl functional groups) that develop during oxidation with ageing in soil (Hilscher and Knicker, 2011; Lehmann et al., 2005), may interact with hydroxyl groups on the edges of phyllosilicates via ligand exchange process (von Lützow et al., 2006).

7.4.3. Effect of biochar and LOM on microbial community structure

In this study, biochar exerted no influence on soil bacterial and fungal communities in contrast to the findings from other short-term studies where biochar addition to soils induced a shift in soil microbial communities (Farrell et al., 2013; O'Neill et al., 2009; Santos et al., 2012). Graber et al. (2010) hypothesised that the low concentrations of residual organic tars (e.g. ethylene glycol, propylene glycol and hydroxyl-propionic) in biochar can promote microbial growth and population diversity in soil. Biochar was found to stimulate the growth of saprophytic fungal communities (Farrell et al., 2013; Steinbeiss et al., 2009) and also mycorrhizal fungi (arbuscular [AM] and ectomycorrihizal [EM]) (Warnock et al., 2007). According to Farrell et al. (2013), the labile C in biochar, which mineralises rapidly after the addition of biochar to soil, may contribute to the changes in soil microbial community. In the present study, a significant proportion of the labile biochar-C component may have been depleted over the 2.1-year incubation period, possibly resulting in the disappearance of any short-term changes in the microbial community between the biochar and the control treatments. The observed changes in the microbial community in some recent biochar studies (Farrell et al., 2013; O'Neill et al., 2009; Santos et al., 2012) could be partially attributed to the increased pH after the addition of biochar in acidic soils (pH: 4.2−5.8). Changes in soil pH has been suggested to influence the substrate utilisation patterns of the microbial communities (Pietikäinen et al., 2000). However, small increases in soil pH (0.06–0.21 pH unit, Table A6.4) with the addition of the two biochars (i.e. 450 and 550°C) in the Vertisol

with different LOM treatments may not have produced any effect on the soil microbial communities. These results are different to the observations from previous studies (Farrell et al., 2013; O'Neill et al., 2009; Pietikäinen et al., 2000; Santos et al., 2012)

The soil microbial community structure was influenced by the application rate of LOM in this study (**Figure 7.8**), which is consistent with the observed shift in microbial community structure from increasing of application rates of an organic amendment, such as poultry litter, in a cultivated soil (Acosta-MartÃnez and Harmel, 2006). Similarly, Griffiths et al. (1999) reported that the microbial community structure changed consistently as substrate, such as glucose, fructose and other compound loading rates increased, resulting in fungal-dominated microbial communities at high substrate loading rates. Although fungal and bacterial biomass were not quantified in the present study, the undetected fungal DNA in the non-LOM treatment and the greatly different fungal communities in the 4% LOM treatments partially reveal the varied fungal biomass with increasing LOM input in the soil. The changes in fungal community structure could be potentially attributed to the increased soil pH with increasing addition of LOM treatments. The increase in soil pH (compared to the control) ranged from 0.43–0.51, 0.67–0.81, 0.81–1.0 pH unit with 1, 2 and 4% LOM treatment, respectively (Table A6.4).

7.4.4. Microbial community structure and priming effect

The detected fungal DNA in the soil with LOM addition and the negative priming in the higher (2 and 4%) LOM application rate treatments suggest that the stimulated fungal community growth could contribute to the greater negative priming effect of biochar on LOM-C mineralisation in 2 and 4% LOM treatments. This stabilisation or decrease of LOM-C mineralisation (relative to the control) could be due to the enhancement of soil aggregation and aggregate stability induced by stimulated fungal growth (Rillig and Mummey, 2006; Tisdall and Oades, 1982; Wright and Upadhyaya, 1998). The presence of biochar did not change fungal community but it may continue to utilise biochar-C therefore decreasing the consumption of LOM in aggregates. On the other hand, there was a significant difference in the fungal communities at 4% compared to 1 and 2% LOM application rates. It is possible that the fungal communities shifted to a structure which can degrade relatively recalcitrant C forms

at higher LOM application rates and therefore causing and sustaining the positive priming of biochar-C mineralisation at 4% LOM treatment (**Figure 7.6**).

The undetected fungal DNA in the soil with 0% LOM addition suggested that there was a lack of fungal growth in the soil and consequently the lack of fungal-induced soil aggregation for protecting soil C from mineralisation. Moreover, the bacterial-dominated microbial communities are associated with higher rates of CO_2 respiration compared to fungal-dominated microbial communities (Six et al., 2006). Hence these two mechanisms may have contributed to the positive priming effect in the 0% LOM treatment.

7.4.5. Implications for C sequestration

Our results provide support that biochars produced through slow pyrolysis at 450 and 550 °C can provide long-term C storage benefit, even in the presence of LOM. The MRT estimated for biochars with LOM application were in the range of a few centuries. The MRT of biochars decreased with the addition of LOM, consistent with the observed increase in mineralisation of biochar-C. Biochar showed a positive priming effect on the LOM-C mineralisation at low LOM rates, e.g. 0% and 1%. However, a negative priming effect of biochar on LOM-C mineralisation occurred at higher application rates of LOM (2 to 4%), suggesting a further enhancement in the biochar-C sequestration potential in clayey soils receiving organic matter input. The addition of biochar did not change microbial community structure in the Vertisol after the long-term incubation period, whereas the addition of LOM induced changes in the structure of microbial communities in the soil, possibly contributing to the negative priming effect of biochar on LOM-C mineralisation, and to the positive priming of biochar. Further research evaluating specific fungal community structures and their role in the degradation of biochar in the presence of LOM is warranted to underpin the C sequestration potential of biochar in soil.

7.5. References

Abdo, Z., Schuette, U.M.E., Bent, S.J., Williams, C.J., Forney, L.J., Joyce, P., 2006. Statistical methods for characterizing diversity of microbial communities by

analysis of terminal restriction fragment length polymorphisms of 16S rRNA genes. Environmental Microbiology 8, 929-938.

Acosta-MartÃnez, V., Harmel, R.D., 2006. Soil microbial communities and enzyme activities under various poultry litter application rates. Journal of Environmental Quality 35, 1309-1318.

Barton, C.V.M., Ellsworth, D.S., Medlyn, B.E., Duursma, R.A., Tissue, D.T., Adams, M.A., Eamus, D., Conroy, J.P., McMurtrie, R.E., Parsby, J., Linder, S., 2010. Whole-tree chambers for elevated atmospheric CO_2 experimentation and tree scale flux measurements in south-eastern Australia: The Hawkesbury Forest Experiment. Agricultural and Forest Meteorology 150, 941-951.

Brodowski, S., John, B., Flessa, H., Amelung, W., 2006. Aggregate-occluded black carbon in soil. European Journal of Soil Science 57, 539-546.

Cheng, C.H., Lehmann, J., Thies, J.E., Burton, S.D., Engelhard, M.H., 2006. Oxidation of black carbon by biotic and abiotic processes. Organic Geochemistry 37, 1477-1488.

Cross, A., Sohi, S.P., 2011. The priming potential of biochar products in relation to labile carbon contents and soil organic matter status. Soil Biology & Biochemistry 43, 2127-2134.

Culman, S.W., Bukowski, R., Gauch, H.G., Cadillo-Quiroz, H., Buckley, D.H., 2009. T-REX: software for the processing and analysis of T-RFLP data. Bmc Bioinformatics 10, 171.

Fang, Y., Singh, B., Singh, B.P., Krull, E., 2014. Biochar carbon stability in four contrasting soils. European Journal of Soil Science, 65, 60–71.

Farrell, M., Kuhn, T.K., Macdonald, L.M., Maddern, T.M., Murphy, D.V., Hall, P.A., Singh, B.P., Baumann, K., Krull, E.S., Baldock, J.A., 2013. Microbial utilisation of biochar-derived carbon. Science of the Total Environment, in press.

Glaser, B., Haumaier, L., Guggenberger, G., Zech, W., 2001. The 'Terra Preta' phenomenon: a model for sustainable agriculture in the humid tropics. Naturwissenschaften 88, 37-41.

Graber, E.R., Harel, Y.M., Kolton, M., Cytryn, E., Silber, A., David, D.R., Tsechansky, L., Borenshtein, M., Elad, Y., 2010. Biochar impact on development and productivity of pepper and tomato grown in fertigated soilless media. Plant and Soil 337, 481-496.

Griffiths, B.S., Ritz, K., Ebblewhite, N., Dobson, G., 1999. Soil microbial community structure: Effects of substrate loading rates. Soil Biology & Biochemistry 31, 145-153.

Hamer, U., Marschner, B., Brodowski, S., Amelung, W., 2004. Interactive priming of black carbon and glucose mineralisation. Organic Geochemistry 35, 823-830.

Hammer, Ø., Harper, D.A.T., Ryan, P.D., 2001. PAST: paleontological statistics software package for education and data analysis. Palaeontologia Electronica 4, 9pp.

Herath, H.M.S.K., Camps-Arbestain, M., Hedley, M., 2013. Effect of biochar on soil physical properties in two contrasting soils: An Alfisol and an Andisol. Geoderma 209-210, 188-197.

Hilscher, A., Knicker, H., 2011. Carbon and nitrogen degradation on molecular scale of grass-derived pyrogenic organic material during 28 months of incubation in soil. Soil Biology & Biochemistry 43, 261-270.

Keith, A., Singh, B., Singh, B.P., 2011. Interactive priming of biochar and labile organic matter mineralization in a smectite-rich soil. Environmental Science & Technology 45, 9611-9618.

Knicker, H., Gonzalez-Vila, F.J., Gonzalez-Vazquez, R., 2013. Biodegradability of organic matter in fire-affected mineral soils of Southern Spain. Soil Biology & Biochemistry 56, 31-39.

Kolb, S.E., Fermanich, K.J., Dornbush, M.E., 2009. Effect of charcoal quantity on microbial biomass and activity in temperate soils. Soil Science Society of America Journal 73, 1173-1181.

Kuzyakov, Y., Friedel, J.K., Stahr, K., 2000. Review of mechanisms and quantification of priming effects. Soil Biology & Biochemistry 32, 1485-1498.

Kuzyakov, Y., Subbotina, I., Chen, H.Q., Bogomolova, I., Xu, X.L., 2009. Black carbon decomposition and incorporation into soil microbial biomass estimated by ^{14}C labeling. Soil Biology & Biochemistry 41, 210-219.

Kwon, S., Pignatello, J.J., 2005. Effect of natural organic substances on the surface and adsorptive properties of environmental black carbon (char): Pseudo pore blockage by model lipid components and its implications for N_2-probed surface properties of natural sorbents. Environmental Science & Technology 39, 7932-7939.

Lehmann, J., Joseph, S., 2009. Biochar for environmental management: Science and technology. Earthscan, London.

Lehmann, J., Liang, B.Q., Solomon, D., Lerotic, M., Luizao, F., Kinyangi, J., Schafer, T., Wirick, S., Jacobsen, C., 2005. Near-edge X-ray absorption fine structure (NEXAFS) spectroscopy for mapping nano-scale distribution of organic carbon forms in soil: Application to black carbon particles. Global Biogeochemical Cycles 19, GB1013.

Lehmann, J., Rillig, M.C., Thies, J., Masiello, C.A., Hockaday, W.C., Crowley, D., 2011. Biochar effects on soil biota - A review. Soil Biology & Biochemistry 43, 1812-1836.

Liang, B., Lehmann, J., Solomon, D., Sohi, S., Thies, J.E., Skjemstad, J.O., Luizao, F.J., Engelhard, M.H., Neves, E.G., Wirick, S., 2008. Stability of biomass-derived black carbon in soils. Geochimica Et Cosmochimica Acta 72, 6069-6078.

Liang, B.Q., Lehmann, J., Sohi, S.P., Thies, J.E., O'Neill, B., Trujillo, L., Gaunt, J., Solomon, D., Grossman, J., Neves, E.G., Luizão, F.J., 2010. Black carbon affects the cycling of non-black carbon in soil. Organic Geochemistry 41, 206-213.

Luo, Y., Durenkamp, M., De Nobili, M., Lin, Q., Brookes, P.C., 2011. Short term soil priming effects and the mineralisation of biochar following its incorporation to soils of different pH. Soil Biology & Biochemistry 43, 2304-2314.

Meidute, S., Demoling, F., Baath, E., 2008. Antagonistic and synergistic effects of fungal and bacterial growth in soil after adding different carbon and nitrogen sources. Soil Biology & Biochemistry 40, 2334-2343.

Miura, A., Shiratani, E., Yoshinaga, I., Hitomi, T., Hamada, K., Takaki, K., 2007. Characteristics of the adsorption of dissolved organic matter by charcoals carbonized at different temperatures. Jarq-Japan Agricultural Research Quarterly 41, 211-217.

MO BIO Laboratories Inc., PowerSoil®DNA Isolation Kit - Instruction Manual. http://www.mobio.com/images/custom/file/protocol/12888.pdf, (cited 5 August, 2013).

O'Neill, B., Grossman, J., Tsai, M.T., Gomes, J.E., Lehmann, J., Peterson, J., Neves, E., Thies, J.E., 2009. Bacterial community composition in Brazilian anthrosols

and adjacent soils characterized using culturing and molecular identification. Microbial Ecology 58, 23-35.

Pietikäinen, J., Kiikkilä, O., Fritze, H., 2000. Charcoal as a habitat for microbes and its effect on the microbial community of the underlying humus. Oikos 89, 231-242.

Pignatello, J.J., Kwon, S., Lu, Y., 2006. Effect of natural organic substances on the surface and adsorptive properties of environmental black carbon (char): Attenuation of surface activity by humic and fulvic acids. Environmental Science & Technology 40, 7757-7763.

Rillig, M.C., Mummey, D.L., 2006. Mycorrhizas and soil structure. New Phytologist 171, 41-53.

Rousk, J., Baath, E., 2007. Fungal and bacterial growth in soil with plant materials of different C/N ratios. FEMS Microbiology Ecology 62, 258-267.

Santos, F., Torn, M.S., Bird, J.A., 2012. Biological degradation of pyrogenic organic matter in temperate forest soils. Soil Biology & Biochemistry 51, 115-124.

Singh, B.P., Cowie, A.L., Smernik, R.J., 2012. Biochar carbon stability in a clayey soil as a function of feedstock and pyrolysis temperature. Environmental Science & Technology 46, 11770-11778.

Six, J., Frey, S.D., Thiet, R.K., Batten, K.M., 2006. Bacterial and fungal contributions to carbon sequestration in agroecosystems. Soil Science Society of America Journal 70, 555-569.

Smith, C.J., Danilowicz, B.S., Clear, A.K., Costello, F.J., Wilson, B., Meijer, W.G., 2005. T-Align, a web-based tool for comparison of multiple terminal restriction fragment length polymorphism profiles. FEMS Microbiology Ecology 54, 375-380.

Steinbeiss, S., Gleixner, G., Antonietti, M., 2009. Effect of biochar amendment on soil carbon balance and soil microbial activity. Soil Biology & Biochemistry 41, 1301-1310.

Tisdall, J.M., Oades, J.M., 1982. Organic-matter and water-stable aggregates in soils. Journal of Soil Science 33, 141-163.

von Lützow, M., Kögel-Knabner, I., Ekschmitt, K., Matzner, E., Guggenberger, G., Marschner, B., Flessa, H., 2006. Stabilization of organic matter in temperate soils: mechanisms and their relevance under different soil conditions - a review. European Journal of Soil Science 57, 426-445.

VSN International, 2011. GenStat for Windows 14th Edition. Hemel Hempstead, UK: VSN International.

Warnock, D.D., Lehmann, J., Kuyper, T.W., Rillig, M.C., 2007. Mycorrhizal responses to biochar in soil - concepts and mechanisms. Plant and Soil 300, 9-20.

Woolf, D., Amonette, J.E., Street-Perrott, F.A., Lehmann, J., Joseph, S., 2010. Sustainable biochar to mitigate global climate change. Nature Communications 1, 56.

Wright, S.F., Upadhyaya, A., 1998. A survey of soils for aggregate stability and glomalin, a glycoprotein produced by hyphae of arbuscular mycorrhizal fungi. Plant and Soil 198, 97-107.

Zimmerman, A.R., 2010. Abiotic and microbial oxidation of laboratory-produced black carbon (biochar). Environmental Science & Technology 44, 1295-1301.

Zimmerman, A.R., Gao, B., Ahn, M.Y., 2011. Positive and negative carbon mineralization priming effects among a variety of biochar-amended soils. Soil Biology & Biochemistry 43, 1169-1179.

Zimmermann, M., Bird, M.I., Wurster, C., Saiz, G., Goodrick, L., Barta, J., Capek, P., Santruckova, H., Smernik, R., 2012. Rapid degradation of pyrogenic carbon. Global Change Biology 18, 3306–3316.

Chapter 8: Summary and future research

The research presented in this thesis evaluates the long-term carbon (C) storage potential of biochar in contrasting Australian soils. The research has provided robust estimates of biochar-C stability through laboratory incubation experiments conducted over 2 years under controlled conditions. Biochar-C stability estimates ranged from decadal to millennia timescales (Chapter 3), which are consistent with the range reported in the literature (Chapter 2). In addition to the pyrolysis temperature, biochar-C stability was found to be influenced by soil properties, such as native soil C content, clay content and clay mineralogy (Chapter 3 and Chapter 4). The temperature sensitivity of the biochars was only influenced by soil properties but not by the pyrolysis temperature of biochars (Chapter 5). The research shows that biochar-C stability estimates change with the incubation period at 20 °C, with the 2-year incubation data providing a more realistic estimate of the mean residence time (MRT) of biochar than the 1-year data (Chapter 4). NEXAFS and XPS analyses of carbon functional groups of the light fraction (< 1.8 g cm^{-3}) of control and biochar amended soil (fresh and aged for 1 and 2 years) did not show any change after incubation for 1 year at 20, 40 and 60 °C (Chapter 6). Furthermore, the research has shown that biochar can influence the mineralisation of native soil organic carbon (SOC) in different soils at different temperatures, with positive to negative priming effects observed in different systems (Chapter 4). Similarly, biochar can also produce variable priming effects on added labile organic matter (LOM). Conversly, the mineralisation of biochar-C can also be negatively or positively primed by the addition of LOM, depending on the application rate of LOM (Chapter 7). The interactive priming effects on C mineralisation in the biochar-amended soils can have implications for the C storage potential of biochar in soil. Further details on the findings of this thesis are summarised below.

Wood biochars (450 and 550 °C) showed high stability in four constrasting soils (Inceptisol, Entisol, Oxisol and Vertisol), with the proportion of added biochar-C mineralised ranged from 0.30−1.14% at 20 °C and 0.97−2.71% at 40 °C over a 1-year incubation period (Chapter 3). Upon extending the incubation experiment to two years, the proportion of added biochar-C mineralised increased to 0.43−1.50% at

20 °C and 1.40−5.19% at 40 °C (Chapter 4). By comparison with 20 and 40 °C, the proportion of biochar-C mineralised was significantly greater at 60 °C, with 2.31−10.58% C mineralised over the 2-year period. MRT of biochars estimated based on the 1-year data ranged from 218−610 years at 20°C and 44−178 years at 40 °C (Chapter 3). The estimated MRT based on 2-year data ranged from 341−1061 years, 41−451 years and 25−127 years at 20, 40 °C and 60 °C, respectively (Chapter 4). The estimated MRT from the 2-year data has been considered to be more realistic than the 1-year data for 20 °C because of greater representation of relatively recalcitrant C pools in the biochar-C mineralisation data used for fitting a two-pool exponential model. However, at elevated temperature, i.e. 40 °C, the MRT of biochars did not change after 1-year, so the short-term may be adequate for determining biochar-C MRT at higher temperature (Chapter 4).

Biochar was more stable when it was produced by slow pyrolysis at 550 °C than at 450 °C. For example, between 0.43 and 3.28% of the added biochar-C was mineralised in the 550 °C biochar amended soils, whereas between 0.80 and 10.58% of the biochar-C was mineralised in the 450 °C biochar amended soils over the 2-year period (Chapter 4). The wood biochar produced at 550 °C, it is possible to sequester C in soil over a century or more even at elevated temperatures (40 or 60 °C) (Chapter 4). Soil characteristics appear to play an important role in influencing the biochar-C stability, especially for the lower (450 °C) temperature biochar. When biochar-C mineralised data were normalised on per unit of the initial native SOC content, the mineralisation of biochar-C occurred in the order of Oxisol < Entisol ≤ Vertisol < Inceptisol. The smallest biochar-C mineralisation in the Oxisol could be due to relatively strong biochar-soil mineral interactions with the variable charged minerals (e.g. hematite, goethite, gibbsite and kaolinite), as compared to relatively weak interactions with the permanent charged phyllosilicates (smectitie and illite) in the other two soils with clay contents > 21.5 %. In this study, the soils used did not have systematic variations in physical and chemical properties, such as, clay content, clay mineralogy, pH and SOC content, which can all influence biochar-C mineralisation. Because of the confounding influences of various soil properties, it was not possible to isolate the effect of a specific soil characteristic on biochar-C mineralisation. Nevertheless, this study provided useful insights into the role of soil characteristics in influencing biochar-C stability. Further studies using soils with a clear gradient in a

single soil property (e.g. organic C or clay content or clay mineral) are required to fully assess the role of a particular soil property in the long-term storage of biochar-C in soil.

In the sandy clayey loam (Entisol) and clayey soils (Oxisol and Vertisol), mineralisation of native SOC was generally suppressed in the presence of biochar (Chapter 4). The interactions between biochar, native SOC and clay minerals were hypothesised to result in an overall increased stabilisation of native SOC. Mineralisation of native SOC in the sandy soil (Inceptisol) was stimulated by biochar addition. In the sandy soil, although there was a positive priming effect initially, the positive priming effect was subsided over time, possibly due to the depletion of labile C components in biochars. Overall, the results suggested that the application of biochar in soil can stabilise native SOC or it does not greatly increase native SOC mineralisation over a longer period, particularly in the presence of clay minerals. Therefore, it can be concluded that the C sequestration potential of biochar would be enhanced in mineral soils due to biochar induced stabilisation of native SOC. In the 2-year incubation study, the results showed that the 550 °C biochar induced a greater stabilisation of native SOC than the 450 °C biochar at 20 and 40 °C (Chapter 4). The incubation temperature had no significant influence on the magnitude of the cumulative priming effect. Considering the two benefits of the 550 °C biochar application to the mineral soils (i.e. greater native SOC stabilisation as well as greater biochar-C stability), wood biochar produced at 550 °C by slow pyrolysis was more effective for long-term C storage in soil relative to the biochar produced at 450 °C.

Although biochar-C mineralisation was significantly greater in the 450 °C biochar than the 550 °C biochar, the two biochars had a similar temperature sensitivity (Q_{10}) (Chapter 5). Moreover, biochars had either smaller or similar Q_{10} relative to native SOC. The presence of biochar decreased Q_{10} of native SOC in the Entisol, Vertisol and Inceptisol. These results addressed the knowledge gap on the temperature senstivity of biochar-C in contrasting soils, including the influence of biochar on native SOC Q_{10}. The Q_{10} of biochar-C was significantly ($p < 0.001$) affected by soil type. For example, Q_{10} of biochar-C were the greatest values in the Vertisol, followed by Inceptisol and Entisol, and the smallest values occurred in the Oxisol at 20−40 °C. The smallest Q_{10} for biochar-C in the Oxisol could be due to relatively strong biochar-soil mineral interactions, which stabilised biochar-C and

decreased its utilisation by soil microbial communities. However, this research did not distinguish the extent of utilisation and mineralisation of biochar by soil microbial communities, relative to abiotic processes, particularly at higher incubation temperatures. Futher research is needed about the influence of soil microbial community versus abiotic processes on biochar-C mineralisation in soil at different temperatures.

The light fraction of the soil amended with the higher-temperature biochar (550 °C) showed a greater proportion of the aromatic C than the light fraction from the soil amended with the lower-temperature biochar (450 °C). After one year of ageing (oxidation) in the soils, NEXAFS and XPS analyses did not consistent change in the C functional group of the light fraction separated from biochar amended soils. This could be due to the mixing of native soil C with the biochar-C in the light fraction, masking any difference in the aromatic C between the fresh and aged biochar samples. However, the XPS analysis of hand-picked biochar samples showed increased oxidation with increasing ageing time and the increasing incubation temperature. These data suggest that the mixed biochar and native soil C light fractions may mask the detection of small amounts of carboxylic functional groups on biochar surfaces that may develop during 1-year ageing. Due to similarities in the spectral features of the biochar and native C it is difficult to determine the changes in biochar-C in the light fraction of biochar amended soils. In the future studies, hand-picked biochar samples representing a range of particle sizes should be analysed, using both NEXAFS and XPS, to determine their C functional groups. There were substantial overlaps between the peaks of various C groups in the spectra of both NEXAFS and XPS, and thus there are limitations in the quantitative analysis of the C functional groups using these techniques. Another spectroscopic techniques, such as nuclear magnetic resonance (NMR) and Fourier transform infrared (FTIR) spectroscopy, should be used in the characterisation of aged biochar samples.

In an extended (2.1-year) incubation experiment (Chapter 7), the results showed that the MRT of biochars (450 and 550 °C) in the Vertisol were in the range of 314−978 years, which was greater than the estimates for the same biochars from a shorter-term study (Keith et al., 2011). The MRT of biochars decreased with the addition of LOM at 1% rate (sugarcane residues), but did not change with further increase in the LOM application rates (i.e. 2 and 4%). Biochar showed a positive

priming effect on native or added LOM-C mineralisation at low LOM application rates (1%). However, negative priming effect of biochar on LOM-C mineralisation was observed at 2 and 4% LOM application rates, suggesting a further enhancement in C sequestration in the Vertisol with high LOM input. The presence of aged biochar (to 2.1 year) did not influence microbial community structure in the Vertisol, possibly due to the depletion of labile C components in the biochars over time. The presence of aged LOM, however, resulted in changes in the structure of microbial communities in the Vertisol; these changes in the microbial community may have contributed to the interactive priming effect of biochar and LOM-C mineralisation. Further research evaluating specific bacterial and fungal community structures and their impact on the interactive biochar and LOM-C mineralisation processes is warranted.

This research on biochar and soil C stability in a variety of soils has shown that wood biochar application to soil is a promising approach for a relatively long-term C storage, possibly achieving a maximum C sequestration benefit in the Oxisol. However, the laboratory-based studies are generally carried out under controlled conditions (constant temperature and moisture), and these controlled conditions and their influence on biochar and soil C stability may differ, relative to those observed under natural conditions in the field. Future research should focus on *in situ* studies examining biochar and soil C stability and stabilisation processes in contrasting soils and environments, over a relatively longer period of at least two years or more. More importantly, future experiments on biochar stability should be conducted in the presence of plants. The effects of rhizosphere processes under field conditions will determine the real potential of biochar for long-term C storage in soils.

References

Keith, A., Singh, B., Singh, B.P., 2011. Interactive priming of biochar and labile organic matter mineralization in a smectite-rich soil. Environmental Science & Technology 45, 9611-9618.

Appendices

Appendix 1: Nutrient Solution recipe (Chapter 3).

In each soil-biochar mixture or control soil container, 18 ml of nutrient solution was added when we set up the incubation studies.

Table A1. Nutrient Solution added to the soil-biochar mixtures or the control soils (for 5 L solution).

Salts	**g/5L**
KNO_3	45.1
$Ca(H_2PO_4)_2$	7.1
$MgSO_47H_2O$	2.125
K_2SO_4	4.2
NH_4NO_3	25.7
	mg/5L
$Na_2EDTA\ 2H_2O$	375
$ZnSO_4\ 2H_2O$	163.35
$MnCl_2\ 4H_2O$	37.5
$FeCl_3\ 6H_2O$	35
$CoSO_4\ 6H_2O$	14.175
$Cu(NO_3)_2\ 2H_2O$	10.9
$Na_2MoO_4\ 2\ H_2O$	11.25
	ml/5L
Soil Solution*	40 ml

*Soil Solution: prepared by gently shaking 50 g of air-dried soil with 100 ml distilled water, the suspension was then filtered through a 100 um sieve.

Appendix 2: Some properties of soils in the incubation experiment (Chapter 3)

Property	Inceptisol	Entisol	Oxisol	Vertisol
pH (1:5 H_2O)	5.70±0.01	8.77±0.01	7.89±0.01	5.65±0.01
pH (1:5 $CaCl_2$)	4.87±0.01	8.06±0.01	7.16±0.01	5.05±0.01
Nitrate nitrogen (NO_3), mg kg^{-1}	5.1	11.0	69.0	22.0
Phosphorus (Colwell), mg kg^{-1}	11	32	34	81
Available potassium, mg kg^{-1}	38	650	72	220
Sulphate sulphur (KCl), mg kg^{-1}	6.3	11.0	7.7	6.6
Chloride, mg kg^{-1}	48.0	120.0	22.0	44.0
CEC -NH_4OAc, $mmol_c$ /kg	20.4	308.0	79.7	421.0
Aluminium (KCl), $mmol_c$ /kg	1.0	-	1.0	-
Calcium (Amm-acet.), $mmol_c$ /kg	15.0	250.0	65.0	270.0
Magnesium (Amm-acet.), $mmol_c$ /kg	2.6	36.0	9.9	140.0
Sodium (Amm-acet.), $mmol_c$ /kg	0.9	5.2	1.9	5.7
Potassium (Amm-acet.), $mmol_c$ /kg	1.0	17.0	1.9	5.5

Appendix 3: XRD analysis method

Clay minerals in the soils were identified by X-ray diffraction (XRD) of oriented specimen (Mg saturated and glycerated, K-saturated and heated at 330° and 550°) and random powder using a GBC MMA diffractometer. The generator was set at 35 kV and 28.5 mA, and monochromatic Cu-Kα radiation (λ = 1.54056 Å) was used. After adequately dispersing the clay using an ultrasonic probe, the clay fraction was deposited on ceramic slides using a Pasteur pipette. Clays were saturated in K or Mg and air dried. X-ray diffraction pattern were obtained for Mg air-dried, Mg saturated-elrylene glycolated, K-air dried and K saturated and heated to 335°C and 550°C, oriented clamp. The samples were scanned for 3-30° 2θ for Mg air-dried and 3-15° 2θ for oriented with a step size of 0.02° at speed 1° min^{-1}. Random powder scans were also analysed over a 2-θ range from 4° to 65° with a step size of 0.02° at speed 1° min^{-1}. Clay minerals in the Entisol were determined before and after removing carbonates with sodium acetate (see below), and the Oxisol was treated with a solution of sodium citrate, sodium bicarbonate and Sodium hydrosulfite (see below) to remove of free ion oxides before the XRD analysis. The clay mineral contents were estimated from their peak areas and comparisons with the standard mixtures.

Removal of carbonates with sodium acetate from Entisol: A suitable amount of sample (< 2 mm) was put into a dialysis membrane. One end of which is tied with a rubber band. Several hundred millilitres of 0.5 M Na-acetate buffer solution (pH 7) were added to the dialysis membrane. The top of the dialysis membrane was tied to a glass “breather” tube (approximately 10 cm long), which was hanged and dipped in a reservoir of the Na-acetate buffer solution. Sodium acetate was changed repeatedly until there was no air bubble coming out. The dialysis membrane was then desalted against a deionised tap water flowing continuously through the container.

Removal of free ion oxides from Oxisol: In 1 g Oxisol soil, 40 ml of Na-citrate solution (0.3 M) and 5 ml $NaHCO_3$ solution (0.5M) was added. The suspension was heated to 80°C in a water bath, and 1 g of solid $Na_2S_2O_4$ was added. The suspension was constantly stirred for 1 min and occasionally for 15 min. It is important to avoid heating above 80°C because FeS can form. About 10 ml of saturated NaCl solution was added to settle the clay. The above treatment procedure was repeated several times until the soil colour became grey.

References

Brown, G. & Brindley, G.W. 1980. X-ray Diffraction procedures for clay mineral identification. In: *Crystal structures of clay minerals and their Xray identification* (eds. Brindley, G.W. & Brown, G.), pp. 305-359. Mineralogical Society, London, UK.

Appendix 4: An example of calculation Q_{10a} (20−40 °C) (Chapter 5).

Fitting the real data of biochar-C mineralised at T_{ref} (20 °C) to the following two-pool exponential model to obtain C_1, C_2, k_1 and k_2 values.

$$C_{min}(t) = C_1 \times \left(1 - e^{-k_1 t}\right) + C_2 \times (1 - e^{-k_2 t})$$

The observed proportion of added biochar-C mineralised over time.

20 °C		**40 °C**	
Time (d)	**WA_B450**	**Time (d)**	**WA_B450**
0	0.00	0	0.00
3	0.08	2	0.07
9	0.16	4	0.16
18	0.20	8	0.34
38	0.31	16	0.50
94	0.41	30	0.77
183	0.55	51	0.90
276	0.66	80	1.16
365	0.72	183	1.50
498	0.80	246	1.63
550	0.83	313	1.66
671	0.88	365	1.74
730	0.91	428	1.82
		469	1.86
		550	1.97
		659	2.39
		730	2.48

The parameters obtained from the two-pool exponential model.

Parameters	**WA_B450**
C_1	0.435
C_2	99.565
k_1	0.029
k_2	6.97×10^{-6}
R^2	0.992

Fitting the observed biochar-C mineralised at 40 °C to the following temperature-incorporated two-pool exponential model. The C_1, C_2, k_1 and k_2 values were obtained from 20 °C. Then Q_{10a} was determined by the common exponential Q_{10} model. The calculated r(T) and Q_{10a} values were 4.59 and 2.14.

$$C_{min}(t,T) = C_1 \times \left(1 - e^{-r(T)k_1 t}\right) + C_2 \times \left(1 - e^{-r(T)k_2 t}\right) \quad (1)$$

$$Q_{10a} = r(T)^{\frac{10}{T - T_{ref}}} \quad (2)$$

Appendix 5: $\delta^{13}C$ signatures (‰) of CO_2-C evolved from soil-biochar mixtures and control soils (Chapter 4 and 5)

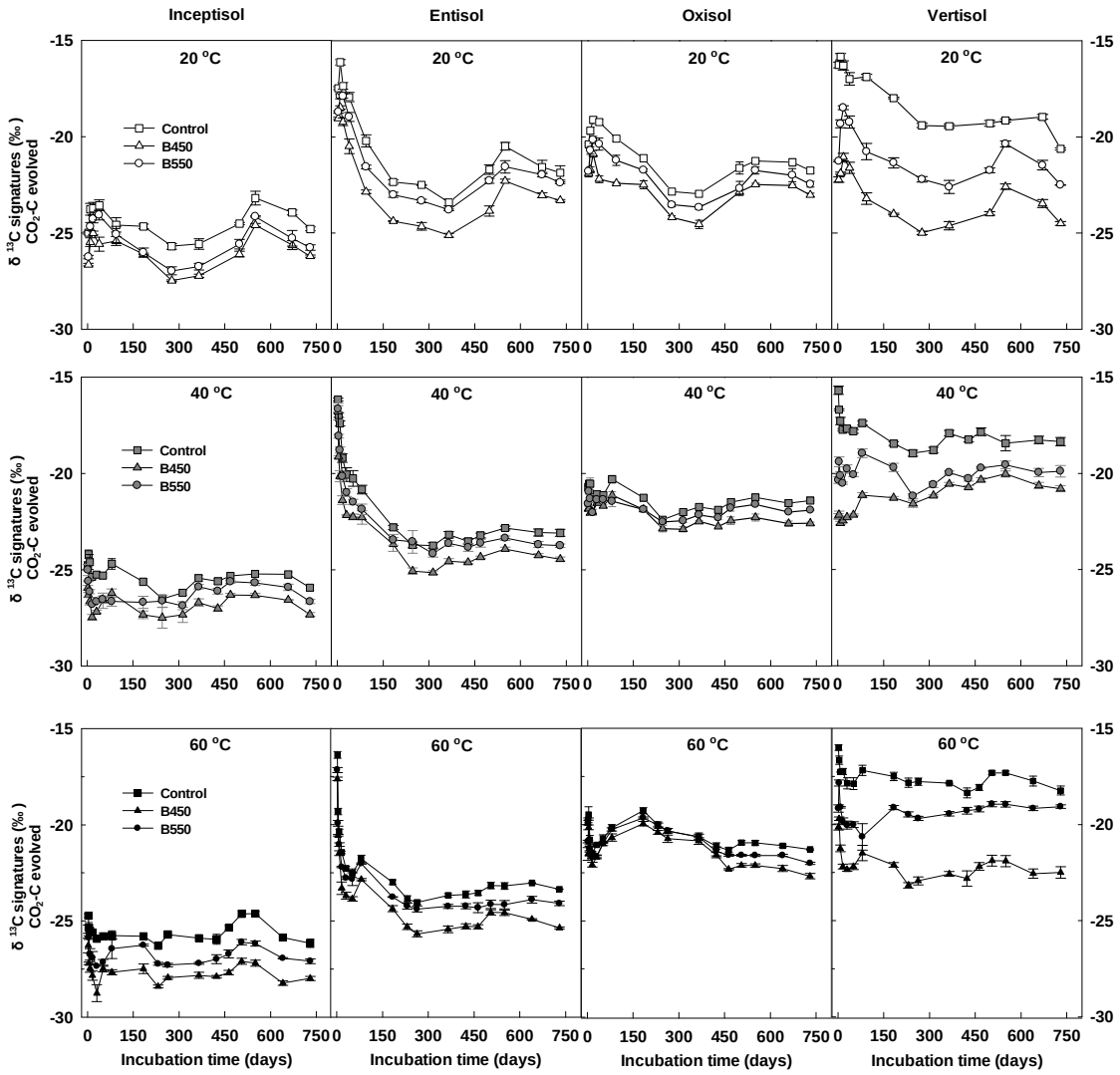

Figure A5.1. $\delta^{13}C$ signatures (‰) of CO_2-C evolved from control (B0), 450 °C (B450) and 550 °C (B550) biochar amended soil incubated at 20 °C (empty symbols) 40 °C (grey filled symbols) and 60 °C (black filled symbols) over the 2-year incubation period. Square, triangle and circle symbols represent B0, B450 and B550 treatments, respectively. Error bars represent ± standard errors of the mean (n=4).

Appendix 6: Soil, biochar and LOM in the 2.1-year incubation study

Surface sample (0-10 cm) of a Vertisol was collected from an experimental plot that has been grown with C4 tussock Mitchell grass (*Astrebla* spp.) for over 100 years. Sugarcane residue (C4 biomass) was used as the source of LOM. Two wood biochars were produced at 450 and 550 °C using slow pyrolysis (5−10 °C per minute heating rate, 40 minutes residence time) by Pacific Pyrolysis (Somersby, Australia) from ^{13}C-depleted woody biomass of *Eucalyptus saligna* Sm. trees that had been grown for two years under an elevated CO_2 environment (Barton et al., 2010). The soil, sugarcane residue and biochars were ground to < 2 mm fraction. Important properties of the soil, biochars and sugarcane residue are shown in Table A6.1.

References

Keith, A., Singh, B., Singh, B.P., 2011. Interactive priming of biochar and labile organic matter mineralization in a smectite-rich soil. Environmental Science & Technology 45, 9611-9618.

Table A6.1. Important properties of the soil, biochars and sugarcane residue used in the incubation experiment (Keith et al., 2011).

Property	Soil	450 °C biochar	550 °C biochar	Sugarcane residue
Total C (%)	0.45	67.8	74.9	39.6
Total N (%)	0.04	0.5	0.6	0.4
$\delta^{13}C$	-14.3	-36.3	-36.4	-12.7
pH (1:5 H_2O)	8.10	8.60	9.90	-
Electrical conductivity (1:5, dS	0.11	0.90	1.10	-
CEC[a] ($mmol_c\ kg^{-1}$)	347	11.4	54.0	-
Clay (%)	53	-	-	-
Silt (%)	14	-	-	-
Sand (%)	33	-	-	-
Specific surface area[b] ($m^2\ g^{-1}$)	-	191.0	228.3	-
Pore volume (%)	-	57.2	67.5	-
Clay minerals	S****, K*, I*	-	-	-

[a]Cation exchange capacity measured by the silver thiorurea method; [b]CO_2 adsorption method; S**** = smectite (>80%), K* = kaolinite (<10%) and I* = illite (<10%).

Table A6.2. Mean residence time of the labile and recalcitrant pools of biochar carbon (C) estimated using a two-pool exponential model fitted to the biochar-C mineralisation data over the 4-month incubation period.

Treatments		Mean residence time		Labile C pool (%)
Biochar (2%)	**LOM (%)**	**Labile (days)**	**Resistant (years)**	
450 °C	0	16	62	0.234
450 °C	1	14	112	0.375
450 °C	2	11	73	0.390
450 °C	4	22	89	0.702
550 °C	0	2	100	0.101
550 °C	1	3	176	0.188
550 °C	2	4	248	0.296
550 °C	4	6	103	0.373

Table A6.3. The sensitivity of LOM and soil $\delta^{13}C$ values in contributing the variation of the proportion of CO_2 derived from biochar.

	$\delta^{13}C$ (biochar)	$\delta^{13}C$ (soil+LOM)	$\delta^{13}C$ (mixture)	Contribution from LOM (%)	Contribution from soil (%)	Biochar-C (%)
Baseline	**-36.40**	**-12.89**	**-15.24**	**88**	**12**	**10.0**
Scnario 1		-12.81		93	7	10.3
Scnario 2		-12.97		83	17	9.7

Table A6.4. pH (n=3) of experimental soils after the 2.1-year incubation period.

Treatments		pH
LOM (%)	**Biochar (%)**	
0	Control	6.56±0.03
	450 °C	6.73±0.08
	550 °C	6.88±0.06
1	Control	7.07±0.02
	450 °C	7.16±0.05
	550 °C	7.30±0.06
2	Control	7.37±0.05
	450 °C	7.45±0.02
	550 °C	7.55±0.02
4	Control	7.56±0.03
	450 °C	7.62±0.05
	550 °C	7.69±0.08

Appendix 7: T-RFLP data (Chapter 7)

Table A7.1. Summary of bacterial T-RFs

Minimum number of T-RFs	156 in sample 33224_17 (YF17_A05.fsa)
Maximum number of T-RFs	269 in sample 33224_28 (YF28_D07.fsa)
Average T-RF richness	213.54
Sample Heterogeneity	1.61
Percent of empty cells in data matrix	61.73

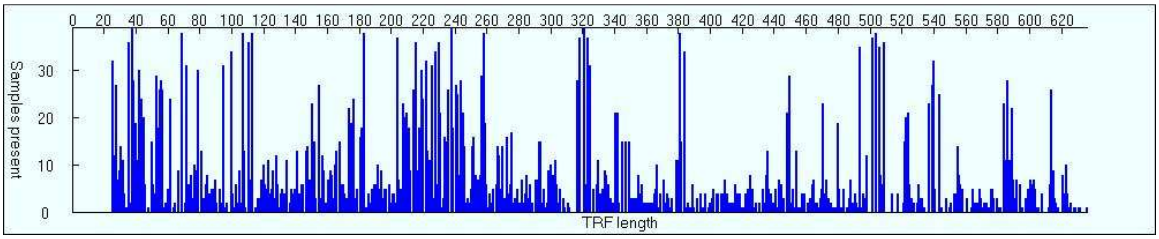

Figure A7.1. Screenshot of bacterial sample details page in *T-REX*.

Table A7.1. Summary of fungal T-RFs

Minimum number of T-RFs	82 in sample 33226_10 (YF16_H03.fsa)
Maximum number of T-RFs	160 in sample 33226_21 (YF30_F07.fsa)
Average T-RF richness	112.56
Sample Heterogeneity	1.19
Percent of empty cells in data matrix	54.43

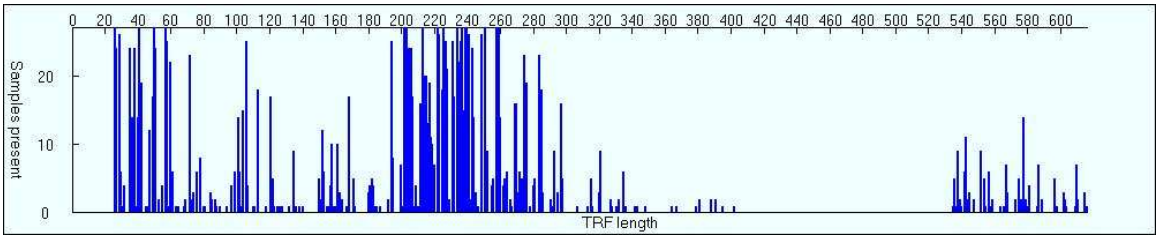

Figure A7.2. Screenshot of fungal sample details page in *T-REX*.

(a)

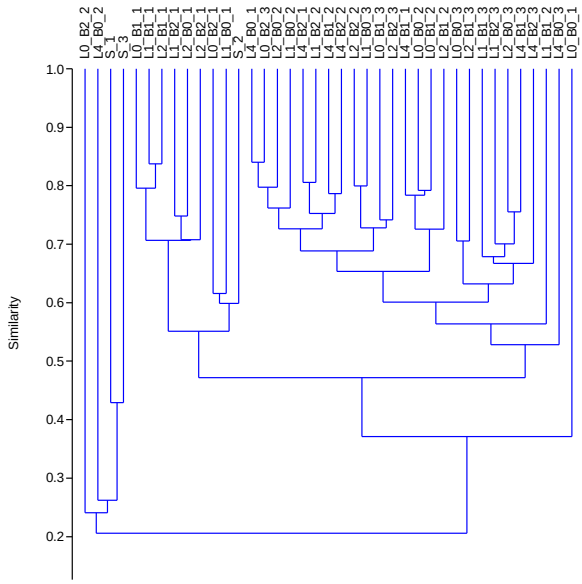

(b)

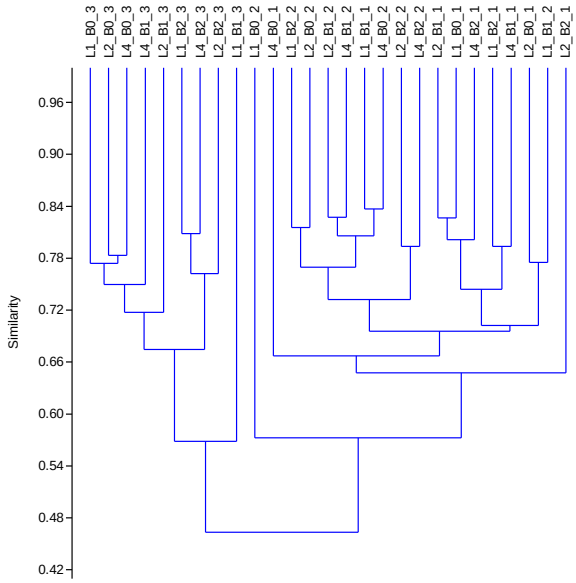

Figure A7.3. Clustering of bacterial (a) and fungal (b) T-RFs peak height. In the labelling, L0, L1, L2 and L4 represent sugarcane addition rates at 0, 1, 2 and 4%; B0, B1 and B2 represent control, 450 °C and 550 °C biochar treatments; 1, 2 and 3 represent three replications.

(a)

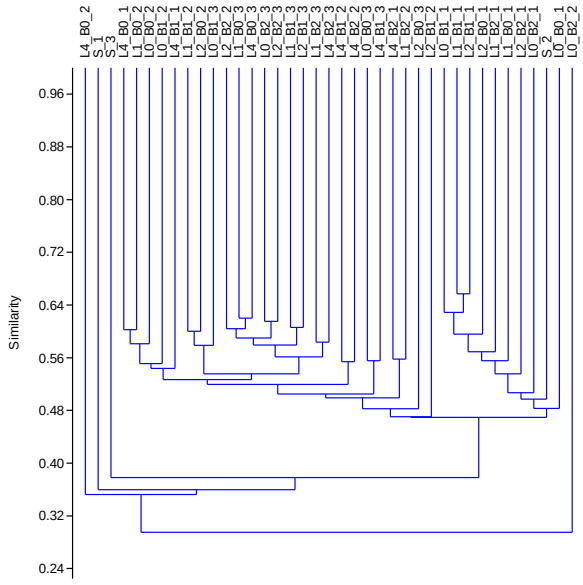

(b)

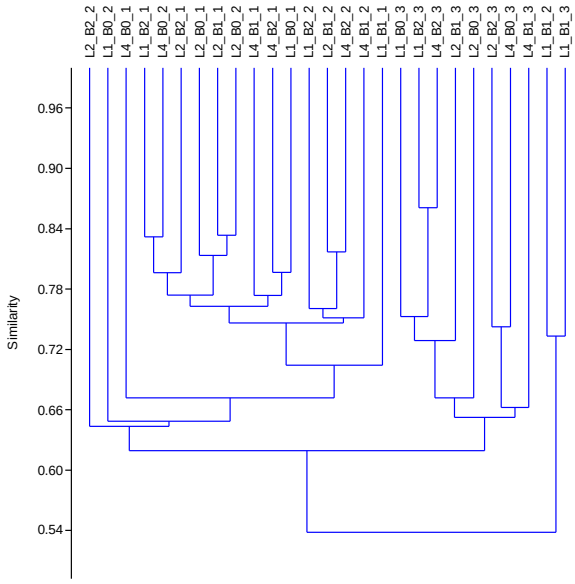

Figure A7.4. Clustering of bacterial (a) and fungal (b) peak appearance and absence. In the labelling, L0, L1, L2 and L4 represent sugarcane addition rates at 0, 1, 2 and 4%; B0, B1 and B2 represent control, 450 °C and 550 °C biochar treatments; 1, 2 and 3 represent three replications; S1, S2 and S3 are original soils.

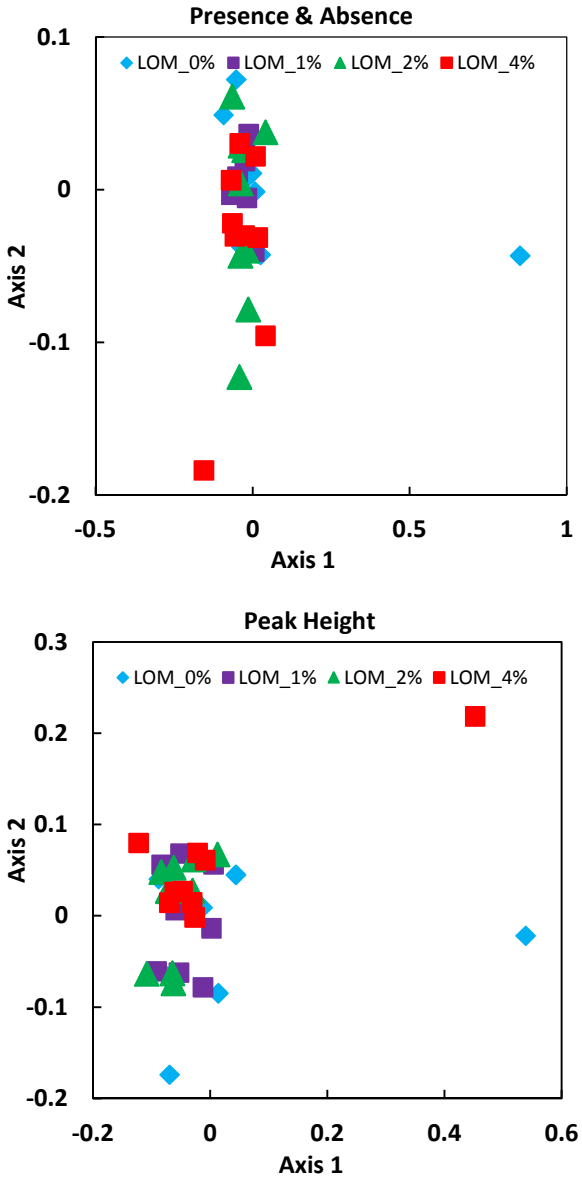

Figure A7.5. Non-metric MDS analysis of the bacterial community structure using peak presence/absence and relativised peak height and peak area.

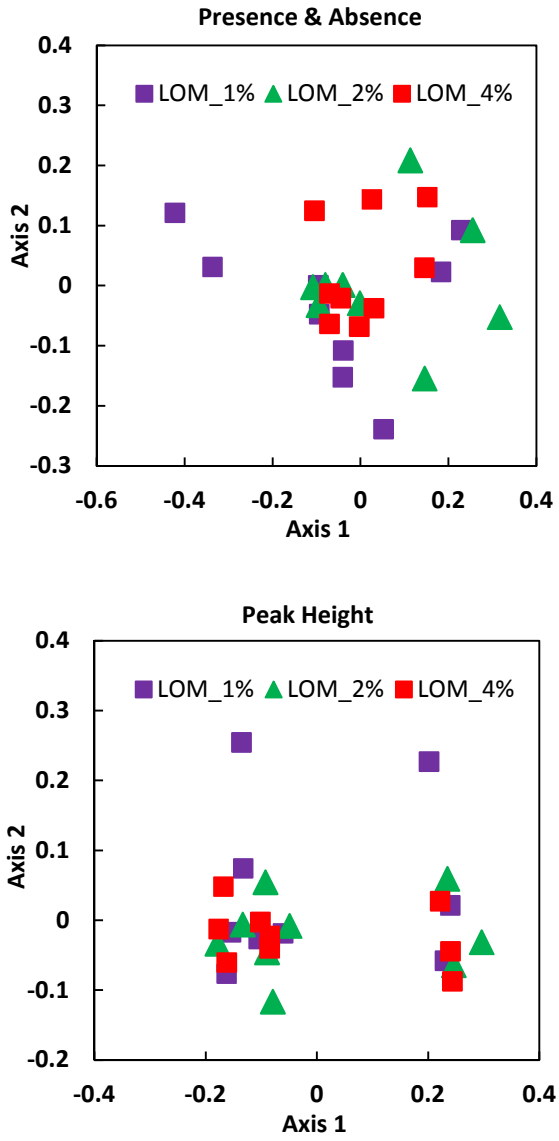

Figure A8.6. Non-metric MDS analysis of the fungal community structure using peak presence/absence and relativised peak height and peak area.